DROUGHT ASSESSMENT OF KIRINDI OYA AND KELANI RIVER BASINS IN SRI LANKA UNDER CLIMATE CHANGE IMPACTS

Farhana Azmi

208346G

Degree of Master of Science

Department of Civil Engineering

University of Moratuwa
Sri Lanka

February 2022

DROUGHT ASSESSMENT OF KIRINDI OYA AND KELANI RIVER BASINS IN SRI LANKA UNDER CLIMATE CHANGE IMPACTS

Farhana Azmi

208346G

Supervised by

Dr R. M. J. Bamunawala

and

Dr T. M. N. Wijayaratna

Thesis submitted in partial fulfillment of the requirements for the degree

Master of Science in Civil Engineering

UNESCO Madanjeet Singh Centre for

South Asia Water Management (UMCSAWM)

Department of Civil Engineering

University of Moratuwa

Sri Lanka

February 2022

DECLARATION OF THE CANDIDATE AND SUPERVISOR

"I declare that this is my own work and this thesis does not incorporate without acknowledgement any material previously submitted for a Degree or Diploma in any other University or institute of higher learning and to the best of my knowledge and belief it does not contain any material previously published or written by another person except where the acknowledgement is made in the text".

Also, I hereby grant to University of Moratuwa the non-exclusive right to reproduce and distribute my thesis, in whole or in part in print, electronic or other medium. I retain the right to use this content in whole or part in future works (such as articles or books).

UOM Verified Signature

---------- 2022-02-06

Farhana Azmi Date

The above candidate has carried out research for the Masters thesis under my supervision

UOM Verified Signature

---------- 2022-02-06

Dr R. M. J. Bamunawala Date

UOM Verified Signature

---------- 2022-02-06

Dr T. M. N. Wijayaratna Date

ABSTRACT

Drought Assessment of Kirindi Oya and Kelani River Basins in Sri Lanka under Climate Change Impacts

Drought is a natural phenomenon that occurs because of climate change. Droughts are localized events influenced by climatic variables such as precipitation, evapotranspiration, and temperature. As a result, the characteristics and implications of drought differ depending on the climatic administrations in various regions around the world. Drought is one of the maximum significant intervals in Sri Lanka. Sri Lanka is very sensitive to the effects of climate change. Drought is an extremely considerable interval in Sri Lanka in terms of people concerned and helps provided, and the country also serves as a recent example for drought interval and risk assessment in tropical regions.

This research investigates the probable use of drought indices at Kirindi Oya and Kelani River basins and provides drought assessment for future climatic scenarios. This research was directed to perceive the changes in drought, their consistencies according to seasonal analysis in the Kirindi Oya and Kelani River basin in Sri Lanka using normalized difference vegetation index (NDVI), standardized precipitation index (SPI), and streamflow drought index (SDI) for future climate change RCP 8.5 which is one of the worst scenarios according to 5th assessment report of the intergovernmental panel on climate change (IPCC). The drought assessment has been divided into three-time intervals such as observed period (1985-2015), mid-century (2040-2059), and end-century (2080-2099). Further, future climate rainfall data has been forecasted by bias correction monthly factor of historical climate rainfall and observed rainfall data using linear scaling.

The NDVI has been calculated by using Landsat images near-infrared (NIR) and RED bands in GIS 10.3. Initially, SPI and SDI have been calculated for observed rainfall and streamflow data respectively. Hydrological model HEC-HMS was set up and calibrated (2002-2006) with a root mean square error standard deviation ratio (RMSE std dev) value of 0.6, nash sutcliffe (NSE) value of 0.59, and percent bias (PBIAS) of 7.63%. The model was validated from 2010 to 2014 with an RMSE std dev value of 0.7, NSE value of 0.51, and PBIAS of 3.22% for Kirindi Oya basin. Further, for the Kelani basin. the HEC-HMS was set up and calibrated (1990-1995) with an RMSE std dev value of 0.6, NSE value of 0.64, and PBIAS of 0.64% and validated (2007-2011) with RMSE std dev value of 0.7, NSE value of 0.56 and Percent Bias of -3.27% for Kelani basin. Thereafter, mid and end-century SPI and SDI have been calculated for future bias-corrected rainfall data and future simulated streamflow, respectively.

To achieve the objectives of this research work, The rate of recurrence of drought occurrences was determined using a combined SPI and SDI evaluation which identified 1989, 1990, 1992, 2001, and 2004 as a severe drought-affected year in the Kirindi Oya river basin in this observed interval. For the Kelani River basin, severe drought has been identified during 1990, 2001, 2012, 2013, and 2014 in the observed interval.

According to seasonal analysis, the probability of occurrence of extreme drought according to SPI values in Kirindi Oya basin is decreasing 25% for mid and 50% end-century, in the Kelani basin 93.75% for mid and 68.75% in end-century. According to SDI values in the Kirindi Oya basin is decreasing 25% for mid and 25% end-century, in the Kelani basin 93.75% for mid and 50% in end-century. First inter monsoon has been found more severe to drought for both SPI and SDI combination in Kirindi Oya river basin, the northeast monsoon period is the driest season for the Kelani River basin which is situated in wet zone in Sri Lanka.

Keywords: Drought indices, Normalized difference vegetation index (NDVI), Standardized precipitation index (SPI), Streamflow drought index (SDI)

DEDICATION

By the grace of Almighty Allah.

ACKNOWLEDGEMENT

I would want to convey my genuine and heartfelt gratitude to Dr. Janaka Bamunawala, my research supervisor, for his constant support for my work, as well as his patience, drive, and vast expertise. This thesis would not have been completed on time without his supervision and ongoing mentoring. Throughout my time with him, he continuously allowed this research to be my responsibility while steering me on the proper path when he felt I needed it. He is a fantastic educator.

I owe a debt of gratitude to Prof. R.L.H. Lalith Rajapakse, Centre Chairman, and program coordinator, for providing me all the essential assistance, guidance, and encouragement, as well as counseling when needed, despite his hectic schedule.

I would also like to express my gratitude to Late. Shri Madanjeet Singh, the University of Moratuwa, and the UNESCO Madanjeet Singh Centre for South Asia Water Management, Department of Civil Engineering, University of Moratuwa, Sri Lanka, for providing me with the opportunity to pursue a master's degree in Water Resource Engineering and Management at the UNESCO Madanjeet Singh Centre for South Asia Water Management, Department of Civil Engineering, University of Moratuwa.

Also, I must thank Irrigation Department for approvals to collect necessary data.

Finally, I must express my very profound gratitude to my SAF friends, especially Virendra Kumar and Utsab Phuyal for all those supports that help me to focus on this research and have provided me with the encouragement to continue my work when I was having a hard time.

TABLE OF CONTENTS

LIST OF FIGURES

LIST OF TABLES

LIST OF ABBREVIATIONS

CMIP5	-	Coupled Model Intercomparison Project Phase 5
DEM	-	Digital Elevation Model
FDC	-	Flow Duration Curve
FIM	-	First Inter Monsoon
HEC	-	Hydrologic Engineering Center
HMS	-	Hydrologic Modeling System
IPCC	-	Intergovernmental Panel on Climate Change
LULC	-	Land-use Landcover
MIT	-	Minimum Inter-event Time
NEM	-	Northeast Monsoon
NSE	-	Nash Sutcliffe Efficiency
PBIAS	-	Percentage Bias
PVE	-	Percentage Streamflow Volume Error
R10	-	Heavy precipitation days
R20	-	Very heavy precipitation days
RAS	-	River Analysis System
RCP	-	Representative Concentration Pathways
RMSE	-	Root Mean Square Error
RMSE std dev	-	RMSE Observed Standard Deviation Ratio
SCS	-	Soil conservation service
SDI	-	Streamflow Drought Index
SEM	-	Second Inter Monsoon
SM	-	Soil Moisture
SMA	-	Soil Moisture Accounting
SPI	-	Standardized Precipitation Index
SWM	-	Southwest Monsoon

CHAPTER 1

1 INTRODUCTION

Drought is a natural occurrence that occurs as part of climate variability, and it is an extended period of parched weather when there is not enough rain. Droughts are localized phenomena whose occurrence is affected by climatic factors while precipitation, evapotranspiration, and temperature. It is a continuous and complicated occurrence that has a significant impact on both human and ecological systems. Lack of precipitation can result in a variety of issues for local communities, including food shortages and a lack of drinking water. As a result, drought's characteristics and subsequent consequences differ depending on climatic regimes worldwide. Droughts' adverse impacts include reducing air and water quality, land degradation, forest fires, and diminished agricultural crop production. It may result in a water conflict, causing people to migrate to a better location (Amarsaikhan et al., 2014). Famine forced migration out from drought-stricken areas and fighting over remaining resources are all possible outcomes of these consequences.

Droughts are identified as an environmental disaster and have concerned the consideration of environmentalists, hydrologists, ecologists, geologists meteorologists, and agricultural scientists. Drought may arise in practically all climatic zones, such as high and minimum rainfall areas, and are generally related to the decrease in the quantity of rainfall obtained over a prolonged period, such as a season or a year (Mishra & Singh, 2010). Sri Lanka is frequently affected by drought, posing a significant threat to the country, including agriculture and the economy (Kottawa-Arachchi & Wijeratne, 2017).

Droughts are mainly categorized into hydrological drought, meteorological drought, and agricultural drought. Drought-related losses of life, human misery, and economic and environmental harm can all be reduced with knowledge of the onset, extent,

intensity, duration, and repercussions. An attempt was made in this study to use RS and GIS approaches to perceive drought.

This study was carried out as part of an ongoing initiative to analyze metrological drought using SPI, hydrological drought using the SDI in the Kirindi Oya river basin in Sri Lanka due to the scarcity of research on the topic. From 1987 to 2015, the SPI and SDI were applied for the corresponding interval of three, six, and twelve months contained by every hydrological year. Agricultural drought risk zones are perceived using the Normalized Difference Vegetation Index (NDVI) and a Landsat satellite image using surface reflectance.

1.1 Drought Types

Droughts can be categorized into four major classifications:

Meteorological drought: It means that precipitation in a certain area is less than 25% of usual in the given area. Because precipitation insufficiency varies greatly from one place to another, these are region-specific.

Hydrological drought: These are attributed to the absence of water on the surface or beneath the ground expected to a lack of precipitation. While all droughts are caused by a shortage of precipitation, hydrological drought is alarmed with how this lack of rain affects hydrological system components such as soil moisture, reservoir levels, streamflow, and groundwater among many others.

Agricultural drought: Drought in agriculture can have serious economic and social effects, especially in areas where water resources are restricted or where water demand exceeds natural supply capacity. Drought in agriculture is defined as a scarcity of rain over a specific timeline that results in a soil moisture deficit, limiting water availability for crops to the point that yields are lowered. As a result, agricultural drought is perceived and monitored using a variety of indicators, which are often based on meteorological data and estimates from remote sensing and/or modeling (Sepulcre-Canto et al., 2012).

Socio-economic drought: The problem is linked to the demand and provide of socioeconomic commodities, as well as meteorological, hydrological, and agricultural

drought conditions. When the demand for an economic item vastly outnumbers the supply due to a weather-related water deficit, a drought occurs.

A correlation between the meteorological, hydrological, and agricultural droughts can be evaluated from the figure below in Figure 1-1.

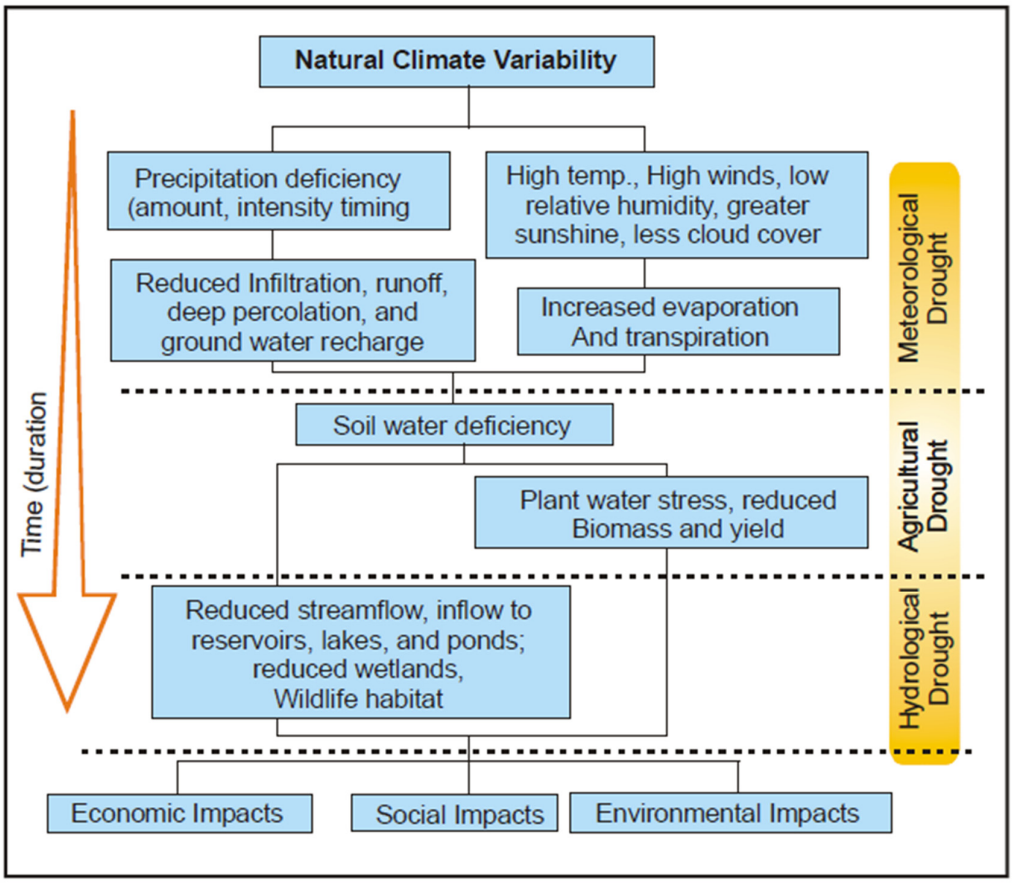

Figure 1-1: Relationship between meteorological, hydrological, and agricultural drought

(Source: National Drought Mitigation Centre, http://enso.unl.edu/ndmc/enigma/def2.htm)

Historically, drought is one of the highly devastating natural disasters for individuals affected and aid supplied in Sri Lanka. The country covers over 65,000 km^2 and has about 20 million population (Department of Census & Statistics 2001). In 2001, the freshwater fisheries, forestry, and agriculture industries accounted for 15% of the national gross domestic product (GDP), and the workforce is employed 35% (Department of Census & Statistics, 2001). Droughts have the probability to destabilize the agrarian economy. The major cash harvests by area cultivated (in

thousands of hectares) are coconut (444), tea (195), rubber (159), and spices. The primary food crop is rice (739), with coconut of secondary significance (Lyon et al., 2009).

The Maha rice-cropping season, which usually begins in late September and finishes off in March, is marked by significant rainfall. Yala, the secondary season, runs from May to early September. Due to a lack of water, only roughly half of the total agricultural land is grown during the second season. Variations in rainfall throughout both seasons have been demonstrated to impact rice and coconut production (Zubair et al., 2003).

The four rainy seasons carry out non produce uniform rainfall regimes over the island, resulting in a high level of agroecological variability despite the country's tiny size. The key increasing seasons of Sri Lanka are the Yala and Maha seasons, which are two consecutive wet seasons out of the four rainfall seasons. Yala season is characterized by a mix of FIM and SWM rainfall. Because SWM rains are heaviest in the country's Southwestern section, the duration (efficiency) of this season in the remaining of the country is often limited to just two months (March to May), and thereafter the Yala season is regarded as the country's minimal growth season. The island's main growth season, known as Maha season, commences in October with the arrival of SIM rains and lasts until late January/February along with the arrival of NEM rains. Showers during the two inter monsoon intervals, which are mostly convective in origin, are typically linked with thunder and lightning, as well as quick-interval high-intensity rains, more than ever during the FIM period (Filho, 2015).

Sri Lanka has much capacity to deal with drought thanks to a system of trans-basin diversions, major storage capacity reservoirs, and over 12,000 small village-level reservoirs. These reservoirs store rainwater from the primary farming season, which begins in October until the secondary cultivation season in April. However, these reservoirs cannot store water for more than a year. Farmers and irrigation managers communicate before each cultivation season, resulting in determining schedules of water deliveries based on storage and projected rainfall. Farmers utilize these calculations to enhance their crop selection and planting area. Farmers are unlikely to

offset the effects of severe drought, even while irrigation efforts provide some water storage (Zubair et al., 2005).

Droughts have immediate consequences in the agricultural and home water supply divisions, and severe droughts can have a broad economic impact. Planned outages of electricity owing to hydropower generating deficiencies, for example, cause disturbances in the industrial and utility services industries, which account for 25% of GDP and 21% of the labour force. The prolonged drought of 2001–02 wreaked havoc on public health, agriculture, water supplies, and hydropower generation, resulting in a 1% reduction in GDP growth. Sri Lanka's climate is heavily influenced by its location and topography. In rural Sri Lanka, agricultural water scarcity is a major issue. Climate change will alter the timing and duration of seasonal monsoons in the future, putting further strain on the island's agricultural production (De Silva et al., 2007).

1.2 Problem Identification

Rendering to the IPCC fifth assessment report (IPCC, 2014), the South Asian section is vulnerable to drought, food deficiencies, and heat-related mortality. Sri Lanka and other South Asian countries have experienced a long-lasting drought once every 3 years, which is only of the main causes for reducing agricultural yield in Sri Lanka (Aadhar & Mishra, 2017). Expected to the reducing effect of monsoon precipitation, Sri Lanka is adversely affected by droughts. Short water storing capacities and increasing demand for water for economic growth further intensify the encouragement of drought on agronomy production all over the country. So, drought has been considered as one of the extremely significant climate intervals in Sri Lanka, especially in the dry and intermediate climate zones of Sri Lanka (Chandimala & Zubair, 2007).

1.3 Problem Statement

Drought is the most frequent problem in Sri Lanka, and some river basins have become dry for decreasing day by day of annual precipitation. The agriculture field has mainly been affected due to the droughts, and this has a direct impact on the agriculture-based economy of Sri Lanka. Thus, understanding the physical characteristics of droughts

and their regularities using multiple indicators will be beneficial in appropriate water management practices and future land use planning.

1.4 Objectives of the study

1.4.1 Main objective

This research investigates the probable use of drought indices (i.e., SPI, SDI & NDVI) at Kirindi Oya and Kelani River basins and drought assessment for future climatic scenarios (mid-and end-century intervals).

1.4.2 Specific Objectives

- To assess the existing drought conditions of the Kirindi Oya and Kelani River basins using multiple drought indices (i.e., SPI, SDI, and NDVI).
- To set up, calibrate, and validate a numerical model (i.e., HEC-HMS) to project future streamflow of Kirindi Oya and Kelani River basins under climate change over the 21st century.
- To compute drought indices (i.e., SPI & SDI) at the Kirindi Oya and Kelani River basins for future scenarios and develop relevant drought assessments over the mid-and end-interval of the 21st century.
- To provide suitable recommendations to minimize drought-induced impacts at the Kirindi Oya and Kelani River basins by comparing the existing and future drought assessment.

CHAPTER 2

2 LITERATURE REVIEW

2.1 Droughts

Droughts have drawn the focus of environmentalists, meteorologists, geologists, ecologists, hydrologists, and agricultural experts as an environmental disaster. Droughts may occur in practically any climatic zone, including areas with high and low rainfall, and are typically accompanied by a long-term drop in precipitation (e.g., seasonal or annual interval). High temperatures and winds, low comparative humidity, and the scheduling and properties of precipitation, such as rain severity and duration, the dispersal of wet periods during the agricultural growing season, and onset and termination, all intensify the effects of droughts. Aridity, alternatively, is a long-lasting characteristic of climate and is limited to places with minimal rainfall (Wilhite, 2021).

Drought is a complex phenomenon because of its dependence on the atmosphere and the hydrologic processes that provide moisture to the environment. Once dry hydrologic conditions are determined, the drought's positive feedback process kicks in, with moisture depletion from topsoil layers lowering evapotranspiration rates and atmospheric comparative humidity. The lower the relative humidity, the lesser extent likely it is that rain will fall, as it will be more difficult for a standard low-pressure system to attain saturation conditions over the region. Only disturbances bringing enough moisture from outside the arid zone will bring enough rain to end the drought (Bravar & Kavvas, 1991).

Drought monitoring and assessment can be done using a variety of indicators. Considering drought exposure, each indicator has its own set of weaknesses and strengths. Meteorological drought indicators amalgamate stored soil moisture, rainfall, and water supply. Nonetheless, they are incapable of reflecting many local geographic details. Furthermore, drought indices determined at a single area are only valid at that

location. As a result, one of the key disadvantages exhibited by climatic-based indicators (in terms of drought) is their shortage of spatial accuracy, together with the fact that they rely on data gathered at weather stations, which can be meagrely dispersed, lowering the fidelity of the drought indices (Brown et al., 2002)

Indicators of drought estimated using the satellite-derived external parameter, on the other hand, have been frequently utilized to investigate droughts. One of the extremely used vegetation indicators is the Normalized Difference Vegetation Index (NDVI). Historical period drought indicators were subjugated by newly produced indices obtained using remote sensing data, and are considered real-time due to developments in remote sensing technology (Murad & Islam, 2011).

Standardized Precipitation Index (SPI) is one of the widely used methods to assess meteorological drought. The interpolation of SPI values is employed to ascertain the spatial distribution and trend of meteorological drought and the values of drought threshold (Himanshu et al., 2015).

The indicators of drought derived using surface parameters derived from satellites have been extensively used in drought research. The extensively used vegetation indicators include the Normalized Difference Vegetation Index (NDVI), Vegetation Condition Index (VCI), and Temperature Condition Index (TCI) (Himanshu et al., 2015).

2.2 Drought Indices

2.2.1 Normalized Difference Vegetation Index (NDVI)

During the late 1970s, scientists discovered that net photosynthesis is proportional to photosynthetically absorbed active light by plants. Photosynthetically absorbed sunlight is proportional to the Normalized Difference Vegetation Index (NDVI). The Normalized Difference Vegetation Index (NDVI) is a metric for determining the intensity and strength of vegetation on the ground. The level of photosynthetic activity in the observed vegetation is related to the magnitude of NDVI. In general, higher NDVI values suggest more vegetation vigor and quantity. As a result, the normalized

difference vegetation index (NDVI) tells us how greener the vegetation is there at a given location over the ground (Murad & Islam, 2011).

The NDVI is an excellent indication of green biomass, leaf area index, and production patterns. The most widely used vegetation index is the NDVI. The NDVI scale runs from -1 to +1, with most values falling between 0 and 0.6. Since red light is comparatively less reflected than near-infrared (NIR) light, healthy green vegetation has a high NDVI score. The NDVI of bare soil, on the other hand, is near zero because both near-infrared and red light is significantly reflected. Because ice and water reflect more red light than NIR light, their values are usually negative (Wang, 2005).

The NDVI is desirable for vegetation surveillance because it has two characteristics: no other surface has higher NDVI values than vegetated surfaces, and it fluctuates as vegetation vigor alters as a response to growth and development or drought-caused environmental stress. As a result, the NDVI can perceive drought and analyse climate impact (Tucker et al., 2005).

Within satellite data, the vegetation index can be utilized as an indicator to calculate the greenness of plants. Among varieties of vegetation indices, the NDVI is the most commonly employed. Researchers can calculate the coverage of vegetation on the Earth's surface by examining photographs captured at visible red and near-infrared (NIR) wavelengths (Taufik et al., 2019).

The agricultural drought index was calculated using Landsat data with 250 m resolution. The vegetation indicator can be applied as an indicator to quantify the abundance of plants within satellite data

The determination of NDVI value for each image was carried out using the following Equation [2-1] and the NDVI is defined as:

$$NDVI = \frac{(\mathrm{NIR} - \mathrm{RED})}{(\mathrm{NIR} + \mathrm{RED})} \qquad [2\text{-}1]$$

The NDVI was determined using bands number as NIR and RED which mentioned in Equation [2-2] and the NDVI is defined as:

$$NDVI = \frac{Band\,5\ -\ Band4}{Band\,5 +\ Band4} \quad [2\text{-}2]$$

2.2.2 Standardized Precipitation Index (SPI)

An index known as Standardized Precipitation Index (SPI) as a tool was generalized in 1993 by Tom McKee in the Colorado Climate Centre to define and monitor drought (Mckee et al., 1993). Standardized precipitation index (SPI) is the most common drought monitoring index (Mckee et al., 1993). It is used by the World Meteorological Organization (WMO) as a reference index for other indices. SPI is determined for any place using the long-term precipitation record for the selected timeframe. Researchers widely use the SPI because it simply needs rainfall data and has been demonstrated to accurately depict drought conditions in many regions, among other things. However, it only takes rainfall data as input and ignores the temperature component, crucial in determining a region's overall water balance. This flaw can make comparing events with comparable SPI levels but different temperature circumstances more challenging (Abeysingha et al., 2020).

The SPI analysis relies on the Gamma probability distribution being used to convert precipitation data to a normal distribution. Positive SPI values reflect higher precipitation compared to the median (wet periods), whereas negative values reflect lower precipitation compared to the median (dry periods) (Al-Qinna et al., 2011). According to McKee et al. (1993, 1995), consistently negative values of SPI and an intensity of 1.0 or less signifies the beginning of a drought event, and the ending of the drought event is signified by the positive SPI values. Precipitation data of a longer duration (minimum 30 years) is needed to compute SPI (Wu et al., 2001).

The SPI, as a tool derived by McKee (1993), used to quantify meteorological drought were calculated from the available rainfall data collected by the Meteorological Department.

For calculating the SPI value following equations are mentioned in Equation [2-3]. The SPI index is defined as:

$$SPI = \frac{(X_i - X_m)}{\sigma} \quad [2\text{-}3]$$

where X_i is the monthly rainfall record of the station, X_m is the rainfall mean, and σ is the standard deviation.

Developing a frequency distribution using precipitation data for a specific time is the first step in computing the SPI (Wu et al., 2001). SPI was calculated using two methods: simple average and moving average. Monthly rainfall records were utilized to calculate SPI. ArcGIS 10.3 was used to map the SPI values at matching drought classifications and intervals. For the SPI interval of 3, 6, and 12 months, the simple average approach established different drought physical characteristics in the study stations. SPI-3 was calculated for January to March, April to June, and October to December. Because the summer months are parched, the period (July-September) was overlooked. SPI-6 values were calculated for January–June, and July–December, and SPI-12 values were generated for a year commencing in January.

2.2.3 Streamflow Drought Index (SDI)

The SDI developed by Nalbantis and Tsakiris (2009) was employed to characterize hydrological drought considering the SPI development concepts. In Iran, the hydrological year spans from October to September of the following year. For each hydrological year, four equivalent intervals are utilized: October to December, October to June, October to March, and October to September (one complete hydrological year) (Tabari et al., 2013).

A lack of water defines drought. As a result, hydrological drought is regarded as the greatest representative drought category, as it not only examines streamflow but also depicts the drought status over an area (Z. Wu et al., 2015). In several elements of the world, different hydrological drought indexes are utilized. The streamflow drought indicator (SDI), like the SPI, is one of them. SDI is straightforward to use, as it allows for missing data.

Furthermore, different time scales can be considered for drought evaluation comparable to SPI. On top of the additional, streamflow input does not account for management actions, and intervals of no flow are capable of skewing the results. In

recent years, several academics have used the SDI methodology to investigate streamflow droughts. As a result, SPI and SDI were utilized in this study to evaluate the climatic and hydrological droughts in the Kirindi Oya river basin, respectively (Abeysingha et al., 2020).

Each Complete hydrological year: October to December, October to March, October to June, and October to September

(j=1 for October and j=12 for September). Based on this series, cumulative streamflow volume is computed as follows:

$$V_{i,k} = \sum_{j=1}^{3K} Q_{ij} \quad i = 1,2,\dots \;\; j = 1,2,\dots,12 \;\; k = 1,2,3,4 \qquad [2\text{-}4]$$

where $V_{i,k}$ is the cumulative streamflow volume for the i^{-th} hydrological year and the k^{-th} reference period, k=1 for October to December, k=2 for October to March, k=3 for October to June, and k=4 for October to September.

The SDI is defined based on cumulative streamflow volumes $V_{i,k}$ for each reference period k of the i^{-th} hydrological year as follows:

$$SDI_{i,k} = \frac{(V_{i,k} - \overline{V})}{s_k} \qquad i = 1,2,\ \dots \qquad k = 1,2,3,4 \qquad [2\text{-}5]$$

The normalization is simply reclaiming the natural logarithms of streamflow. The SDI index is defined as:

$$SDI_{i,k} = \frac{Y_{i,k} - \overline{Y_k}}{S_{y,k}} \qquad i = 1,\ 2,\ \dots,\ k = 1,\ 2,\ 3,\ 4 \qquad [2\text{-}6]$$

in which

$$Y_{i,k} = \ln\left(V_{i,k}\right), \qquad i = 1,\ 2,\ \dots,\ k = 1,\ 2,\ 3,\ 4 \qquad [2\text{-}7]$$

where V_k and S_k are the averages and the standard deviation of cumulative streamflow volumes, respectively.

Given the great reliance of numerous operations (industrial, urban water supply, and hydropower generation) on surface water resources, the hydrological component is the

most crucial. A basin's reservoirs or lake levels are generally connected with hydrological drought, first caused by rainfall deficiencies (Liu et al., 2012). Hydrological droughts may have a wide range of effects, including deteriorating water quality, reducing or disregarding water supplies, causing crop failure, constraining irrigation water requirements, reduction in power generation, limiting recreational activities, disorderly riparian habitats, and affecting a wide range of social and economic activities (Mishra & Singh, 2010).

In general, the indices developed to characterize hydrological drought are data-heavy and computationally costly. The streamflow drought index (SDI), on the other hand, was recently established by Nalbantis and Tsakiris (2009) and is a straightforward and efficient index for studying hydrological droughts.

2.3 Remote sensing in drought

Traditional drought monitoring methods relied solely on rainfall data, which had several drawbacks, including a limited network of stations, climate data that was often inadequate and inaccurate due to human error, and maximum importantly, it was difficult to attain data in close real-time spatially and temporally. Remote sensing technology has revolutionized monitoring and managing natural resources, notably in water resources, to address such shortcomings.

Remote sensing methods provide new opportunities for gathering this vital information because of their ability to collect regional-scale information in a short period. As a consequence, remote sensing techniques are employed to monitor disasters at critical stages (i.e., before, during, and after the disaster). Most importantly, this equipment is being utilized to collect baseline data against which future changes may be evaluated, and GIS techniques, on the other hand, provide an appropriate framework for integrating a variety of data sources. Remote Sensing and GIS can be used to determine geomorphologic parameters and project floods (Himanshu et al., 2015).

Drought risk assessment has been substantially facilitated by advances in the areas of GIS and remote sensing (RS) over the last three decades. Most of the data needed to assess drought risk have a spatial component and changes over time. As a result, the

use of GIS and RS has become necessary. GIS has a significant role to play in assessing drought risk. Remote sensing techniques provide frequent and consistent information concerning drought monitoring, including the surface characteristics of flat surfaces while fully utilizing information from the ground surface variety of time, space, and direction. For real-time and dynamic drought monitoring, it can provide macro, dynamic, and real-time monitor data sources (Tucker & Choudhury, 1987).

The key benefit of using GIS for drought risk assessment is that it creates a visual representation of the interval and opens the possibility of further analysing this product to estimate the likely damage caused by drought. Drought risk assessment necessitates current and accurate information on terrain topography and land use. Remotely sensed photos from satellites and planes are frequently the only source of this data for broad areas at a reasonable cost (Wipulanusat et al., 2009).

A meteorological station can link to a GIS and continue to receive meteorological data straight into GIS. That data is then handled and evaluated universally by the system database. GIS translates the model into its language, analyses the data using advanced analysis functions, and integrates drought early warning into the drought assessment system (Belal et al., 2014).

2.4 Use of HEC-HMS in Drought Analysis

The Hydrologic Engineering Centre–Hydrologic Modelling System (HEC–HMS) is a commonly used model supporting lumped parameter-based and distributed parameter-based modeling (Agrawal, 2005). HEC–HMS' ability to model long-term daily flows demonstrates its utility as a tool for water resource development planning. Low flows were successfully reproduced by the HEC–HMS, making it a valuable tool for predicting low flows in advance based on drought projections. The HEC–HMS is beneficial for examining future severe circumstances by combining the advantages of several modeling methodologies and different data availability. The information presented here can create adaptation and mitigation efforts (De Silva et al., 2014).

To calculate direct runoff, HEC-HMS uses a variety of approaches, including user-specified unit hydrographs, Clark unit hydrographs, Snyder unit hydrographs, SCS

unit hydrographs, Modclark (distributed model), and kinematic wave (Hamedi & Fuentes, 2015).

2.5 Pros and Cons of different models

The MIKE-SHE model contains ranges of physical procedures with high obligations on parameters and data, and hence its operation seems more sophisticated than the other three above-mentioned distributed models (Refsgaard et al., 1995). Further, MIKE-SHE is a commercial model, thus requires a subscription for researchers to undertake modeling activities.

The Soil-Water Assessment Tool (i.e., SWAT) is an open-source model maintained by international academics who have created many modules to account for human influences and agricultural development. The SWAT is commonly used for non-point source pollution simulation (Jayakrishnan et al., 2005), although it is rarely employed for drought predictions. It is preferable to enhance low flow simulations and the association to climate forecasting when applied to drought forecasting (Xing et al., 2020).

Drought forecast is possible if an Artificial Neural Network (i.e., ANN) is trained with the input of the two climatic signals about the preceding spring. The use of these climatic signals of other intervals did not contribute to the NDVI forecast (Marj & Meijerink, 2014). However, a large amount of data is needed to train and validate an ANN, while the method would also take a significantly longer time.

The Hydrologic Engineering Centre–Hydrologic Modelling System (HEC–HMS) is one such model that supports both lumped parameter-based modeling and distributed parameter-based modeling (Agrawal, 2005). The model provides various choices for simulating rainfall-runoff processes in watersheds. The HEC–HMS successfully reproduced low flows and, thus, is a useful tool to estimate low flows in advance based on drought forecasts. HEC-HMS incorporates several methods in calculating direct runoff: user-specified unit hydrograph, Clark unit hydrograph, Snyder unit hydrograph, SCS unit hydrograph, Modclark (distributed model), and kinematic wave (Hamedi & Fuentes, 2015).

According to this performance rating table, objective functions are evaluated which is mentioned in Table 2-1.

Table 2-1 Performance rating of the objective functions (Gunathilake et al., 2019)

Performance rating	NSE	RMSE	Percent Bias
Very good	0.75 to 1	0 to 0.5	< ± 10
Good	0.65 to 0.75	0.5 to 0.6	± 10 to ± 15
Satisfactory	0.5 to 0.65	0.6 to 0.7	± 15 to ± 25
Unsatisfactory	< 0.50	≥ 0.7	> ± 25

2.6 HEC-HMS Model

2.6.1 Simple canopy method-

Initial canopy storage (%): It is an initial condition input that reflects the percentage of the maximum canopy storage that has been filled at the beginning of the simulation. As a beginning value, we advise starting the simulation after a time of no rainfall, which makes a value of 0% reasonable. This assumption should be followed when selecting simulation periods later in the hydrologic modeling process. It is an initial condition input that reflects the percentage of the maximum canopy storage that has been filled at the beginning of the simulation. As a beginning value, we advise starting the simulation after a time of no rainfall, which makes a value of 0% reasonable. This assumption should be followed when selecting simulation periods later in the hydrologic modeling process (Ahbari et al., 2018).

Max canopy storage (mm): A formalism parameter reflecting the greatest depth of water that vegetation may intercept. The original value is estimated using the basin's SCS land use map. , and the suggested values are mentioned in Table 2-3 (Ahbari et al., 2018).

2.6.2 Surface Storage

Initial surface storage (%): It is an initial condition input that reflects the percentage of the maximum surface storage that has been filled at the start of the simulation. As a

starting point, we advise starting the simulation after a period of no rainfall, which causes all of the water held in the basin depression to either evaporate or penetrate. A value of 0% is reasonable in this situation (Ahbari et al., 2018).

Max surface storage (mm): It is estimated in correlation with the slope (%) of the catchment surface.

2.6.3 Transform

Mockus invented the SCS approach for the watershed lag in 1961. It encompasses a wide range of circumstances, from severely wooded watersheds with steep channels and a high percentage of runoff occurring from subsurface flow through meadows with strong surface runoff retardance, to smooth land surfaces and huge paved areas (USDA-NRCS, 2010).

Time of Concentration- The time of concentration (*Tc*) is the amount of time it takes for runoff to flow from the watershed's furthest distant point to the outlet (USDA-NRCS, 2010).

The Kirpich Equation- According to Subramanya (2013), formula relating the time of concentration of the length of travel and slope of the catchment as

$$t_c = 0.01947^{L^{0.7}} S^{-0.385} \quad [2\text{-}8]$$

t_c= time of concentration (minutes)

L = maximum length of travel of water (m), and

S = slope of catchment = $\Delta H \ / \ L$ in which

ΔH =distinction in elevation among the most remote point on the catchment and the outlet

Relation between lag and time of concentration- According to USDA-NRCS (2010), For average natural watershed conditions and approximately uniform distribution of runoff:

$$L = 0.6T_c \quad [2\text{-}9]$$

where, L= lag, h, and *Tc* = time of concentration, h.

2.6.4 Baseflow

Baseflow as defined by Hall (1968) is the proportion of flow derived from groundwater or other delayed sources Appleby (1970) expanded on the recession and baseflow problem, citing Hall's work in particular l.

Ahbari et al (2018), explained method for calculating baseflow recession as-

- Calculate *Kr* (Constant recession) using the equation,

$$k_r = t\sqrt{\frac{Q_t}{Q_0}} \qquad [2\text{-}10]$$

where, Q_t is discharge at time t after the peak; Q_0 is the initial discharge at the beginning of the event, t is the time step

2.6.5 Routing

Muskingum Routing Method-

According to the US Army Corps of Engineers (2018), the Muskingum *K* parameter is comparable to the reach's travel time. This parameter can be calculated in a variety of methods, including:

Flood wave velocity- The travel time, *T*, of a flood wave flowing through a reach may be calculated by dividing the reach length, L, by the flood wave velocity, V_w:

$$T = \frac{L}{v_w} \qquad [2\text{-}11]$$

To evaluate a flood wave velocity, various methods can be used including:

a) Manning's Equation (Manning, 1891)
b) Kleitz-Seddon Law (Seddon, 1900)

Kleitz-Seddon Law which can be written as:

$$v_w = \frac{1}{B}\frac{dQ}{dy} \qquad [2\text{-}12]$$

where B = water surface's top width and $\frac{dQ}{dy}$ = slope of the flow-stage rating curve

According to the US Army Corps of Engineers (2018), Muskingum *X* is a dimensionless coefficient having no physical meaning. This value must be set between 0.0 (the greatest attenuation) and 0.5 (the least attenuation) (no attenuation). When this option is set to 0, storage inside the reach is only computed based on outflow. When this value is set to 0.5, the inflow and outflow are given equal weight when evaluating storage within reach. As a consequence, the input hydrograph experiences no attenuation as it travels throughout the reach. In most circumstances, model calibration refines an initial estimate of 0.25.

2.7 Climate Change

Water resources are increasingly handled in situations of great unpredictability because of naturally variable rainfall, anthropogenic climate change, and changing societal needs. Hence, it is a complex undertaking to manage water supplies to suit the requirements of society, the economy, and the environment. Climate change and drought have been linked in several studies based on climate models, which forecast that the influence of climate change would lead to additional frequent and severe droughts, higher temperatures, and lower and more unpredictable precipitation levels in the Eastern Mediterranean region and Syria (De Châtel, 2014). According to climate change predictions, drought frequency may rise in the future because of climate change, and water will become scarcer in all areas. Perception of people's views of drought and climate change is crucial in achieving long-term water management (i.e., identifying behavioral impediments) (Dessai & Sims, 2010).

Climate change caused by humans may worsen water scarcity. According to the Fourth Assessment Report of the Intergovernmental Panel on Climate Change (IPCC), "it is quite probable that areas impacted by droughts and warm spells will rise" (IPCC, 2007, p. 5). According to climate change projections, the UK would suffer more frequent hot, dry summers, possibly leading to additional droughts (Hulme et al., 2002). Wade et al. (2006a, p. 14) state that a repeat of severe drought would have "much higher repercussions than droughts in the twentieth century" in terms of climate change implications. The eastern and southern portions of England may experience the most drastic variations in precipitation. The eastern and southern portions of England may

experience the most drastic variations in precipitation. By the 2080s, extreme drought might occur every two years in three in the southeast, with short-duration droughts taking place up to three times as frequently in the 2020s as they did from 1961 to 1990 (Wade et al., 2006b, p. 18).

CHAPTER 3

3 MATERIALS AND METHODS

3.1 Study Area Selection

Based on regular annual rainfall besides with some other biophysical parameters, Sri Lanka has been general into 3 major climatic zones: (1) Wet Zone in the southwestern region including Central Highlands country, (2) Dry Zone covering predominantly, northern, and eastern part of the country, and (3) Intermediate zone separating the wet and dry zones, avoidance the Central Highlands omitting in the south and the west. For this research project, two basins are selected from two different climatic zones in Sri Lanka (Figure 3-1).

- Kirindi Oya basin is selected from the dry zone and partially in the intermediate zone.
- Kelani River basin is selected from the wet zone, which is entirely located in the wet zone.

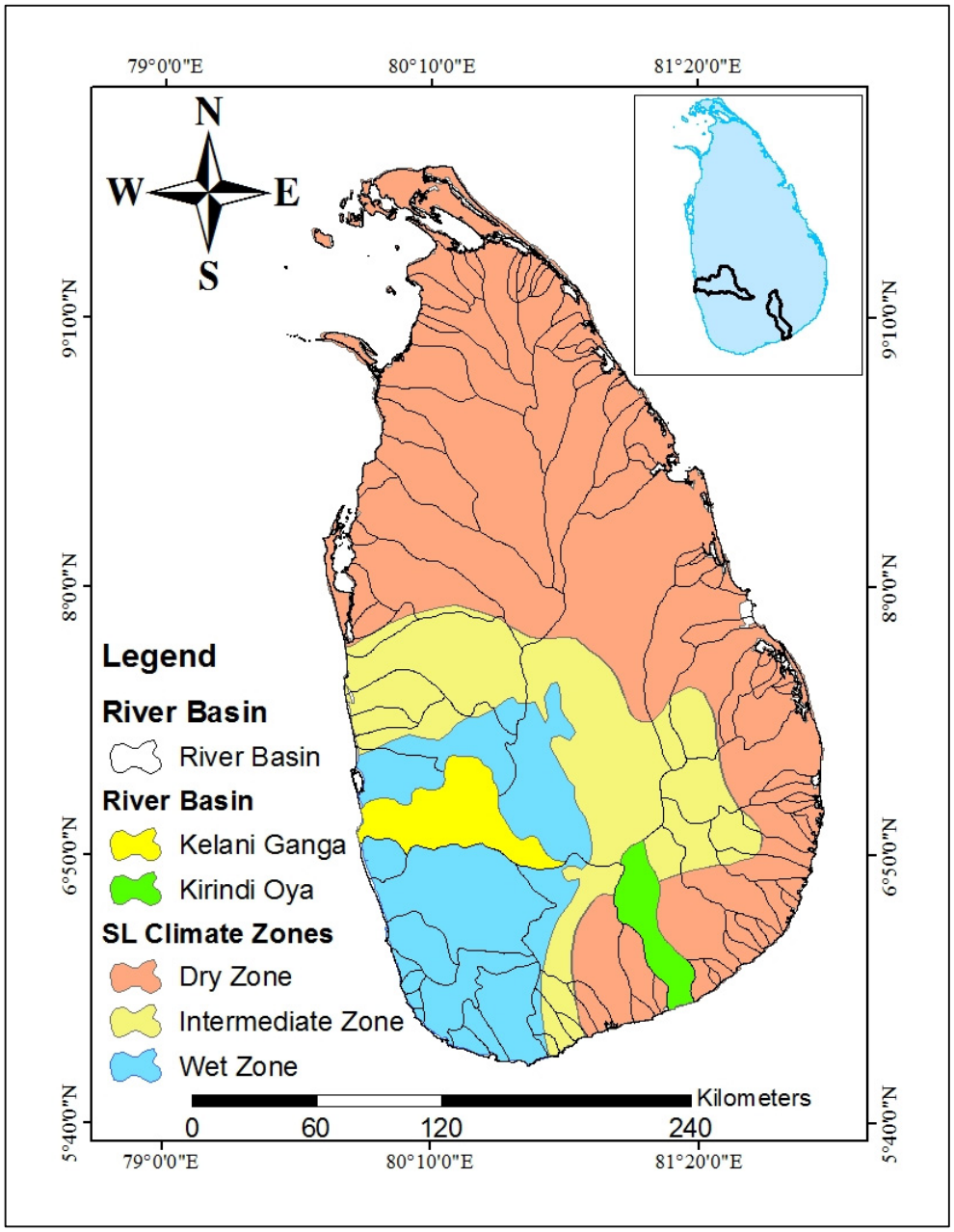

Figure 3-1: Kirindi Oya river basin from the dry zone and Kelani River basin from the wet zone

Kirindi Oya River Basin: The Kirindi Oya river basin (Figure 3-2), with a watershed area of 1,203 km^2, is located in the south-eastern region of Sri Lanka's dry zone. This river flows for a 118 km distance initiating from the medium-range hills of Sri Lanka to the Indian Ocean. Since ancient times, the basin's water resources have been utilized for agriculture (Abeysingha et al., 2020). The basin's downstream tanks, Badagiriya

Tank, Yoda Wewa, Debara Wewa, and Lunugamwehera reservoir, utilize the basin's upstream streamflow to feed irrigation and other uses.

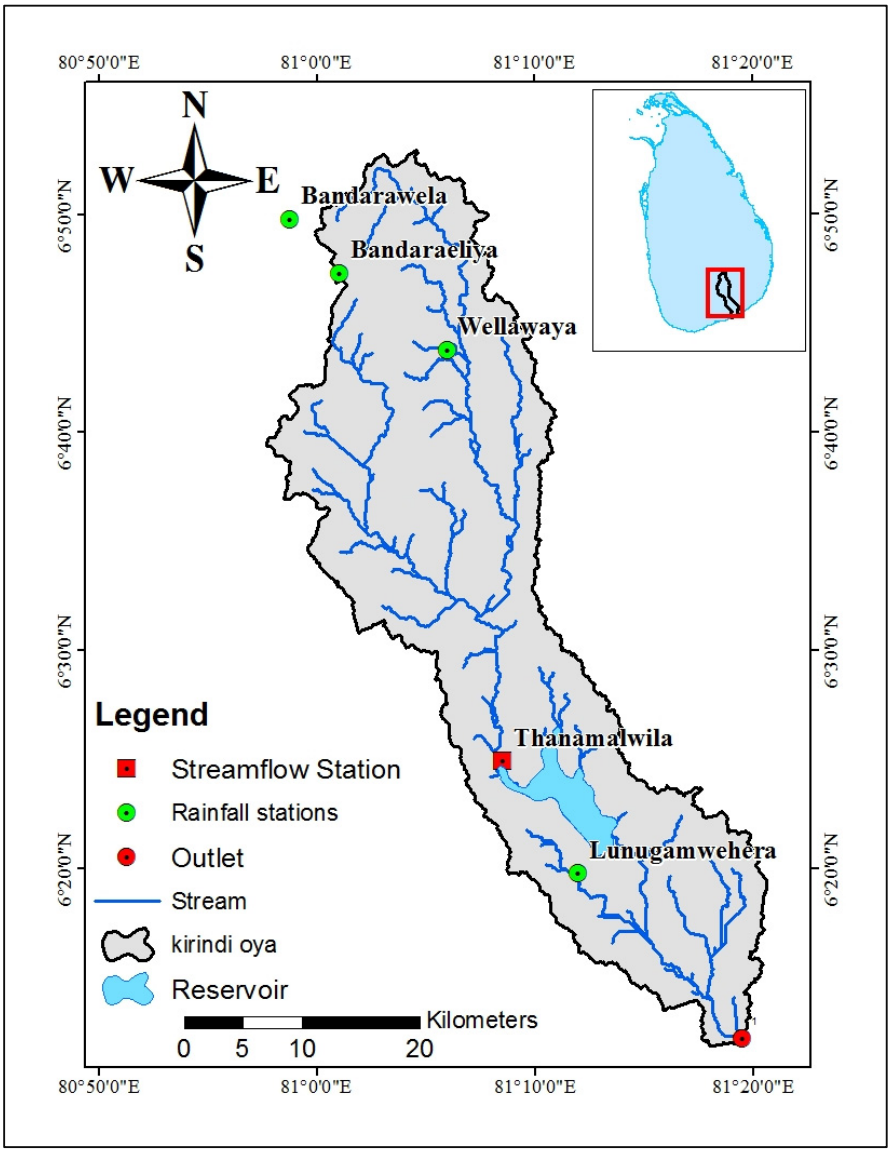

Figure 3-2: Study area of Kirindi Oya River basin including streamflow station and rainfall stations

Kelani River Basin: The Kelani River is a 145 km long river in Sri Lanka (Figure 3-3). It is the country's fourth-longest river, stretching from the Sri Pada Mountain Range to Colombo. It flows through or borders the Sri Lankan districts of Nuwara Eliya, Ratnapura, Kegalle, Gampaha, and Colombo. The Kelani River also passes

through Sri Lanka's capital, Colombo, and delivers 80 percent of the country's drinking water.

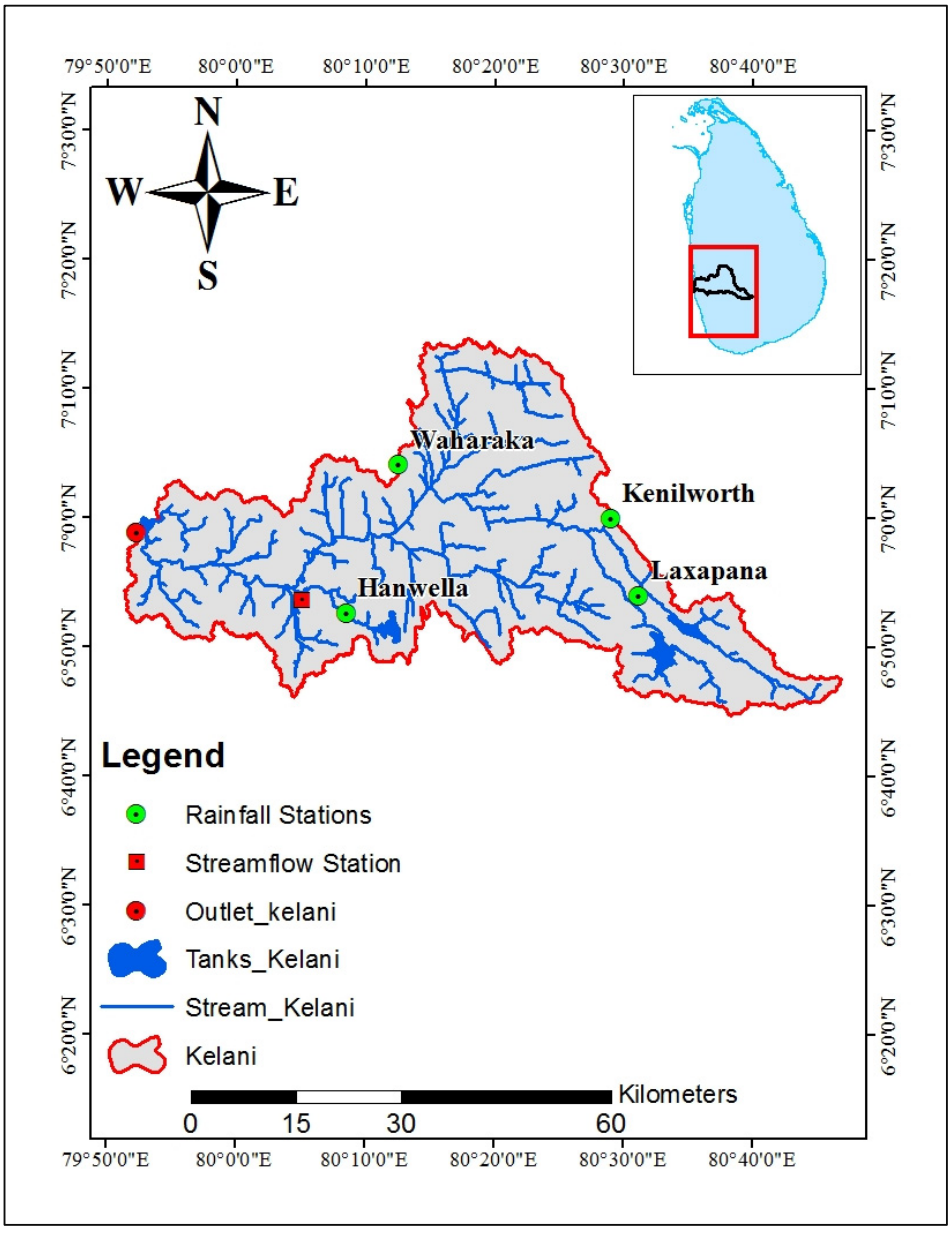

Figure 3-3: Study area of Kelani River basin including streamflow station and rainfall station

3.2 Methodology

Figure 3-4 illustrates the methodology used for this study project. Two river basins (Kirindi Oya and Kelani) are selected from two different climatic zones in Sri Lanka. After selecting river basins, various drought-related problems were identified in these basins through literature analysis, and specific objectives were created for the identified problems. Afterward, various forms of data were collected from relevant departments/organizations.

Land use and soil maps are collected from the survey department, observed precipitation is collected from the meteorological department, and observed streamflow is collected from the Irrigation Department (Table 3-1). All the collected data were checked for consistency and verified.

HEC-HMS model was set up, calibrated, and validated using the observed data. According to model parameter optimization, if it satisfies the performance, it goes to simulated runoff and if it does not satisfy the performance, it goes back to HEC-HMS data again, then it needs to improve the model's parameters. Drought indices were calculated for the present situation using the observed data, and the calibrated and validated model was used to project streamflow required for indices calculation under future scenarios. After calculating all the indices, the statistical calculation was completed, followed by the drought risk assessments for the selected river basins. According to the assessment, recommendations were given to minimize the identified drought-related problem in the river basins.

NDVI calculations were performed only for the present conditions because a reliable projection of land use is not available for future periods.

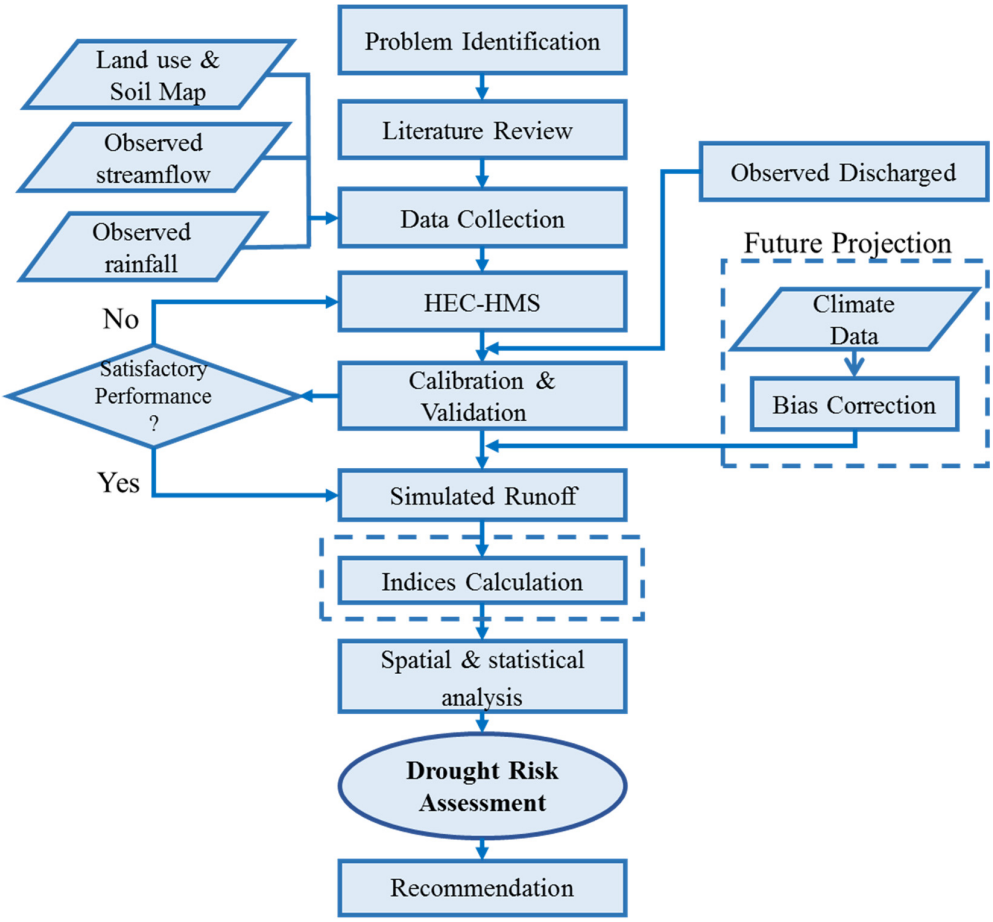

Figure 3-4: Methodology flow chart

3.2.1 Methodology for indices – reference conditions

Observed data were used for the calculation of indices in the present scenario. Standardized Precipitation Index (SPI), Streamflow Drought Index (SDI), and agricultural drought index (NDVI) were calculated from the observed rainfall, streamflow, and Landsat data, respectively. Those indices were used to assess the drought conditions of the river basin.

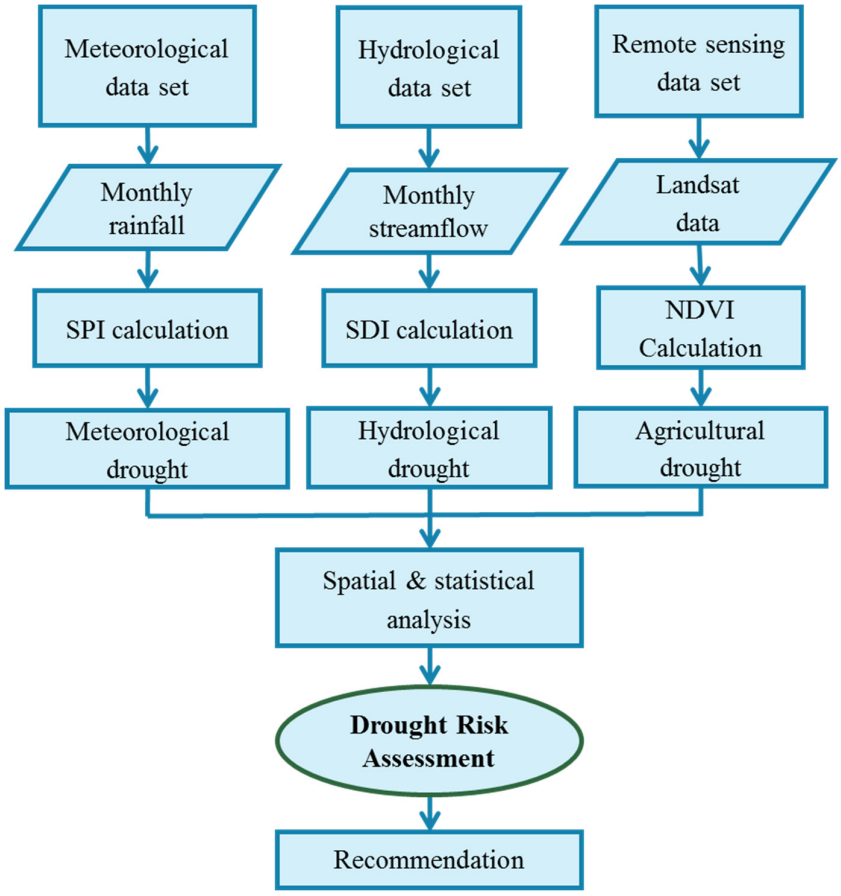

Figure 3-5: Methodology flow chart for indices calculation

3.2.2 Methodology for future indices

For future scenario model calibrated and validated data and downloaded RCM afterward bias-corrected climate data are used for calculating future drought index SPI and SDI. After that, statistical analysis is performed and go for risk assessment.

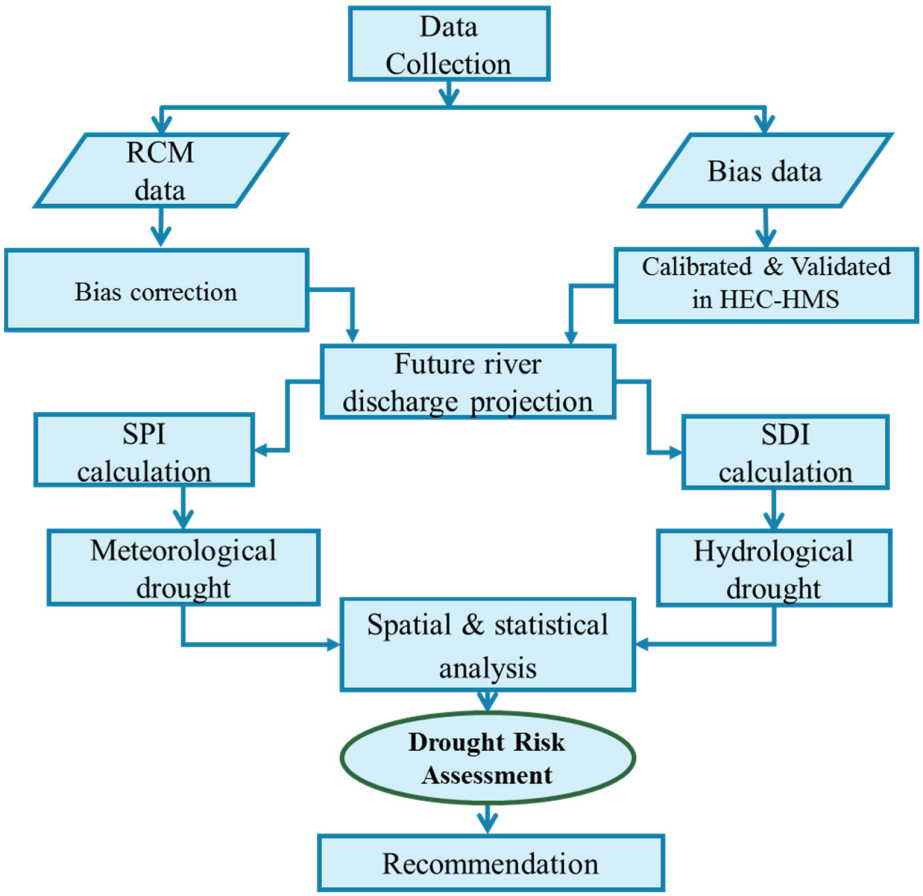

Figure 3-6: Methodology flow chart for future scenario

3.3 Data collection

The primary data sources for this study were streamflow, rainfall, land use, and climate data. Streamflow and rainfall data for the research project area were collected from the Irrigation Department and Meteorology Department respectively from 1985 to 2015. Both river data sources are mentioned in Table 3-1. For the Kirindi Oya River basin, Thanamalwila catchment's rainfall and streamflow stations and their coordinates are mentioned in Table 3-2 and Kelani river basin at Hanwella catchment's rainfall and streamflow station and their coordinates are indicated in Table 3-3 below.

Table 3-1 Data type, resolution, and data sources for this research both river basin

Data Type	Spatial/Temporal Resolution	Data Source
Digital Elevation Model	30 m	Survey Department, Sri Lanka
Rainfall Data	Daily	Meteorology Department, Sri Lanka
Streamflow	Daily	Irrigation Department, Sri Lanka
Evaporation	Monthly	Meteorology Department (Agromet Division), Sri Lanka
Land use & Soil	1:50,000	Survey Department, Sri Lanka
Climate Scenario Data (CMIP5)-RCP 8.5	RCM (25 km)	https://esgf-data.dkrz.de/search/cordex-dkrz/

Table 3-2: Streamflow and Rainfall data of Kirindi Oya river basin with the station's coordinate

Name of the Station	Latitude	Longitude	Period of Record	
			From	To
Streamflow				
Tanamalwila	6.4449° N	81.1375° E	Oct-87	Sep-15
Rainfall				
Bandaraeliya	6.7808° N	81.0220° E	Jan-85	Dec-15
Lunugamwehera	6.3308° N	81.1220° E	Jan-85	Dec-15
Wellawaya	6.7033° N	81.1137° E	Jan-85	Dec-15
Bandarawela	6.6808° N	80.0220° E	Jan-85	Dec-15

Table 3-3: Streamflow and rainfall data with their station's coordinate in Kelani River basin

Name of the Station	Latitude	Longitude	Time Period of Record	
			From	To
Streamflow				
Hanwella	6.88° N	80.12° E	Oct-85	Sep-15
Rainfall				
Hanwella	6.88° N	80.12° E	Oct-85	Sep-15
Waharaka	7.03° N	80.28° E	Jan-85	Dec-15
Kenilworth	6.08° N	80.38° E	Jan-85	Dec-15
Laxapana	6.87° N	80.63° E	Jan-85	Dec-15

3.4 Land use map

Land use maps with a resolution of 1:50,000 were obtained from the Survey Department, Sri Lanka. Homesteads/gardens, rubber cultivation, forest, tea cultivation, paddy, scrubland, stream, rock, reservoir boundary, marsh, coconut cultivation, water hole boundaries grassland, tank, unclassified region, and other cultivations were among the land-use classifications.

3.4.1 Land-use map in Kirindi Oya River Basin

The land use details of Thanamalwila catchments are presented in Table 3-4 and graphically shown in Figure 3-7. A land-use map was prepared for the Thanamalwila catchment study area.

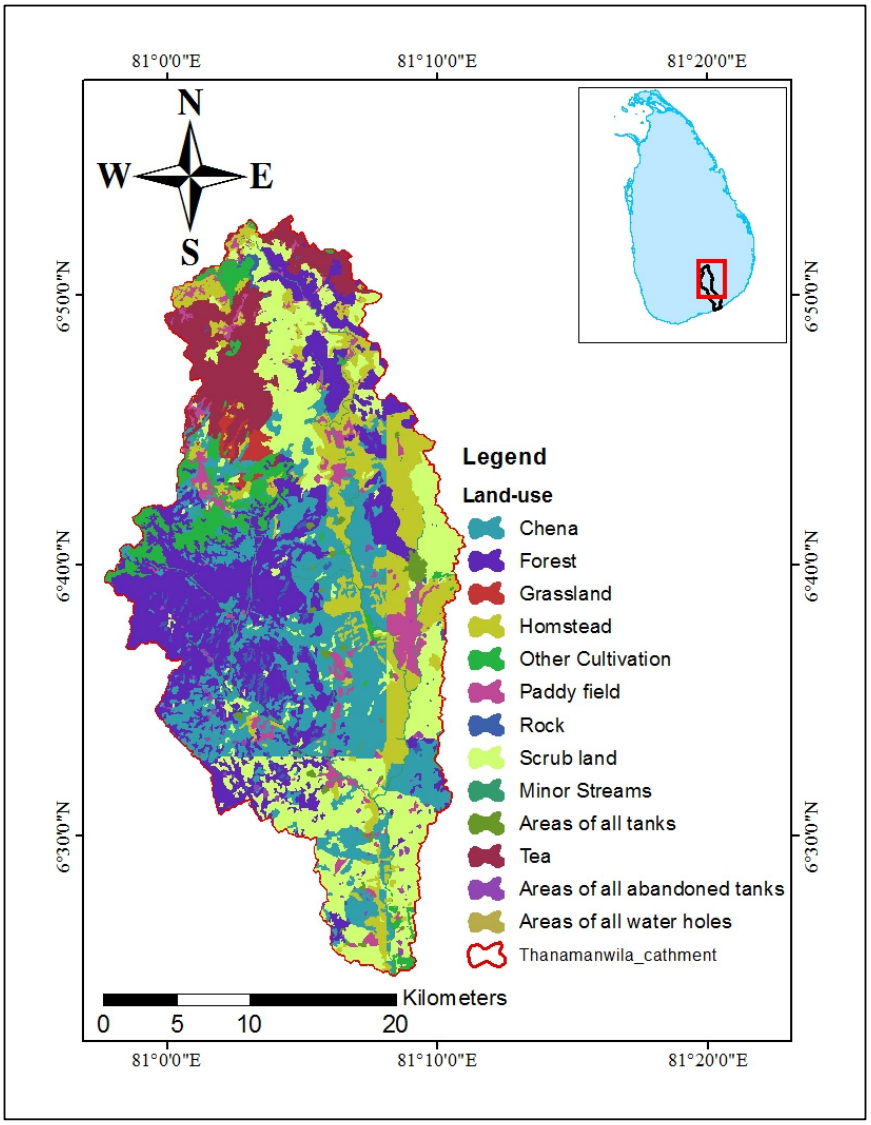

Figure 3-7 Land-use of Thanamalwila catchment in Kirindi Oya River basin

(Source: Survey Department, Sri Lanka)

Table 3-4 Land use distribution of Kirindi Oya River basin at Thanamalwila catchment

GFCODE	Land-use type	Area (km²)	Area in percentage
CHENA	Chena	154.20	21.10
FRSUA	Forest	172.67	23.63
GRSLA	Grassland	6.04	0.83
HOMSA	Homestead/Garden	95.86	13.12
OTHRA	Other Cultivation	35.68	4.88
PDDYA	Paddy field	32.31	4.42
ROCKA	Rock	9.64	1.32
SCRBA	Scrub land	147.04	20.12
STRMA	Minor Streams	11.45	1.57
TANKA	Areas of all tanks	5.69	0.78
TEAA	Tea	55.27	7.56
TNKAA	Areas of all abandoned tanks	4.87	0.67
WTRHA	Areas of all water holes	0.02	0.00

3.4.2 Land-use map in Kirindi Oya River Basin

The land use details of Hanwella catchments are presented in Table 3-5 and graphically shown in Figure 3-8. A land-use map was prepared for the Hanwella catchment study area.

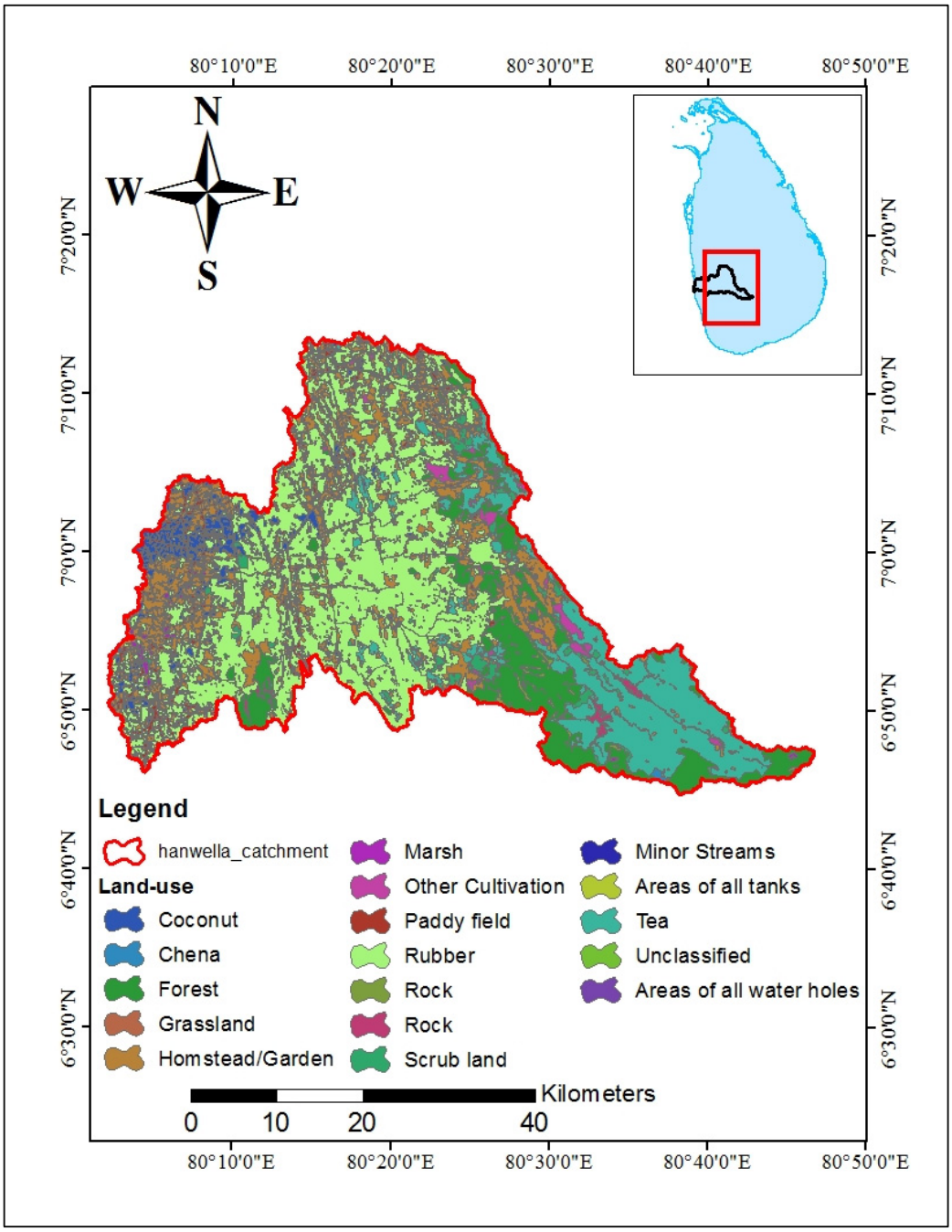

Figure 3-8 Land-use of Hanwella catchment in Kelani River basin

(Source: Survey Department, Sri Lanka)

Table 3-5 Land use distribution of Kelani River basin at Hanwella catchment

GFCODE	Land-use type	Area (km²)	Area in percentage
CCNTA	Coconut	67.97	3.49
CHENA	Chena	1.75	0.09
FRSUA	Forest	238.57	12.26
GRSLA	Grassland	0.10	0.01
HOMSA	Homestead/Garden	357.81	18.39
MRSHA	Marsh	6.98	0.36
OTHRA	Other Cultivation	23.35	1.20
PDDYA	Paddy field	111.20	5.72
RBBRA	Rubber	762.42	39.19
ROCKA	Rock	26.07	1.34
SCRBA	Scrubland	49.85	2.56
STRMA	Minor Streams	22.20	1.14
TANKA	Areas of all tanks	0.06	0.00
TEAA	Tea	276.89	14.23
UNCLA	Unclassified	0.01	0.00
WTRHA	Areas of all water holes	0.30	0.02

3.5 Missing data filling

Spatial interpolation techniques are commonly used to fill in gaps in daily precipitation series by approximating the unidentified rainfall amount to some extent using known data from nearby stations (Hasan & Croke, 2013). Normal ratio, inverse distance, correlation coefficient, arithmetic average, and other spatial interpolation methods refer to the process of predicting unknown data values for a point utilizing well-known data values from adjacent stations (Ismail & Ibrahim, 2017). Empirical approaches, statistical methods, and function fitting can all be used to estimate missing data. Multiple regression analysis is the most suited method among the traditional methods (Kashani & Dinpashoh, 2012).

Missing data is filled using Regression analysis.

Equations for different stations are

- Wellawewa

$$y = 0.3259x + 2.9943 \quad [3\text{-}1]$$

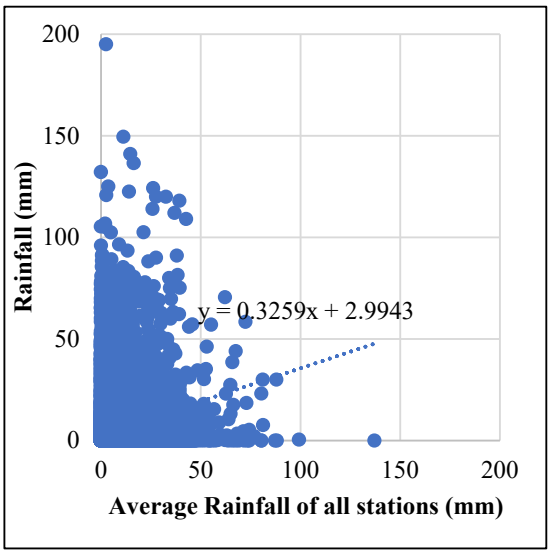

Figure 3-9 Linear regression equation for Wellawewa rainfall station

- Bandarawela

$$y = 0.9745x - 0.0485 \quad [3\text{-}2]$$

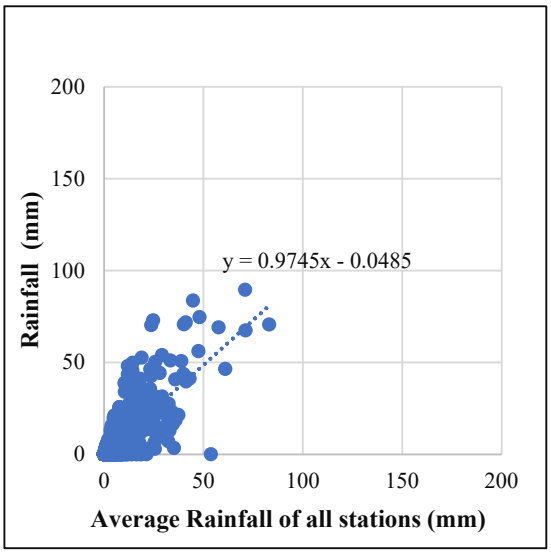

Figure 3-10 Linear regression equation for Bandarawela rainfall station

- Bandaraeliya

$$y = 1.1106x + 0.0134 \quad [3\text{-}3]$$

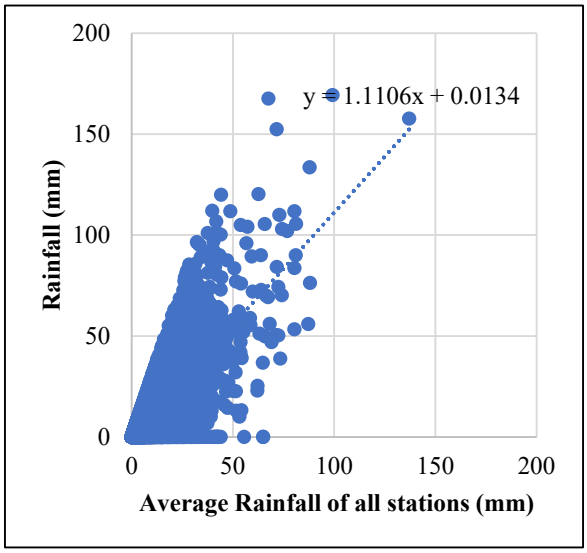

Figure 3-11 Linear regression equation for Bandaraeliya rainfall station

- Lunugamwehera

$$y = 0.89x + 0.2791 \quad [3\text{-}4]$$

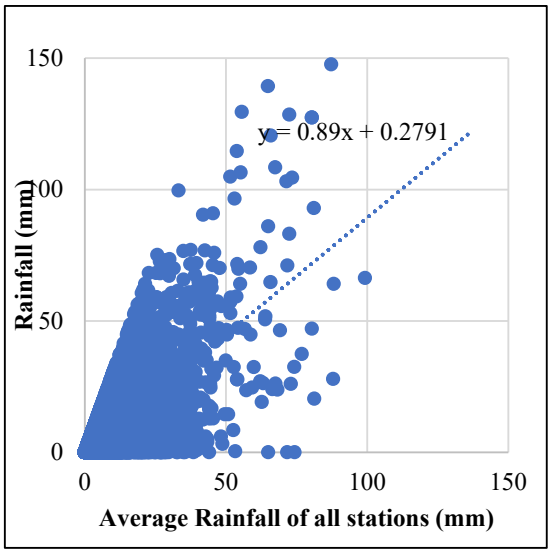

Figure 3-12 Linear regression equation for Lunugamwehara rainfall station

For the missing data filling these equations are used from Equation [3-1] to Equation [3-4]. Those equations came from the scatter plot of all the different rainfall stations which are showing Figure 3-9 to Figure 3-12.

3.6 Data Analysis of Kirindi Oya River Basin

Daily data on streamflow, rainfall, and evaporation from 1985 to 2015 were acquired from the Irrigation and Meteorological departments. Inconsistencies in the rainfall, streamflow, and evaporation data were examined, including visual and consistency verifications. Following that, yearly and monthly measurements were taken over the entire watershed up to the measuring streamflow stations in both river basins. Thanamalwila and Hanwella streamflow measuring stations were considered for Kirindi Oya and Kelani River Basin, respectively.

Inconsistencies and non-homogeneities in hydrological and meteorological data series might be identified using statistical data tests that discover trends and change points. For proper time series analysis, inconsistency, which indicates systematic errors during recording, and non-homogeneity, which results from either natural or man-made alterations to the gauging environment, are both significant. It has also been determined that statistical tests, as well as physical or historical proof and justifications from metadata, must be included for a very comprehensive study (Wijesekera & Perera, 2012).

Seasonal Analysis

The topography of the nation, as well as the regional scale wind regimes of the Southwest and Northeast monsoons, determine the climate of Sri Lanka. The climate of Sri Lanka may be characterized into four seasons -

- Second Inter Monsoon – October and November
- Northeast Monsoon – December to February
- First Inter Monsoon – March and April
- Southwest Monsoon – May to September

3.6.1 Thanamalwila Streamflow Gauging Station

Thanamalwila streamflow gauging station is only considering the streamflow station in the Kirindi Oya river basin for this study.

In the Thanamalwila catchment, for the selected data period (1987-2015) and four monsoon variations are shown in Figure 3-13. The monthly average streamflow for four different monsoons is Second Inter monsoon- 2 m^3/s but 1997/98 year shown 4.75 m^3/s value, Northeast monsoon- 26 m^3/s, First Inter monsoon- 22 m^3/s and Southwest monsoon- 38 m^3/s.

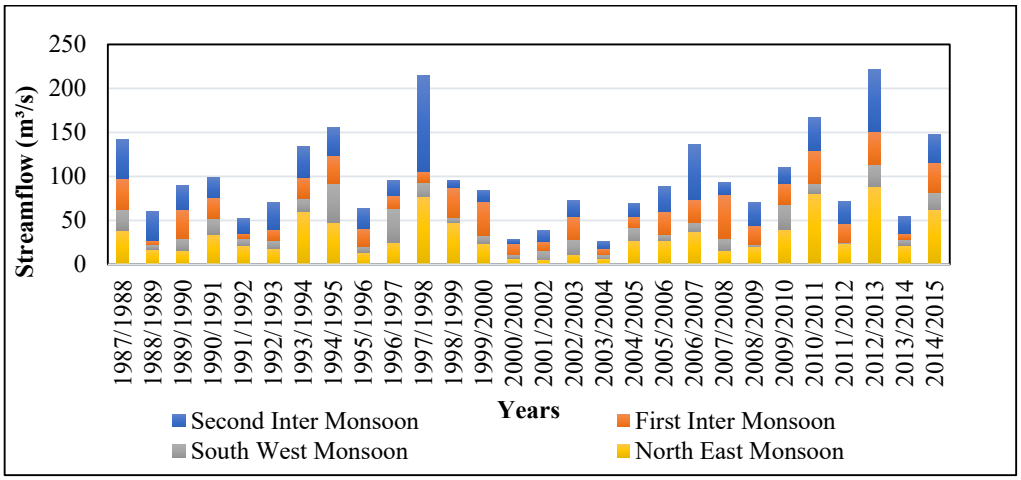

Figure 3-13 Streamflow seasonal variation of Thanamalwila streamflow gauging stations including four monsoon seasons in Sri Lanka

In the Thanamalwila catchment, for the selected data period (1987-2015), monthly maximum, minimum, and mean are shown in Figure 3-14 by box plot. The monthly mean of Streamflow varies from 0.5 ~ 17 m^3/s, the minimum streamflow varies from 0 ~ 4 m^3/s and the maximum streamflow varies from 2 ~ 82 m^3/s.

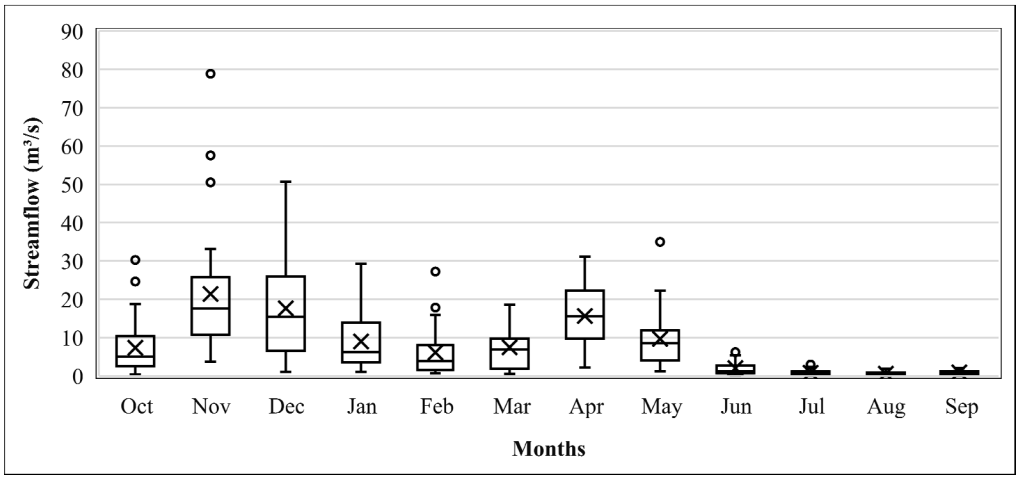

Figure 3-14 Streamflow variation of Thanamalwila streamflow gauging stations according to hydrological year (1987/88 – 2014/15)

3.6.2 Wellawewa Rainfall station

From data analysis of Wellawewa rainfall station, for the selected data period (1985-2015), four monsoon variations are shown in Figure 3-15. The monthly average rainfall for four different monsoons is Inter monsoon- 658 mm, Northeast monsoon-406 mm, First Inter monsoon 436 mm, and Southwest monsoon 297 mm.

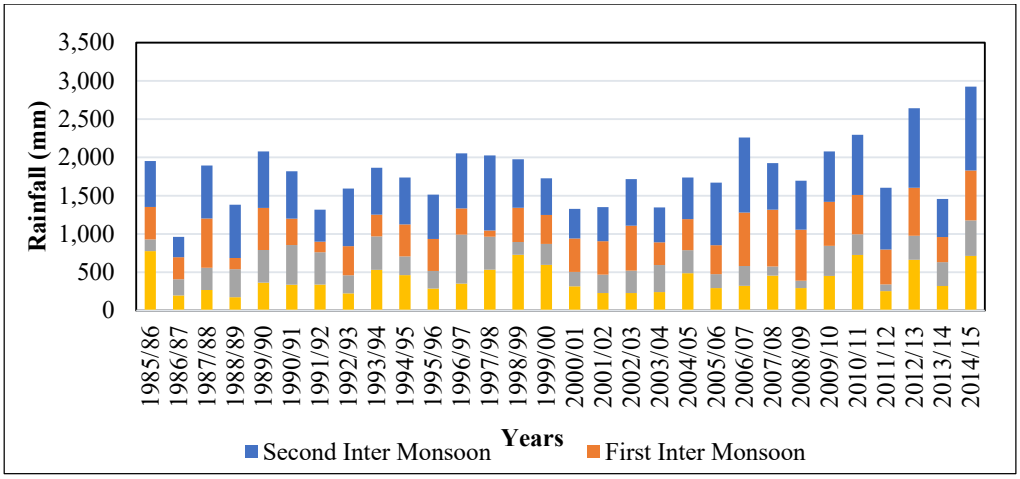

Figure 3-15 Rainfall seasonal variation of Wellawewa rainfall stations including four monsoon seasons in Sri Lanka

In the Thanamalwila catchment, in Wellawewa rainfall station for the selected data period (1985-2015), monthly maximum, minimum, and mean are shown in Figure 3-16 by box plot. The monthly mean of rainfall varies from 21 ~ 373 mm, the minimum streamflow varies from 0 ~ 109 mm and the maximum streamflow varies from 85 ~ 688 mm.

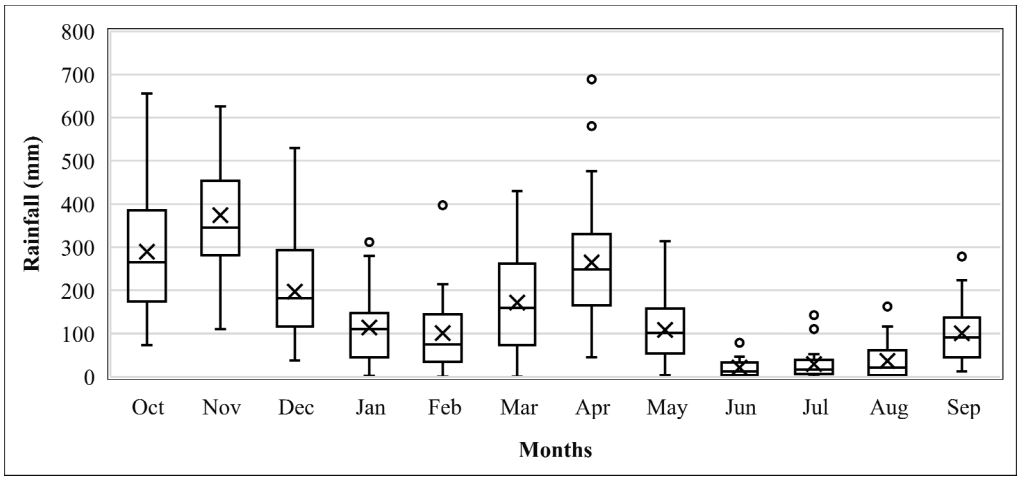

Figure 3-16 Rainfall variation of Wellawewa rainfall station according to hydrological year (1985/86 – 2014/15)

In Thanamalwila catchment, Wellawewa rainfall station and Thanamalwila streamflow station's yearly total are shown in Figure 3-17 for visual checking. Rainfall data does not match the streamflow pattern. 1989/90 rainfall is high, but streamflow is not as high as rainfall.

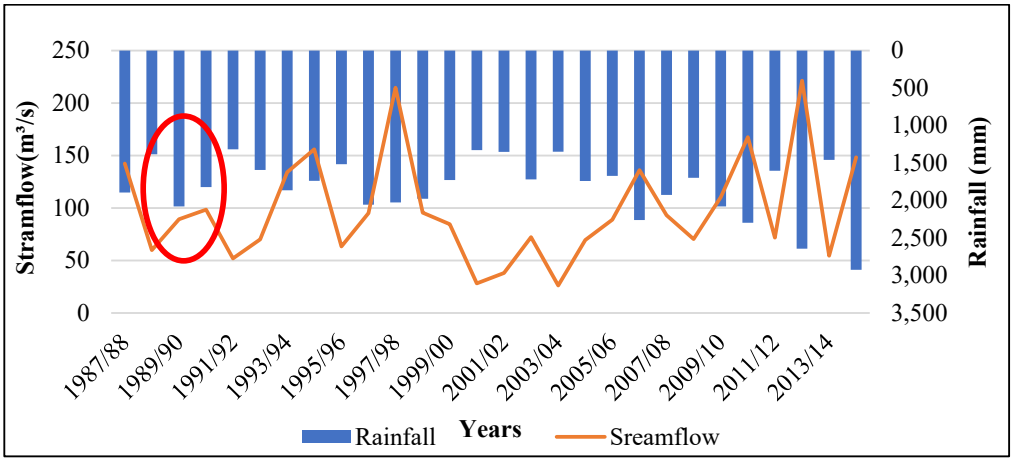

Figure 3-17 Yearly streamflow vs yearly rainfall of wellawewa station in the Kirindi Oya River basin

3.6.3 Bandarawela Rainfall Station

From data analysis of Bandarawela rainfall station, for the selected data period (1985-2015), four monsoon variations are shown in Figure 3-18. The monthly average rainfall for four different monsoons is Inter monsoon- 497 mm, Northeast monsoon-378 mm, First Inter monsoon 290 mm, and Southwest monsoon 436 mm.

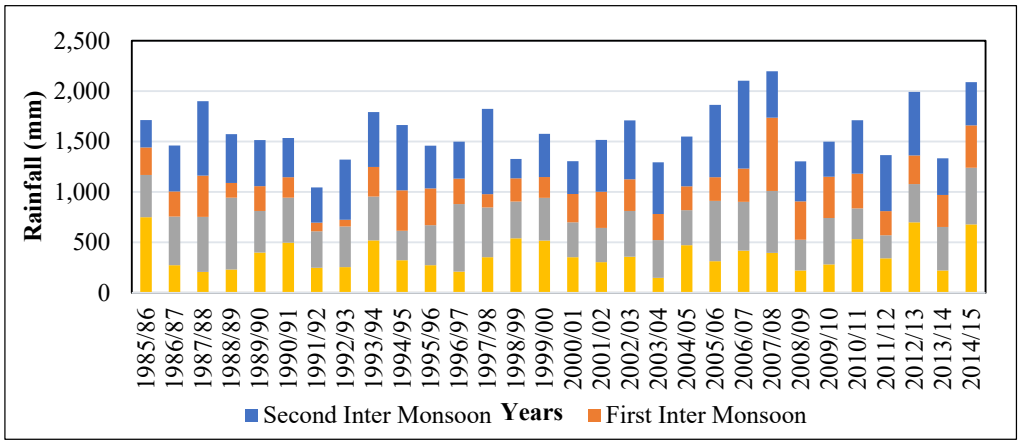

Figure 3-18 Rainfall seasonal variation of Bandarawela rainfall stations including four monsoon seasons in Sri Lanka

In the Thanamalwila catchment, in Bandarawela rainfall station for the selected data period (1985-2015), monthly maximum, minimum, and mean are shown in Figure 3-16 by box plot. The monthly mean of rainfall varies from 54 ~ 256 mm, the minimum streamflow varies from 0 ~ 32 mm and the maximum streamflow varies from 183 ~ 536 mm.

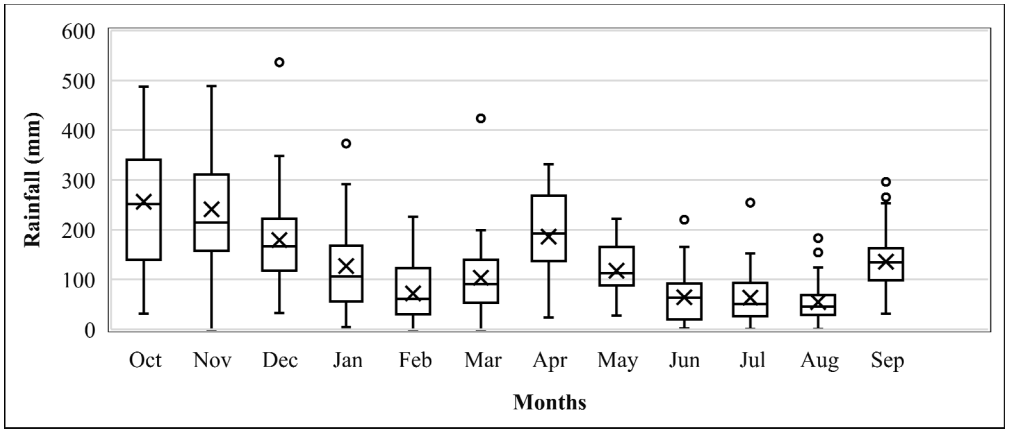

Figure 3-19 Streamflow variation of Bandarawela rainfall station according to hydrological year (1985/86 – 2014/15)

In Thanamalwila catchment, Bandarawela rainfall station and Thanamalwila streamflow station's yearly total are shown in Figure 3-20 for visual checking. Rainfall data does not match the streamflow pattern. 2007/08 rainfall is high, but streamflow is not as high as rainfall.

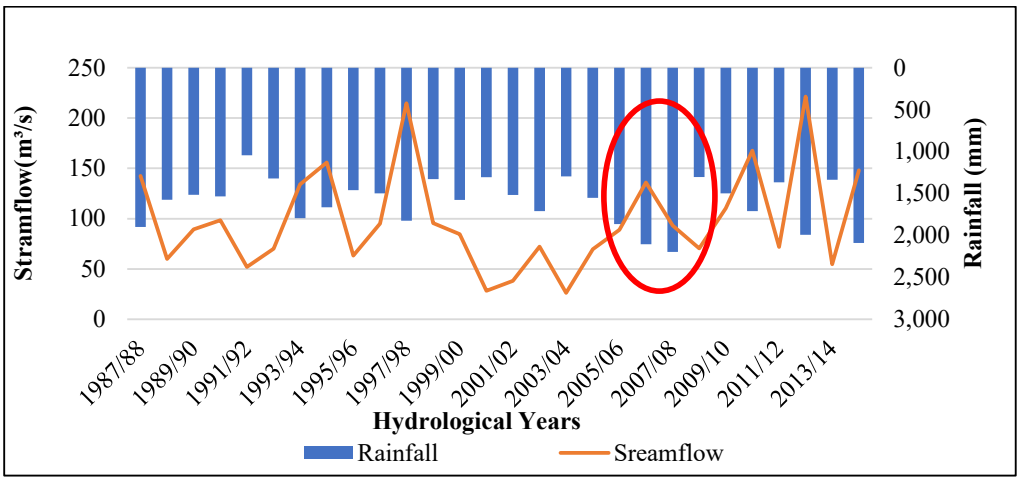

Figure 3-20 Yearly streamflow vs yearly rainfall of Bandarawela station in the Kirindi Oya River basin

3.6.4 Bandaraeliya Rainfall Station

From data analysis of Bandaraeliya rainfall station, for the selected data period (1985-2015), four monsoon variations are shown in Figure 3-18. The monthly average rainfall for four different monsoons is Inter monsoon- 708 mm, Northeast monsoon- 505 mm, First Inter monsoon 494 mm, and Southwest monsoon 481 mm.

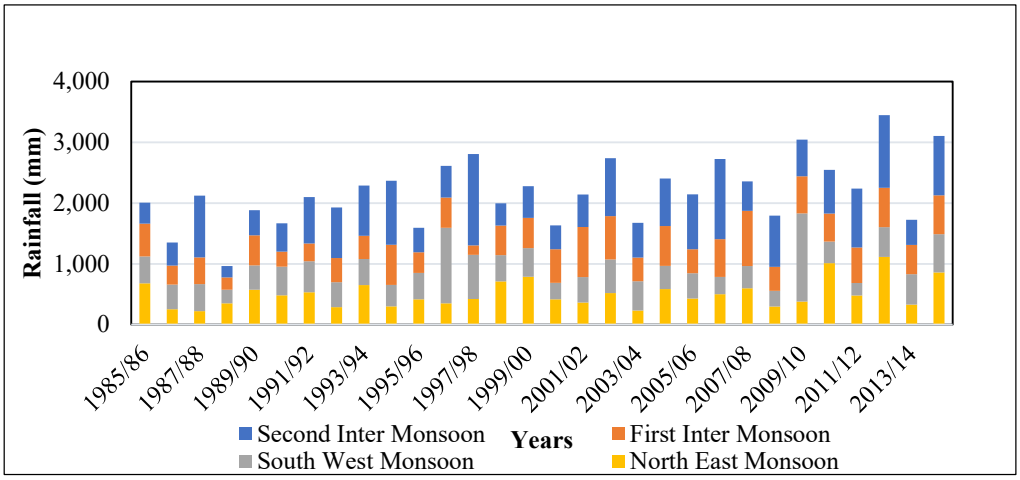

Figure 3-21 Rainfall seasonal variation of Bandaraeliya rainfall stations including four monsoon seasons in Sri Lanka

In the Thanamalwila catchment, in Bandaraeliya rainfall station for the selected data period (1985-2015), monthly maximum, minimum, and mean are shown in Figure 3-22 by box plot. The monthly mean of rainfall varies from 42 ~ 365 mm, the minimum streamflow varies from 0 ~ 70 mm and the maximum streamflow varies from 222 ~ 772 mm.

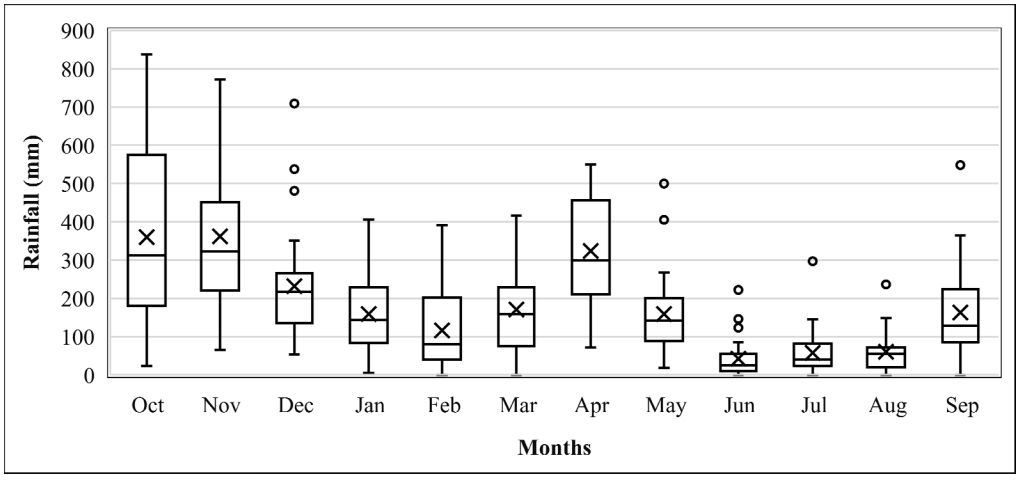

Figure 3-22 Rainfall variation of Bandaraeliya rainfall station according to hydrological year (1985/86 – 2014/15)

In Thanamalwila catchment, Bandaraeliya rainfall station and Thanamalwila streamflow station's yearly total are shown in Figure 3-23 for visual checking. Rainfall data does not match the streamflow pattern. 2003/04 rainfall is high, but streamflow is not as high as rainfall.

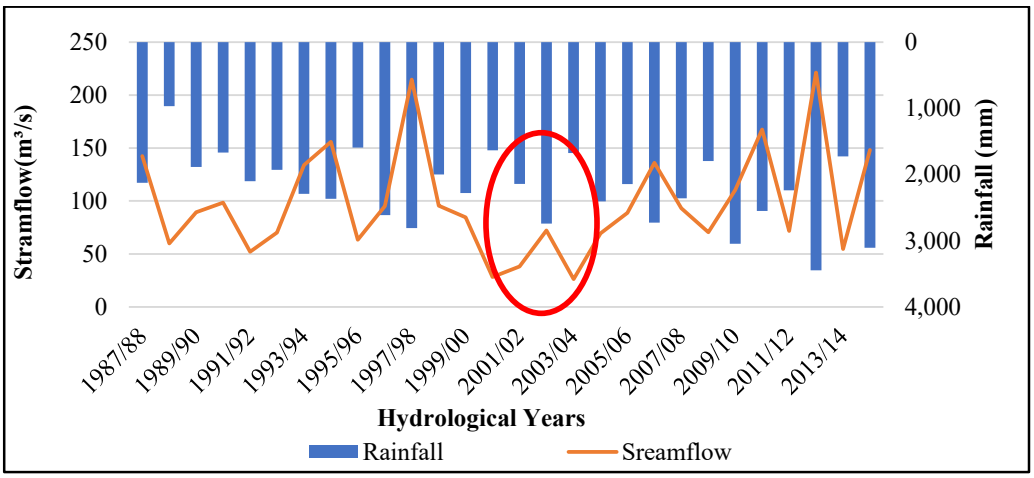

Figure 3-23 Yearly streamflow vs yearly rainfall of Bandaraeliya station in the Kirindi Oya River basin

3.6.5 Lunugamwehera Rainfall Station

From data analysis of the Lunugamwehera rainfall station, for the selected data period (1985-2015), four monsoon variations are shown in Figure 3-24. The monthly average rainfall for four different monsoons is Inter monsoon- 448 mm, Northeast monsoon- 335 mm, First Inter monsoon 215 mm, and Southwest monsoon 210 mm.

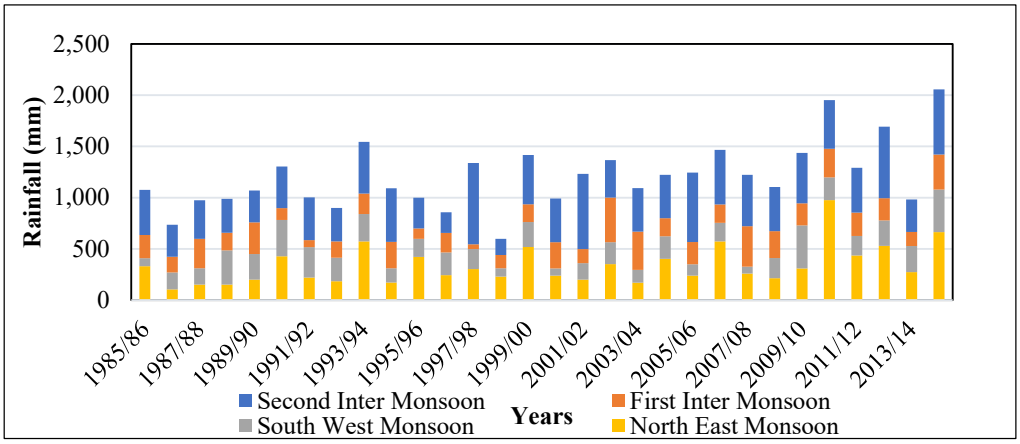

Figure 3-24 Rainfall seasonal variation of Lunugamwehera rainfall stations including four monsoon seasons in Sri Lanka

In the Thanamalwila catchment, in the Lunugamwehera rainfall station for the selected data period (1985-2015), monthly maximum, minimum, and mean are shown in Figure 3-25 by box plot. The monthly mean of rainfall varies from 23 ~ 267 mm, the minimum streamflow varies from 0 ~ 106 mm and the maximum streamflow varies from 90 ~ 558 mm.

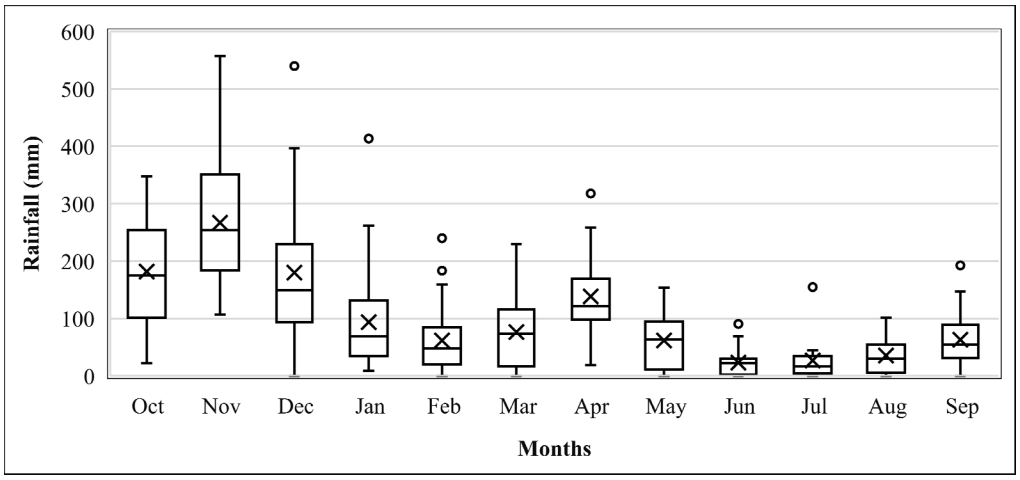

Figure 3-25 Rainfall variation of Lunugamwehera rainfall station according to hydrological year (1985/86 – 2014/15)

In Thanamalwila catchment, Lunugamwehera rainfall station and Thanamalwila streamflow station's yearly total are shown in Figure 3-23 for visual checking. Rainfall data does not match the streamflow pattern. 2000 - 2006 rainfall is high, but streamflow is not as high as rainfall.

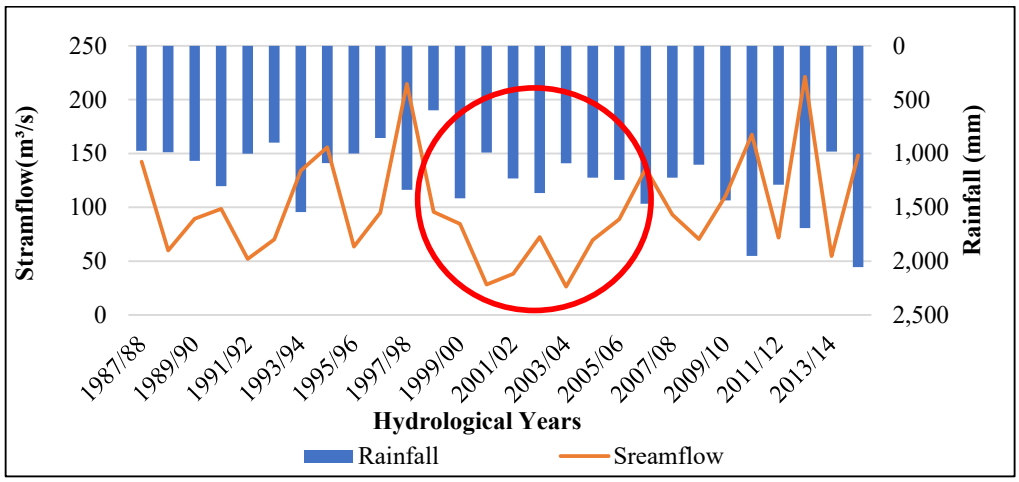

Figure 3-26 Yearly streamflow vs yearly rainfall of Lunugamwehera station in the Kirindi Oya River basin

3.7 Data Analysis of Kelani River Basin

The Kelani River basin also considers four rainfall stations, and one streamflow station and these stations' locations are described in the 3.3 section.

3.7.1 Hanwella Streamflow Station

In the Hanwella catchment, for the selected data period (1985-2015) and four monsoon variations are shown in Figure 3-27. The monthly average streamflow for four different monsoons is Second Inter monsoon- 411 m^3/s, Northeast monsoon- 169 m^3/s, First Inter monsoon- 139 m^3/s, and Southwest monsoon- 676 m^3/s.

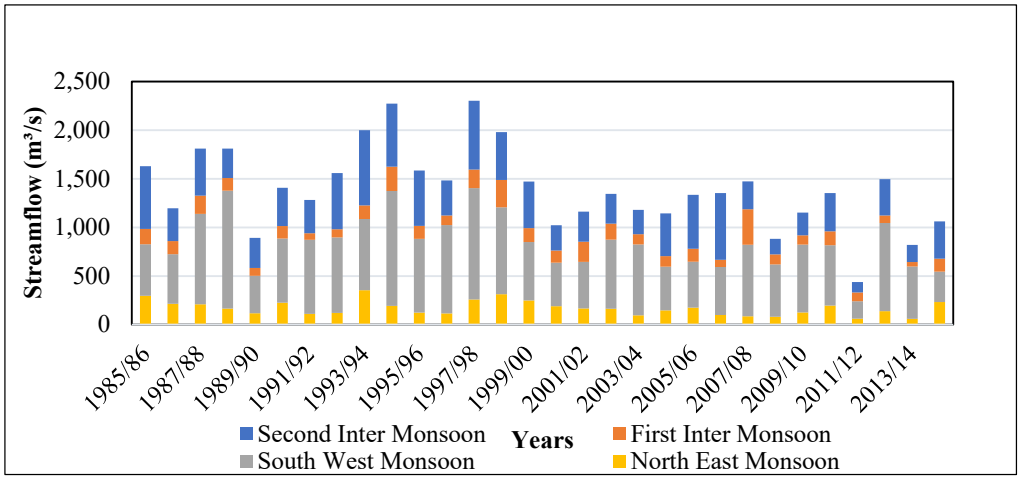

Figure 3-27 Streamflow seasonal variation of Hanwella streamflow gauging stations including four monsoon seasons in Sri Lanka

In the Hanwella catchment, for the selected data period (1985-2015), monthly maximum, minimum, and mean are shown in Figure 3-28 by box plot. The monthly mean of Streamflow varies from 40 ~ 209 m³/s, the minimum streamflow varies from 15 ~ 57 m³/s and maximum streamflow varies from 85 ~ 442 m³/s.

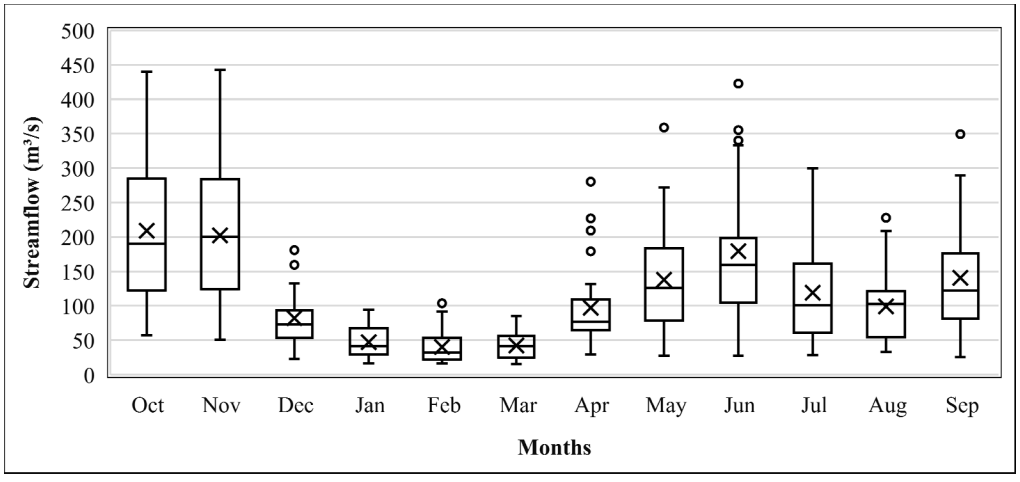

Figure 3-28 Streamflow variation of Hanwella streamflow gauging stations according to hydrological year (1987/88 – 2014/15)

3.7.2 Hanwella Rainfall Station

From data analysis of Hanwella rainfall station, for the selected data period (1985-2015), four monsoon variations are shown in Figure 3-29. The monthly average rainfall for four different monsoons is Inter monsoon- 839 mm, Northeast monsoon- 427 mm, First Inter monsoon 510 mm, and Southwest monsoon 1,312 mm.

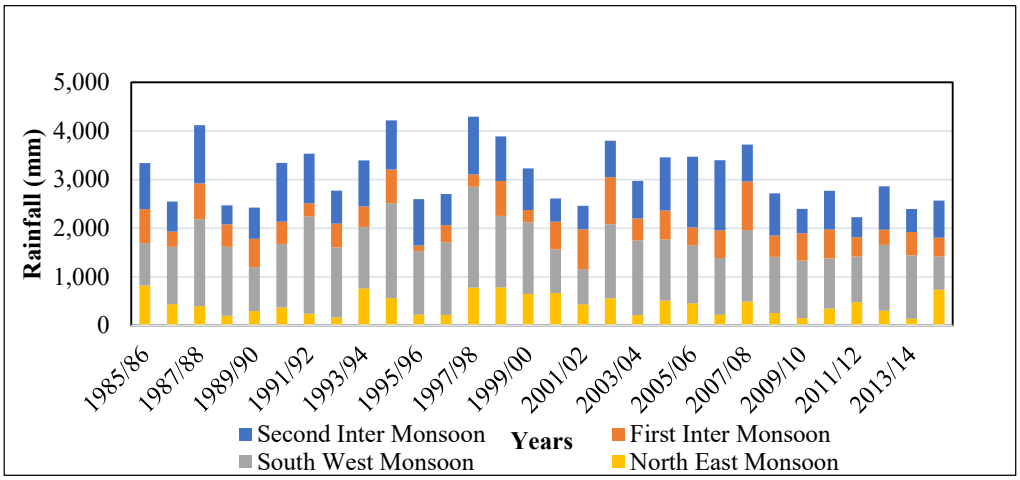

Figure 3-29 Rainfall seasonal variation of Hanwella rainfall stations including four monsoon seasons in Sri Lanka

In the Hanwella catchment, in Hanwella rainfall station for the selected data period (1985-2015), monthly maximum, minimum, and mean are shown in Figure 3-31 by box plot. The monthly mean of rainfall varies from 104 ~ 456 mm, the minimum streamflow varies from 0 ~ 112 mm and the maximum streamflow varies from 315 ~ 847 mm.

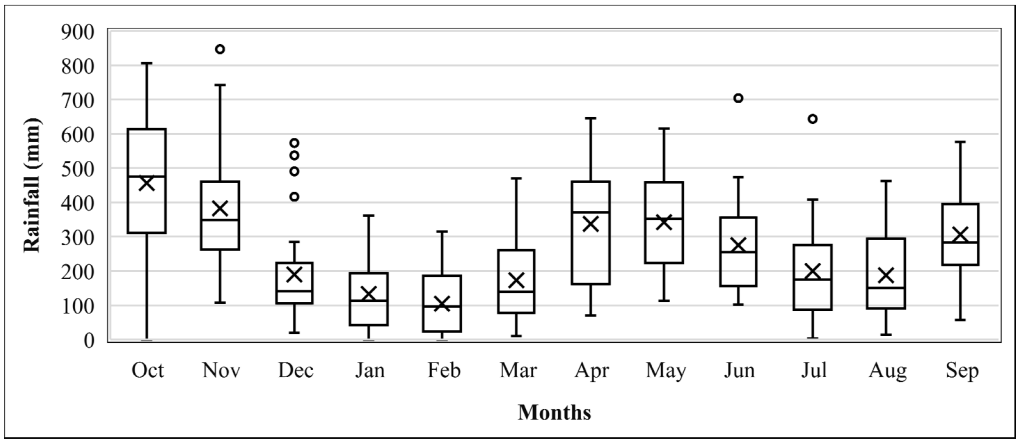

Figure 3-30 Streamflow variation of Hanwella rainfall station according to hydrological year (1985/86 – 2014/15)

In the Hanwella catchment, the Hanwella rainfall station and Hanwella streamflow station's yearly total are shown in Figure 3-31 for visual checking. Rainfall data are matched with streamflow patterns almost every year.

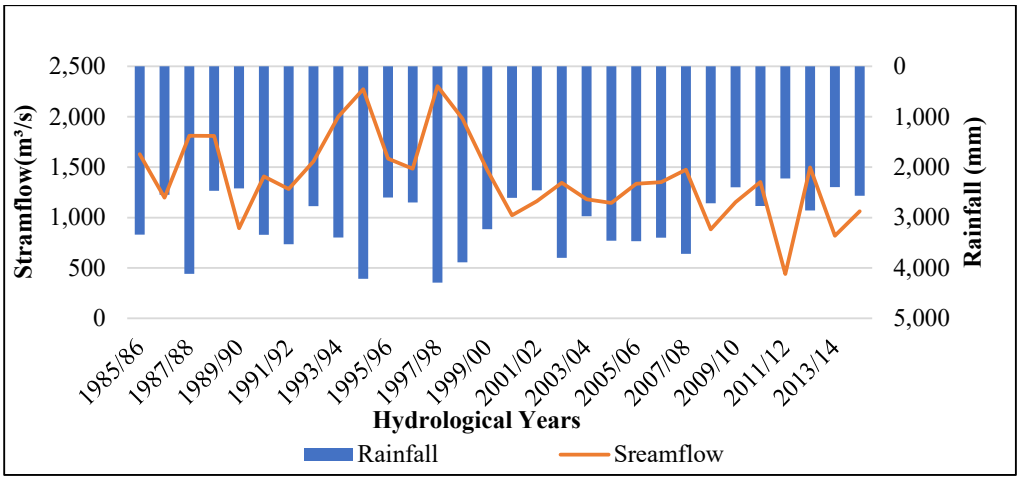

Figure 3-31 Yearly streamflow vs yearly rainfall of Hanwella station in the Kelani River basin

3.7.3 Waharaka Rainfall Station

From data analysis of Waharaka rainfall station, for the selected data period (1985-2015), four monsoon variations are shown in Figure 3-32. The monthly average rainfall for four different monsoons is Inter monsoon- 588 mm, Northeast monsoon-345 mm, First Inter monsoon 367 mm, and Southwest monsoon 685 mm.

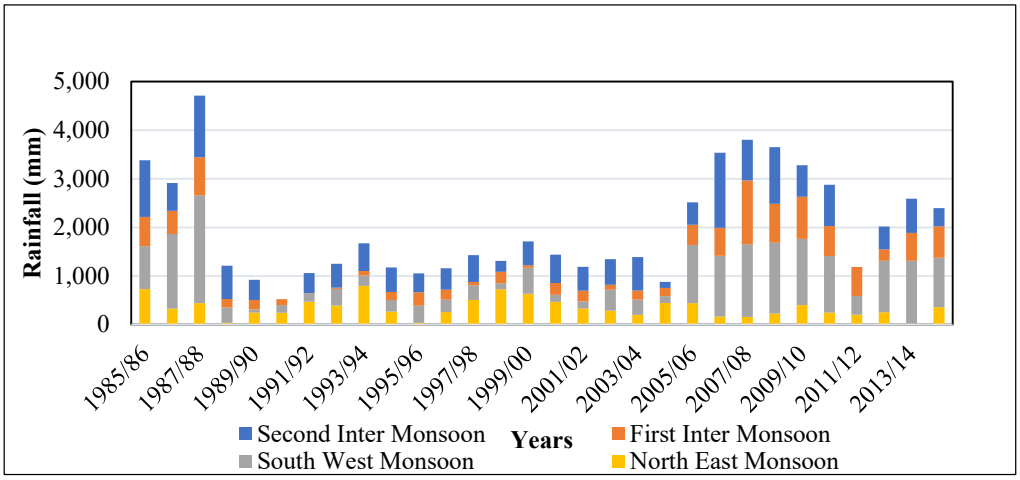

Figure 3-32 Rainfall seasonal variation of Waharaka rainfall stations including four monsoon seasons in Sri Lanka

In the Hanwella catchment, in Hanwella rainfall station for the selected data period (1985-2015), monthly maximum, minimum, and mean are shown in Figure 3-33 by box plot. The monthly mean of rainfall varies from 76 ~ 306 mm, the minimum streamflow varies from 0 ~ 180 mm and the maximum streamflow varies from 226 ~ 847 mm.

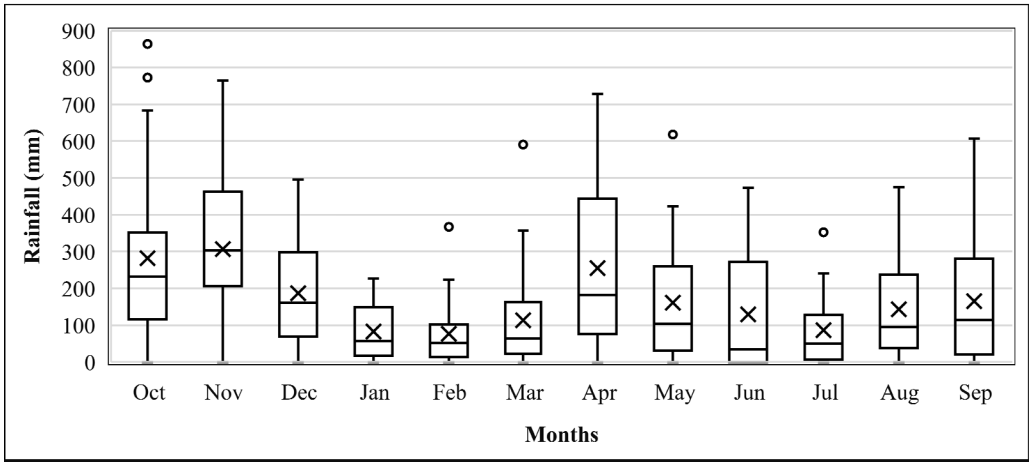

Figure 3-33 Rainfall variation of Waharaka rainfall station according to hydrological year (1985/86 – 2014/15)

In the Hanwella catchment, Waharaka rainfall station and Hanwella streamflow station's yearly total are shown in Figure 3-34 for visual checking. Rainfall data are not matched with streamflow pattern in 1987/88 as per graph rainfall is high but streamflow is not high as rainfall.

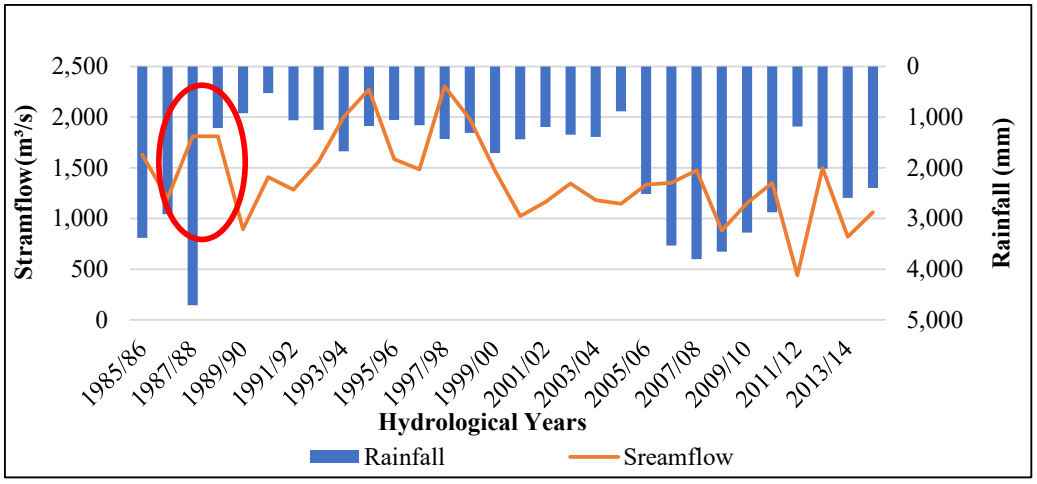

Figure 3-34 Yearly streamflow vs yearly rainfall of Waharaka station in the Kelani River basin

3.7.4 Kenilworth Rainfall Station

From data analysis of Kenilworth rainfall station, for the selected data period (1985-2015), four monsoon variations are shown in Figure 3-35. The monthly average rainfall for four different monsoons is Inter monsoon- 1,216 mm, Northeast monsoon-455 mm, First Inter monsoon 638 mm, and Southwest monsoon 3,590 mm.

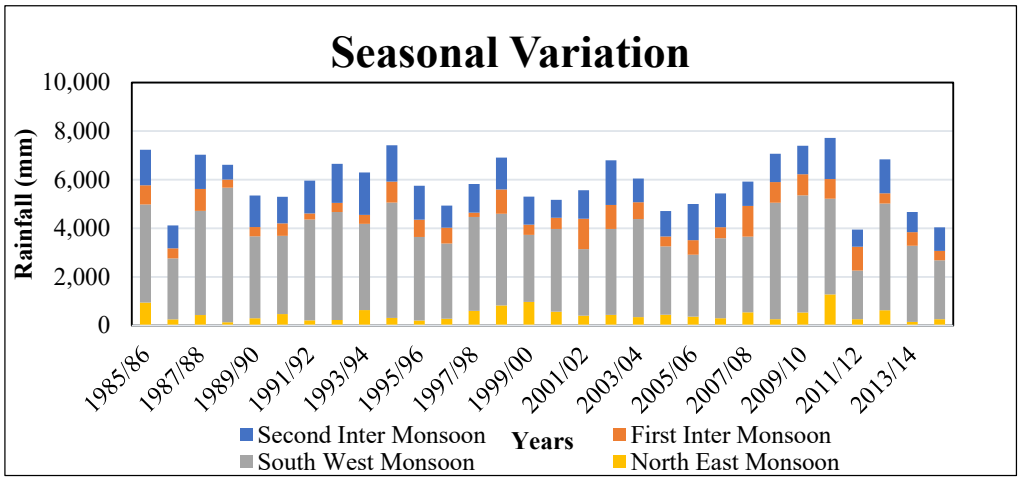

Figure 3-35 Rainfall seasonal variation of Kenilworth rainfall stations including four monsoon seasons in Sri Lanka

In the Hanwella catchment, in Kenilworth rainfall station for the selected data period (1985-2015), monthly maximum, minimum, and mean are shown in Figure 3-36 by box plot. The monthly mean of rainfall varies from 123 ~ 850 mm, the minimum streamflow varies from 0 ~ 346 mm and the maximum streamflow varies from 410 ~ 1,557 mm.

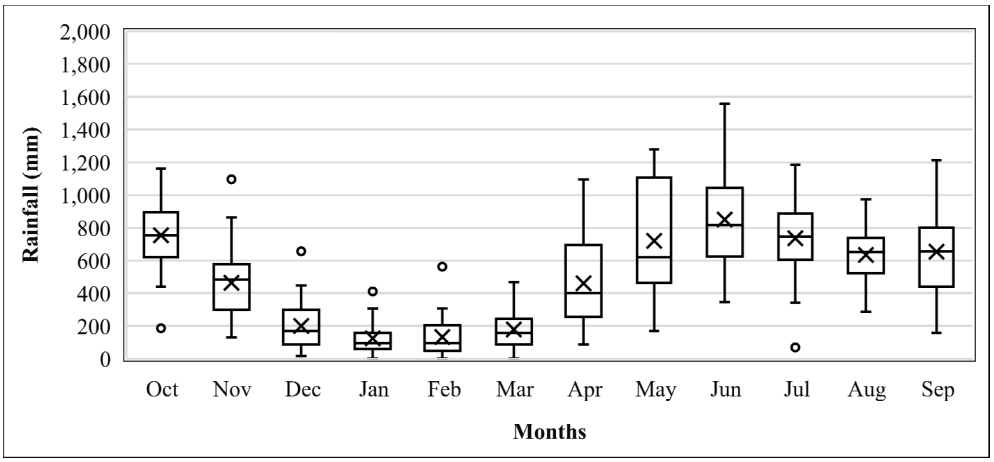

Figure 3-36 Rainfall variation of Kenilworth rainfall station according to hydrological year (1985/86 – 2014/15)

In Hanwella catchment, Kenilworth rainfall station and Hanwella streamflow station's yearly total are shown in Figure 3-37 for visual checking. Rainfall data are matched with streamflow patterns almost every year but 1999/2000 as per graph rainfall peak and streamflow peaks are not matching.

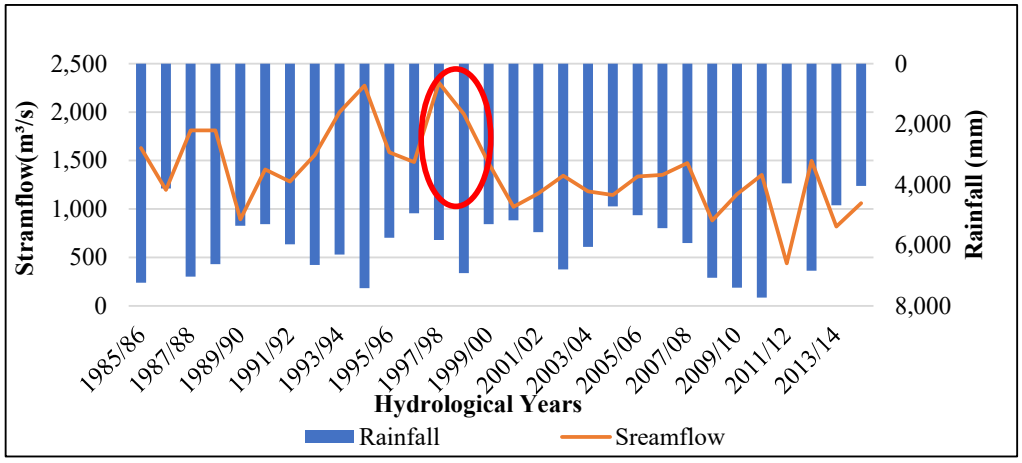

Figure 3-37 Yearly streamflow vs yearly rainfall of Kenilworth station in the Kelani River basin

3.7.5 Laxapana Rainfall Station

From data analysis of the Laxapana rainfall station, for the selected data period (1985-2015), four monsoon variations are shown in Figure 3-38. The monthly average rainfall for four different monsoons is Inter monsoon- 952 mm, Northeast monsoon-343 mm, First Inter monsoon 492 mm, and Southwest monsoon 2,741 mm.

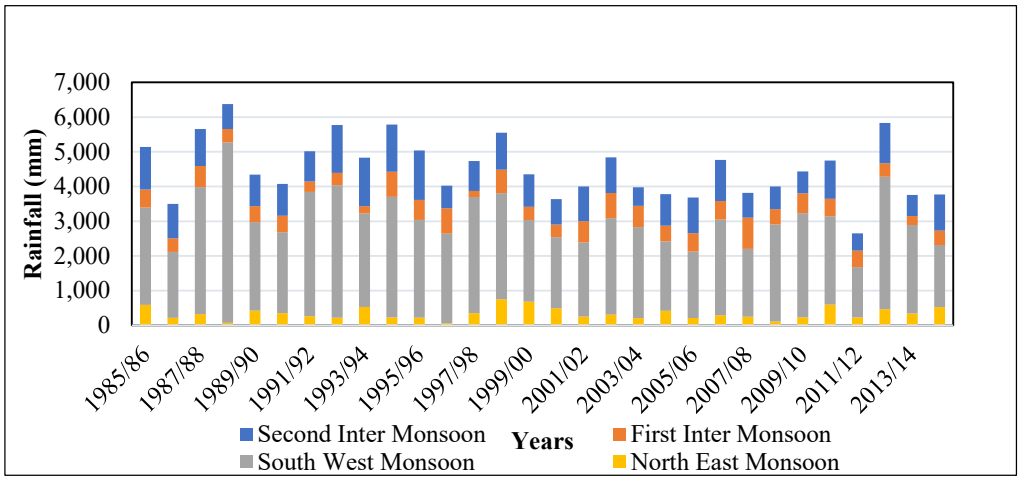

Figure 3-38 Rainfall seasonal variation of Laxapana rainfall stations including four monsoon seasons in Sri Lanka

In the Hanwella catchment, in the Laxapana rainfall station for the selected data period (1985-2015), monthly maximum, minimum, and mean are shown in Figure 3-39 by box plot. The monthly mean of rainfall varies from 95 ~ 660 mm, the minimum streamflow varies from 0 ~ 261 mm and the maximum streamflow varies from 289 ~ 1,555 mm.

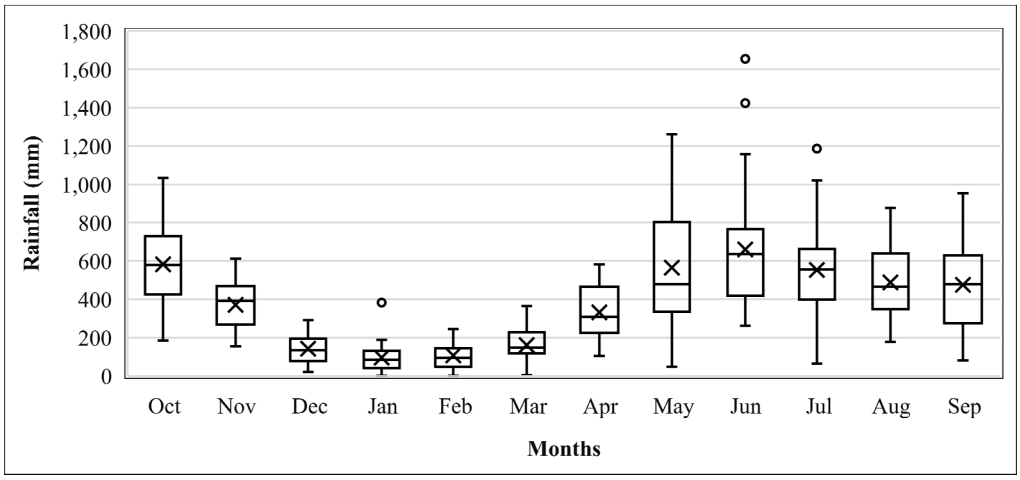

Figure 3-39 Rainfall variation of Laxapana rainfall station according to hydrological year (1985/86 – 2014/15)

In the Hanwella catchment, the Laxapana rainfall station and Hanwella streamflow station's yearly total are shown in Figure 3-40 for visual checking. Rainfall data are matched with streamflow patterns almost every year but 1999/2000 as per graph rainfall peak and streamflow peaks are not matching.

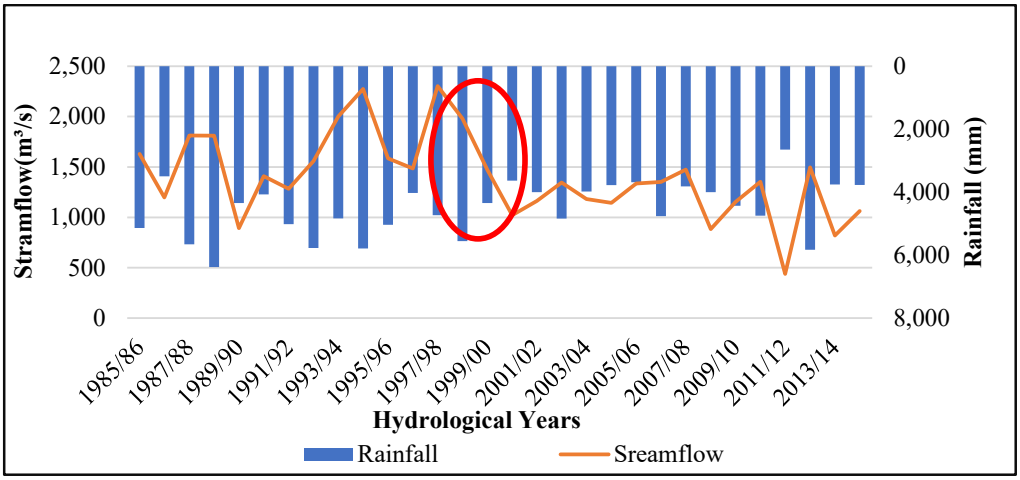

Figure 3-40 Yearly streamflow vs yearly rainfall of Laxapana station in the Kelani River basin

3.8 Single Mass Curve

The single mass curve was utilized to determine the data's quality. The cumulative rainfall was plotted against time, and the plot revealed that the data for the four stations utilized in the study were homogenous. As a result, the rainfall data were considered of high quality and hence eligible for further research analysis. The single mass curve for the Kirindi Oya is shown in Figure 3-41 and the Kelani River basin is shown in Figure 3-42.

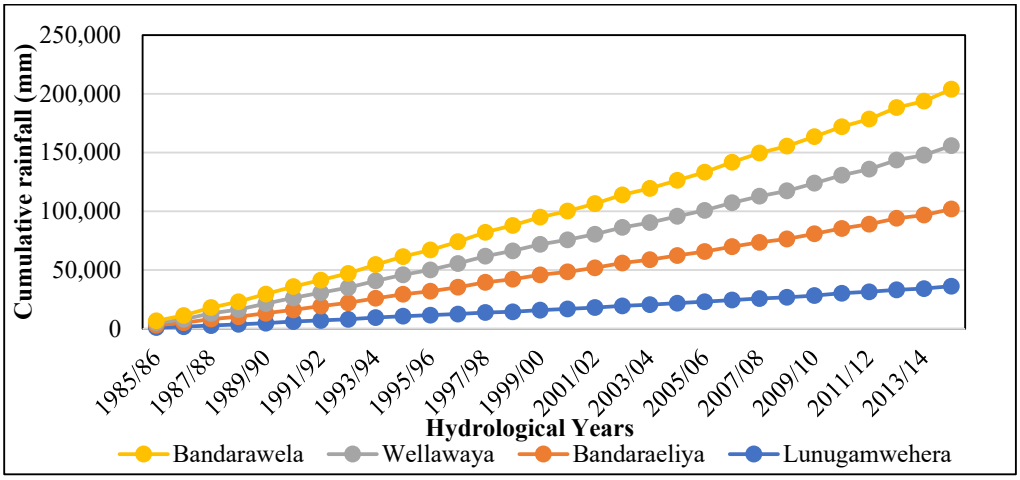

Figure 3-41 Single mass curve including four rainfall stations of Kirindi Oya River basin

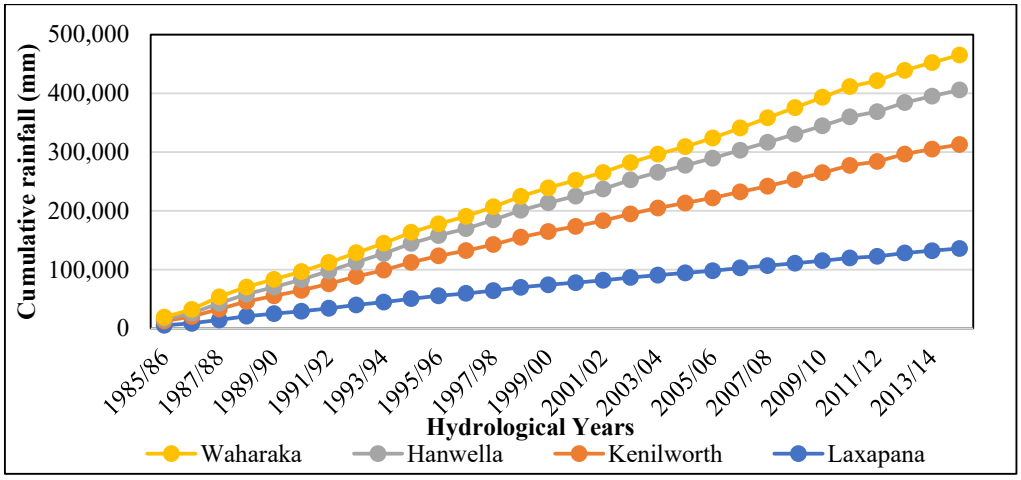

Figure 3-42 Single mass curve including four rainfall stations of Kelani River basin

3.9 Double Mass curve

The double mass curve is utilized to measure the consistency of various types of hydrological data by evaluating data from a single station to a pattern built of data from multiple other stations in the region. The double-mass curve can be used to smooth out inconsistent precipitation data (Subramanya, 2013).

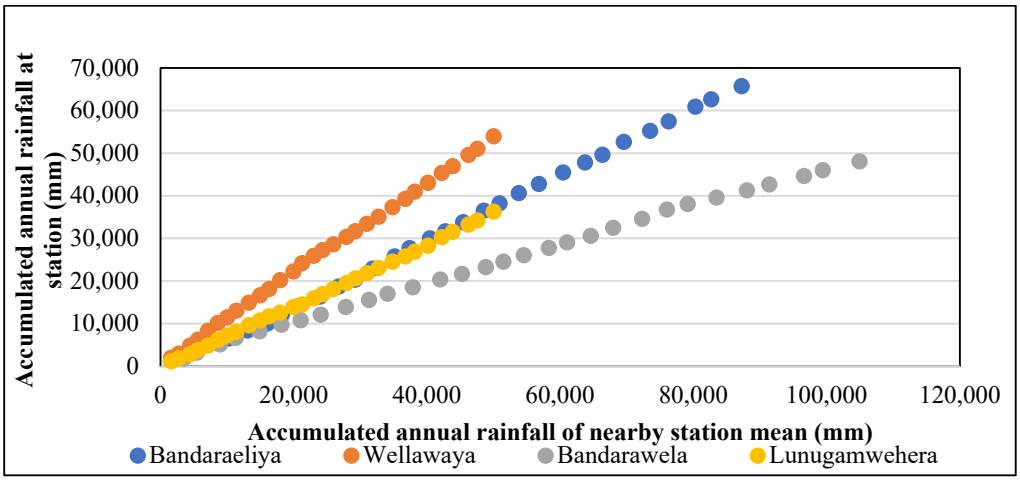

Figure 3-43 Double mass curve including four rainfall Stations of Kirindi Oya River basin

3.10 Indices calculation

3.10.1 Normalized Difference Vegetation Index (NDVI)

The agricultural drought index was calculated using Landsat data with 250 m resolution. The vegetation index can be utilized as an indicator to measure the greenness of plants within satellite data.

The NDVI value for every image was calculated utilizing the equation [3-5] and as follows:

$$NDVI = \frac{(\text{NIR} - \text{RED})}{(\text{NIR} + \text{RED})} \qquad [3\text{-}5]$$

The NDVI was determined using by bands and as follows:

$$NDVI = \frac{Band\,5\ -\ Band4}{Band\,5 +\ Band4} \quad [3\text{-}6]$$

Table 3-6 NDVI value ranges for the high, moderate, and severe situation (Taufik et al., 2019)

Class	Descriptions	Value of NDVI	Coverage
1	Low NDVI	0.1 or less	Water (low coverage)
2	Moderate NDVI	0.2 to 0.5	Non-vegetation (medium coverage)
3	Severe NDVI	0.6 to 0.9	Vegetation (Severe coverage)

3.10.2 Standardized Precipitation Index (SPI)

Standardized Precipitation Index (SPI), a tool derived by McKee (1993), the number of meteorological droughts were estimated from the existing precipitation data collected by the Meteorological Department.

For calculating the SPI value following equations are mentioned in Equation [2-3]. The SPI index is defined as:

$$SPI = \frac{(X_i - X_m)}{\sigma} \quad [3\text{-}7]$$

Where X_i is the monthly precipitation record of the station, X_m is the precipitation mean, and σ is the standard deviation.

These indices are assessed on a 3, 6, and 12-month scale for Meteorological drought risks categorization using SPI values (McKee et al., 1993).

Table 3-7 Metrological Drought Index SPI value ranges according to McKee et al., 1993

Code	Category	SPI values
1	Extremely wet	> 2
2	Severely wet	1.50 to 1.99
3	Moderately wet	1.00 to 1.49
4	Near normal	0.99 to – 0.99
5	Moderately dry	– 1.00 to – 1.49
6	Severely dry	– 1.50 to – 1.99
7	Extremely dry	< –2

3.10.3 Streamflow Drought Index (SDI)

SDI is a hydrological drought index SDI was initially proposed by Nalbantis (2008) and Nalbantis and Tsakiris (2009).

Each Complete hydrological year: October to December, October to March, October to June, and October to September

(j=1 for October and j=12 for September). Based on this series, cumulative streamflow volume is defined as:

$$V_{i,k} = \sum_{j=1}^{3K} Q_{ij} \quad i = 1,2,\ldots \;\; j = 1,2,\ldots,12 \;\; k = 1,2,3,4 \qquad [3\text{-}8]$$

where $V_{i,k}$ is the cumulative streamflow volume for the i^{-th} hydrological year and the k^{-th} reference period, k=1 for October to December, k=2 for October to March, k=3 for October to June, and k=4 for October to September.

The SDI is well-defined based on accumulative streamflow volumes $V_{i,k}$ for each reference period k of the i^{-th} hydrological year defined as:

$$SDI_{i,k} = \frac{(V_{i,k} - \overline{V})}{s_k} \qquad i = 1,2,\ldots \qquad k = 1,2,3,4 \qquad [3\text{-}9]$$

The normalization is simply reclaiming the natural logarithms of streamflow. The SDI index is defined as:

$$SDI_{i,k} = \frac{Y_{i,k} - \overline{Y_k}}{S_{y,k}} \qquad i = 1,\ 2,\ \ldots,\ k = 1,\ 2,\ 3,\ 4 \qquad [3\text{-}10]$$

in which

$$Y_{i,k} = \ln\left(V_{i,k}\right), \qquad i = 1,\ 2,\ \ldots,\ k = 1,\ 2,\ 3,\ 4 \qquad [3\text{-}11]$$

where V_k and S_k are the averages and the standard deviation of accumulative streamflow volumes, respectively.

3.11 HEC-HMS Model Development

The HEC-HMS model has been used to predict streamflow and floods in Sri Lanka's major river basins under future climatic conditions. Findings of such studies indicate that the HEC-HMS was capable of both continuous and event-based simulations in the Kelani River basin in Sri Lanka (Gunathilake et al., 2019).

Watershed hydrologic modeling, as well as the calibration and validation processes that go along with it, necessitate a huge amount of spatial and temporal data. In practice, data accessibility and quality are frequently a concern that must be addressed. Due to a lack of high-resolution data for constructing, calibrating, and validating the model, it is sometimes necessary to sacrifice the overall quality of the modeling.

The efficiency of a model is determined by its parameters once it has been chosen and developed. These settings were optimized for matching. The model was calibrated using data from 2010/11 to 2014/15 during five years, with RMSE as the objective function. The model's generated streamflow was evaluated using model performance criteria after each calibration run. By adjusting the parameter's initial values until the model performance criteria showed significant evidence for each criterion, the optimum or best-calibrated parameter set was found.

3.11.1 Kirindi Oya

The Thanamalwila catchment was selected for hydrological modeling, and this area was divided into 5 sub-catchments Figure 3-44. HEC-HMS model parameters and selected methods are shown in Table 3-8.

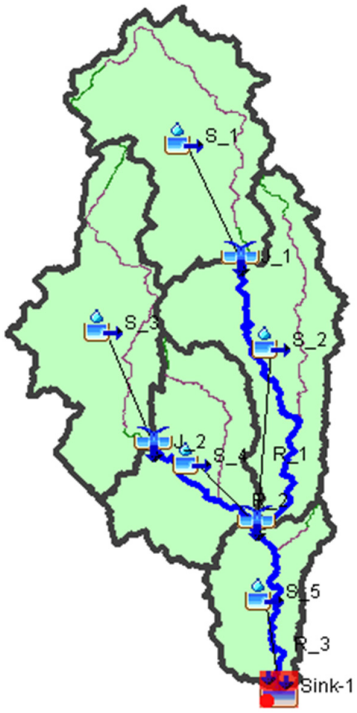

Figure 3-44 Catchment, sub-catchments, reaches, and streams delineated in HEC-HMS development

Table 3-8 Model Parameters and selected methods for calculating these methods

Model Parameters	Method
Canopy method	Simple Canopy
Surface Method	Simple Surface
Loss method	Deficit and Constant
Transform method	SCS Unit Hydrograph
Baseflow method	Recession
Evapotranspiration	Monthly Average
Precipitation	Thiessen method
Routing Method	Muskingum

3.11.1.1 Simple canopy method

This approach provides a straightforward representation of a plant canopy. If no surface representation is provided, all rainwater that falls to the surface or directly to

the soil is included. All probable evapotranspiration will be used to empty the canopy storage until all water in the storage is drained. The crop coefficient is multiplied by the probable evapotranspiration to estimate the evapotranspiration from canopy storage and, ultimately, the surface and soil components. Excess probable evapotranspiration will be exploited by the surface and soil components only after the canopy storage has been drained. Vegetation types and canopy interception mentioned in Table 3-9 used for the canopy calculation and Kirindi Oya basin according to sub-catchment canopy calculation are presented in Table 3-10

Table 3-9 Vegetation type and canopy interception

Vegetation Type	Canopy interception
General vegetation	1.27
Grasses and deciduous trees	2.03
Trees and coniferous trees	2.54

Table 3-10 Canopy interception in Thanamalwila each sub-catchment

Sub-Catchment Number	Canopy interception
S 1	1.58
S 2	1.04
S 3	1.71
S 4	1.46
S 5	0.93

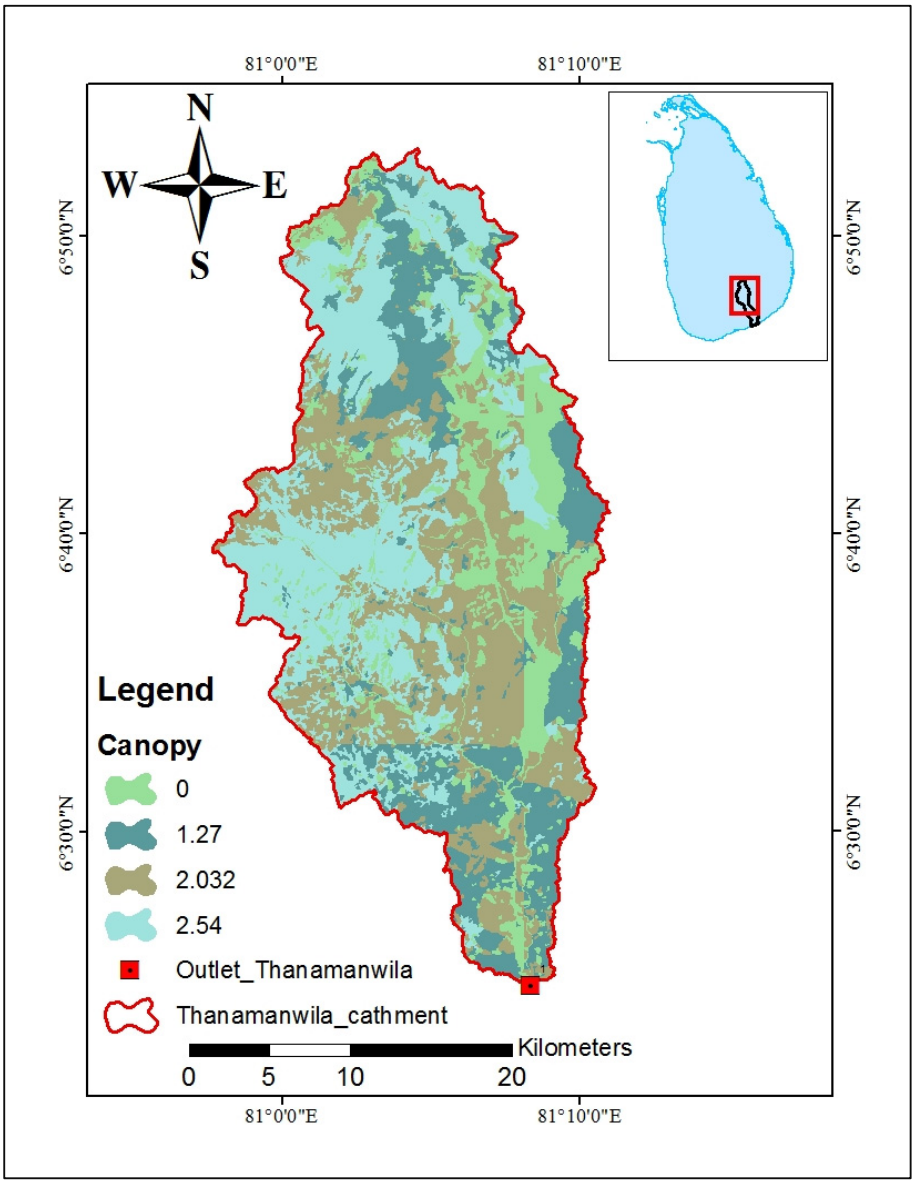

Figure 3-45 Canopy interception in Thanamalwila catchment

3.11.1.2 Surface Method

This method straightforwardly depicts the soil surface. All rainfall that falls on the soil surface is caught and stored until the surface's storage capacity is reached. Water in surface storage penetrates the soil whenever it is available, and even when the storage capacity is not full, water will infiltrate. When the storage capacity is full and the rainfall through-fall rate exceeds the infiltration rate, surface runoff is generated.

3.11.1.3 Loss method

To account for continual fluctuations in moisture content, the deficit constant loss approach employs a single soil layer. Using the deficit constant method allows for continuous simulation. It should be utilized in conjunction with a canopy approach that extracts water from the soil in response to probable evapotranspiration calculated by the meteorologic model. As the canopy drains soil water between precipitation events, the soil layer will dry up. Unless a canopy approach is used, there will be no soil water extraction. It can also be used with a surface approach for retaining water on the land's surface. The water in surface storage percolates into the soil layer. The ability of the soil layer to receive water determines the rate of infiltration. For this study, the deficit and constant methods were used as the loss method for all calculations.

The maximum deficit is obtained from the curve number using Equation [3-12], and the initial deficit parameter is taken 20% of the maximum deficit (Malpass et al., 2009). The maximum storage is identified as:

$$S = \frac{25{,}400}{CN} - 254 \qquad [3\text{-}12]$$

where

S = maximum probable storage, mm

CN = curve number

Maximum storage and deficit calculation for HEC-HMS for Kirindi Oya River basin are shown in Table 3-11 and all the reach-related information is shown in Table 3-12.

Table 3-11 Maximum storage and deficit calculation for HEC-HMS for Kirindi Oya River basin

Sub-Catchment Number	CN	Maximum Storage (mm)	Initial Deficient (mm)	Initial constant rate (mm/hrs)
S 1	73.94	89.53	17.91	1.27
S 2	77.83	72.36	14.47	1.27
S 3	69.71	110.36	22.07	1.27
S 4	70.72	105.16	21.03	1.27
S 5	72.40	96.83	19.37	1.27

Table 3-12 Preparation data in HEC-HMS

Sub-Catchment Number	Flow path (km)	Centroidal flow path length (km)	Centroidal flow path slope	Basin Slope	Drainage Density (km/km²)
S 1	38.70	17.52	0.01	0.31	0.28
S 2	34.93	11.54	0.00	0.22	0.25
S 3	38.50	20.84	0.00	0.09	0.30
S 4	22.54	7.63	0.00	0.08	0.24
S 5	21.26	9.35	0.00	0.04	0.24

Lag time

Time of Concentration is computed by utilizing Equation [3-13] by the Kirpich method. For the Kirindi Oya basin time of concentration is shown in Table 3-13 according to sub-catchments.

$$t_c = 0.0078L^{0.77}S^{-0.385} \quad [3\text{-}13]$$

where

t_c = Time of concentration

L = Length longest flow path (ft)

S = Basin slope

CN = Curve number

Table 3-13 Calculation of Time of Concentration

Sub catchment	CN	Maximum probable Retention (S), inch	Initial abstraction, mm	L	S	Time of concentration, t_c (min)
S 1	72.40	3.52	17.91	66.36	1.56	103.82
S 2	70.72	2.85	14.47	61.34	1.79	109.78
S 3	69.71	4.34	22.07	66.10	2.55	168.86
S 4	77.83	4.14	21.03	43.77	2.59	113.18
S 5	73.94	3.81	19.37	41.84	3.42	143.07

3.11.1.4 Baseflow Method

While a subbasin element illustrates the interaction of surface runoff, infiltration, and subsurface processes, the actual subsurface computations are carried out by a baseflow process embedded within the subbasin. There are 6 various baseflow approaches available. Some of the approaches are meant for event simulations, while others are for continuous simulations.

The recession baseflow approach is intended to simulate the normal behavior experienced in watersheds when channel flow recedes exponentially following an incident. This approach is primarily designed for event simulation. It does, however, have the probable to automatically reset after every storm event and, as a consequence, may be utilized for continuous simulation. It does not conserve mass inside the subbasin.

3.11.1.5 Thiessen Rainfall

The Thiessen method is a common method used for deriving the average areal precipitation shown in Figure 3-46. This process assigns an area called a Thiessen polygon for each rainfall measuring station. Each point within this polygon is expected to have a similar rainfall along with a constant weight. Thiessen polygons for the Kirindi Oya River basin at the Thanamalwila outlet were produced by Arc-GIS using four rain gauging stations. The coverage area of each rainfall measuring station is characterized by colour boundaries. The areas of the Thiessen polygon and their weight were computed, and the values are presented in Table 3-14.

Table 3-14 Thiessen weights for the Kirindi Oya River basin at Thanamalwila catchment

Station name	Thiessen polygon area (km^2)	Thiessen weight
Wellaweya	130.208	0.69
Bandarawela	13.170	0.02
Bandaraeliya	81.687	0.18
Lunughamhara	505.675	0.11

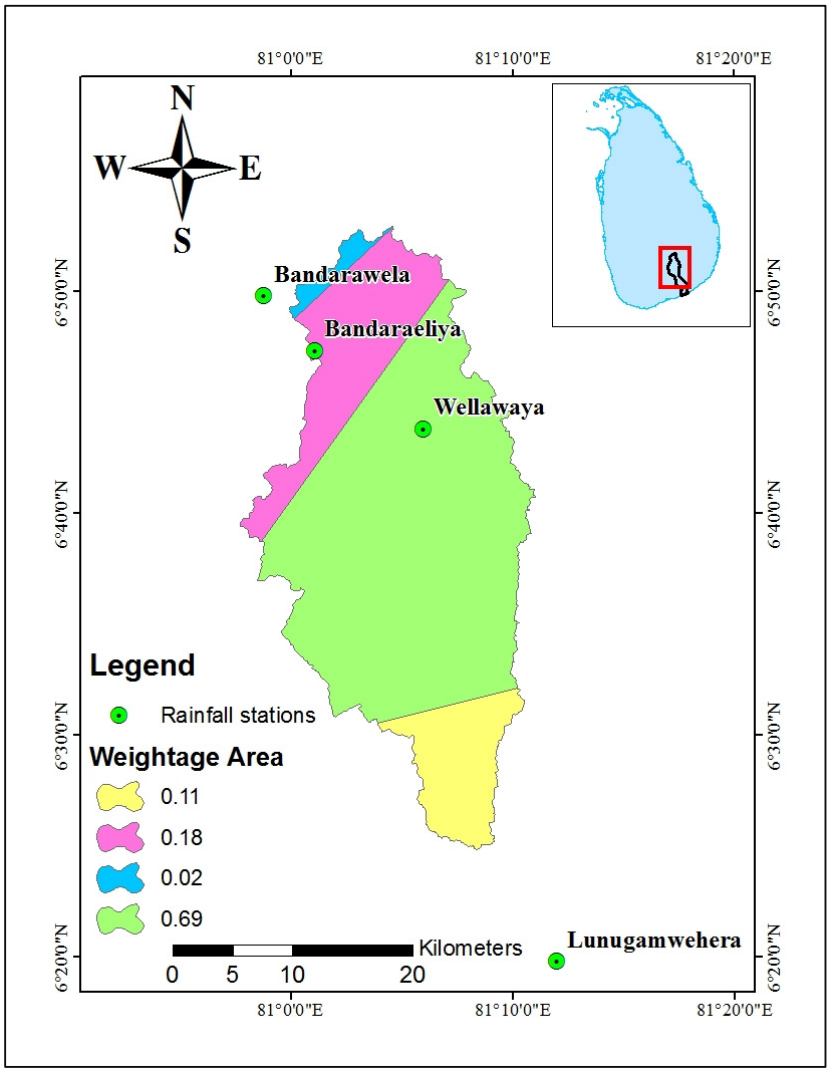

Figure 3-46 Thiessen rainfall distribution in Thanamalwila catchment

3.11.1.6 Routing Method

While a reach element theoretically represents a section of a stream or river, the actual computations are carried out by a routing method included within the reach. There are a total of nine distinct routing strategies available. Every technique employs a hydrologic routing methodology, as opposed to a hydraulic strategy that utilizes the entire set of unsteady flow equations. Each approach in the program provides a different level of information, and not all methods are similarly capable of expressing numerous streams.

The Muskingum *K* is essentially the time it takes to traverse across the reach. It may be approximated based on information of the cross-section and flow parameters. In certain circumstances, it might be a calibration parameter.

The Muskingum *X* is a weighted mean of inflow and outflow effect that fluctuates from 0.0 to 0.5. In practice, a value of 0.0 results in maximum attenuation, and a value of 0.5 results in no attenuation. The majority of stream reaches require an intermediate value determined by calibration.

3.11.2 Kelani River

For modeling, this Hanwella streamflow has been selected and according to this station's name named Hanwella catchment this area has been divided into 4 sub-catchments Figure 3-47. HEC-HMS model parameters and selected methods are shown in the table Table 3-15.

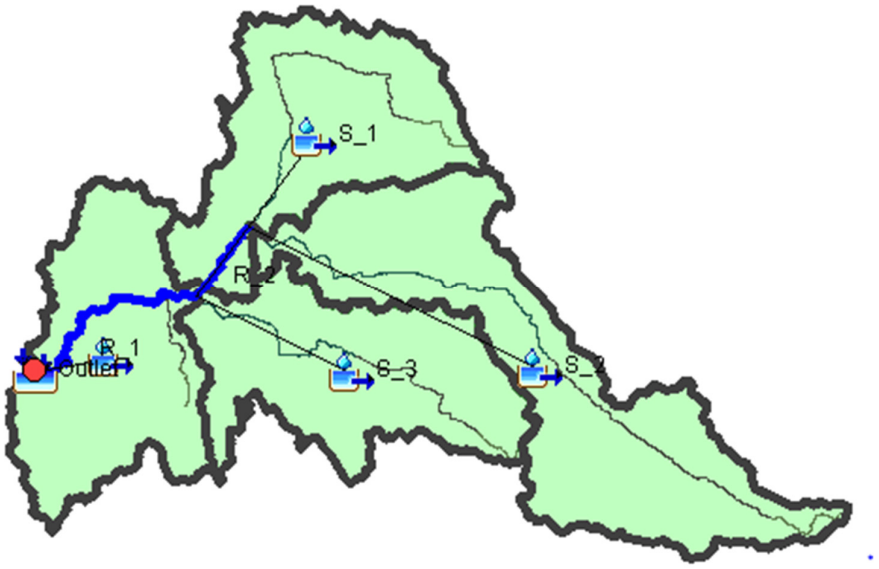

Figure 3-47 Catchment, sub catchments, reaches, and streams delineated in HEC-HMS development

Table 3-15 Model Parameters and selected methods for calculating these methods

Model Parameters	Method
Canopy method	Simple Canopy
Surface Method	Simple Surface
Loss method	Deficit and Constant
Transform method	SCS Unit Hydrograph
Baseflow method	Recession
Evapotranspiration	Monthly Average
Precipitation	Thiessen method
Routing Method	Muskingum

3.11.2.1 Canopy Method

Simple canopy method

This method straightforwardly depicts a plant canopy. All precipitation refers to any additional precipitation that falls to the surface, or directly to the soil if the surface is not represented. The canopy storage will be emptied using all available evapotranspiration until the water in the store is disappeared. To calculate the amount of evapotranspiration from canopy storage and later the surface and soil components, multiply the probable evapotranspiration by the crop coefficient.

3.11.2.2 Surface Method

This approach offers a straightforward depiction of the soil surface. All precipitation that falls on the soil surface is collected and stored until the storage capacity of the surface is depleted. Storage on the groundwater infiltrates the soil whenever it is there, and water will infiltrate even if the storage capacity is not full. Surface runoff occurs when the storage capacity is reduced, and the precipitation through-fall rate exceeds the infiltration rate.

3.11.2.3 Loss method

The extreme deficit is obtained from the curve number using Equation [3-12], and the initial deficit parameter is taken 20% of the maximum deficit (Malpass et al., 2009). All the information about length and slope which are received from HEC-HMS are

shown in Table 3-16. Maximum deficit and constant have been calculated for the Kelani River basin and these are shown in Table 3-17.

Table 3-16 Preparation data in HEC-HMS in Kelani River basin

Sub-Catchment Number	Flow Path (km)	Centroidal Flow Path Length (km)	Centroidal Flow Path Slope	Basin Slope	Drainage Density (km/km²)
S 1	59.05	21.12	0.00	0.27	0.05
S 2	86.53	43.19	0.02	0.33	0.05
S 3	48.97	23.05	0.00	0.30	0.05
S 4	36.98	9.45	0.00	0.14	0.06

Table 3-17 Maximum storage and deficit calculation for HEC-HMS for Kelani River basin

Sub-Catchment Number	CN	Maximum Storage (mm)	Initial Deficient (mm)	Initial Constant Rate (mm/hrs)
S 1	75	81.03	16.21	1.27
S 2	73	93.93	18.79	1.27
S 3	70	107.01	21.40	1.27
S 4	77	74.35	14.87	1.27

Table 3-18 Calculation of time of concentration

Sub-Catchment Number	CN	Maximum probable Retention (S), inch	Initial abstraction, mm	L	S	Time of concentration, t_c (min)
S 1	75.81	3.19	114.00	91.89	1.65	151.47
S 2	73.00	3.70	75.76	123.32	1.54	190.01
S 3	70.36	4.21	82.61	79.56	1.59	126.27
S 4	77.36	2.93	0.00	64.08	2.15	137.68

3.11.2.4 Baseflow Method

The recession baseflow approach is intended to simulate the normal behavior observed in watersheds when channel flow recedes exponentially following an incident. This approach is primarily meant for event simulation. It does, however, can automatically reset after each storm occurrence and may therefore be utilized for continuous simulation. Within the subbasin, it does not retain mass.

3.11.2.5 Thiessen Rainfall

Using four rain gauging stations, Arc-GIS 10.3 developed thiessen polygons for the Kelani River basin near the Thanamalwila outflow. Colour boundaries demarcate the coverage area of each gauging station. The areas and weights of the thiessen polygons were calculated, and the results are reported in Table 3-19.

Table 3-19 Thiessen weights for the Kirindi Oya River basin at Thanamalwila catchment

Station name	Thiessen polygon area (km^2)	Thiessen weight
Waharaka	583	0.30
Kenilworth	387	0.20
Hanwella	467	0.24
Laxapana	507	0.26

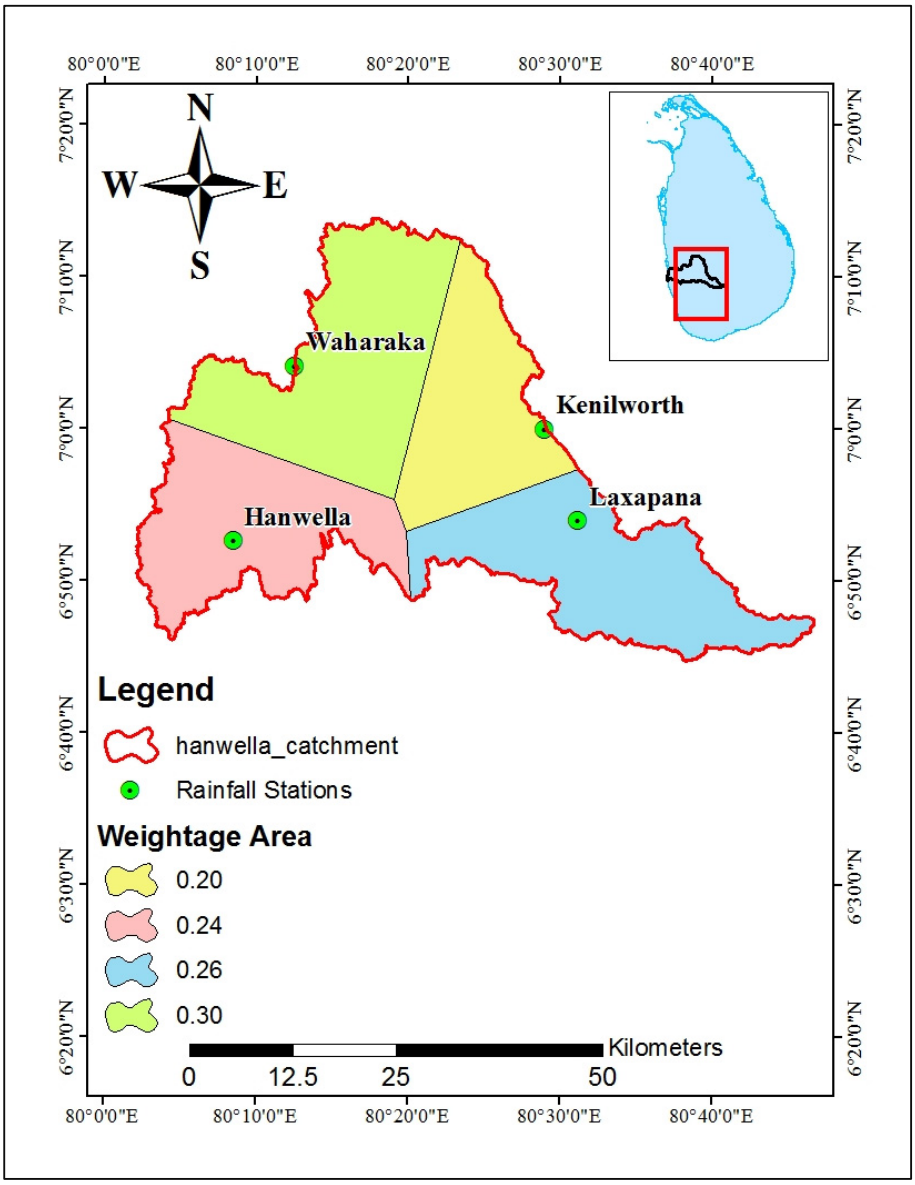

Figure 3-48 Thiessen rainfall distribution in Hanwella catchment

3.11.2.6 Routing Method

Muskingum Routing

The Muskingum *K* is essentially the time it takes to travel across the reach. It may be approximated based on information of the cross-section and flow parameters. In certain circumstances, it might be a calibration parameter.

The Muskingum X is a weighted average of the inflow and outflow effect that extends from 0.0 to 0.5. In practice, a value of 0.0 leads to maximum attenuation, and a value of 0.5 leads to no attenuation. The majority of stream reaches need an intermediate value discovered by calibration.

CHAPTER 4

4 RESULTS AND DISCUSSIONS

4.1 Introduction

This research project has two river basins named Kirindi Oya and Kelani River basin. These two-river basin indices calculations are separately 4.3 and 4.4. for both river basin results are including Normalized Difference Vegetation Index, Standardized Precipitation Index, and Streamflow Drought Index.

For this study rainfall and streamflow data are the main component and the Kirindi Oya River basin in the Southern province of Sri Lanka along with a data set containing four stations obtaining daily precipitation data for 30 years. The second river basin is the Kelani River basin in the Western province of Sri Lanka with a data set comprising of four stations having daily rainfall data for 30 years. By using these rainfall and streamflow drought indices have been calculated.

In 0 mentioned the bias-corrected results for bias correction, it has been used linear scaling method. In this project for the bias correction using three different models and which model gives the best result further work has been done using this model.

Also mentioned are the results of HEC-HMS models for both river basin calibration 5 years and validation for 5 years. Then validated parameters are used for mid and end century climate data.

4.2 Bias Correction

Linear scaling method

The RCP 8.5 which is the worst scenario for climate change has been adopted for the future time period for this research (IPCC, 2014). The Linear scaling (LS) technique employs a constant correction factor calculated from the difference between original

RCM simulations and observations for each calendar month. This technique can adjust for climatic factors when monthly mean values are involved. Precipitation is adjusted with a multiplier, and temperature is corrected by the additive term, equation mentioned as:

$$P_{hst,m,d}^{cor} = P_{hst,m,d} * \left[\frac{\mu\left(P_{obs,m}\right)}{\mu\left(P_{hst,m}\right)}\right] \quad [4\text{-}1]$$

where

$P^{cor}_{hst,m,d}$ = Precipitation on the d^{th} day of the m^{th} month,

$P_{hst,m,d}$ = precipitation from original RCM outputs during the relevant period

d = day

m = month

μ = mean value

Three RCMs with 25-50 km resolution (MPI-M-MPI-ESM-MR) were evaluated for the bias correction. After checking all three models from which one showed the highest R^2 the RCM model is used for further climate drought assessment. It has shown here Wellawewa station's three models Figure 4-1 and the rest of the models are shown in annexure1. From these three models, 25 km resolution WAS_22 MPI-M-MPI-ESM-MR has shown the highest R^2 value is 0.3378. For this research work, it has been using WAS_22 MPI-M-MPI-ESM-MR models value.

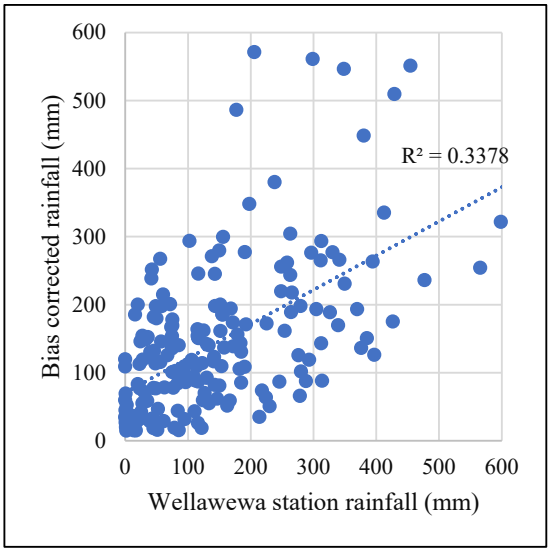

Figure 4-1 Bias corrected rainfall (mm) for WAS_22 MPI-M-MPI-ESM-MR

The RCM data (WAS_22 MPI-M-MPI-ESM-MR) has been downloaded from the CORDEX-DKRZ website as NetCDF files. After the downloading of RCM data extract those data by using MATLAB. Extracted data has biased in linear Regression method in monthly coefficient value as shown in Figure 4-1. Same monthly coefficients are used for future period mid-century and end-century. These biased data have been used for calculating future drought indices SPI and SDI.

4.3 Study Area 1 (Kirindi Oya)

4.3.1 Normalized Difference Vegetation Index (NDVI)

For calculating 1986, 1995, and 2006 NDVI values, relevant images were collected from Landsat 4-5 and Landsat 8 (2015 image). In this study, the reference time scale is from 1985 to 2015, and the decadal NDVI variations are shown in Figure 4-2.

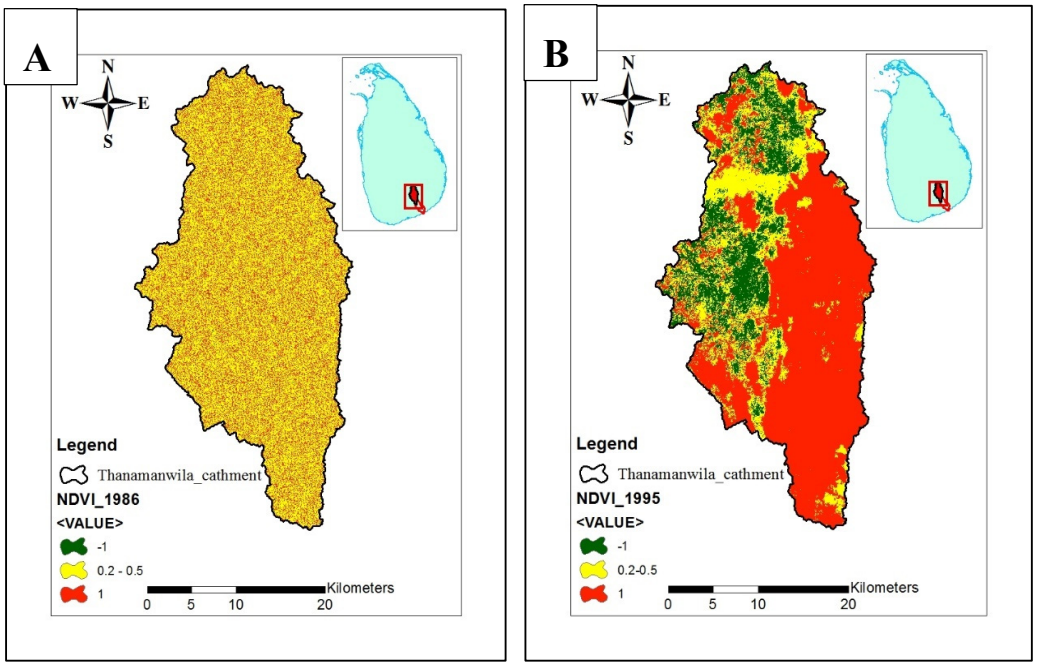

Figure 4-2 NDVI for (A) 1986 and (B) 1995 in the Thanamalwila basin, which is a sub-basin of the Kirindi Oya River basin

The 1986 NDVI plot comprises its maximum values between 0.2 to 0.5 (moderate range), which indicate non-vegetation coverage (map (A) of Figure 4-2). Map (B) of the same figure shows a high NDVI value in 1995, indicating maximum area vegetation coverage.

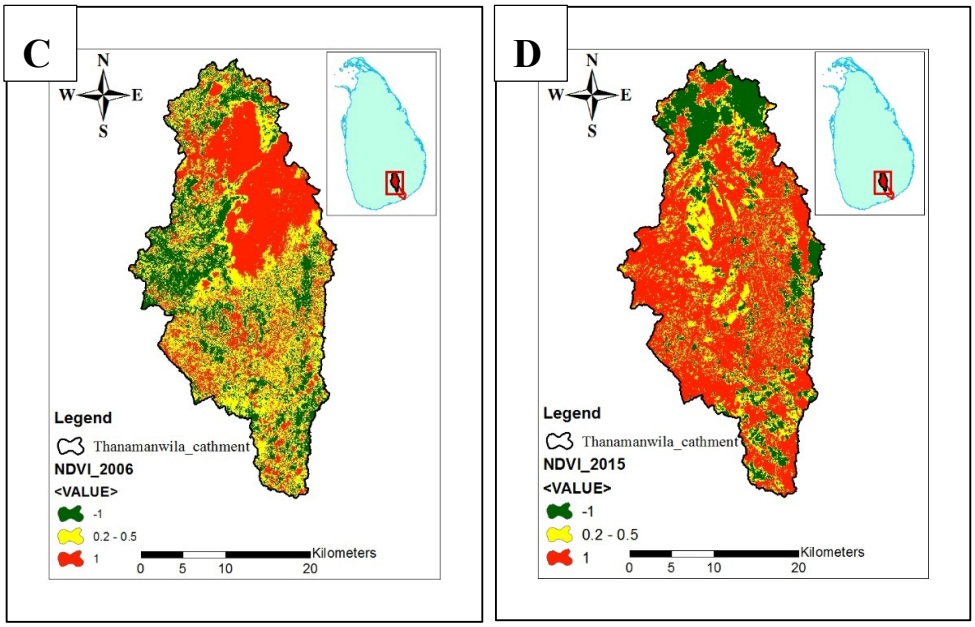

Figure 4-3 NDVI for (C) 2006 and (B) 2015 in the Thanamalwila basin which is sub basin of the Kirindi Oya River basin

The 2006 NDVI plot comprises its maximum values between 0.2 to 0.5 (moderate range), which indicate non-vegetation coverage (map (C) of Figure 4-2). Map (D) of the same figure shows a high NDVI which most of the area in severe coverage. Upstream of the catchment shows low coverage of NDVI.

4.3.2 Standardized Precipitation Index (SPI)

SPI is for meteorological drought index, computed on a three-, six-, and twelve-month scale. SPI was estimated for four rainfall stations covering the complete river basin.

4.3.2.1 Observed Period (1985/86 -2014/15)

The yearly SPI variation over the entire Kirindi Oya river basin is presented in Figure 4-4. Corresponding to SPI values, 1986, 1989, 1992, 1993, 1996, 1998, 2000, 2004, 2009, and 2014 years can be categorized as moderate dry (Table 3-7). In terms of SPI, the most severe drought (–1.5 to – 1.99) was reported for the whole river basin in 1987 (Figure 4-4). Drought frequently occurs in 3 or 4 years within this 30 years observed

period. SPI for this basin can be utilized to monitor the drought and also to determine the degree of drought since this study identified roughly similar years as drought years.

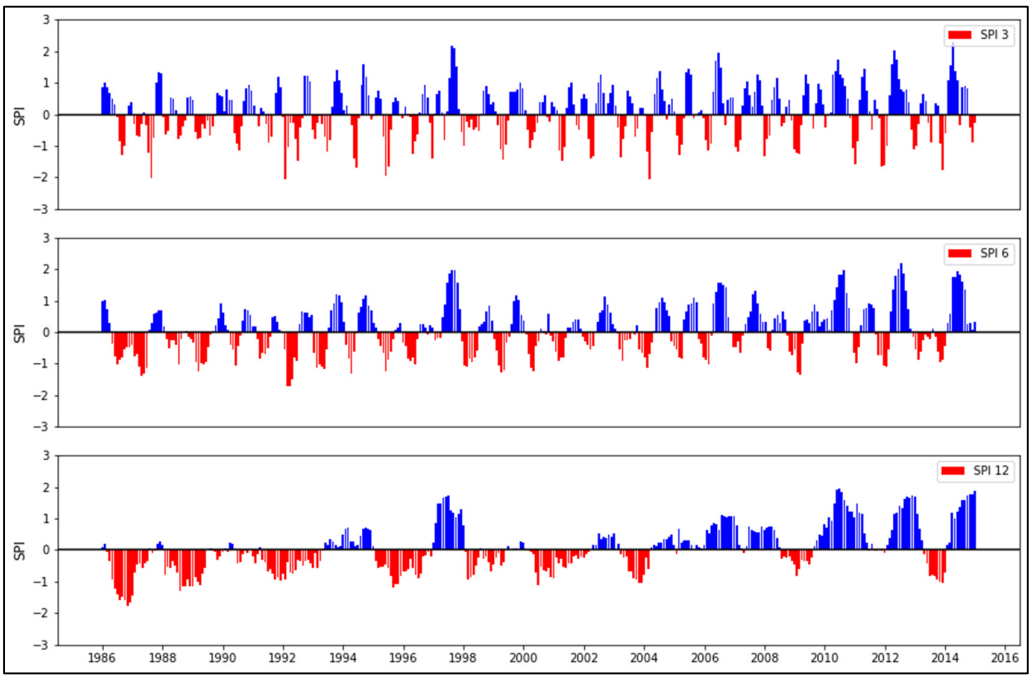

Figure 4-4 SPI variation in the Kirindi Oya river basin based on 3, 6, and 12 months for the observed period (1986-2015)

From 1985 to 2015, the time series of SPI at 3-month (October–December) were computed to demonstrate their probable value for identifying drought and monitoring drought risk (Figure 4-5). In the 3-month SPI time scale, the SPI frequencies fluctuated significantly above and below the zero line. Drought occurs whenever the SPI is negative, and the intensity decreases below –1.0. Drought occurrence events found in the observed period are 67 extreme, 129 severe, 294 moderate, and 650 mild droughts for 3-month scale, according to Figure 4-5.

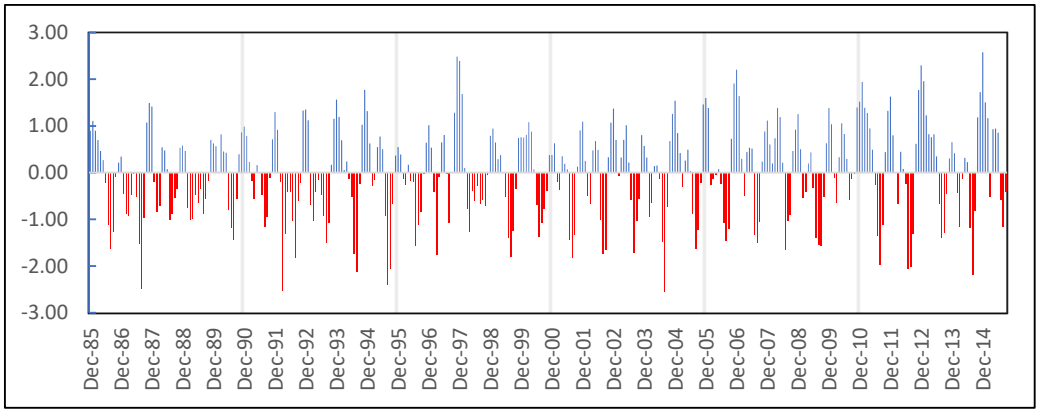

Figure 4-5 SPI variation in the Kirindi Oya river basin based on 3-month for the observed period (1986-2015)

From 1985 to 2015, the time series of SPI at 6-month periods (October–March) were computed to demonstrate their probable value for identifying drought and monitoring drought risk (Figure 4-6). In the 6-month SPI time scale, the SPI frequencies fluctuated significantly above and below the zero line. Drought occurs whenever the SPI is negative, and the intensity decreases below –1.0. Drought occurrence events found in the observed period are 2 extremes, 13 severe, 48 moderate, and 120 mild droughts for 6-month scale, according to Figure 4-6.

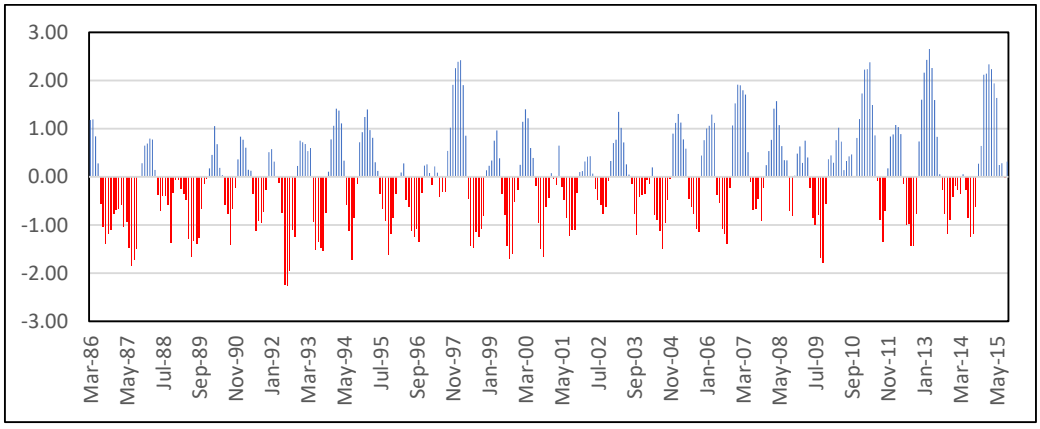

Figure 4-6 SPI variation in the Kirindi Oya river basin based on 6-month for the observed period (1986-2015)

From 1985 to 2015, the time series of SPI at 12-month/annual periods (October–September) were computed to demonstrate their probable value for identifying drought and observing drought risk (Figure 4-7). In the 12-month SPI time scale, the SPI frequencies fluctuated significantly above and below the zero line. Drought occurs whenever the SPI is negative, and the intensity decreases below –1.0. Drought occurrence events found in the observed period are no extreme events, 52 severe, 247 moderate, and 840 mild droughts for 12-month scale, according to Figure 4-7. As a result, the severity of drought changes throughout time. Furthermore, the magnitude of wet occurrences during all three SPI periods, 3-month, 6-month, and annual, is nearly the same (Figure 4-4).

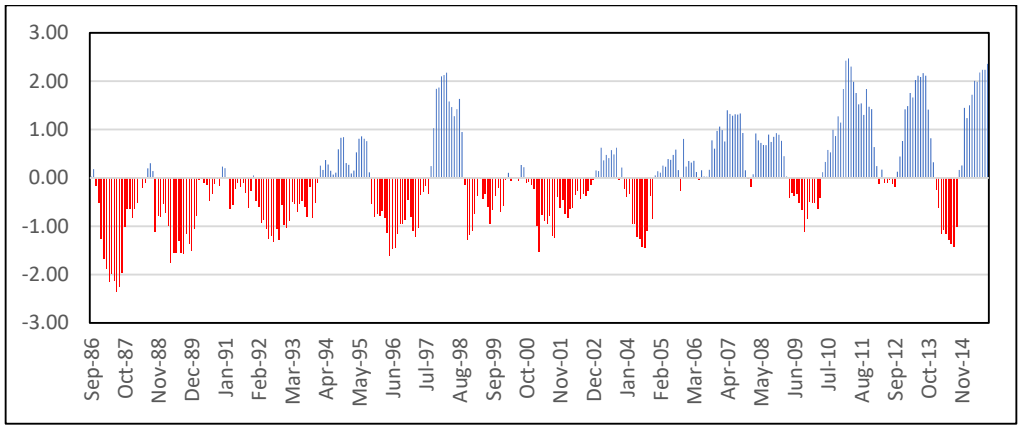

Figure 4-7 SPI variation in the Kirindi Oya river basin based on 12-month for the observed period (1986-2015)

4.3.2.2 Mid Century (2040 -2059)

From 2040 to 2059, the time series of SPI at 3-month (October–December) were computed to demonstrate their probable value for identifying drought and observing drought risk (Figure 4-8). In the 3-month SPI time scale, the SPI frequencies fluctuated significantly above and below the zero line. Drought occurs whenever the SPI is negative, and the intensity decreases below –1.0. Drought occurrence events found in the observed period are no extreme event, 16 severe, 25 moderate, and 78 mild droughts for 3-month scale, according to Figure 4-8.

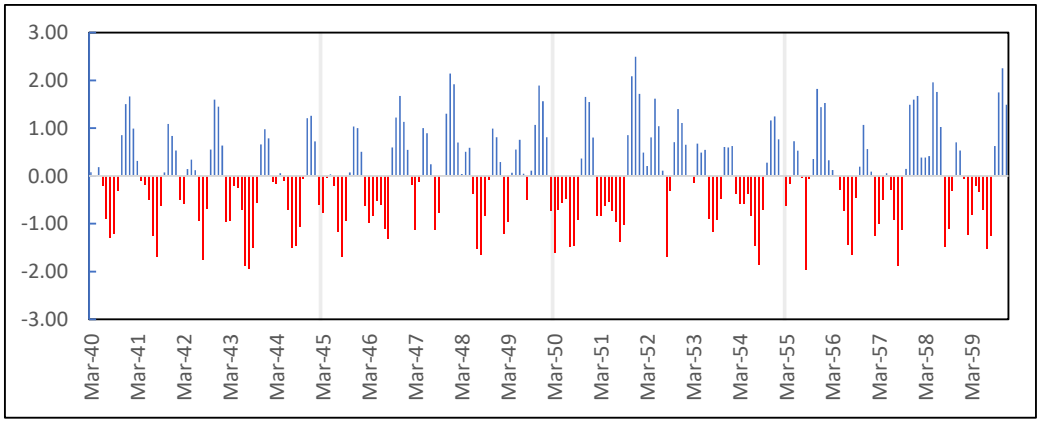

Figure 4-8 SPI variation in the Kirindi Oya river basin based on 3-month for mid-century (2040-2059) in RCP 8.5

From 2040 to 2059, the time series of SPI at 6-month periods (October–March) were computed to demonstrate their probable value for identifying drought and observing drought risk (Figure 4-9). In the 6-month SPI time scale, the SPI frequencies fluctuated significantly above and below the zero line. Drought occurs whenever the SPI is negative, and the intensity decreases below –1.0. Drought occurrence events found in the observed period are no extreme event, 16 severe, 35 moderate, and 62 mild droughts for 6-month scale, according to Figure 4-9.

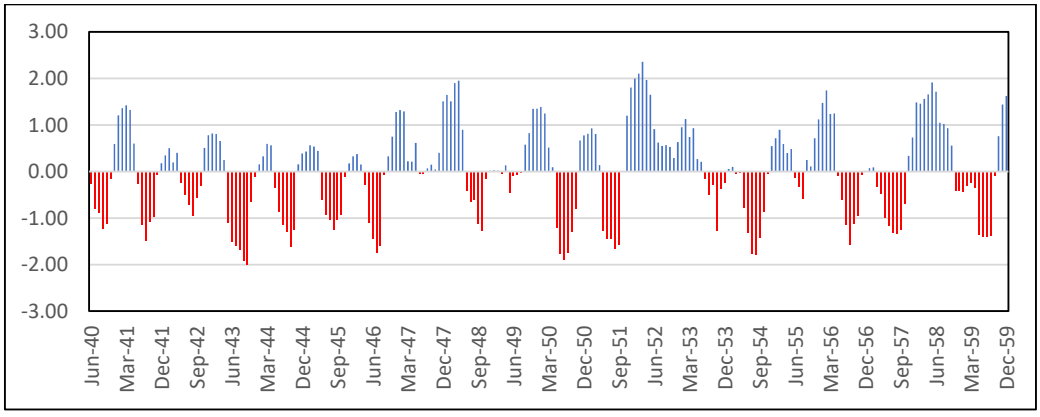

Figure 4-9 SPI variation in the Kirindi Oya river basin based on 6-month for mid-century (2040-2059) considering RCP 8.5

From 2040 to 2059, the time series of SPI at 12-month/annual periods (October–September) were computed to demonstrate their probable value for identifying drought and observing drought risk (Figure 4-10). In the 12-month SPI time scale, the SPI frequencies fluctuated significantly above and below the zero line. Drought occurs whenever the SPI is negative, and the intensity decreases below –1.0. Drought occurrence events found in the observed period are no extreme event, 89 severe, 122 moderate, and 584 mild droughts for 12-month scale, according to Figure 4-10. As a result, the severity of drought changes throughout time. Furthermore, the magnitude of wet occurrences during all three SPI periods, 3-month, 6-month, and annual, is nearly the same (Figure 4-10).

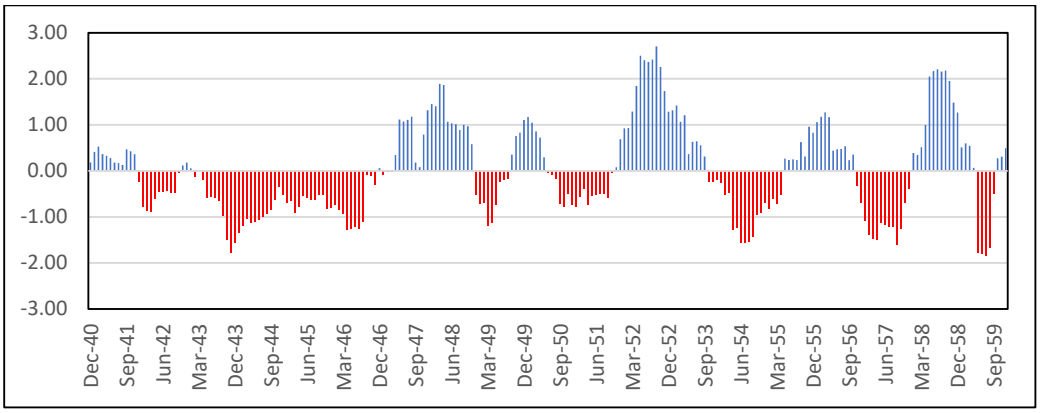

Figure 4-10 SPI variation in the Kirindi Oya river basin based on 12-month for mid-century (2040-2059) considering RCP 8.5

4.3.2.3 End Century (2080 -2099)

From 2080 to 2099, the time series of SPI at 3-month (October–December) were computed to demonstrate their probable value for identifying drought and monitoring drought risk (Figure 4-11). In the 3-month SPI time scale, the SPI frequencies fluctuated significantly above and below the zero line. Drought occurs whenever the SPI is negative, and the intensity decreases below –1.0. Drought occurrence events found in the observed period are 1 extreme event, 7 severe, 35 moderate, and 89 mild droughts for 3-month scale, according to Figure 4-11.

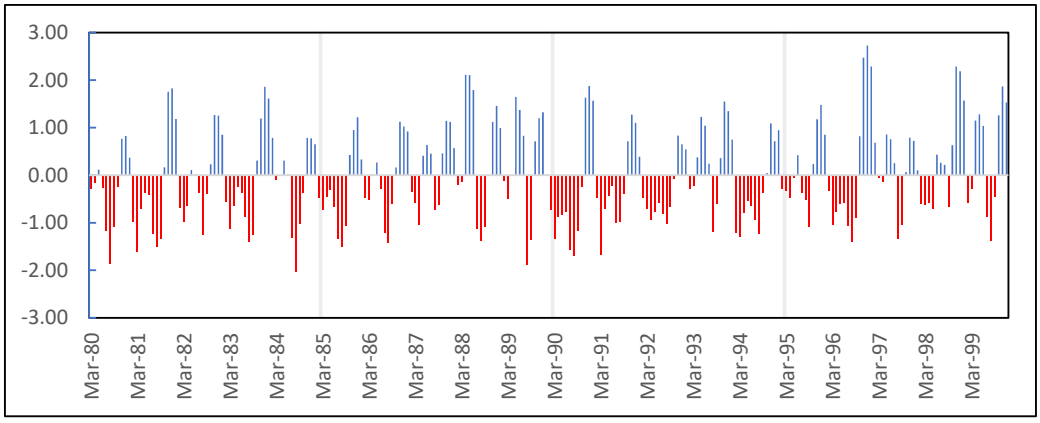

Figure 4-11 SPI variation in the Kirindi Oya river basin based on 3-month for End-century (2080-2099)

From 2080 to 2099, the time series of SPI at 6-month periods (October–March) were computed to demonstrate their probable value for identifying drought and observing drought risk (Figure 4-12). In the 6-month SPI time scale, the SPI frequencies fluctuated significantly above and below the zero line. Drought occurs whenever the SPI is negative, and the intensity decreases below –1.0. Drought occurrence events found in the observed period are 2 extreme events, 19 severe, 25 moderate, and 63 mild droughts for 6-month scale, according to Figure 4-12.

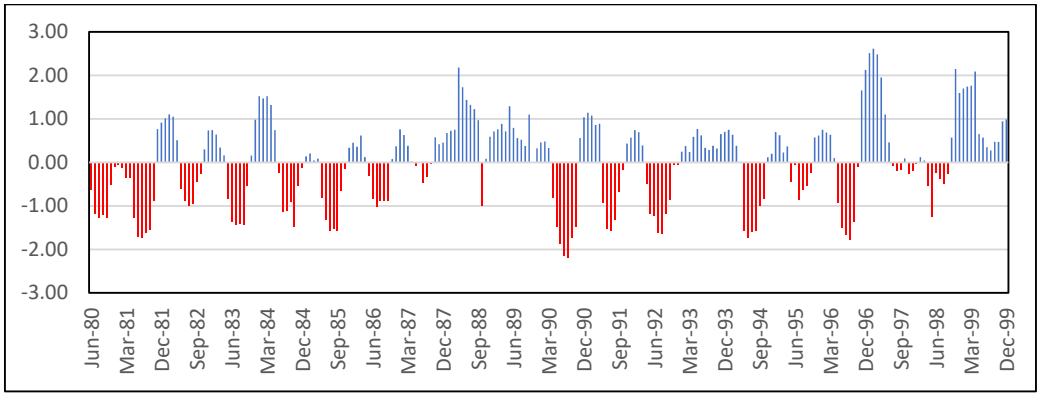

Figure 4-12 SPI variation in the Kirindi Oya river basin based on 6-month for End-century (2080-2099) considering RCP 8.5

From 2040 to 2059, the time series of SPI at 12-month/annual periods (October–September) were computed to demonstrate their probable value for identifying drought and observing drought risk (Figure 4-13). In the 12-month SPI time scale, the SPI frequencies fluctuated significantly above and below the zero line. Drought occurs whenever the SPI is negative, and the intensity decreases below –1.0. Drought occurrence events found in the observed period are 10 extreme events, 42 severe, 151 moderate, and 630 mild droughts for 12-month scale, according to Figure 4-13. As a result, the severity of drought changes throughout time. Furthermore, the magnitude of wet occurrences during all three SPI periods, 3-month, 6-month, and annual, is nearly the same (Figure 4-13).

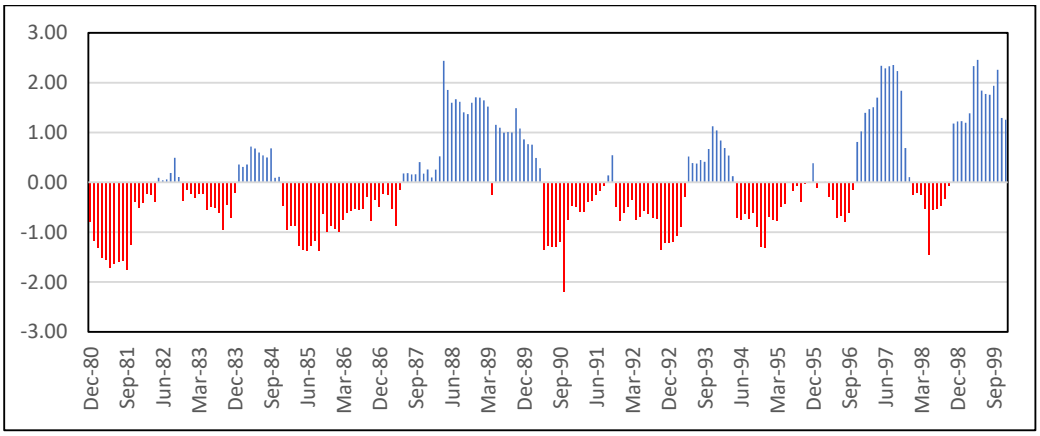

Figure 4-13 SPI variation in the Kirindi Oya river basin based on 12-month for End-century (2080-2099) considering RCP 8.5

4.3.3 HEC-HMS Results

The modeling of continuous streamflow in the Kirindi Oya River is used to calculate drought indicators for the future time period. Assuming curve number to be constant for future calculation.

Model Calibration

In the Thanamalwila catchment, hydrographs in normal and semi-log scales are compared for both actual and modeled streamflow Figure 4-14 to Figure 4-17, respectively. At the Thanamalwila catchment, flow duration curves for both sorted and

sort only observed streamflow are shown in Figure 4-16. Four parameters (Recession constant, Ratio to peak, Muskingum *K*, and Muskingum *X*) are optimized for calibrating the HEC-HMS model for the observed period and initial parameters and optimized parameters are shown in Table 4-1. The calibration and validation objectives functions of the Kirindi Oya river basin are mentioned in Table 4-2.

Table 4-1 Initial parameters and optimized parameters of HEC-HMS model in the Kirindi Oya river basin

Method	Sub-Catchment	Parameters	Initial Value	Optimized value
Baseflow (Recession)	S_1	Recession Constant	0.7	0.920
	S_2	Recession Constant	0.7	0.095
	S_3	Recession Constant	0.7	0.153
	S_4	Recession Constant	0.7	0.132
	S_5	Recession Constant	0.7	0.815
	S_1	Ratio to peak	0.509	0.352
	S_2	Ratio to peak	0.501	0.532
	S_3	Ratio to peak	0.513	0.919
	S_4	Ratio to peak	0.495	0.463
	S_5	Ratio to peak	0.525	0.104
Routing (Muskingum)	R_1	Muskingum K	35	40
	R_2	Muskingum K	39	35
	R_3	Muskingum K	29	32
	R_1	Muskingum x	0.0536	0.1004
	R_2	Muskingum x	0.0501	0.173
	R_3	Muskingum x	0.0879	0.100

Table 4-2 Objective function's performance rating of calibration and validation in Kirindi Oya River basin

Objective Functions	Calibration	Performance Rating	Validation	Performance Rating
RMSE	0.60	Good	0.70	Satisfactory
NSE	0.59	Good	0.505	Satisfactory
Percent Bias	7.63%	Very Good	3.22%	Very Good

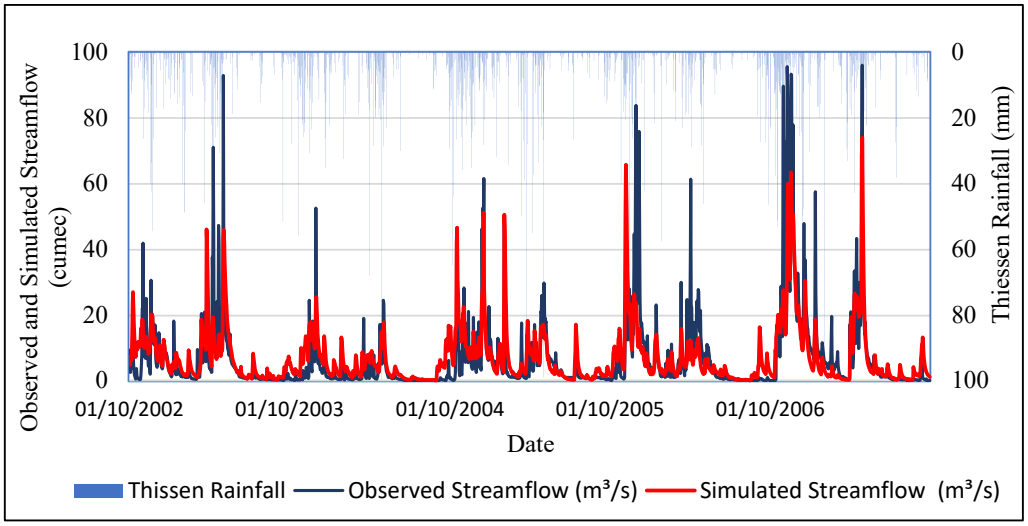

Figure 4-14 Observed and simulated streamflow hydrograph along thissen rainfall of Kirindi Oya river basin calibration period (2002/03-2006/07)

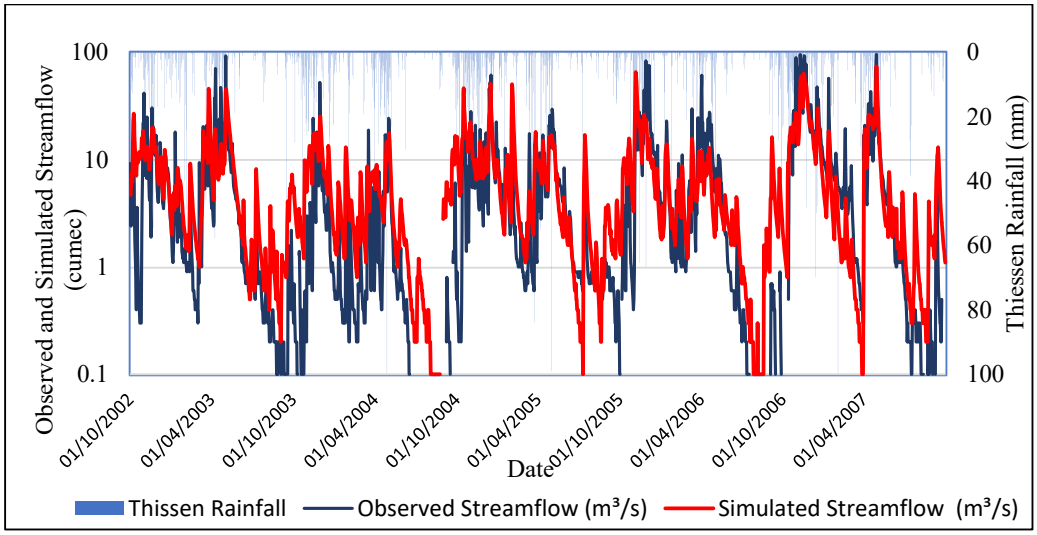

Figure 4-15 Observed and simulated streamflow hydrograph along thissen rainfall of Kirindi Oya river basin calibration period (2002/03-2006/07) in log scale

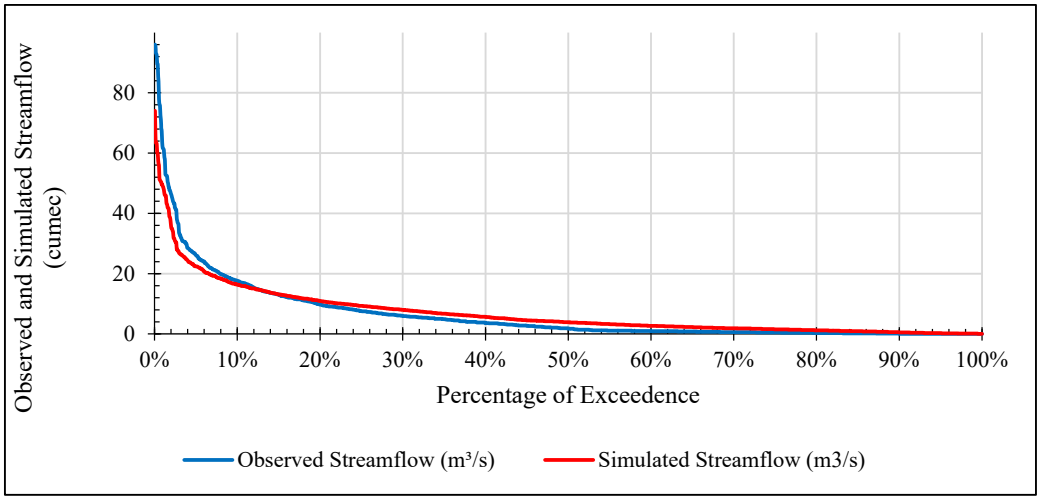

Figure 4-16 Observed and simulated streamflow Flow Duration Curve (FDC) of Kirindi Oya river basin calibration period (2002/03-2006/07)

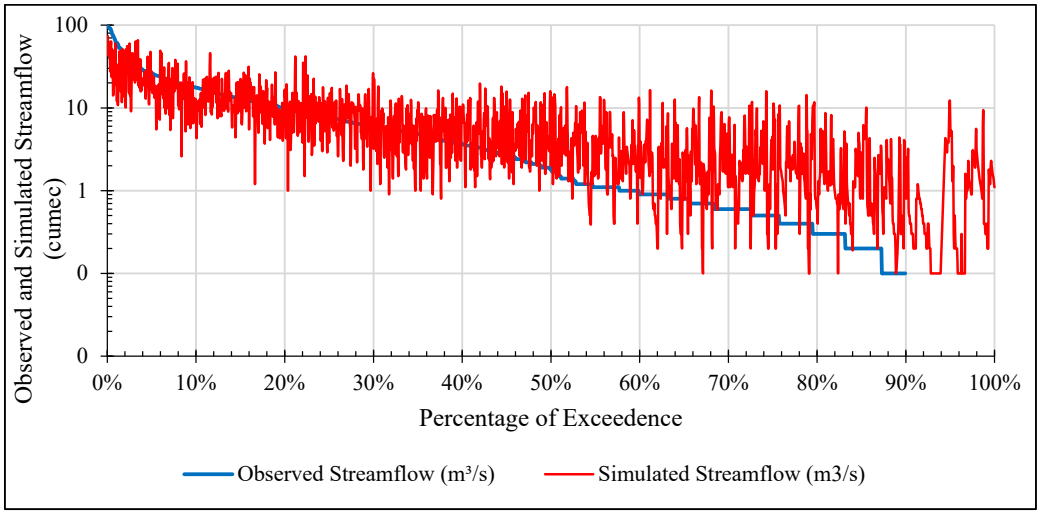

Figure 4-17 Observed and simulated streamflow thresholds of Kirindi Oya river basin calibration period (2002/03-2006/07)

Model Validation

Hydrographs comparison for both observed and simulated streamflow in normal and semi-log scales for Thanamalwila catchment are illustrated in Figure 4-18 to Figure 4-21 respectively. Flow duration curves for both sorted and sort only observed streamflow at the Thanamalwila catchment.

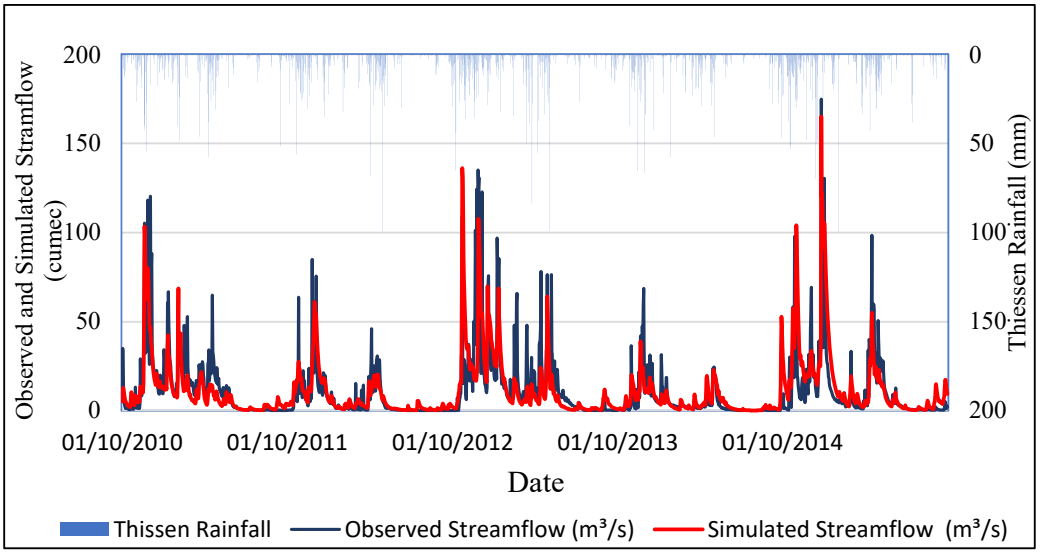

Figure 4-18 Observed and simulated streamflow hydrograph along thissen rainfall of Kirindi Oya river basin validation period (2010/11-20014/15)

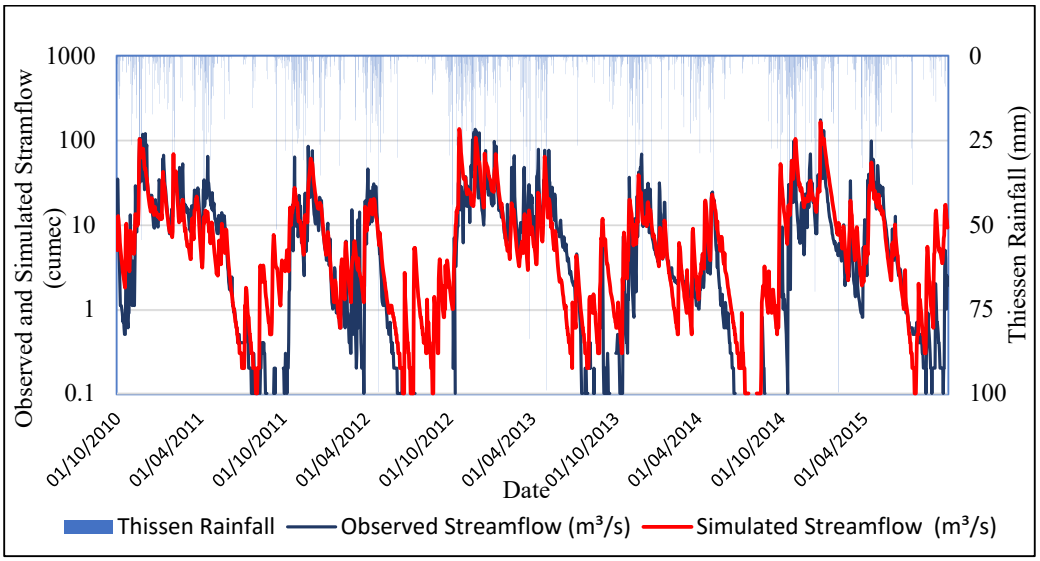

Figure 4-19 Observed and simulated streamflow hydrograph along thissen rainfall of Kirindi Oya river basin validation period (2010/11-2014/15) in log scale

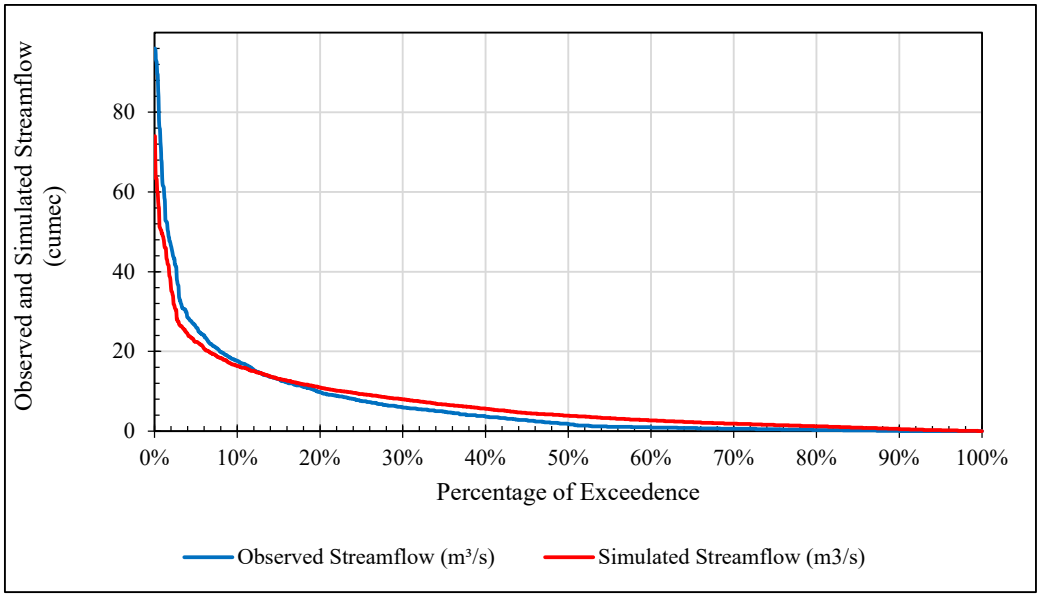

Figure 4-20 Observed and simulated streamflow Flow Duration Curve (FDC) of Kirindi Oya river basin validation period (2010/11-2014/15)

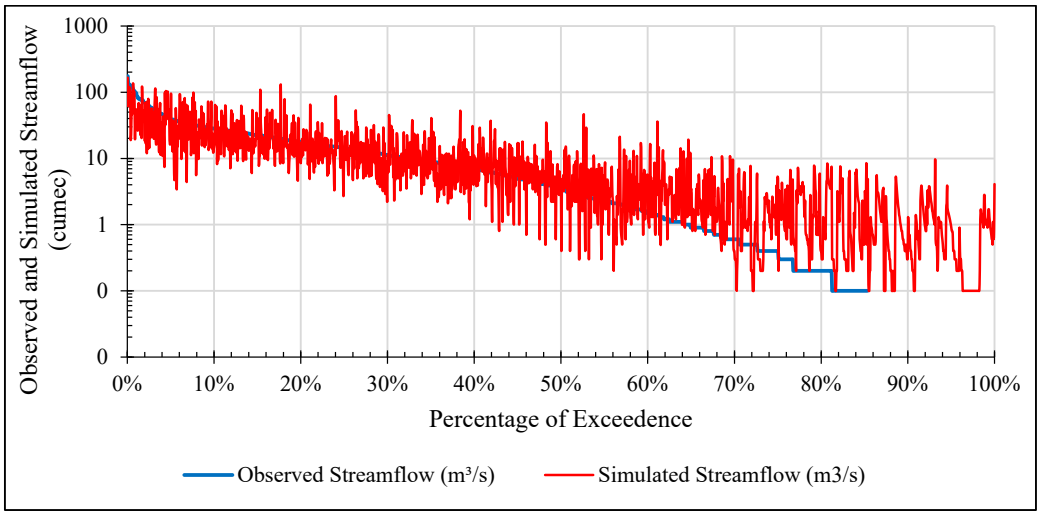

Figure 4-21 Observed and simulated streamflow thresholds of Kirindi Oya river basin validation period (2010/11-2014/15)

Model Run for Mid and End Century Period

Figure 4-22, represents 2048 has a high peak that is increased 3.0% from observed rainfall and 2nd peak occurs in 2058 has 2.5%. Runoff is increasing by the time period.

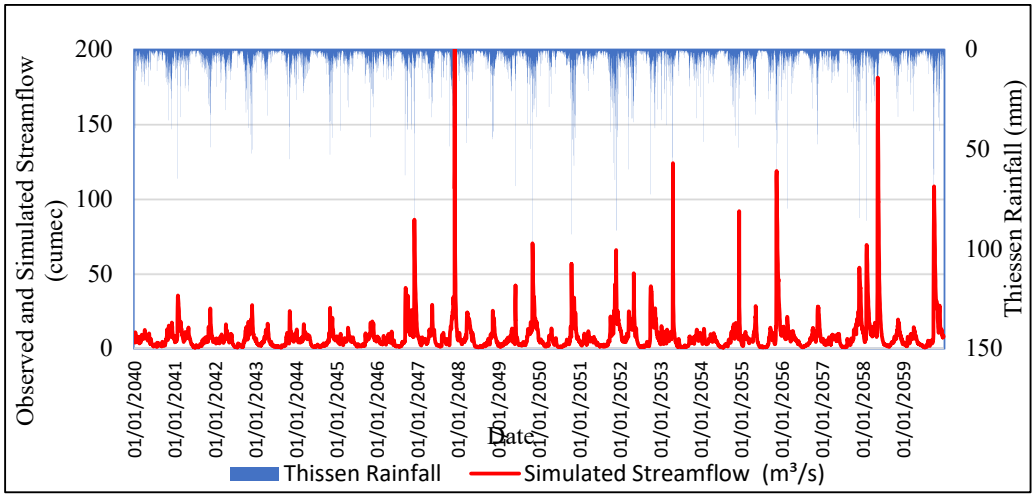

Figure 4-22 Simulated streamflow hydrograph along thissen rainfall of Kirindi Oya river basin Mid-century period (2040-2059) in validate HEC-HMS

Figure 4-23 shows 2088 has a high peak of 200 m^3/s and 2nd peak occurs in 2098 has 183 m^3/s but the maximum value is less than 50 m^3/s.

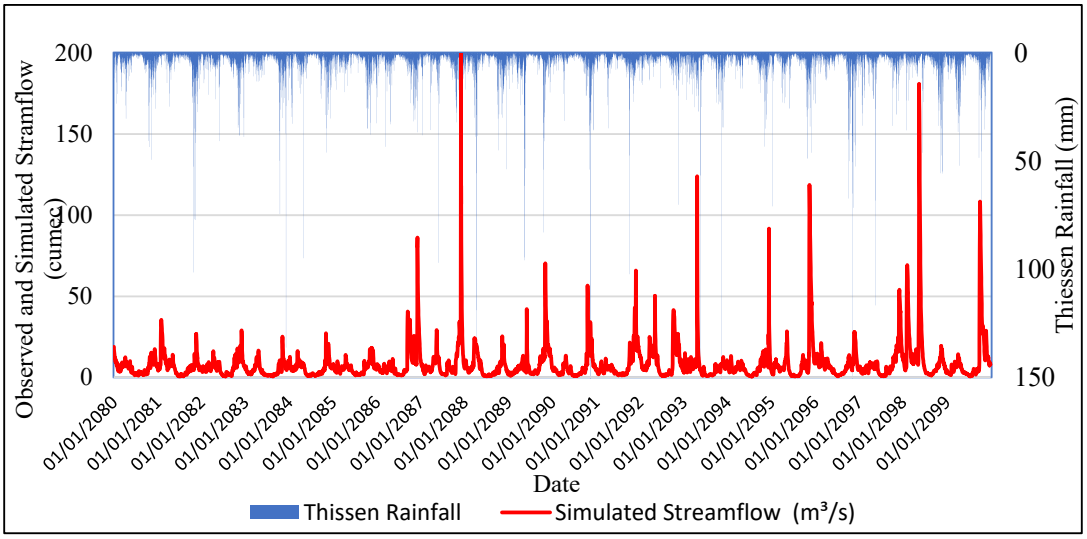

Figure 4-23 Simulated streamflow hydrograph along thissen rainfall of Kirindi Oya river basin End-century period (2080-2099) in validate HEC-HMS

4.3.4 Streamflow Drought Index (SDI)

4.3.4.1 Observed Period (1985/86 -2014/15)

At the Thanamalwila streamflow gauging stations, the SDI was estimated for three different time frames of 3, 6, and 12 months (Figure 4-24). Negative anomalies appear lower than the x-axis, whereas positive anomalies appear directly above. The time scale plays a role in drought severity, as shown by the red color bars which indicate severe drought according to Table 3-7. At annual time scales (October–September), the hydrological years 2000–2001 and 2003–2004 at Thanamalwila stations revealed various severe drought occurrences.

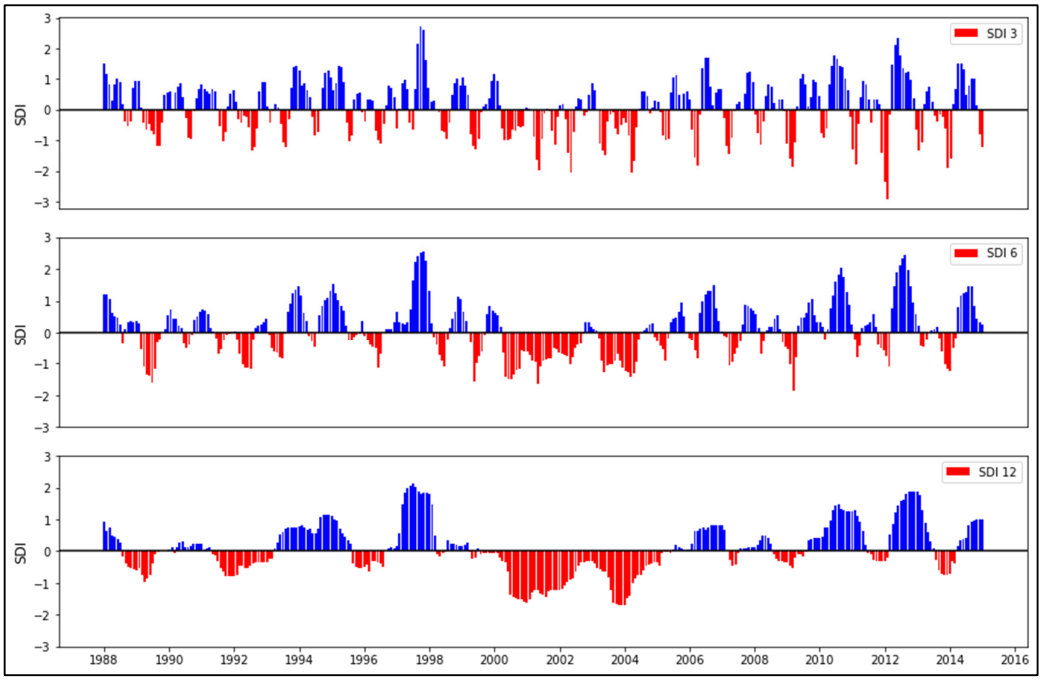

Figure 4-24 SDI variation in the Kirindi Oya river basin based on 3, 6, and 12 months for the observed period (1986-2015)

From 1985 to 2015, the time series of SDI at 3-month (October–December) were computed to demonstrate their probable value for identifying drought and monitoring drought risk (Figure 4-25). In the 3-month SDI time scale, the SDI frequencies fluctuated significantly above and below the zero line. Drought occurs whenever the SDI is negative, and the intensity decreases below –1.0. Drought occurrence events

found in the observed period are 9 extreme events, 14 severe, 36 moderate, and 101 mild droughts for 3-month scale, according to Figure 4-25.

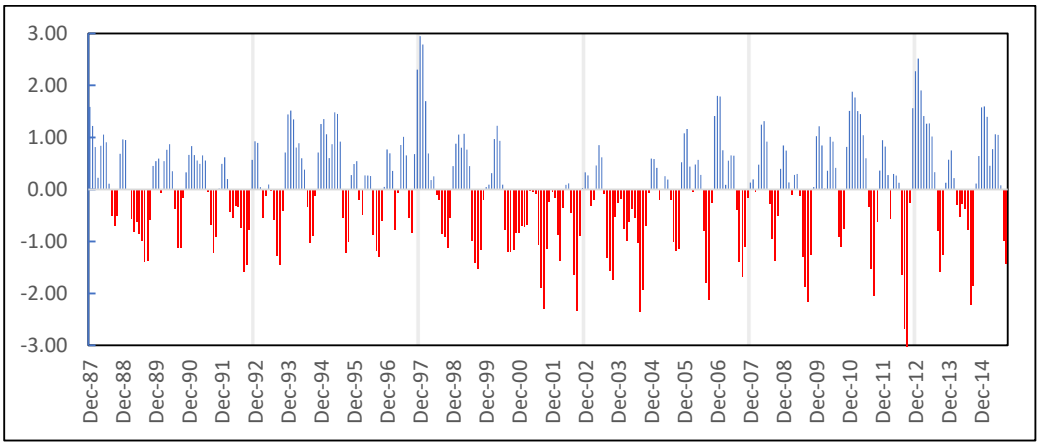

Figure 4-25 SDI variation in the Kirindi Oya river basin based on 3-month for the observed period (1986-2015)

From 1985 to 2015, the time series of SDI at 6-month periods (October–March) were computed to demonstrate their probable value for identifying drought and monitoring drought risk (Figure 4-26). In the 6-month SDI time scale, the SDI frequencies fluctuated significantly above and below the zero line. Drought occurs whenever the SDI is negative, and the intensity decreases below –1.0. Drought occurrence events found in the observed period are 2 extreme events, 14 severe, 41 moderate, and 107 mild droughts for 6-month scale, according to Figure 4-26.

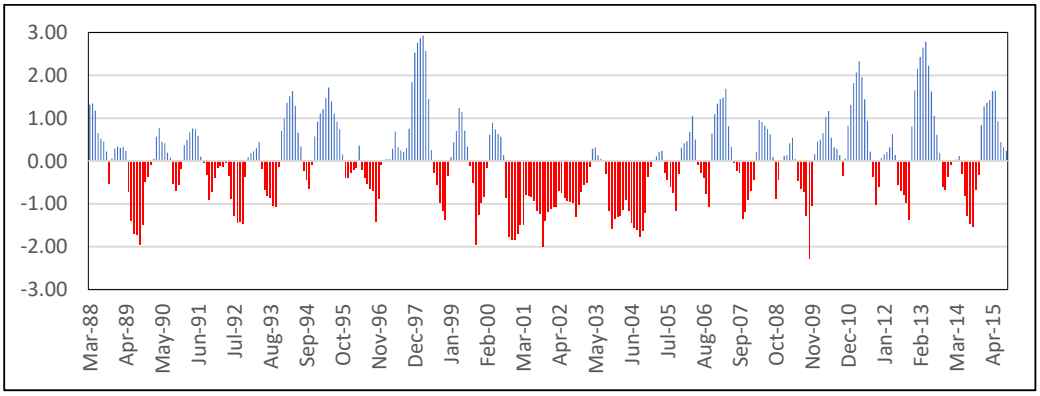

Figure 4-26 SDI variation in the Kirindi Oya river basin based on 6-month for the observed period (1986-2015)

From 1985 to 2015, the time series of SDI at 12-month/annual periods (October–September) were computed to demonstrate their probable value for identifying drought and monitoring drought risk (Figure 4-27). In the 12-month SDI time scale, the SDI frequencies fluctuated significantly above and below the zero line. Drought occurs whenever the SPI is negative, and the intensity decreases below –1.0. Drought occurrence events found in the observed period are 7 extreme events, 21 severe, 16 moderate, and 128 mild droughts for 12-month scale, according to Figure 4-27. As a result, the severity of drought changes throughout time. Furthermore, the magnitude of wet occurrences during all three SDI periods, 3-month, 6-month, and annual, is nearly the same (Figure 4-24).

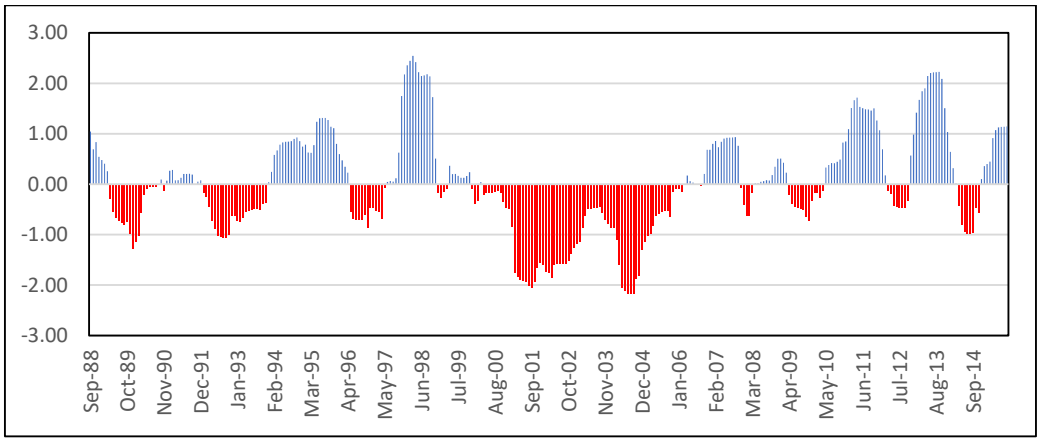

Figure 4-27 SDI variation in the Kirindi Oya river basin based on 12 months for the observed period (1986-2015)

4.3.4.2 Mid Century (2040 -2059)

From 2040 to 2059, the time series of SDI at 3-month (October–December) were computed to demonstrate their probable value for identifying drought and monitoring drought risk (Figure 4-28). In the 3-month SDI time scale, the SDI frequencies fluctuated significantly above and below the zero line. Drought occurs whenever the SDI is negative, and the intensity decreases below –1.0. Drought occurrence events found in the observed period are no extreme event, 9 severe, 30 moderate, and 94 mild droughts for 3-month scale, according to Figure 4-28.

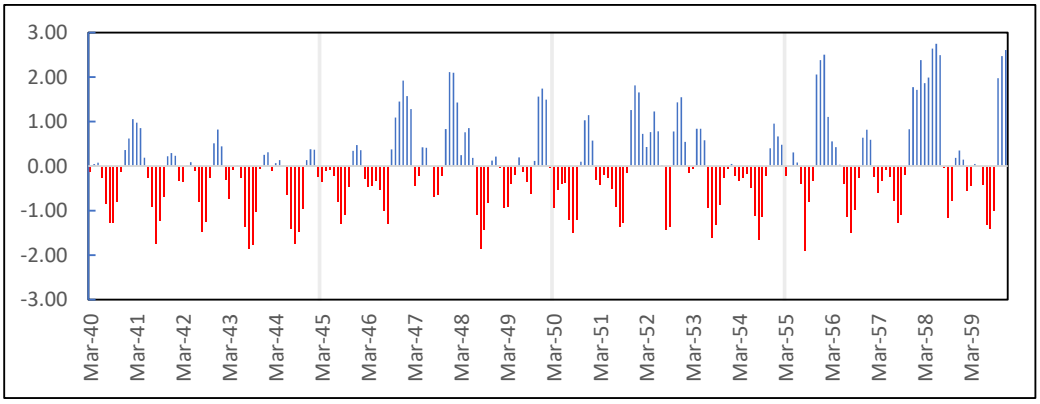

Figure 4-28 SDI variation in the Kirindi Oya river basin based on 3-month for mid-century (2040-2059) in RCP 8.5

From 2040 to 2059, the time series of SDI at 6-month periods (October–March) were computed to demonstrate their probable value for identifying drought and monitoring drought risk (Figure 4-29). In the 6-month SDI time scale, the SDI frequencies fluctuated significantly above and below the zero line. Drought occurs whenever the SDI is negative, and the intensity decreases below –1.0. Drought occurrence events found in the observed period are no extreme event, 3 severe, 26 moderate, and 110 mild droughts for 6-month scale, according to Figure 4-29.

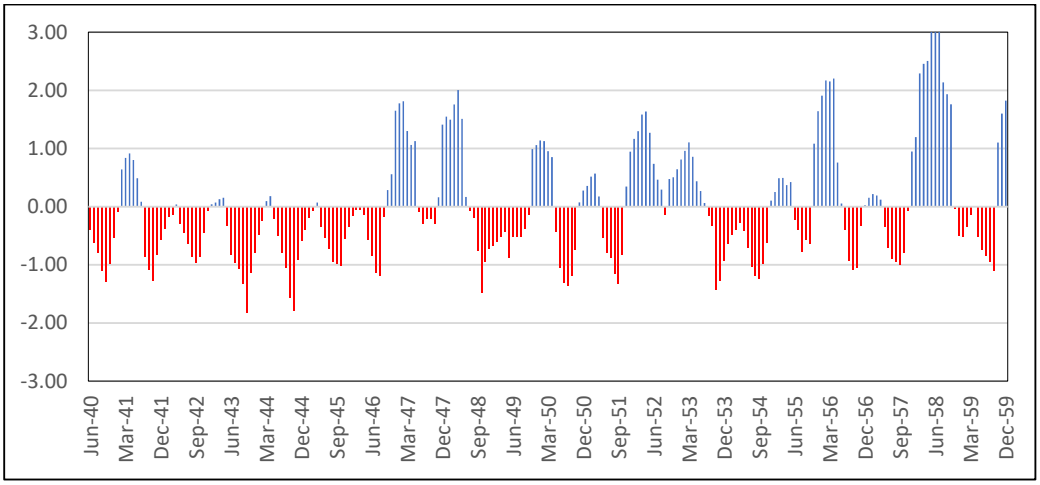

Figure 4-29 SDI variation in the Kirindi Oya river basin based on 6-month for mid-century (2040-2059) considering RCP 8.5

From 2040 to 2059, the time series of SDI at 12-month/annual periods (October–September) were computed to demonstrate their probable value for identifying drought and monitoring drought risk (Figure 4-30). In the 12-month SDI time scale, the SDI frequencies fluctuated significantly above and below the zero line. Drought occurs whenever the SDI is negative, and the intensity decreases below –1.0. Drought occurrence events found in the observed period are no extreme event, no severe, 29 moderate, and 109 mild droughts for 12-month scale, according to Figure 4-30. As a result, the severity of drought changes throughout time. Furthermore, the magnitude of wet occurrences during all three SDI periods, 3-month, 6-month, and annual, is nearly the same (Figure 4-30).

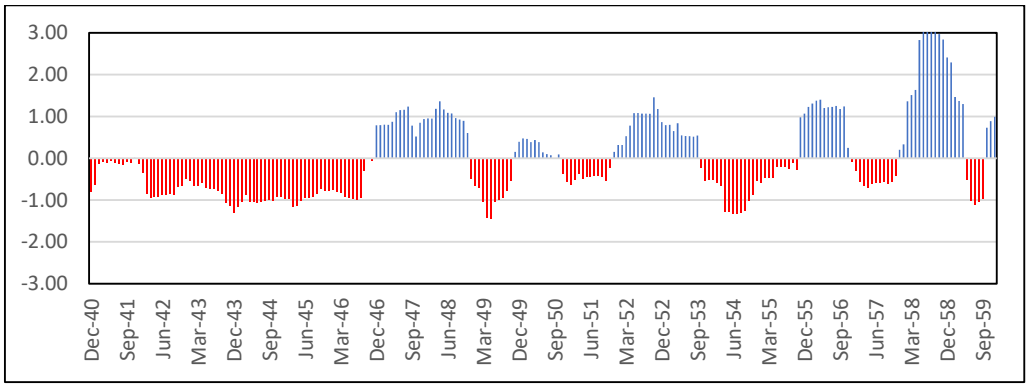

Figure 4-30 SDI variation in the Kirindi Oya river basin based on 12-month for mid-century (2040-2059) considering RCP 8.5

4.3.4.3 End Century (2080 -2099)

From 2080 to 2099, the time series of SDI at 3-month (October–December) were computed to demonstrate their probable value for identifying drought and monitoring drought risk (Figure 3-32). In the 3-month SDI time scale, the SDI frequencies fluctuated significantly above and below the zero line. Drought occurs whenever the SDI is negative, and the intensity decreases below –1.0. Drought occurrence events found in the observed period are no extreme event, no severe, 30 moderate, and 119 mild droughts for 3-month scale, according to Figure 3-32.

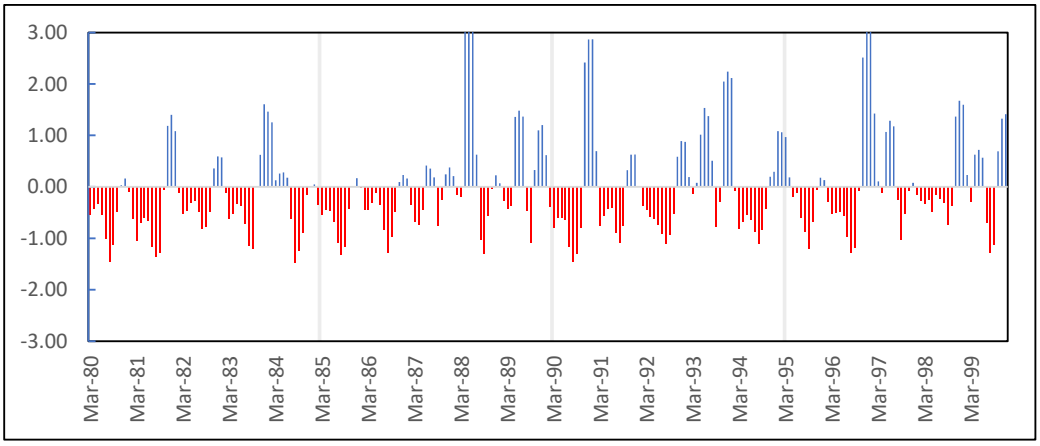

Figure 4-31 SDI variation in the Kirindi Oya river basin based on 3-month for mid-century (2080-2099) considering RCP 8.5

From 2080 to 2099, the time series of SDI at 6-month periods (October–March) were computed to demonstrate their probable value for identifying drought and monitoring drought risk (Figure 4-32). In the 6-month SDI time scale, the SDI frequencies fluctuated significantly above and below the zero line. Drought occurs whenever the SDI is negative, and the intensity decreases below –1.0. Drought occurrence events found in the observed period are no extreme event, no severe, 33 moderate, and 109 mild droughts for 6-month scale, according to Figure 4-32.

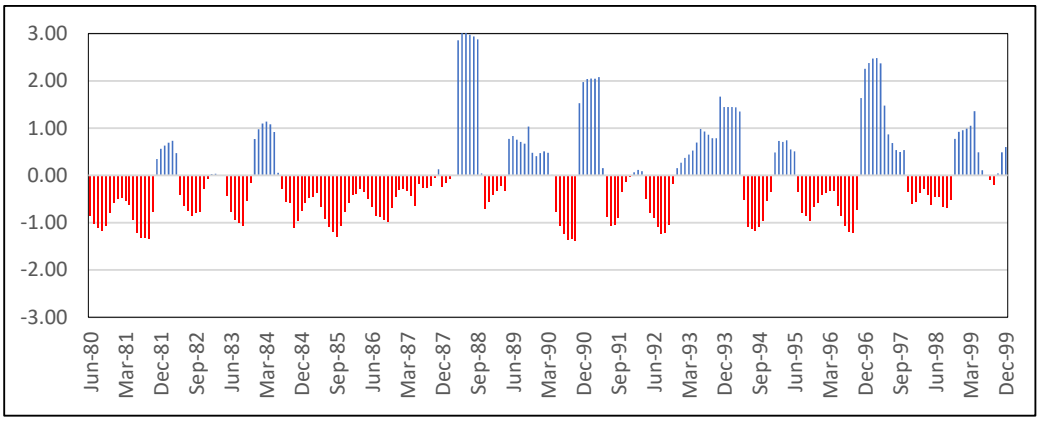

Figure 4-32 SDI variation in the Kirindi Oya river basin based on 6-month for mid-century (2080-2099)

From 2080 to 2099, the time series of SDI at 12-month/annual periods (October–September) were computed to demonstrate their probable value for identifying drought and monitoring drought risk (Figure 4-33). In the 12-month SDI time scale, the SDI frequencies fluctuated significantly above and below the zero line. Drought occurs whenever the SDI is negative, and the intensity decreases below –1.0. Drought occurrence events found in the observed period are no extreme event, no severe, 40 moderate, and 91 mild droughts for 12-month scale, according to Figure 4-33. As a result, the severity of drought changes throughout time. Furthermore, the magnitude of wet occurrences during all three SDI periods, 3-month, 6-month, and annual, is nearly the same (Figure 4-33).

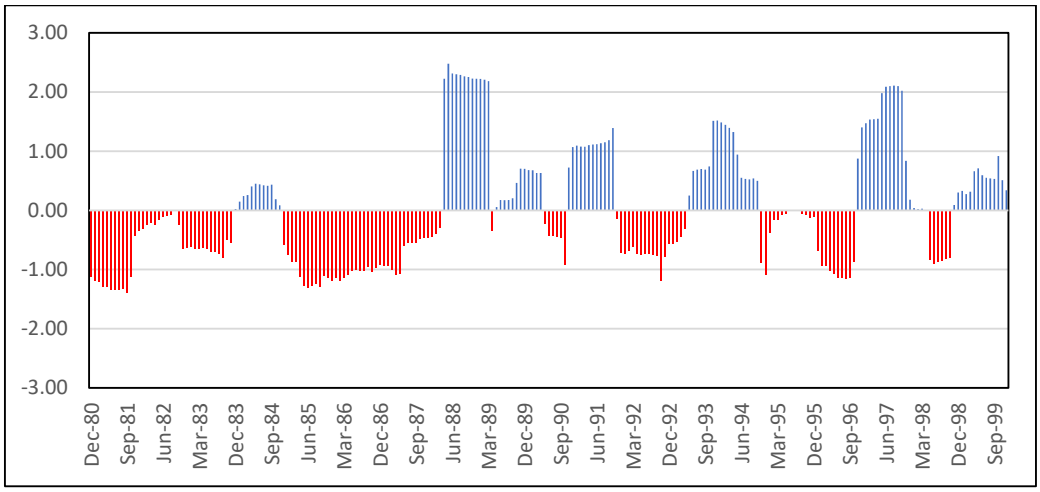

Figure 4-33 SDI variation in the Kirindi Oya river basin based on 12-month for mid-century (2080-2099) considering RCP 8.5

4.3.5 Seasonal Analysis (Kirindi Oya)

As mentioned in 3.6 about four seasons in Sri Lanka. The frequency analysis of selected drought indices has shown according to seasonal analysis. Among these four seasons which season shows the most drought-affected season. For analysing this seasonal situation consider hydrological water year which one following in Sri Lanka.

4.3.5.1 Second Inter Monsoon Period

This season considering October and November. This research work considers the observed period starts from 1985 to 2015.

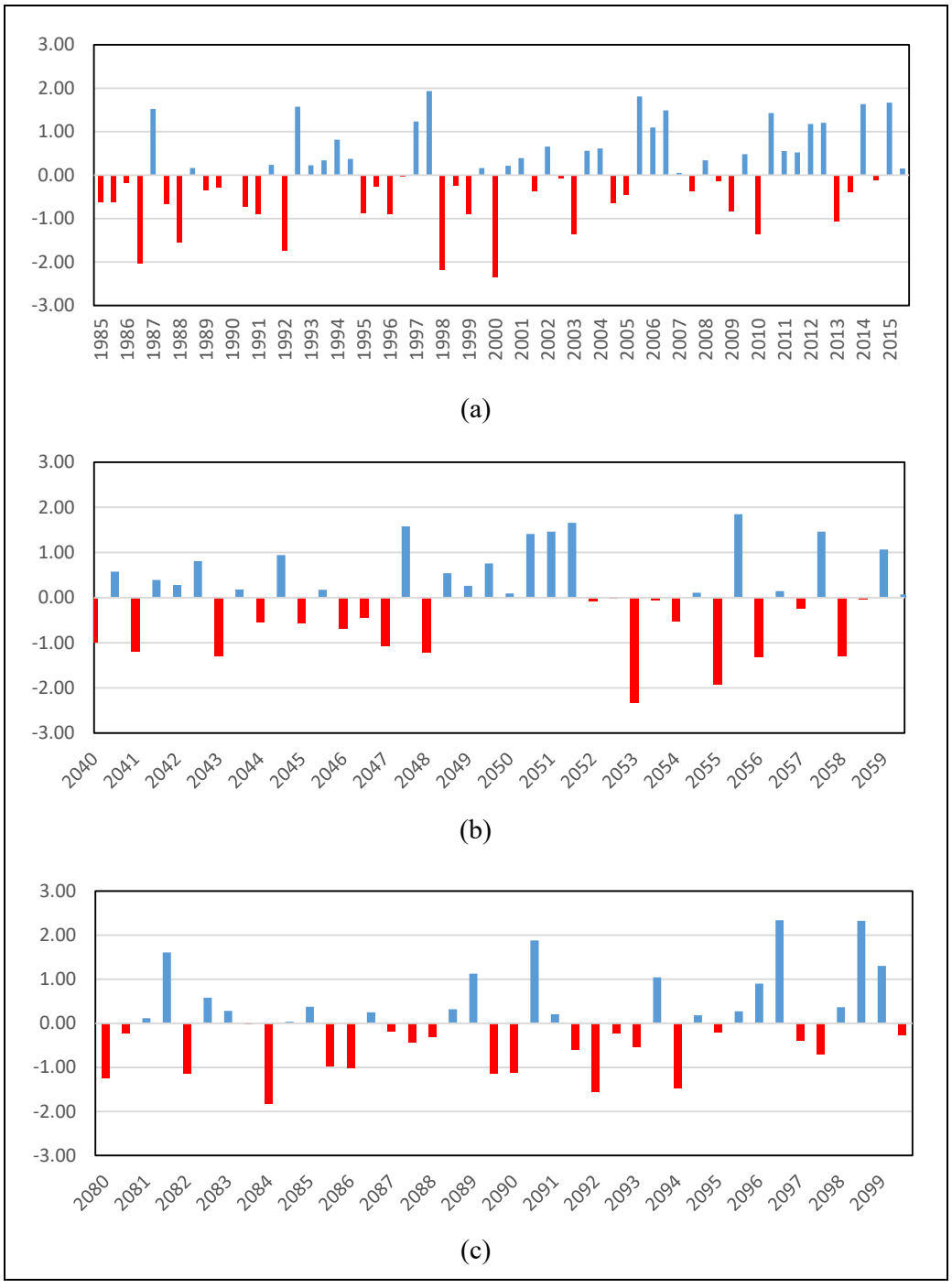

Figure 4-34 Standardized Precipitation Index in Second Inter Monsoon for (a) observed period, (b) mid-Century period, and (c) end-Century period in Kirindi Oya River basin

Standardized Precipitation Index in Second Inter Monsoon for the observed period, mid-century period, and end-century period in Kirindi Oya river basin are shown in Figure 3-34. For the seasonal analysis, all those monthly SPI values are plotted as a graph.

The second inter monsoon drought classification for different periods shows in Table 4-3. According to historical data, extreme drought may decrease by 50% in the mid-century period, and extreme drought may not occur that much in the end-of-century period. In the mid-century, severe droughts may decrease by 50%, and in the end-century, the same type of drought as observed may occur. In the case of mild drought, the probability of occurrence could be doubled as compared to the observed period. Mild drought is less harmful to the environment, however, in this study, the percentage variation of mild drought will decrease by 48% in the mid-century and by 38% at the end of the century. During the last non-drought percentage variation may reduce by 25% in the mid-century and 32% in the end-century.

Table 4-3 Event identification of SPI values in Second Inter Monsoon and the percentage variation of the mid and end-century based on the observed period

Drought Type	Observed Period	Mid-Century	End-Century
Non-drought	28	21 (-25%)	19 (-32%)
Mild drought	21	11 (-48%)	13 (-38%)
Moderate drought	3	6 (100%)	6 (100%)
Severe drought	2	1 (-50%)	2 (0%)
Extreme drought	2	1 (-50%)	0 (-100%)

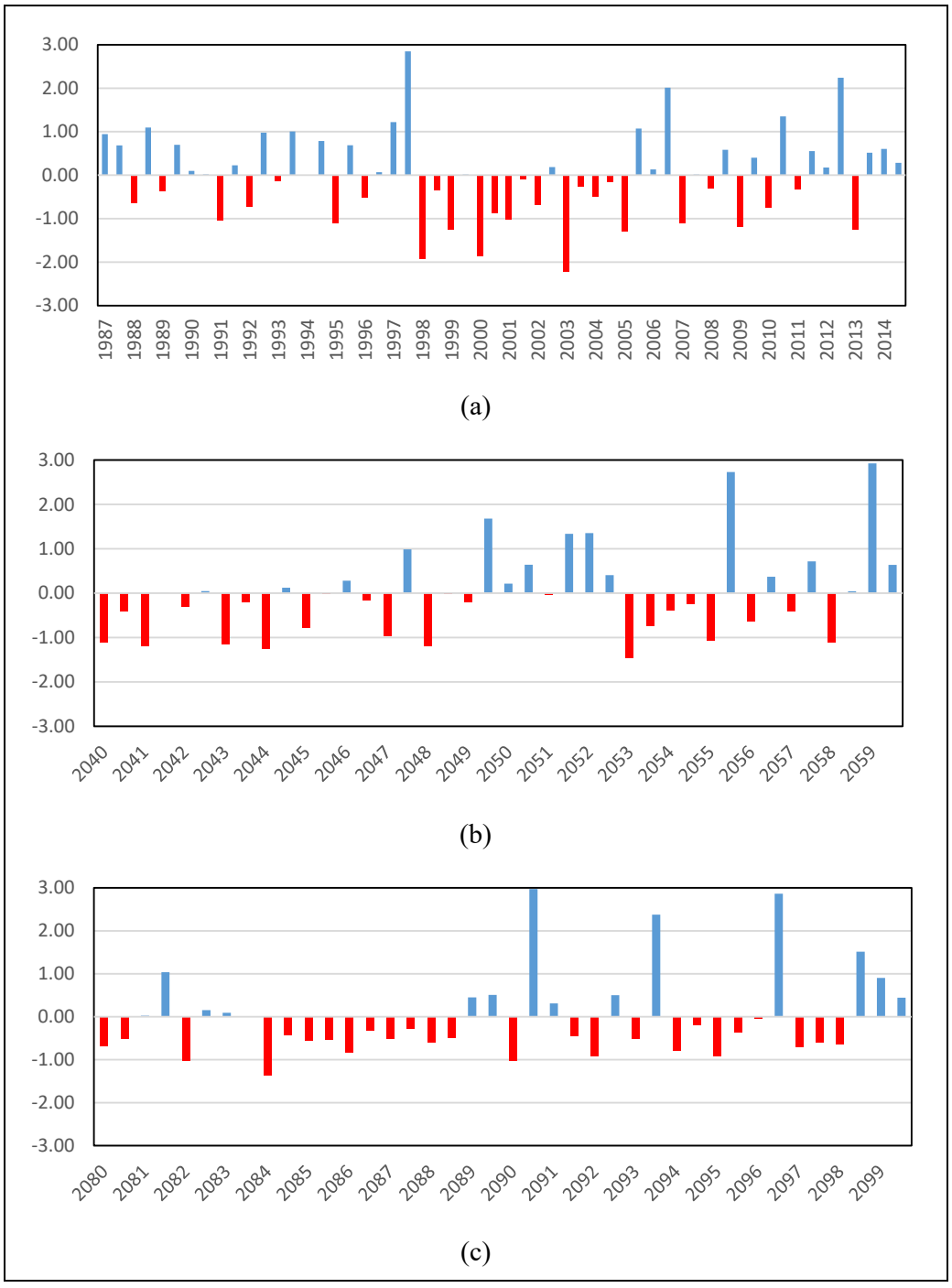

Figure 4-35 Streamflow Drought Index in Second Inter Monsoon for (a) observed period, (b) mid-century period, and (c) end-century period in Kirindi Oya River basin

Streamflow Drought Index in Second Inter Monsoon for the observed period, Mid-Century period, and End-Century period in Kirindi Oya river basin is shown in Figure 4-35. For the seasonal analysis, all those monthly SDI values are plotted as a graph.

The second inter monsoon drought classification for different periods shows in Table 4-4. According to observed data, extreme and severe drought may not occur that much in both mid and end century periods. The moderate drought may occur the same in the mid-century but at the end of the century, it may decrease 63%. The percentage mild drought variation may occur same as observed period but in the end-century 47% may increase. During the non-drought percentage, variation may reduce by 43% in the mid-century and 50% in the end-century.

Table 4-4 Event identification of SDI values in Second Inter Monsoon and the percentage variation of the Mid and End-century based on the observed period

Drought Type	Observed Period	Mid-Century	End-Century
Non-drought	30	17 (-43%)	15 (-50%)
Mild drought	15	15 (0%)	22 (47%)
Moderate drought	8	8 (0%)	3 (-63%)
Severe drought	2	0 (-100%)	0 (-100%)
Extreme drought	1	0 (-100%)	0 (-100%)

4.3.5.2 Northeast Monsoon

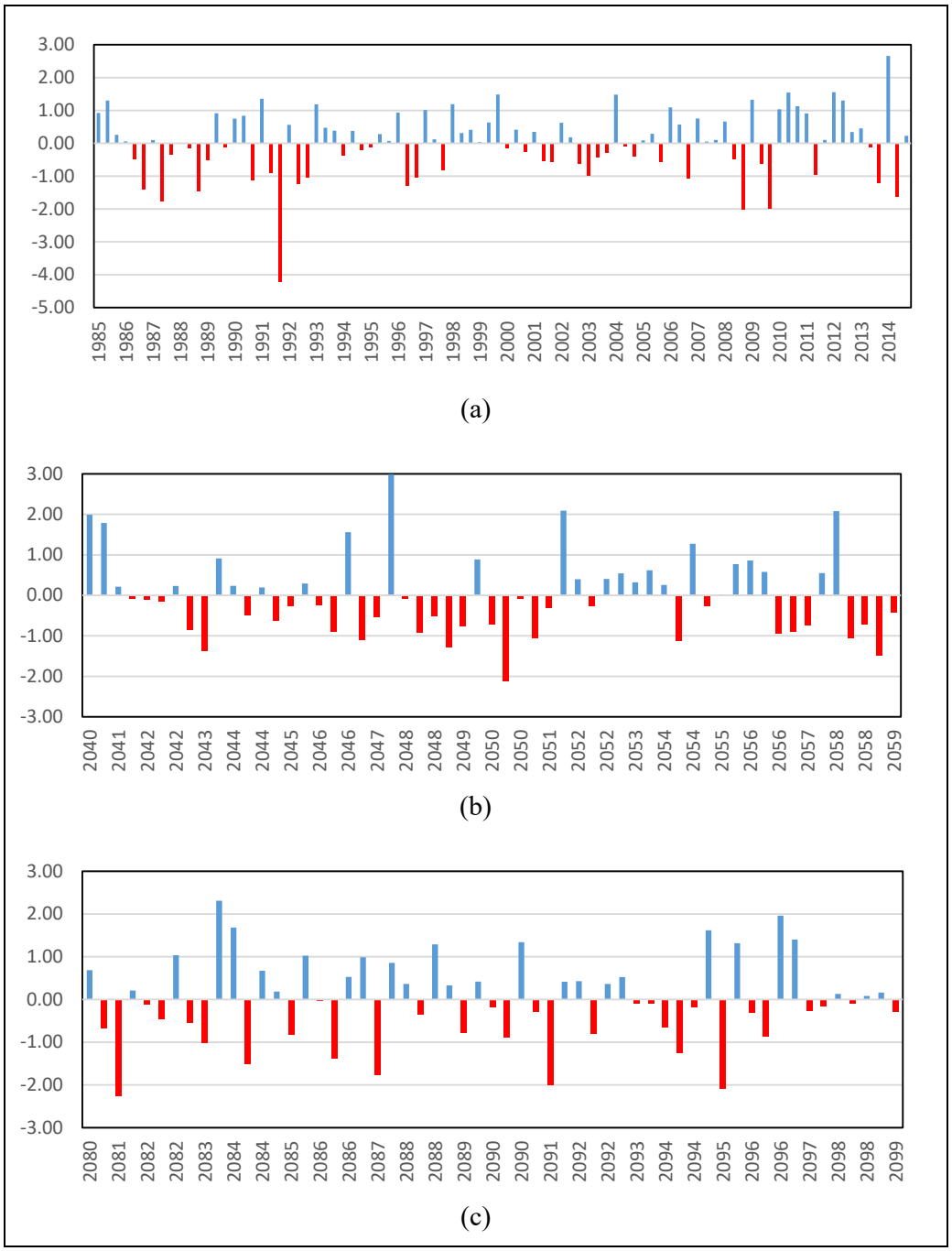

Figure 4-36 Standardized Precipitation Index in Northeast Monsoon for (a) observed period, (b) mid-century period, and (c) end-century period in Kirindi Oya River basin

Standardized Precipitation Index in Northeast Monsoon for the observed period, Mid-Century period, and End-Century period in Kirindi Oya river basin are shown in the Figure 4-36. For the seasonal analysis, all those monthly SPI values are plotted as a graph.

In the Northeast Monsoon, drought classification for different periods shows in Table 4-5. According to observed period data, extreme drought may decrease by 50% in the mid-century period and may increase 50% in the end-of-century period. In the mid-century, severe droughts may decrease by 100%, and in the end-century drought has decreased by 33%. In the case of moderate and mild drought, the probability of occurrence may not increase in this NEM period.

Table 4-5 Event identification of SPI values in Northeast Monsoon and the percentage variation of the mid and end-century based on the observed period

Drought Type	Observed Period	Mid-Century	End-Century
Non-drought	47	25 (-47%)	27 (-43%)
Mild drought	24	24 (0%)	22 (-8%)
Moderate drought	8	7 (-13%)	3 (-63%)
Severe drought	3	0 (-100%)	2 (-33%)
Extreme drought	2	1 (-50%)	3 (50%)

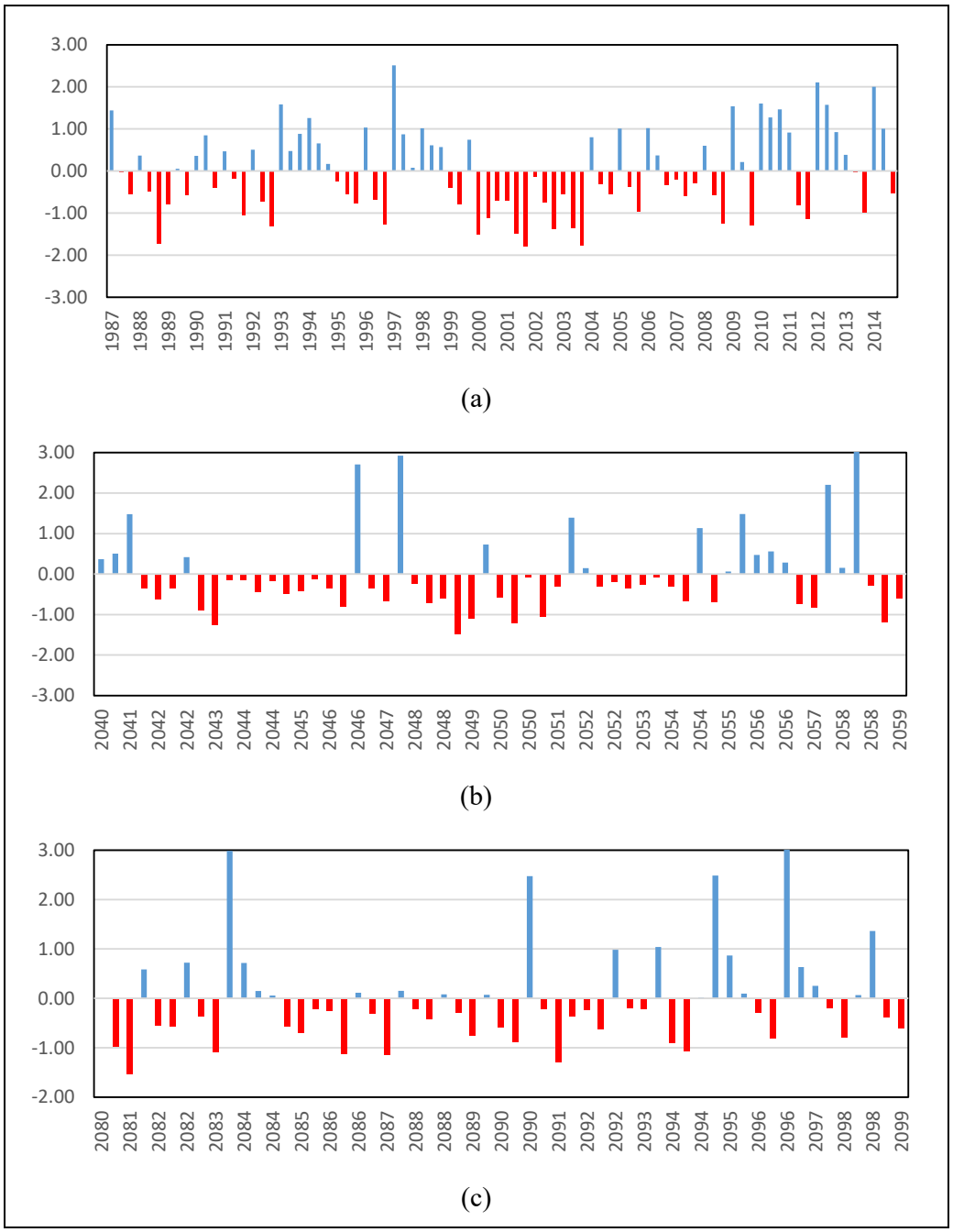

Figure 4-37 Streamflow Drought Index in Northeast Monsoon for (a) observed period, (b) mid-Century period, and (c) end-Century period in Kirindi Oya River basin

Streamflow Drought Index in Second Inter Monsoon for the observed period, Mid-Century period, and End-Century period in Kirindi Oya river basin is shown in Figure 4-37. For the seasonal analysis, all those monthly SDI values are plotted as a graph.

The second inter monsoon drought classification for different periods shows in Table 4-6. According to Observed data, in this monsoon all the types will decrease then it can be predicted that in this season probability of occurrence will reduce.

Table 4-6 Event identification of SDI values in Northeast Monsoon and the percentage variation of the mid and end-century based on the observed period

Drought Type	Observed Period	Mid-Century	End-Century
Non-drought	0	0 (0%)	0 (0%)
Mild drought	32	33 (3%)	29 (-9%)
Moderate drought	10	6 (-40%)	5 (-50%)
Severe drought	4	0 (-100%)	1 (-75%)
Extreme drought	1	0 (-100%)	0 (-100%)

4.3.5.3 First Inter Monsoon Period

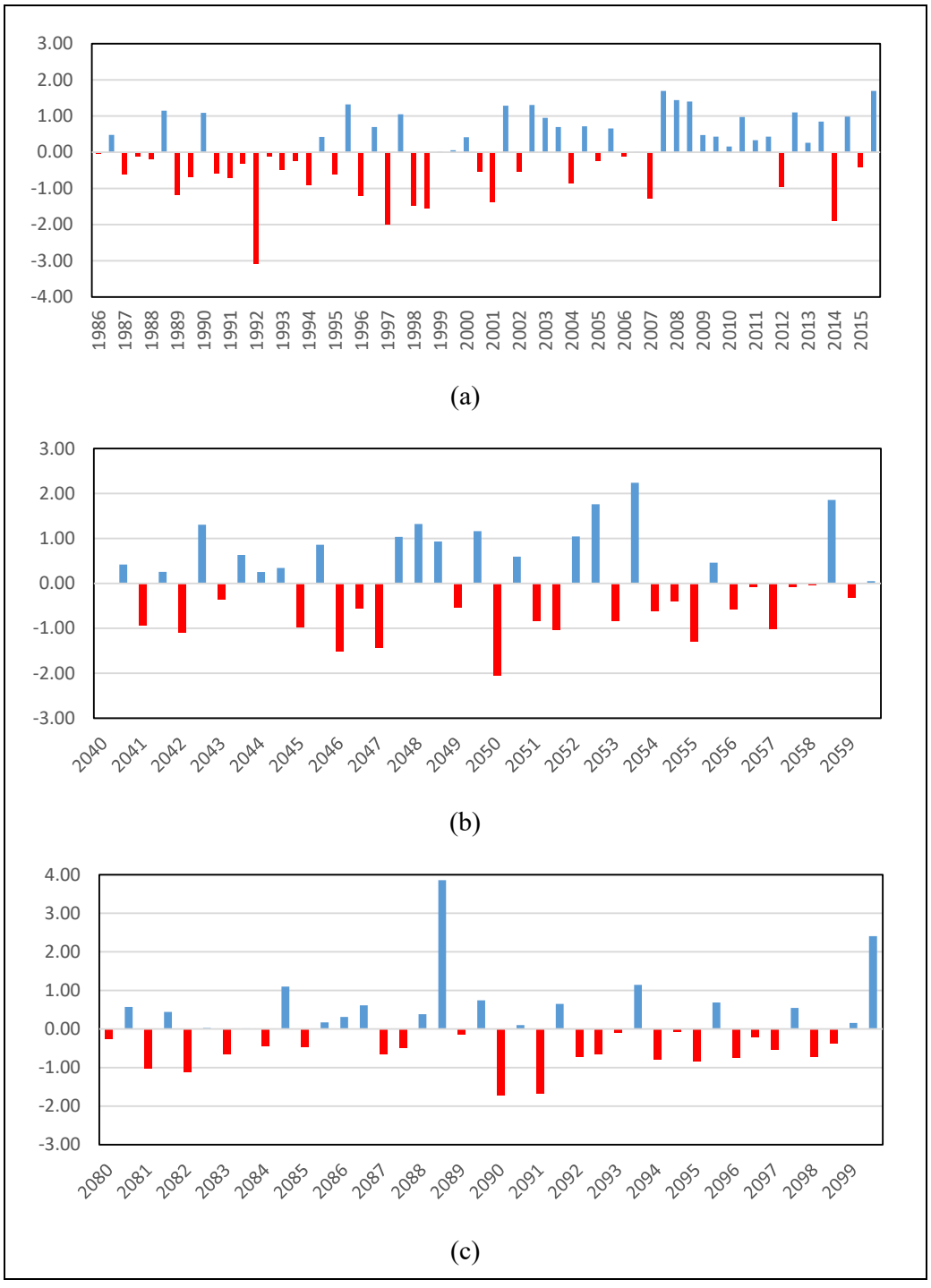

Figure 4-38 Standardized Precipitation Index in First Inter Monsoon for (a) observed period, (b) mid-century period, and (c) end-century period in Kirindi Oya River basin

Standardized Precipitation Index in First Inter Monsoon for the observed period, Mid-Century period, and End-Century period in Kirindi Oya river basin are shown in Figure 4-38. For the seasonal analysis, all those monthly SPI values are plotted as a graph.

In the First Inter Monsoon drought classification for different periods shown in Table 4-7. Compare the observed data all the drought types will reduce in the both mid and end-century the probability of occurrence may not increase in this FIM season.

Table 4-7 Event identification of SPI values in First Inter Monsoon and the percentage variation of the mid and end-century based on the observed period

Drought Type	Observed Period	Mid-Century	End-Century
Non-drought	30	18 (-40%)	18 (-40%)
Mild drought	17	15 (-12%)	18 (6%)
Moderate drought	5	5 (0%)	2 (-60%)
Severe drought	3	1 (-67%)	2 (-33%)
Extreme drought	1	1 (0%)	0 (-100%)

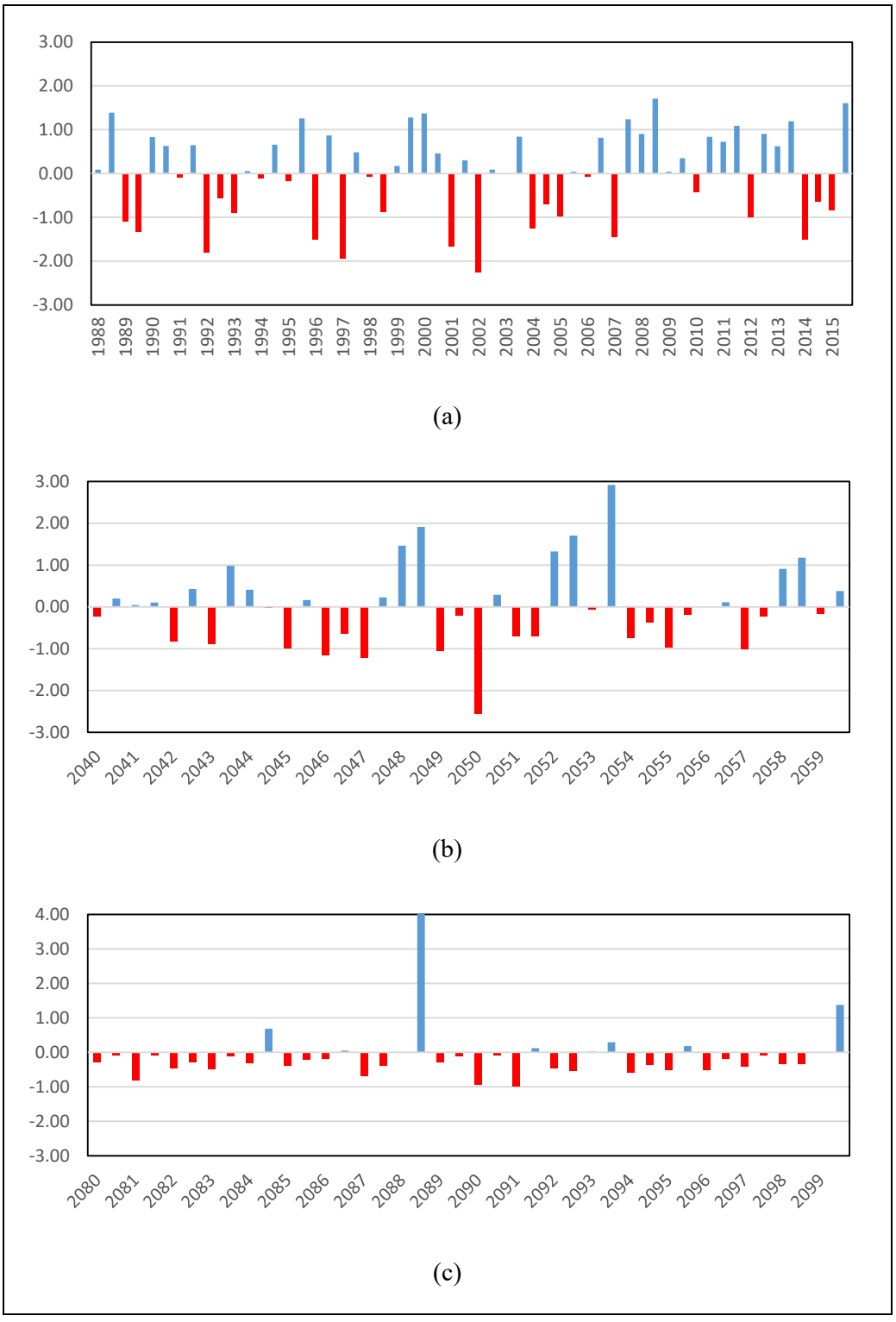

Figure 4-39 Streamflow Drought Index in First Inter Monsoon for (a) observed period, (b) mid-century period, and (c) end-century period in Kirindi Oya River basin

Streamflow Drought Index in First Inter Monsoon for the observed period, Mid-Century period, and End-Century period in Kirindi Oya river basin are shown in Figure 4-39. For the seasonal analysis, all those monthly SDI values are plotted as a graph.

The First inter monsoon drought classification for different periods shows in Table 4-8. According to Observed data, extreme drought may same in mid-century, but the end century may not occur, and severe drought may not occur that much in both mid and end century periods. The moderate drought may occur the same in the mid-century but at the end of the century, it will occur. The percentage of mild drought variation may increase by 7% in the mid-century but in the end-century, 107% may increase. During the non-drought percentage, variation may reduce by 39% in the mid-century and 71% in the end-century.

Table 4-8 Event identification of SDI values in First Inter Monsoon and the percentage variation of the mid and end-century based on the observed period

Drought Type	Observed Period	Mid-Century	End-Century
Non-drought	31	19 (-39%)	9 (-71%)
Mild drought	15	16 (7%)	31 (107%)
Moderate drought	4	4 (0%)	0 (-100%)
Severe drought	5	0 (-100%)	0 (-100%)
Extreme drought	1	1 (0%)	0 (-100%)

4.3.5.4 Southwest Monsoon Period

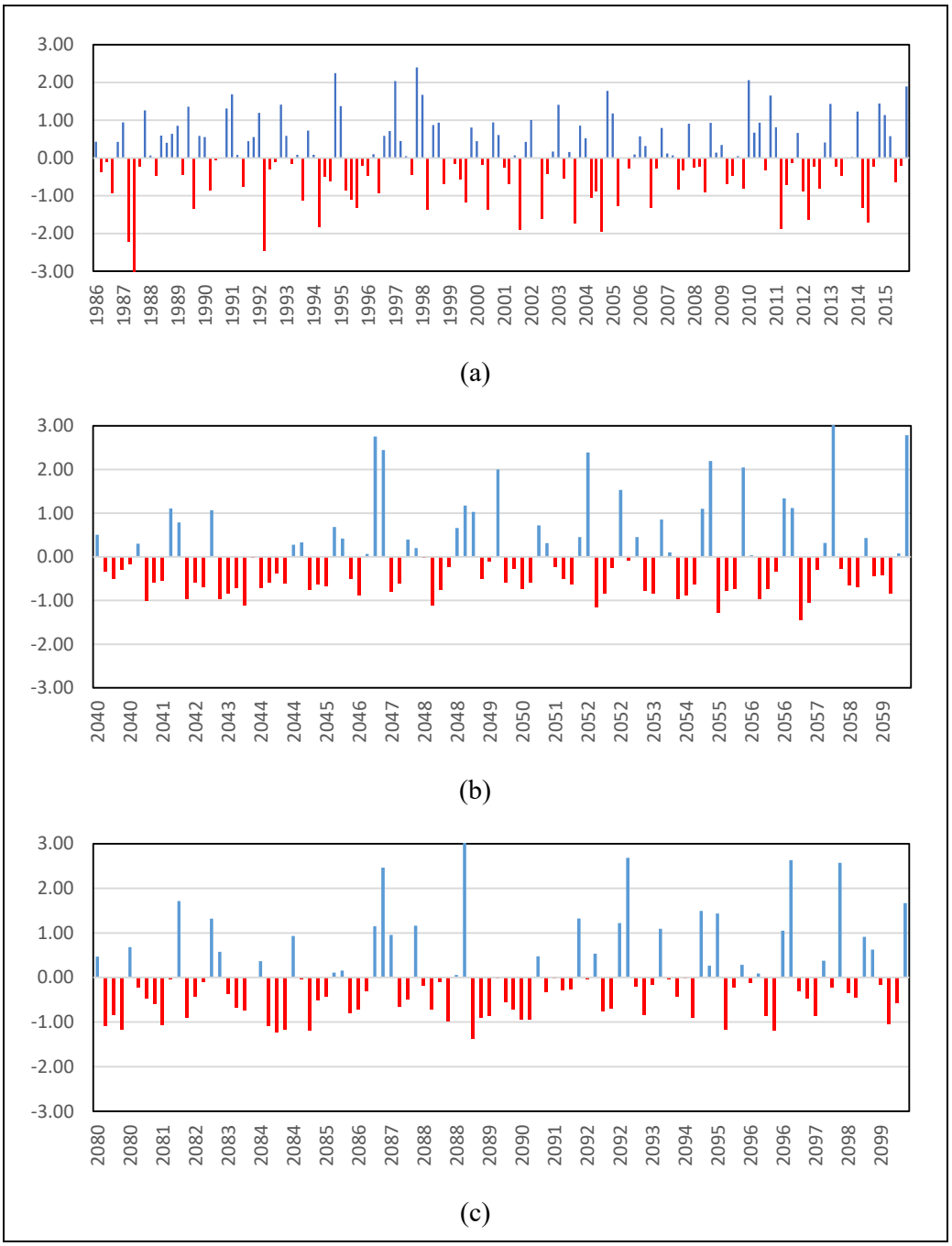

Figure 4-40 Standardized Precipitation Index in Southwest Monsoon for (a) observed period, (b) mid-century period, and (c) end-century period in Kirindi Oya River basin

Standardized Precipitation Index in Southwest Monsoon for the observed period, Mid-Century period, and End-Century period in Kirindi Oya river basin are shown in Figure 4-40. For the seasonal analysis, all those monthly SPI values are plotted as a graph.

In the Southwest Monsoon drought classification for different periods shows in Table 4-9. Compare the observed data all the drought types will reduce in the both mid and end-century but for mild drought, it will increase 19% in mid-century and 17% in end-century.

Table 4-9 Event identification of SPI values in Southwest Monsoon and the percentage variation of the mid and end-century based on the observed period

Drought Type	Observed Period	Mid-Century	End-Century
Non-drought	73	37 (-49%)	34 (-53%)
Mild drought	47	56 (19%)	55 (17%)
Moderate drought	11	7 (-36%)	11 (0%)
Severe drought	9	0 (-100%)	0 (-100%)
Extreme drought	0	0 (0%)	0 (0%)

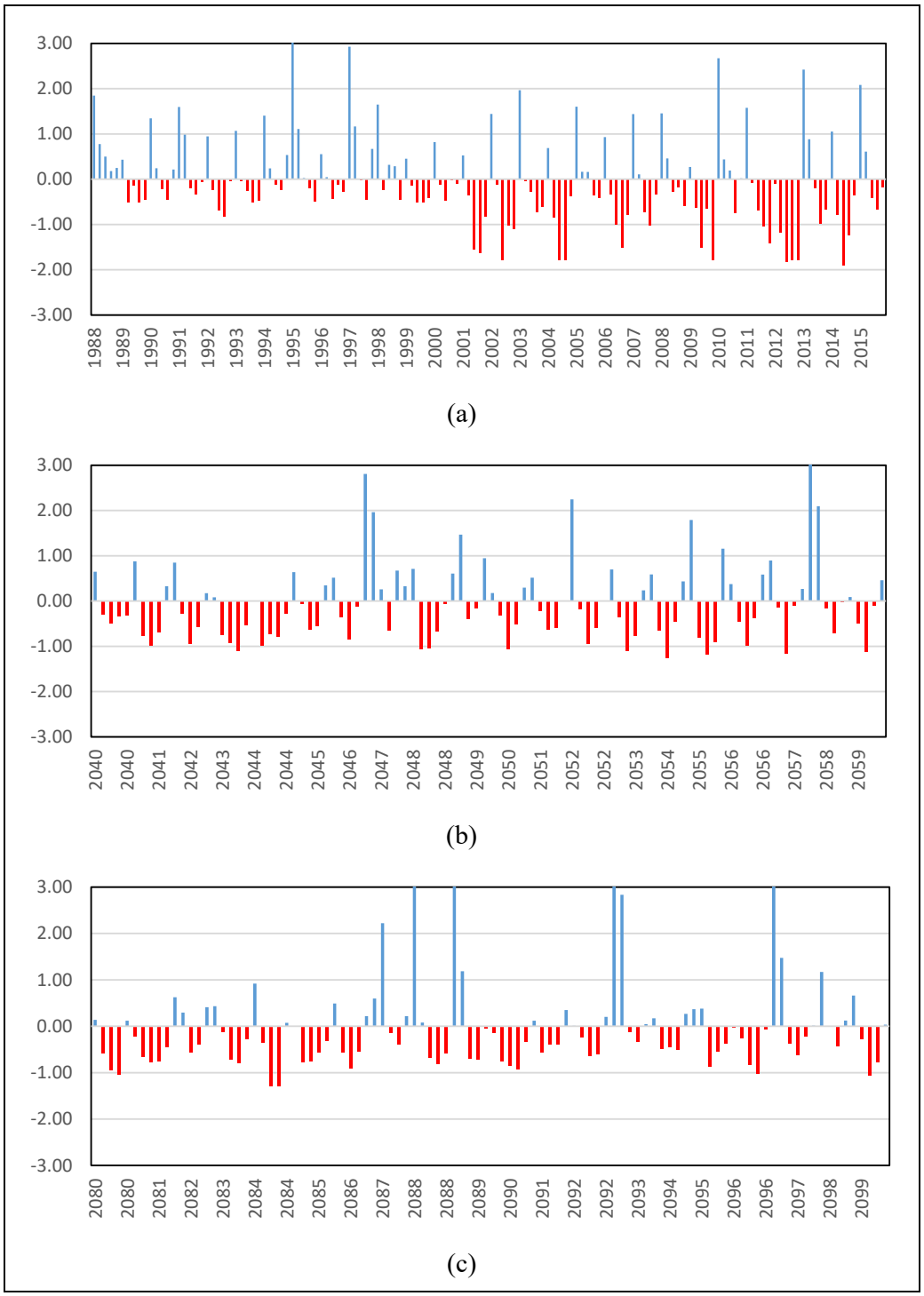

Figure 4-41 Streamflow Drought Index in Southwest Monsoon for (a) observed period, (b) mid-century period, and (c) end-century period in Kirindi Oya River basin

Streamflow Drought Index in First Inter Monsoon for the observed period, Mid-Century period, and End-Century period in Kirindi Oya river basin are shown in Figure 4-39. For the seasonal analysis, all those monthly SDI values are plotted as a graph.

In the Northwest monsoon drought classification for different periods shows in Table 4-10. According to Observed data, all types of may reduce for both mid and end-century only in the moderate drought 13% will increase for the mid-century period.

Table 4-10 Event identification of SDI values in Northwest Monsoon and the percentage variation of the mid and end-century based on the observed period

Drought Type	Observed Period	Mid-Century	End-Century
Non-drought	52	37 (-29%)	35 (-33%)
Mild drought	68	54 (-21%)	60 (-12%)
Moderate drought	8	9 (13%)	5 (-38%)
Severe drought	12	0 (-100%)	0 (-100%)
Extreme drought	0	0 (0%)	0 (0%)

4.4 Study Area 2 (Kelani River)

4.4.1 Normalized Difference Vegetation Index (NDVI)

This project observed time scale is from 1985 to 2015 and for this NDVI shown here every decade one map. For calculating 1986, 1995, and 2006 NDVI values, relevant images were collected from Landsat 4-5 and Landsat 8 (2015 image). In this study, the reference time scale is from 1985 to 2015, and the decadal NDVI variations are shown in Figure 4-42.

The 1986 NDVI plot comprises its maximum values between 0.2 to 0.5 (moderate range), which indicate non-vegetation coverage (map (A) of Figure 4-42). Map (B) of the same figure shows a high NDVI value in 1995, indicating maximum area vegetation coverage.

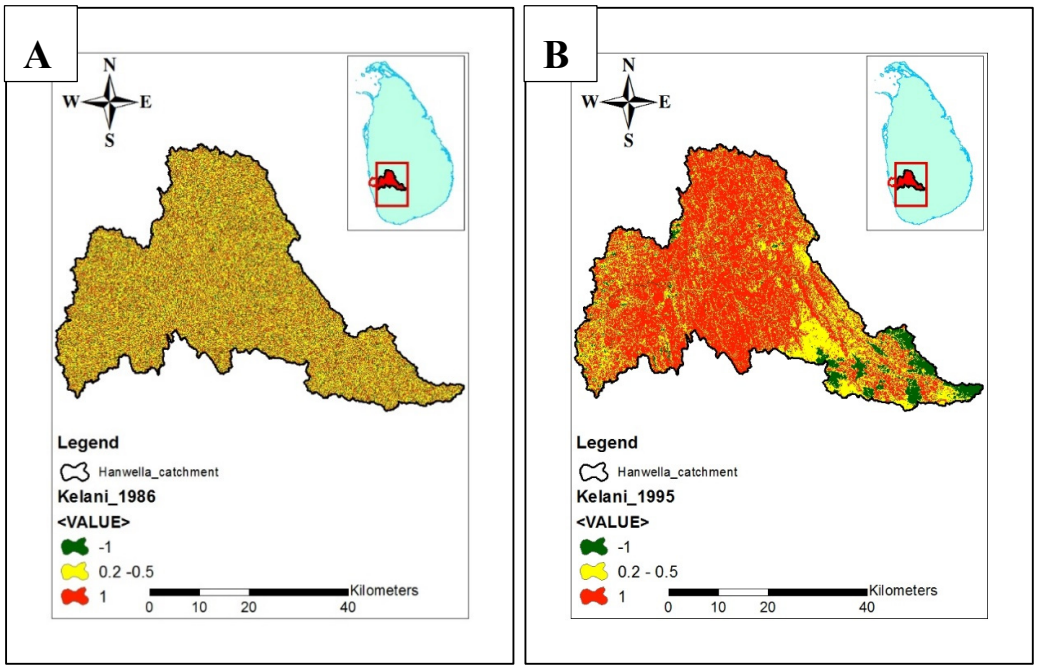

Figure 4-42 NDVI for A. 1986 and B. 1995 in the Hanwella basin which is sub basin of the Kelani River basin

Map (C) of Figure 4-43 shows 2006 NDVI and it has been showing low coverage and moderate coverage also. Map (D) of Figure 4-43 is showing 2015 NDVI which most of the area is in severe coverage. Upstream of the catchment shows low coverage of NDVI.

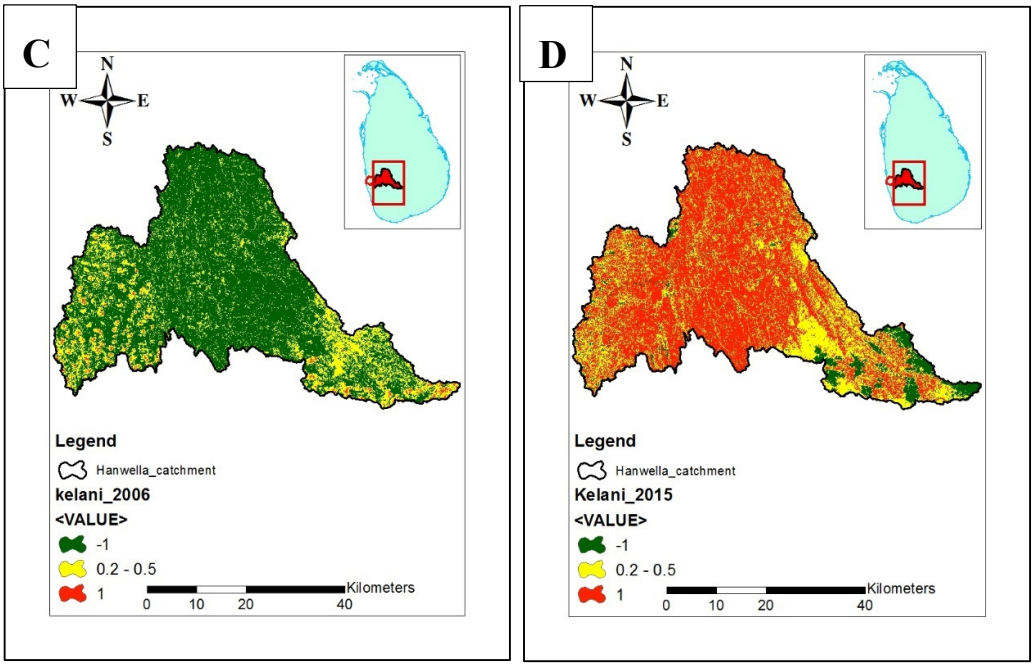

Figure 4-43 NDVI for C. 2006 and B. 2015 in the Hanwella basin which is sub basin of the Kelani River basin

4.4.2 Standardized Precipitation Index (SPI)

4.4.2.1 *Observed Period (1985/86 -2014/15)*

The yearly SPI variation over the complete Kelani River basin is presented in Figure 4-44. According to SPI values, 1990, 1992, 1996, 1998, 2000, 2002, and 2006 years can be categorized as moderate dry (Table 3-7). In terms of SPI, the most severe drought (–1.5 to – 1.99) was reported for the whole river basin in 2012 (Figure 4-44). Drought frequently occurs in 3 or 4 years within this 30 years observed period. SPI for this basin can be utilized to monitor the drought and also to determine the degree of drought since this study identified roughly the same years as drought years.

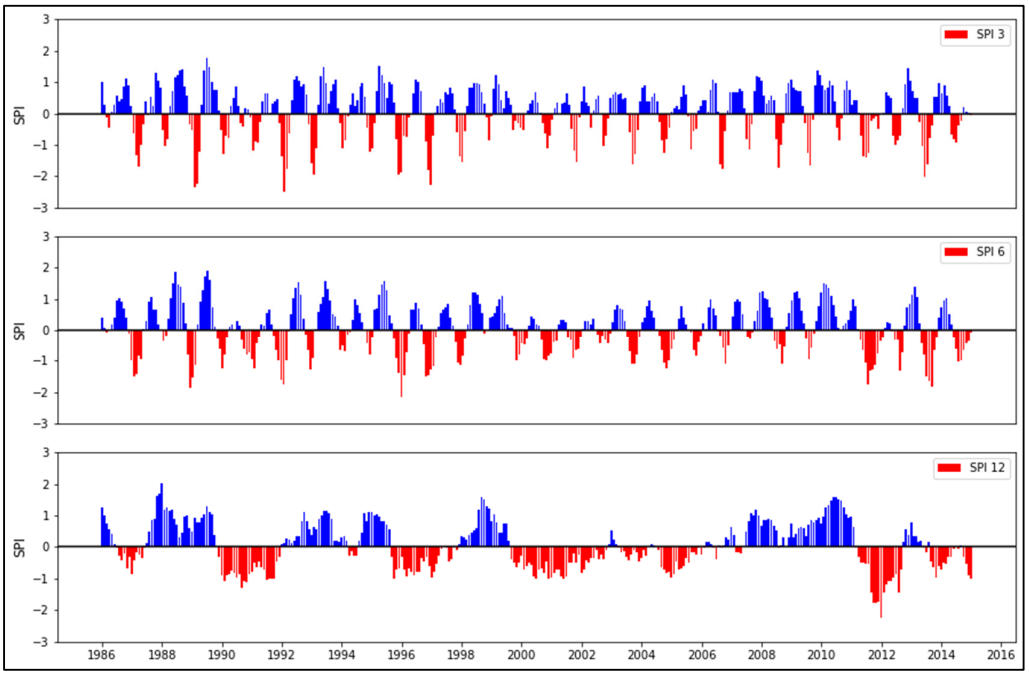

Figure 4-44 SPI variation in the Kelani River basin based on 3, 6, and 12 months for the observed period (1986-2015)

From 1985 to 2015, the time series of SPI at 3-month (October–December) were computed to demonstrate their probable value for identifying drought and monitoring drought risk (Figure 4-45). In the 3-month SPI time scale, the SPI frequencies fluctuated significantly above and below the zero line. Drought occurs whenever the SPI is negative, and the intensity decreases below –2.0. Drought occurrence events found in the observed period are 17 extremes, 17 severe, 29 moderate, and 87 mild droughts for the 3-month scale, according to Figure 4-45.

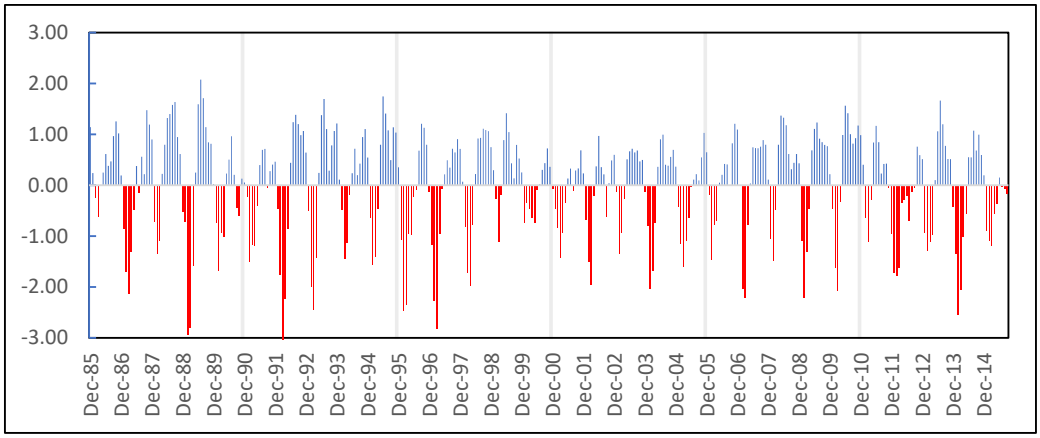

Figure 4-45 SPI variation in the Kelani River basin based on 3-month for the observed period (1986-2015)

From 1985 to 2015, the time series of SPI at 6-month periods (October–March) were computed to demonstrate their probable value for identifying drought and monitoring drought risk (Figure 4-46). In the 6-month SPI time scale, the SPI frequencies fluctuated significantly above and below the zero line. Drought occurs whenever the SPI is negative, and the intensity decreases below –2.0. Drought occurrence events found in the observed period are 8 extremes, 19 severe, 36 moderate, and 108 mild droughts for 6-month scale, according to Figure 4-46.

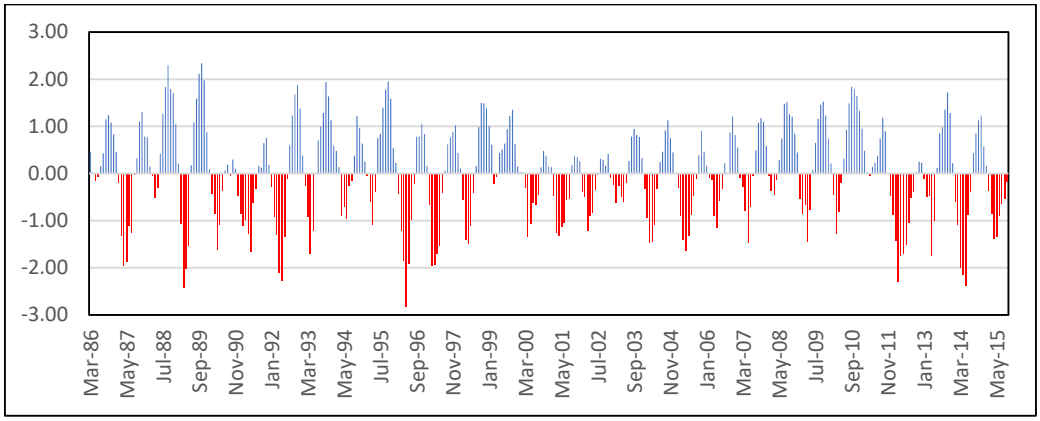

Figure 4-46 SPI variation in the Kelani River basin based on 6-month for the observed period (1986-2015)

From 1985 to 2015, the time series of SPI at 12-month/annual periods (October–September) were computed to demonstrate their probable value for identifying drought and observing drought risk (Figure 4-47). In the 12-month SPI time scale, the SPI frequencies fluctuated significantly above and below the zero line. Drought occurs whenever the SPI is negative, and the intensity decreases below –1.0. Drought occurrence events found in the observed period are 30 extreme, 42 severe, 304 moderate, and 801 mild droughts for 12-month scale, according to Figure 4-47. As a result, the severity of drought changes throughout time. Furthermore, the magnitude of wet occurrences during all three SPI periods, 3-month, 6-month, and annual is nearly the same (Figure 4-44).

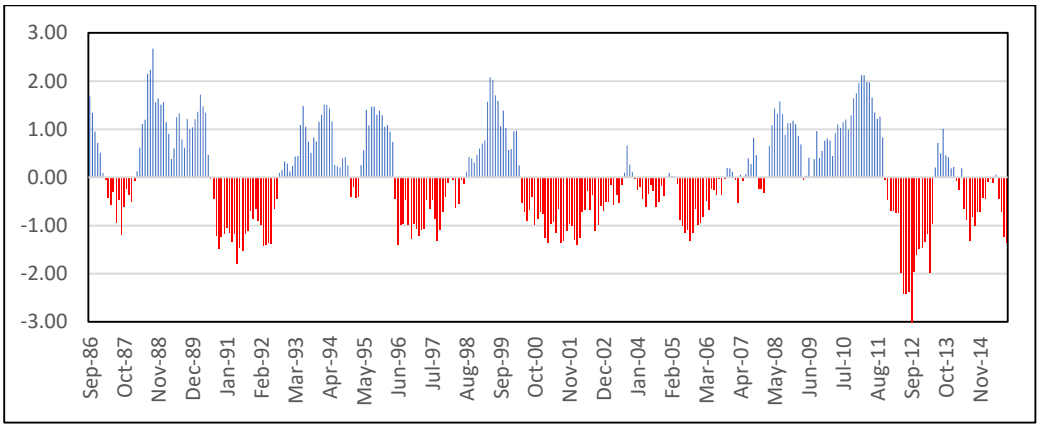

Figure 4-47 SPI variation in the Kelani River basin based on 12-month for the observed period (1986-2015)

4.4.2.2 Mid Century (2040 -2059)

From 2040 to 2059, the time series of SPI at 3-month (October–December) were computed to demonstrate their probable value for identifying drought and observing drought risk (Figure 4-48). In the 3-month SPI time scale, the SPI frequencies fluctuated significantly above and below the zero line. Drought occurs whenever the SPI is negative, and the intensity decreases below –1.0. Drought occurrence events found in the observed period are 3 extremes, 18 severe, 32 moderate, and 46 mild droughts for 3-month scale, according to Figure 4-48.

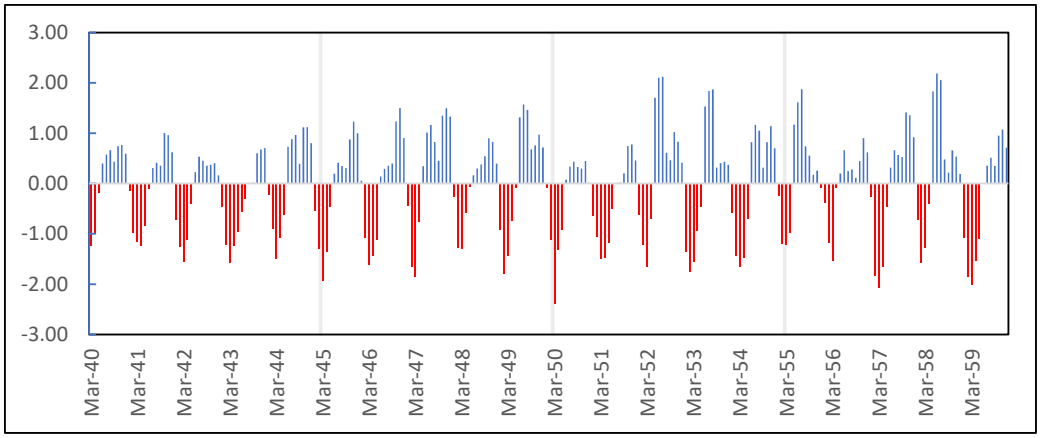

Figure 4-48 SPI variation in the Kelani River basin based on 3-month for mid-century (2040-2059) considering RCP 8.5

From 2040 to 2059, the time series of SPI at 6-month periods (October–March) were computed to demonstrate their probable value for identifying drought and observing drought risk (Figure 4-49). In the 6-month SPI time scale, the SPI frequencies fluctuated significantly above and below the zero line. Drought occurs whenever the SPI is negative, and the intensity decreases below –1.0. Drought occurrence events found in the observed period are 3 extremes, 17 severe, 25 moderate, and 65 mild droughts for 6-month scale, according to Figure 4-49.

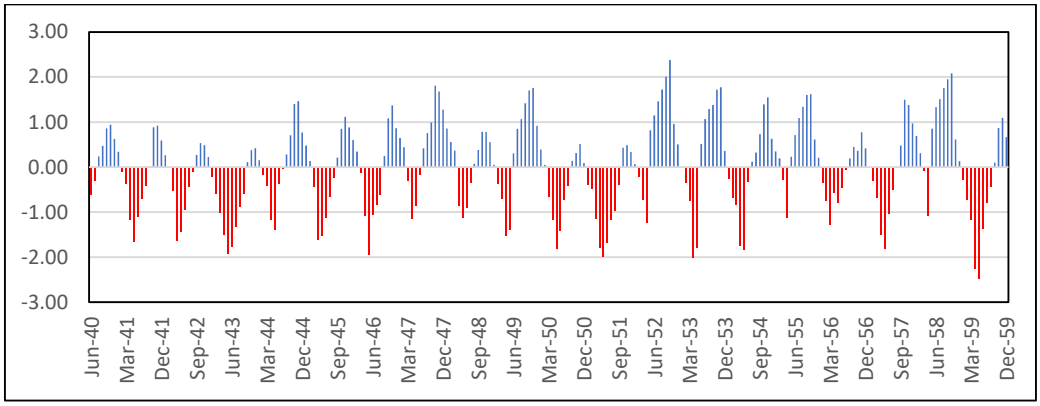

Figure 4-49 SPI variation in the Kelani River basin based on 6-month for mid-century (2040-2059) considering RCP 8.5

From 2040 to 2059, the time series of SPI at 12-month/annual periods (October–September) were computed to demonstrate their probable value for identifying drought and observing drought risk (Figure 4-50). In the 12-month SPI time scale, the SPI frequencies fluctuated significantly above and below the zero line. Drought occurs whenever the SPI is negative, and the intensity decreases below –1.0. Drought occurrence events found in the observed period are no extreme events, 42 severe, 304 moderate, and 801 mild droughts for 12-month scale, according to Figure 4-50. As a result, the severity of drought changes throughout time. Furthermore, the magnitude of wet occurrences during all three SPI periods, 3-month, 6-month, and annual, is nearly the same (Figure 4-50).

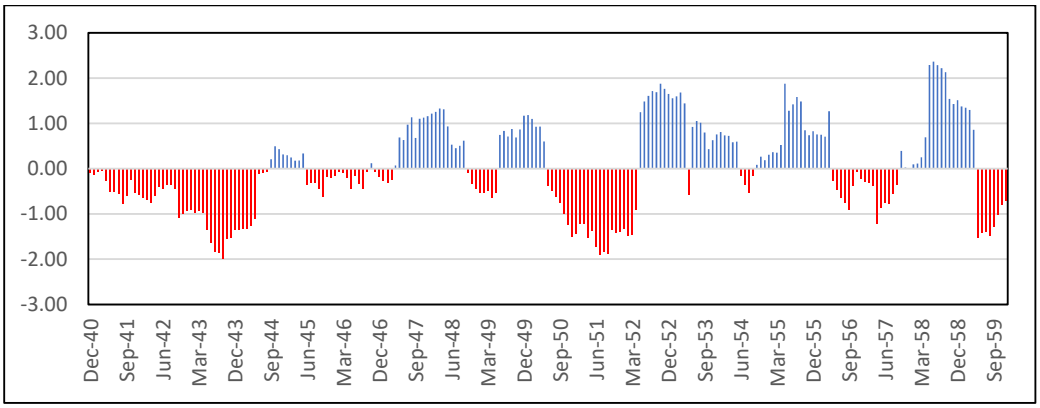

Figure 4-50 SPI variation in the Kelani River basin based on 12-month for mid-century (2040-2059) considering RCP 8.5

4.4.2.3 End Century (2080 -2099)

From 2080 to 2099, the time series of SPI at 3-month (October–December) were computed to demonstrate their probable value for identifying drought and observing drought risk (Figure 4-51). In the 3-month SPI time scale, the SPI frequencies fluctuated significantly above and below the zero line. Drought occurs whenever the SPI is negative, and the intensity decreases below –1.0. Drought occurrence events found in the observed period are 2 extreme events, 11 severe, 38 moderate, and 48 mild droughts for 3-month scale, according to Figure 4-51.

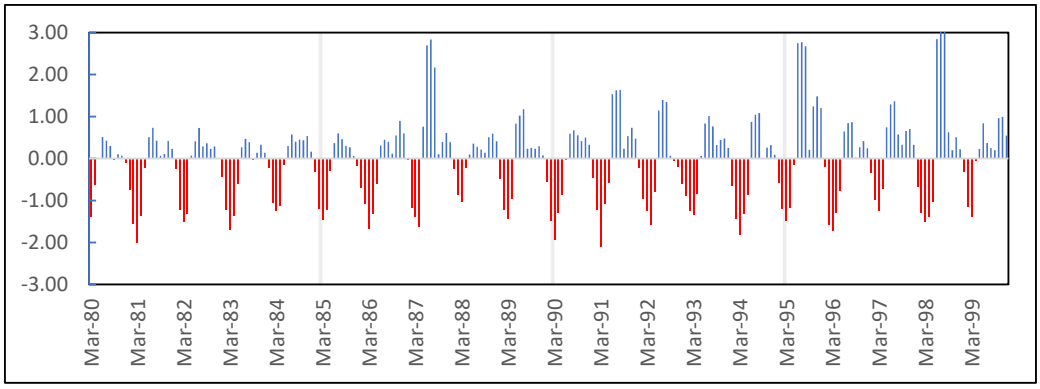

Figure 4-51 SPI variation in the Kelani River basin based on 3-month for mid-century (2080-2099) considering RCP 8.5

From 2080 to 2099, the time series of SPI at 6-month periods (October–March) were computed to demonstrate their probable value for identifying drought and observing drought risk (Figure 4-52). In the 6-month SPI time scale, the SPI frequencies fluctuated significantly above and below the zero line. Drought occurs whenever the SPI is negative, and the intensity decreases below –1.0. Drought occurrence events found in the observed period are no extreme events, 14 severe, 22 moderate, and 89 mild droughts for 6-month scale, according to Figure 4-52.

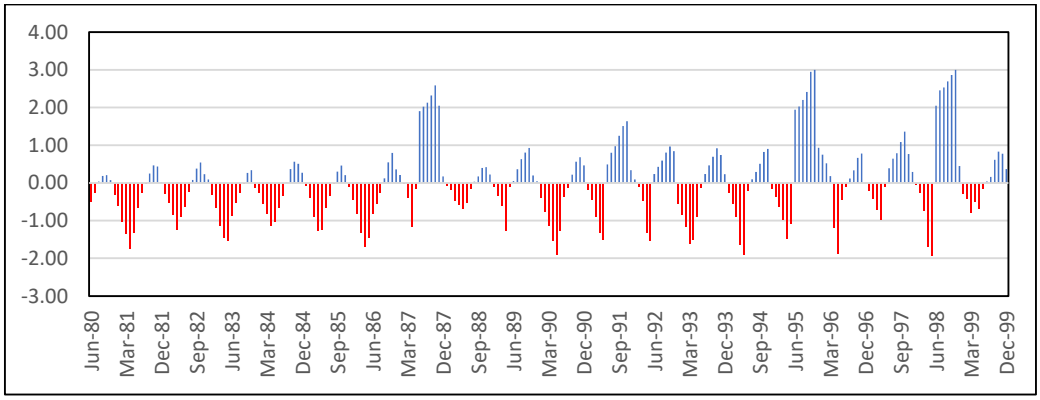

Figure 4-52 SPI variation in the Kelani River basin based on 6-month for mid-century (2080-2099) considering RCP 8.5

From 2040 to 2059, the time series of SPI at 12-month/annual periods (October–September) were computed to demonstrate their probable value for identifying drought

and observing drought risk (Figure 4-53). In the 12-month SPI time scale, the SPI frequencies fluctuated significantly above and below the zero line. Drought occurs whenever the SPI is negative, and the intensity decreases below –1.0. Drought occurrence events found in the observed period are no extreme events, no severe, 84 moderate, and 833 mild droughts for 12-month scale, according to Figure 4-53. As a result, the severity of drought changes throughout time. Furthermore, the magnitude of wet occurrences during all three SPI periods, 3-month, 6-month, and annual, is nearly the same (Figure 4-53).

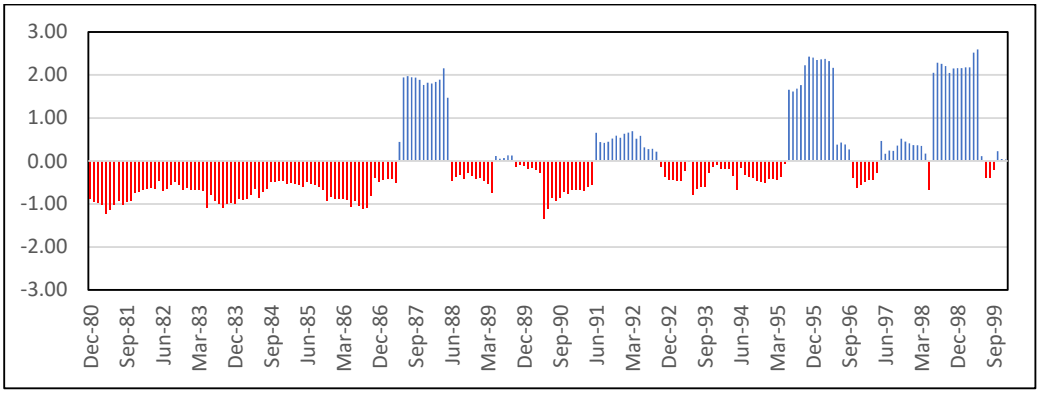

Figure 4-53 SPI variation in the Kelani River basin based on 12-month for mid-century (2080-2099) considering RCP 8.5

4.4.3 HEC-HMS Results

Water management and decision-makers need to be able to simulate continuous streamflow in the Kelani River.

Model Calibration

Hydrographs comparison for both observed and simulated streamflow in normal and semi-log scales for Hanwella catchment are illustrated in Figure 4-54 to Figure 4-57 respectively. Flow duration curves for both sorted and sort only observed streamflow at the Hanwella catchment are shown in Figure 4-56. Four parameters (Recession Constant, Ratio to peak, Muskingum K, and Muskingum X) are optimized for calibrating the HEC-HMS model for the observed period and initial parameters and optimized parameters are shown in Table 4-12. The calibration and validation objectives functions of the Kelani River basin are mentioned in Table 4-12.

Table 4-11 Initial parameters and optimized parameters of HEC-HMS model in the Kelani River basin

Method	Sub-catchment Number	Parameters	Initial Value	Optimized value
Baseflow (Recession)	S_1	Recession Constant	0.948	0.179
	S_2	Recession Constant	0.253	0.276
	S_3	Recession Constant	0.105	0.178
	S_4	Recession Constant	0.957	0.115
	S_1	Ratio to peak	0.30	0.351
	S_2	Ratio to peak	0.30	0.531
	S_3	Ratio to peak	0.30	0.609
	S_4	Ratio to peak	0.30	0.381
Routing (Muskingum)	R_1	Muskingum K	41.839	55.919
	R_2	Muskingum K	10.137	32.568
	R_1	Muskingum x	0.260	0.180
	R_2	Muskingum x	0.125	0.114

Table 4-12 Objective function's performance rating of calibration and validation in Kelani River basin

Objective Functions	Calibration	Performance Rating	Validation	Performance Rating
RMSE	0.60	Good	0.70	Satisfactory
NSE	0.64	Satisfactory	0.56	Satisfactory
Percent Bias	0.64%	Very Good	-3.27%	Very Good

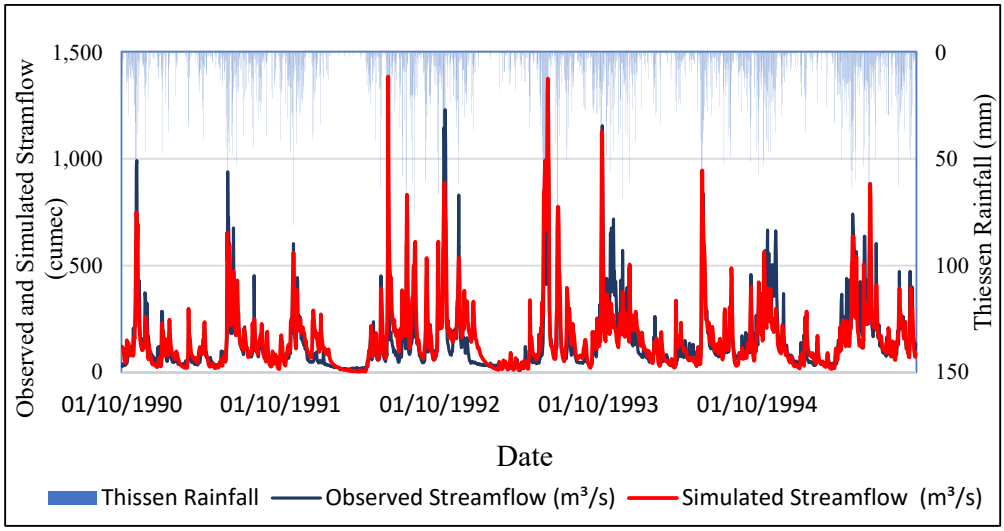

Figure 4-54 Observed and simulated streamflow hydrograph along thissen rainfall of Kelani River basin calibration period (1990/91-1994/95)

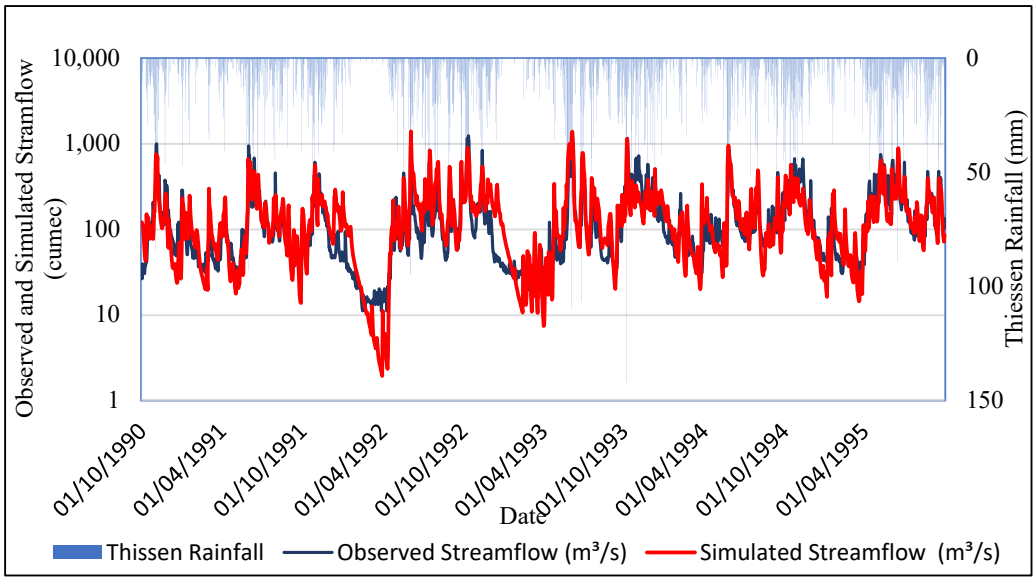

Figure 4-55 Observed and simulated streamflow hydrograph along thissen rainfall of Kelani River basin calibration period (1990/91-1994/95) in log scale

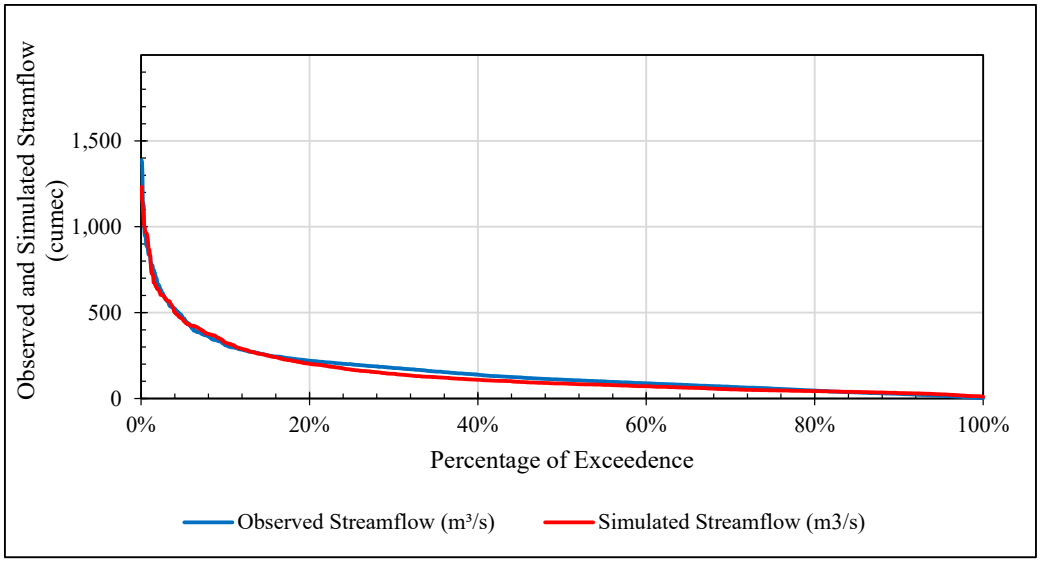

Figure 4-56 Observed and simulated streamflow Flow Duration Curve (FDC) of Kelani River basin calibration period (1990/91-1994/95)

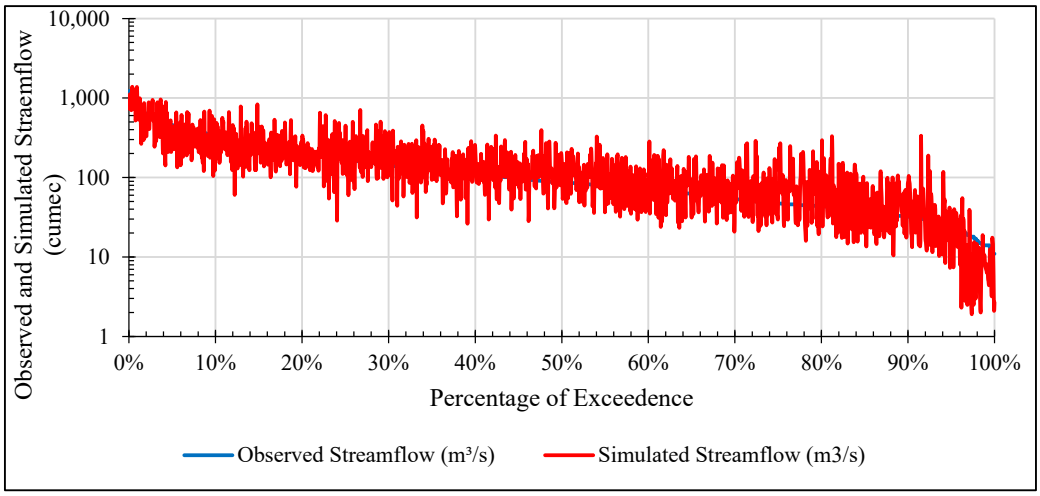

Figure 4-57 Observed and simulated streamflow thresholds of Kelani River basin calibration period (1990/91-1994/95)

Model Validation

Hydrographs comparison for both observed and simulated streamflow in normal and semi-log scales for Hanwella catchment are illustrated in Figure 4-58 to Figure 4-61 respectively. Flow duration curves for both sorted and sort only observed streamflow at the Hanwella catchment.

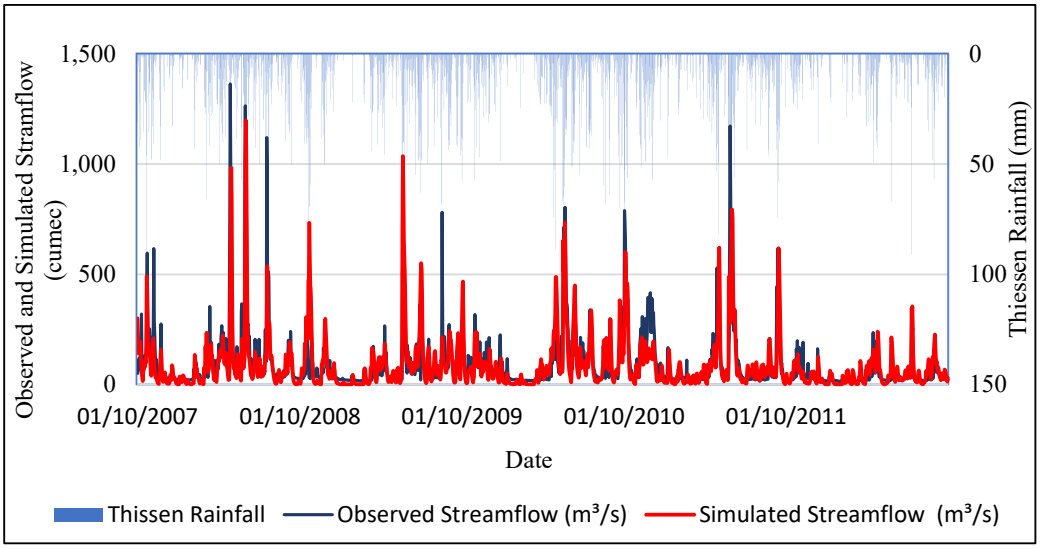

Figure 4-58 Observed and simulated streamflow hydrograph along thissen rainfall of Kelani River basin validation period (2007/08 - 2011/12)

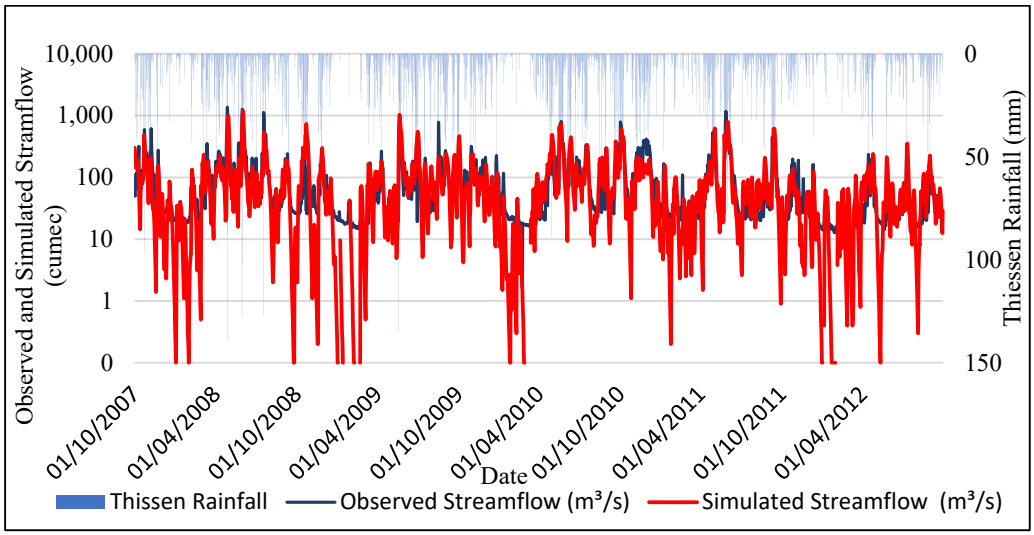

Figure 4-59 Observed and simulated streamflow hydrograph along thissen rainfall of Kelani River basin validation period (2007/08 - 2011/12) in log scale

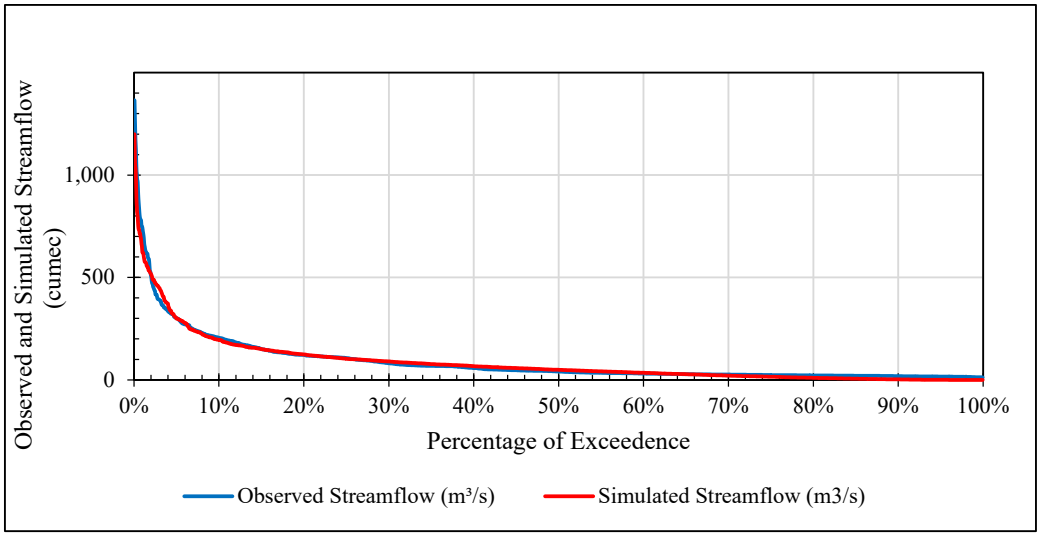

Figure 4-60 Observed and simulated streamflow Flow Duration Curve (FDC) of Kelani River basin validation period (2007/08 - 2011/12)

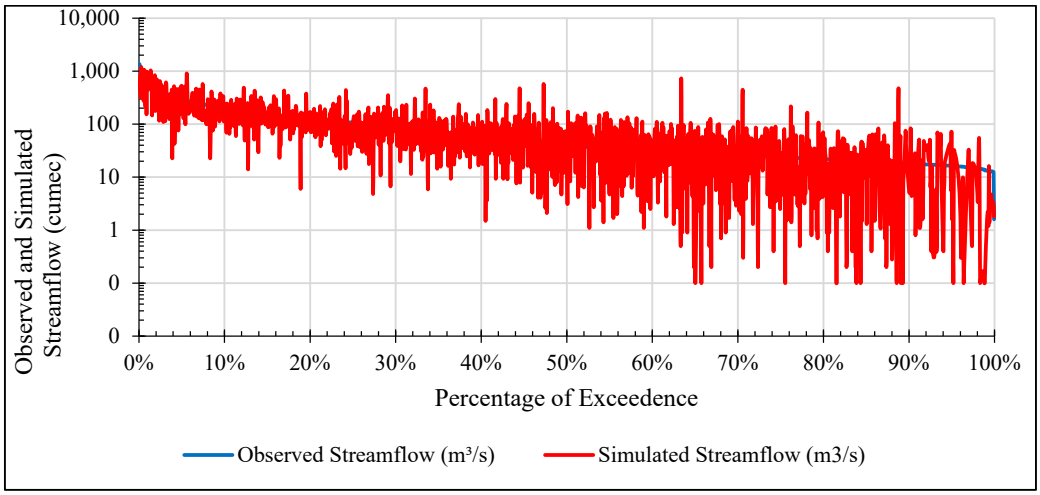

Figure 4-61 Observed and simulated streamflow thresholds of Kelani River basin validation period (2007/08 - 2011/12)

Model Run for Mid and End Century Period

Figure 4-62 shows 2048 has a high peak of 200 m^3/s and 2nd peak occurs in 2058 has 183 m^3/s but the maximum value is less than 50 m^3/s.

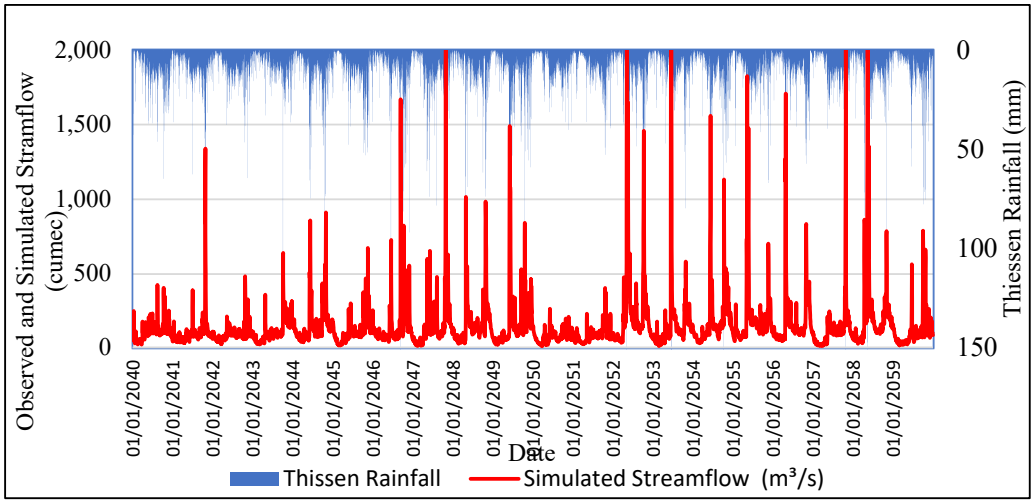

Figure 4-62 Simulated streamflow hydrograph along thissen rainfall of Kelani River basin mid-century period (2040-2059) in validate HEC-HMS model

Figure 4-63 shows 2088 has a high peak of 200 m^3/s and 2nd peak that occurs in 2098 has 183 m^3/s but the maximum value is less than 50 m^3/s.

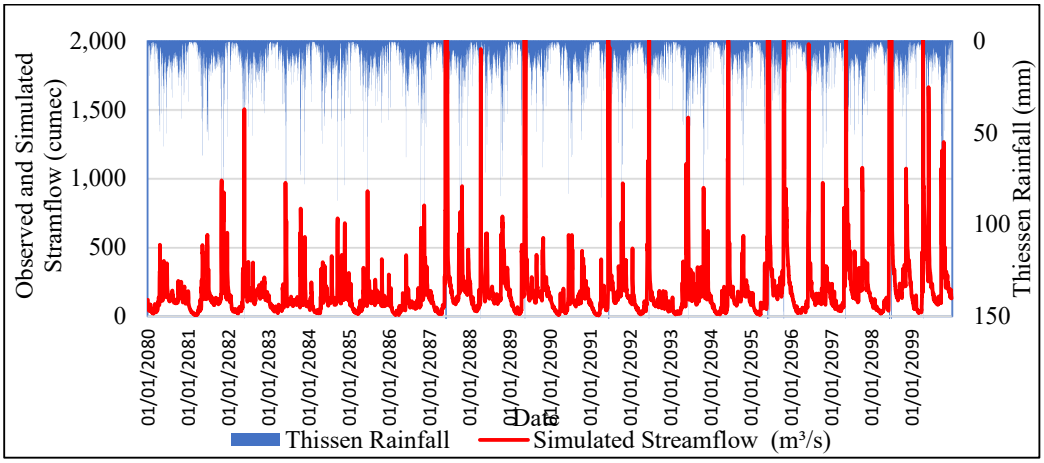

Figure 4-63 Simulated streamflow hydrograph along thissen rainfall of Kelani River basin end-century period (2080-2099) in validate HEC-HMS

4.4.4 Streamflow Drought Index (SDI)

4.4.4.1 Observed Period (1985/86 -2014/15)

At the Hanwella streamflow gauging stations, the SDI was estimated for three different time frames of 3, 6, and 12 months (Figure 4-64). Negative anomalies appear lower than the x-axis, whereas positive anomalies appear above. The time scale plays a role in drought severity, as shown by the red color bars which indicate severe drought according to Table 3-7. At annual time scales (October–September), the hydrological years 2008, 2012, and 2014 at Hanwella stations revealed various severe drought occurrences. Drought does not frequently occur in the early days but after 2006 frequency is increased and every 2 years it occurs within this last 10 years observed period.

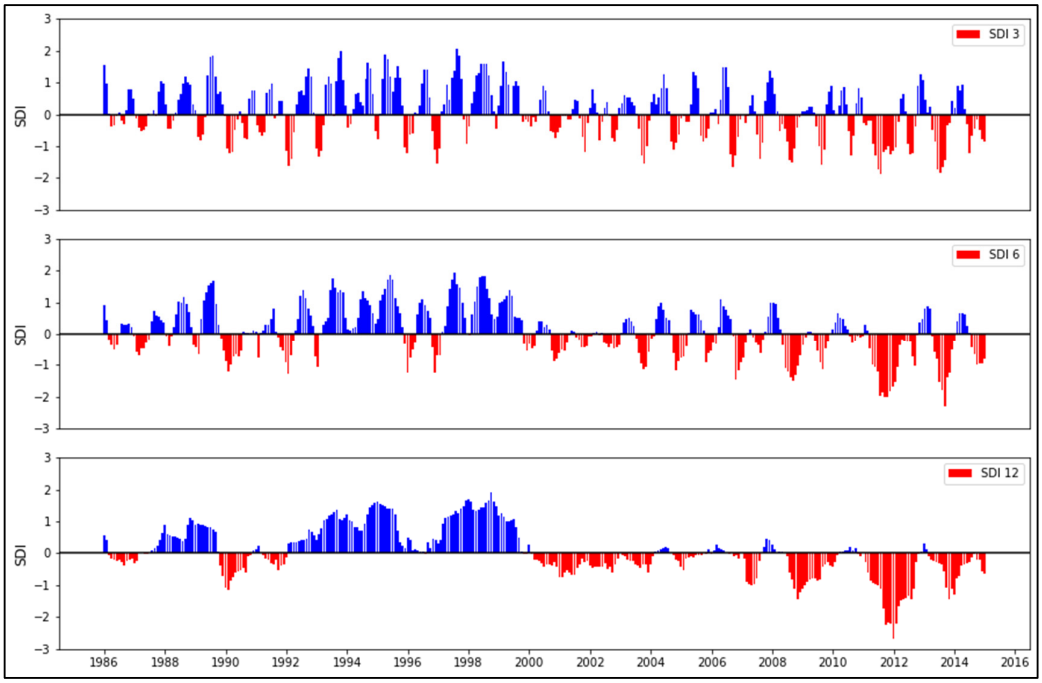

Figure 4-64 SDI variation in the Kelani River basin based on 3, 6, and 12 months for the observed period (1986-2015)

From 1985 to 2015, the time series of SDI at 3-month (October–December) were computed to demonstrate their probable value for identifying drought and observing drought risk (Figure 4-65). In the 3-month SDI time scale, the SDI frequencies

fluctuated significantly above and below the zero line. Drought occurs whenever the SDI is negative, and the intensity decreases below –1.0. Drought occurrence events found in the observed period are 6 extreme events, 23 severe, 32 moderate, and 122 mild droughts for 3-month scale, according to Figure 4-65.

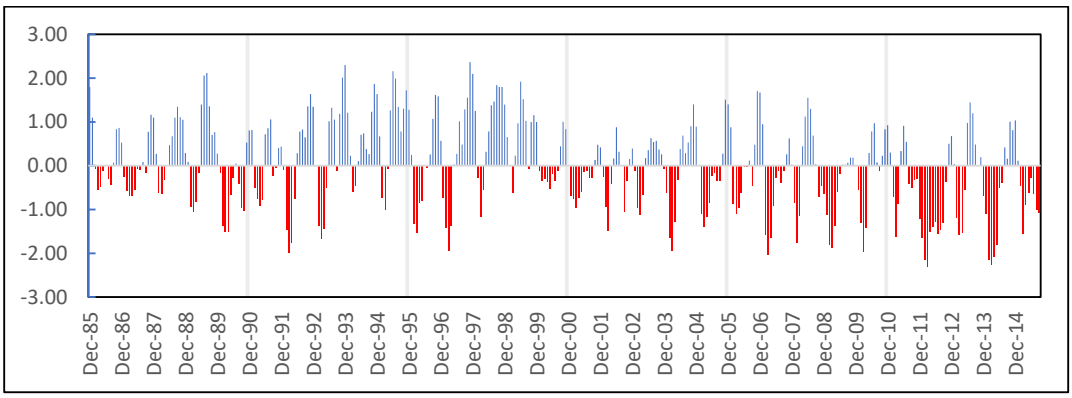

Figure 4-65 SDI variation in the Kelani River basin based on 3-month for the observed period (1986-2015)

From 1985 to 2015, the time series of SDI at 6-month periods (October–March) were computed to demonstrate their probable value for identifying drought and observing drought risk (Figure 4-66). In the 6-month SDI time scale, the SDI frequencies fluctuated significantly above and below the zero line. Drought occurs whenever the SDI is negative, and the intensity decreases below –1.0. Drought occurrence events found in the observed period are 8 extreme events, 16 severe, 29 moderate, and 128 mild droughts for 6-month scale, according to Figure 4-66.

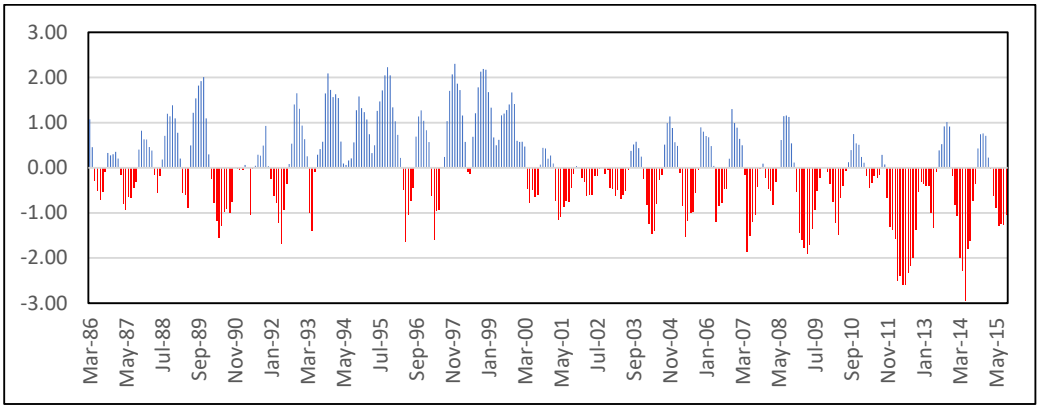

Figure 4-66 SDI variation in the Kelani River basin based on 6-month for the observed period (1986-2015)

From 1985 to 2015, the time series of SDI at 12-month/annual periods (October–September) were computed to demonstrate their probable value for identifying drought and observing drought risk (Figure 4-67). In the 12-month SDI time scale, the SDI frequencies fluctuated significantly above and below the zero line. Drought occurs whenever the SPI is negative, and the intensity decreases below –1.0. Drought occurrence events found in the observed period are 56 extreme events, 69 severe, 188 moderate, and 959 mild droughts for 12-month scale, according to Figure 4-67. As a result, the severity of drought changes throughout time. Furthermore, the magnitude of wet occurrences during all three SDI periods, 3-month, 6-month, and annual, is nearly the same (Figure 4-64).

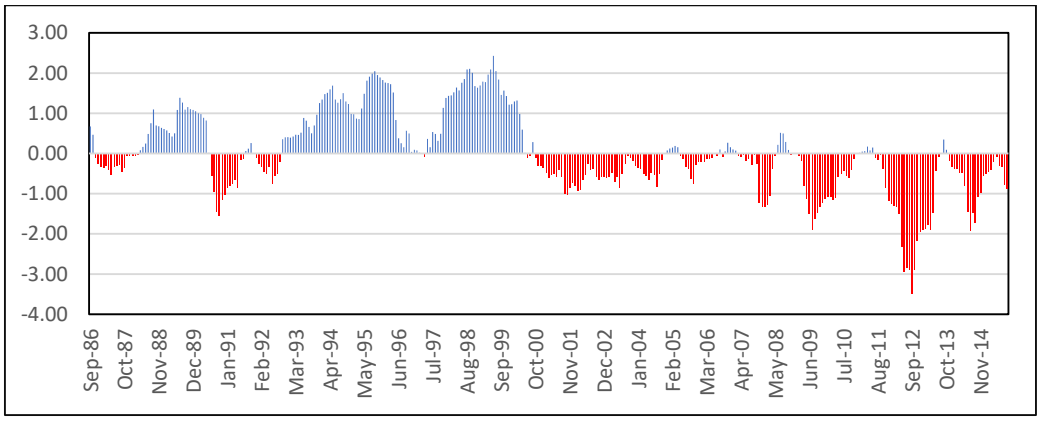

Figure 4-67 SDI variation in the Kelani River basin based on 12-month for the observed period (1986-2015)

4.4.4.2 Mid Century (2040 -2059)

From 2040 to 2059, the time series of SDI at 3-month (October–December) were computed to demonstrate their probable value for identifying drought and observing drought risk (Figure 4-68). In the 3-month SDI time scale, the SDI frequencies fluctuated significantly above and below the zero line. Drought occurs whenever the SDI is negative, and the intensity decreases below –1.0. Drought occurrence events found in the observed period are 1 extreme event, 9 severe, 25 moderate, and 88 mild droughts for 3-month scale, according to Figure 4-68.

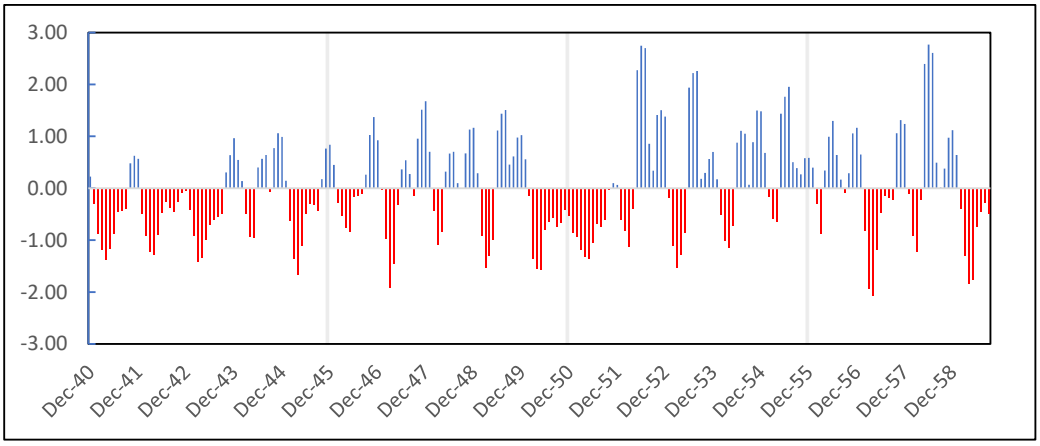

Figure 4-68 SDI variation in the Kelani River basin based on 3-month for mid-century (2040-2059) in RCP 8.5

From 2040 to 2059, the time series of SDI at 6-month periods (October–March) were computed to demonstrate their probable value for identifying drought and observing drought risk (Figure 4-69). In the 6-month SDI time scale, the SDI frequencies fluctuated significantly above and below the zero line. Drought occurs whenever the SDI is negative, and the intensity decreases below –1.0. Drought occurrence events found in the observed period are no extreme events, 16 severe, 32 moderate, and 58 mild droughts for 6-month scale, according to Figure 4-69.

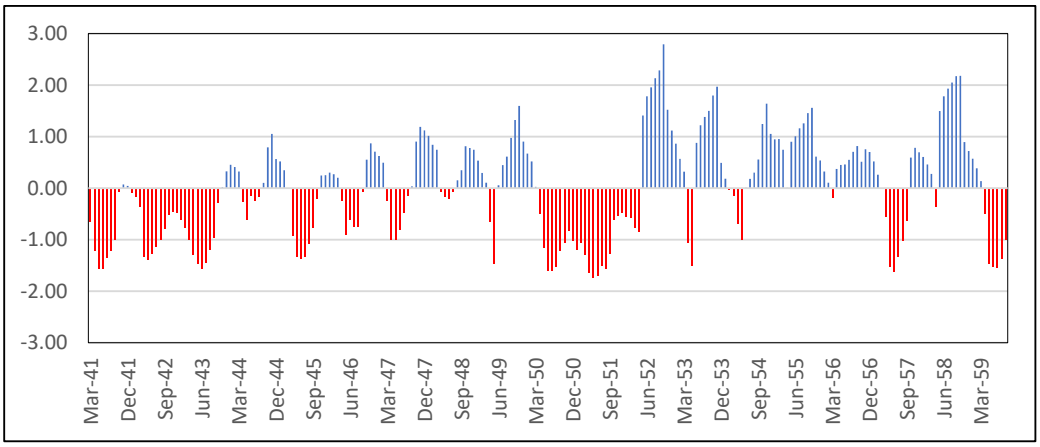

Figure 4-69 SDI variation in the Kelani River basin based on 6-month for mid-century (2040-2059) considering RCP 8.5

From 2040 to 2059, the time series of SDI at 12-month/annual periods (October–September) were computed to demonstrate their probable value for identifying drought and observing drought risk (Figure 4-70). In the 12-month SDI time scale, the SDI frequencies fluctuated significantly above and below the zero line. Drought occurs whenever the SDI is negative, and the intensity decreases below –1.0. Drought occurrence events found in the observed period are no extreme events, 16 severe, 32 moderate, and 58 mild droughts for 12-month scale, according to Figure 4-70. As a result, the severity of drought changes throughout time. Furthermore, the magnitude of wet occurrences during all three SDI periods, 3-month, 6-month, and annual, is nearly the same (Figure 4-70).

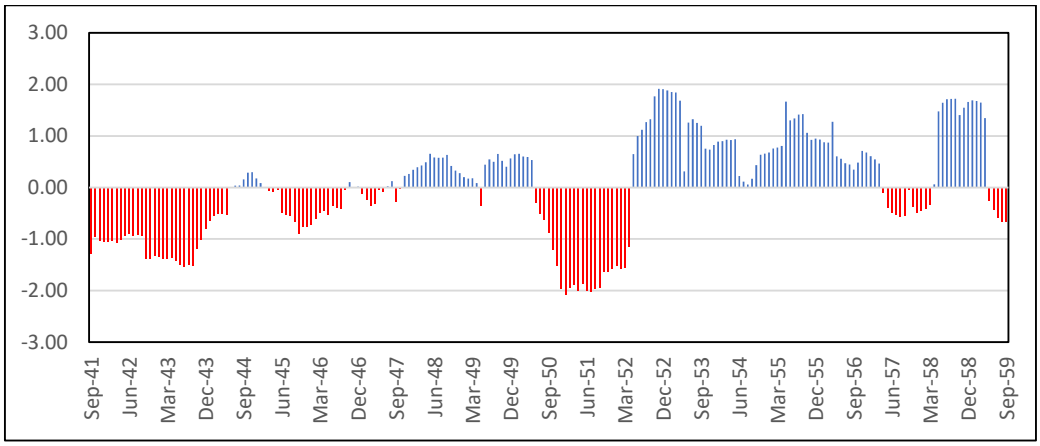

Figure 4-70 SDI variation in the Kelani River basin based on 12-month for mid-century (2040-2059) considering RCP 8.5

4.4.4.3 End Century (2080 -2099)

From 2080 to 2099, the time series of SDI at 3-month (October–December) were computed to demonstrate their probable value for identifying drought and observing drought risk (Figure 4-71). In the 3-month SDI time scale, the SDI frequencies fluctuated significantly above and below the zero line. Drought occurs whenever the SDI is negative, and the intensity decreases below –1.0. Drought occurrence events found in the observed period are no extreme events, 6 severe, 29 moderate, and 97 mild droughts for 3-month scale, according to Figure 4-71.

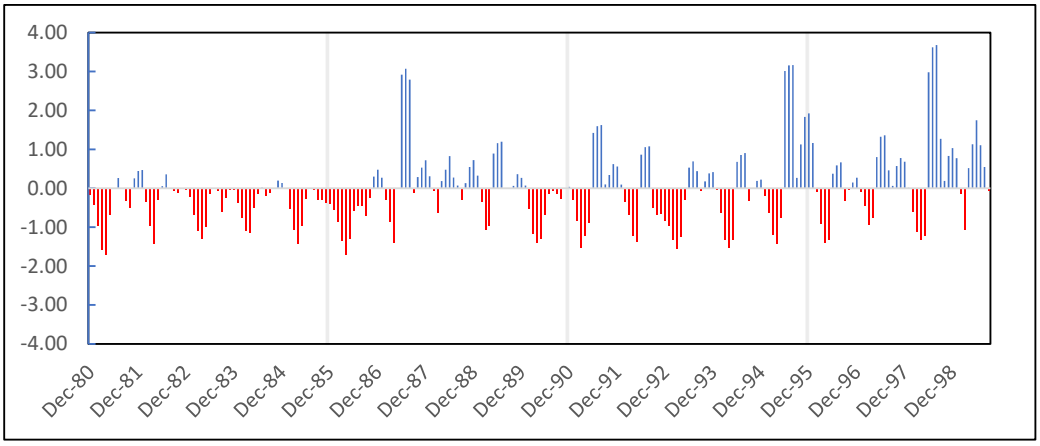

Figure 4-71 SDI variation in the Kelani River basin based on 3-month for mid-century (2080-2099) considering RCP 8.5

From 2080 to 2099, the time series of SDI at 6-month periods (October–March) were computed to demonstrate their probable value for identifying drought and observing drought risk (Figure 4-72). In the 6-month SDI time scale, the SDI frequencies fluctuated significantly above and below the zero line. Drought occurs whenever the SDI is negative, and the intensity decreases below –1.0. Drought occurrence events found in the observed period are no extreme events, 3 severe, 26 moderate, and 101 mild droughts for 6-month scale, according to Figure 4-72.

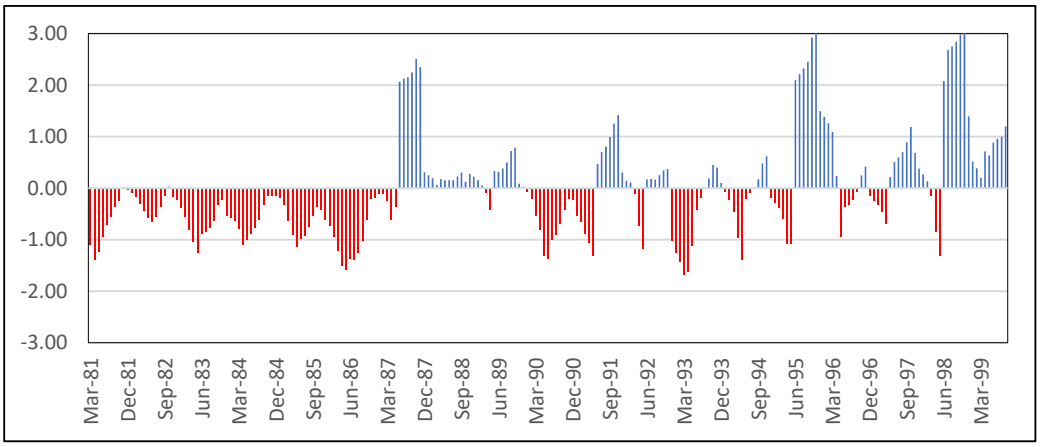

Figure 4-72 SDI variation in the Kirindi Oya river basin based on 6-month for mid-century (2080-2099) considering RCP 8.5

From 2080 to 2099, the time series of SDI at 12-month/annual periods (October–September) were computed to demonstrate their probable value for identifying drought and observing drought risk (Figure 4-73). In the 12-month SDI time scale, the SDI frequencies fluctuated significantly above and below the zero line. Drought occurs whenever the SDI is negative, and the intensity decreases below –1.0. Drought occurrence events found in the observed period are no extreme events, 9 severe, 121 moderate, and 646 mild droughts for 12-month scale, according to Figure 4-73. As a result, the severity of drought changes throughout time. Furthermore, the magnitude of wet occurrences during all three SDI periods, 3-month, 6-month, and annual, is nearly the same (Figure 4-73).

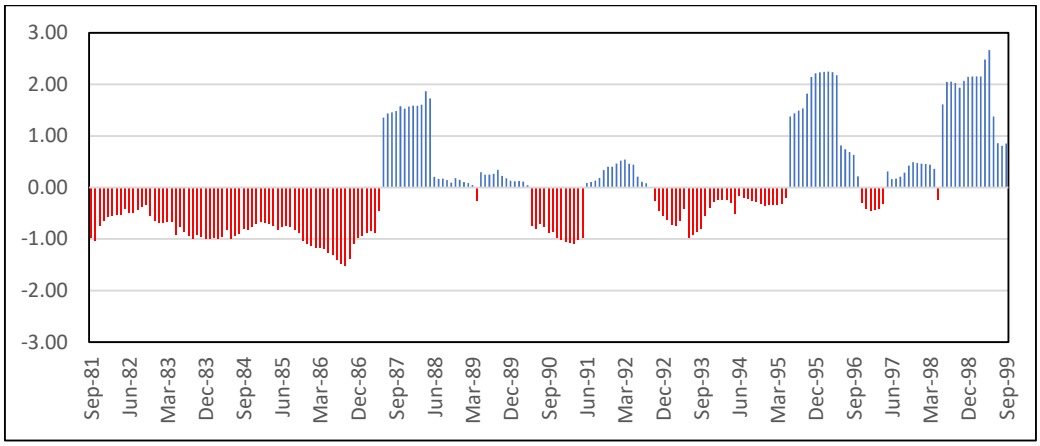

Figure 4-73 SDI variation in the Kirindi Oya river basin based on 12-month for mid-century (2080-2099) considering RCP 8.5

4.4.5 Seasonal Analysis (Kelani River)

4.4.5.1 Second Inter Monsoon Period

This season considers October and November according to Sri Lankan hydrological year. This research work considers the observed period starts from 1985 to 2015.

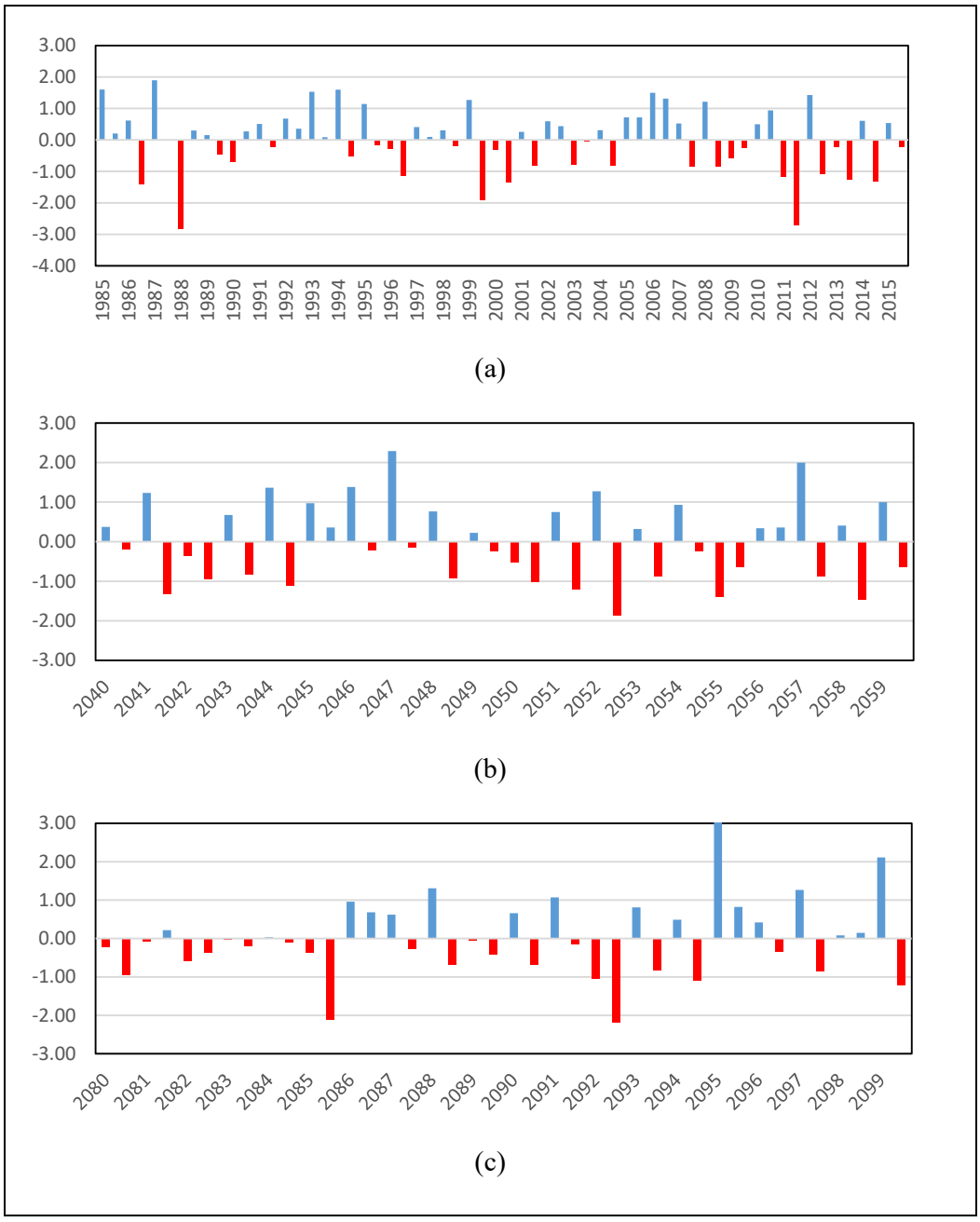

Figure 4-74 Standardized Precipitation Index in Second Inter Monsoon for (a) observed period, (b) mid-century period, and (c) end-century period in Kelani River basin

Standardized Precipitation Index in Second Inter Monsoon for the observed period, Mid-Century period, and End-Century period in Kelani River basin are shown in Figure 4-74. For the seasonal analysis, all those monthly SPI values are plotted as a graph. The Second Inter Monsoon drought classification for different periods shows in Table 4-13. Compare the observed data all the drought types will reduce in the both mid and end-century.

Table 4-13 Event identification of SPI values in Second Inter Monsoon and the percentage variation of the mid and end-century based on the observed period

Drought Type	Observed Period	Mid-Century	End-Century
Non-drought	32	19 (-41%)	17 (-47%)
Mild drought	18	14 (-22%)	18 (0%)
Moderate drought	7	6 (-14%)	3 (-57%)
Severe drought	1	1 (0%)	0 (-100%)
Extreme drought	2	0 (-100%)	2 (0%)

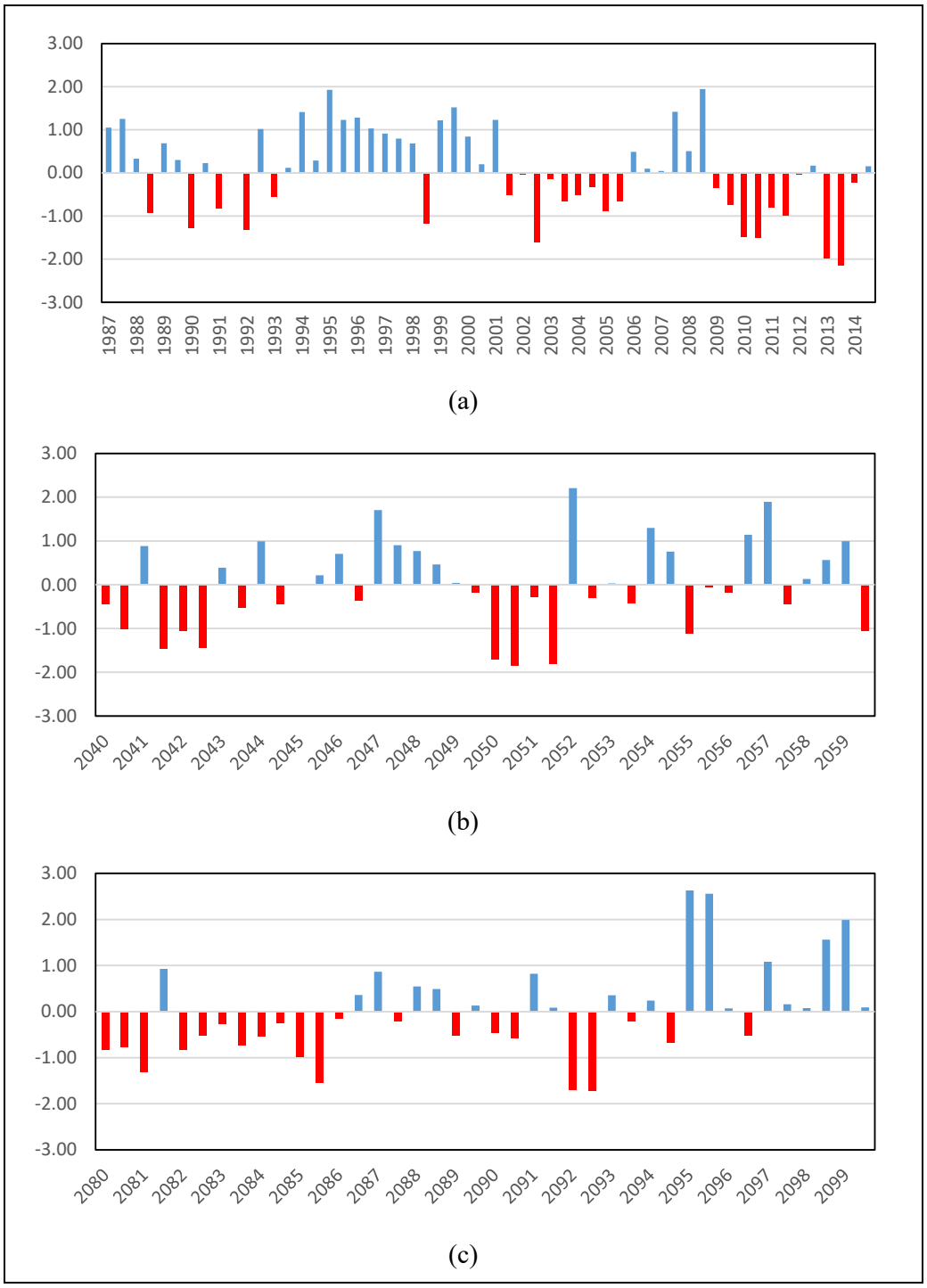

Figure 4-75 Streamflow Drought Index in Second Inter Monsoon for (a) observed period, (b) mid-century period, and (c) end-century period in Kelani River basin

Streamflow Drought Index in Second Inter Monsoon for the observed period, Mid-Century period, and End-Century period in Kelani River basin is shown in Figure 4-75. For the seasonal analysis, all those monthly SPI values are plotted as a graph. The Second Inter Monsoon drought classification for different periods shows in Table 4-14. Compare the observed data all the drought types will reduce in the both mid and end-century.

Table 4-14 Event identification of SDI values in Second Inter Monsoon and the percentage variation of the mid and end-century based on the observed period

Drought Type	Observed Period	Mid-Century	End-Century
Non-drought	32	19 (-41%)	19 (-41%)
Mild drought	18	14 (-22%)	17 (-6%)
Moderate drought	5	6 (20%)	1 (-80%)
Severe drought	4	1 (-75%)	3 (-25%)
Extreme drought	1	0 (-100%)	0 (-100%)

4.4.5.2 Northeast Monsoon

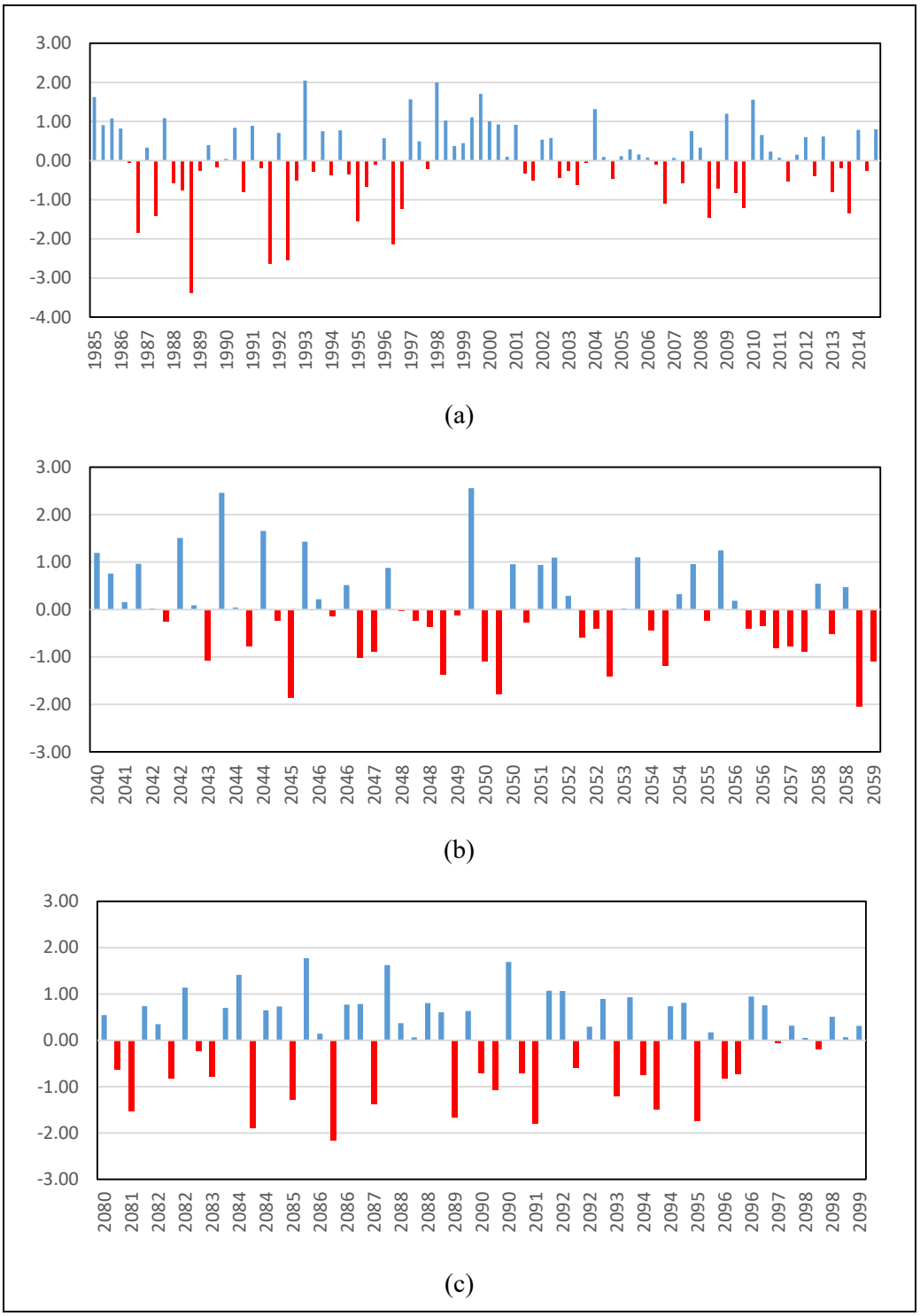

Figure 4-76 Standardized Precipitation Index in Northeast Monsoon for (a) observed period, (b) mid-century period, and (c) end-century period in Kelani River basin

Standardized Precipitation Index in Northeast Monsoon for the observed period, Mid-Century period, and End-Century period in Kelani River basin are shown in Figure 4-76. For the seasonal analysis, all those monthly SPI values are plotted as a graph. In the Northeast Monsoon, drought classification for different periods shows in Table 4-15. Compare the observed data all the drought types will reduce in the both mid and end-century.

Table 4-15 Event identification of SPI values in Northeast Monsoon and the percentage variation of the mid and end-century based on the observed period

Drought Type	Observed Period	Mid-Century	End-Century
Non-drought	48	27 (-44%)	34 (-29%)
Mild drought	30	20 (-33%)	12 (-60%)
Moderate drought	6	7 (17%)	5 (-17%)
Severe drought	2	2 (0%)	5 (150%)
Extreme drought	4	1 (-75%)	1 (-75%)

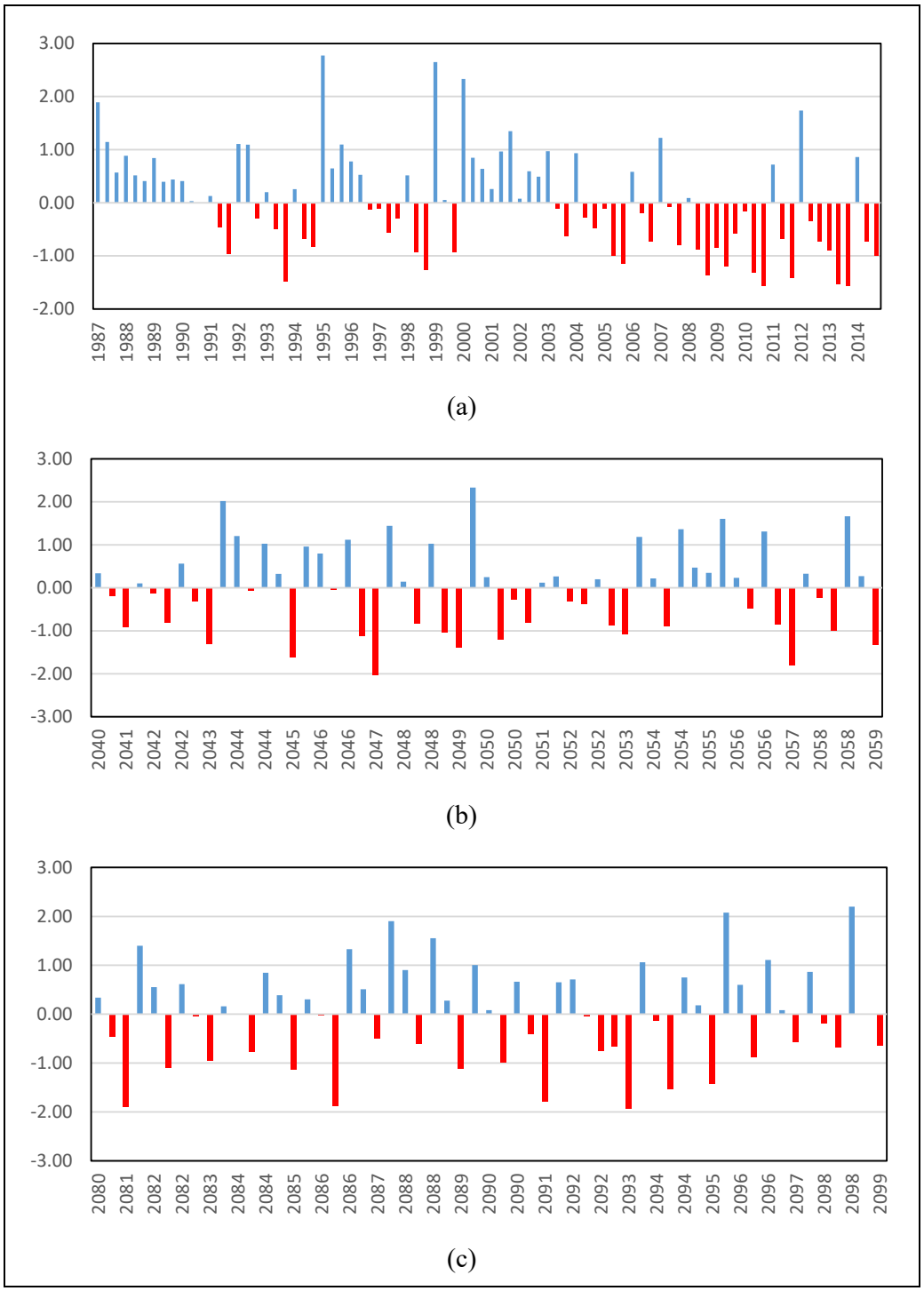

Figure 4-77 Streamflow Drought Index in Northeast Monsoon for (a) observed period, (b) mid-century period, and (c) end-century period in Kelani River basin

Streamflow Drought Index in Northeast Monsoon for the observed period, Mid-Century period, and End-Century period in Kelani River basin is shown in Figure 4-77. For the seasonal analysis, all those monthly SPI values are plotted as a graph. In the Northeast Monsoon, drought classification for different periods shows in Table 4-16. Compare the observed data all the drought types will reduce in the both mid and end-century.

Table 4-16 Event identification of SDI values in Northeast Monsoon and the percentage variation of the mid and end-century based on the observed period

Drought Type	Observed Period	Mid-Century	End-Century
Non-drought	42	29 (-31%)	28 (-33%)
Mild drought	35	18 (-49%)	20 (-43%)
Moderate drought	10	7 (-30%)	4 (-60%)
Severe drought	3	2 (-33%)	5 (67%)
Extreme drought	0	1 (0%)	0 (0%)

4.4.5.3 First Inter Monsoon Period

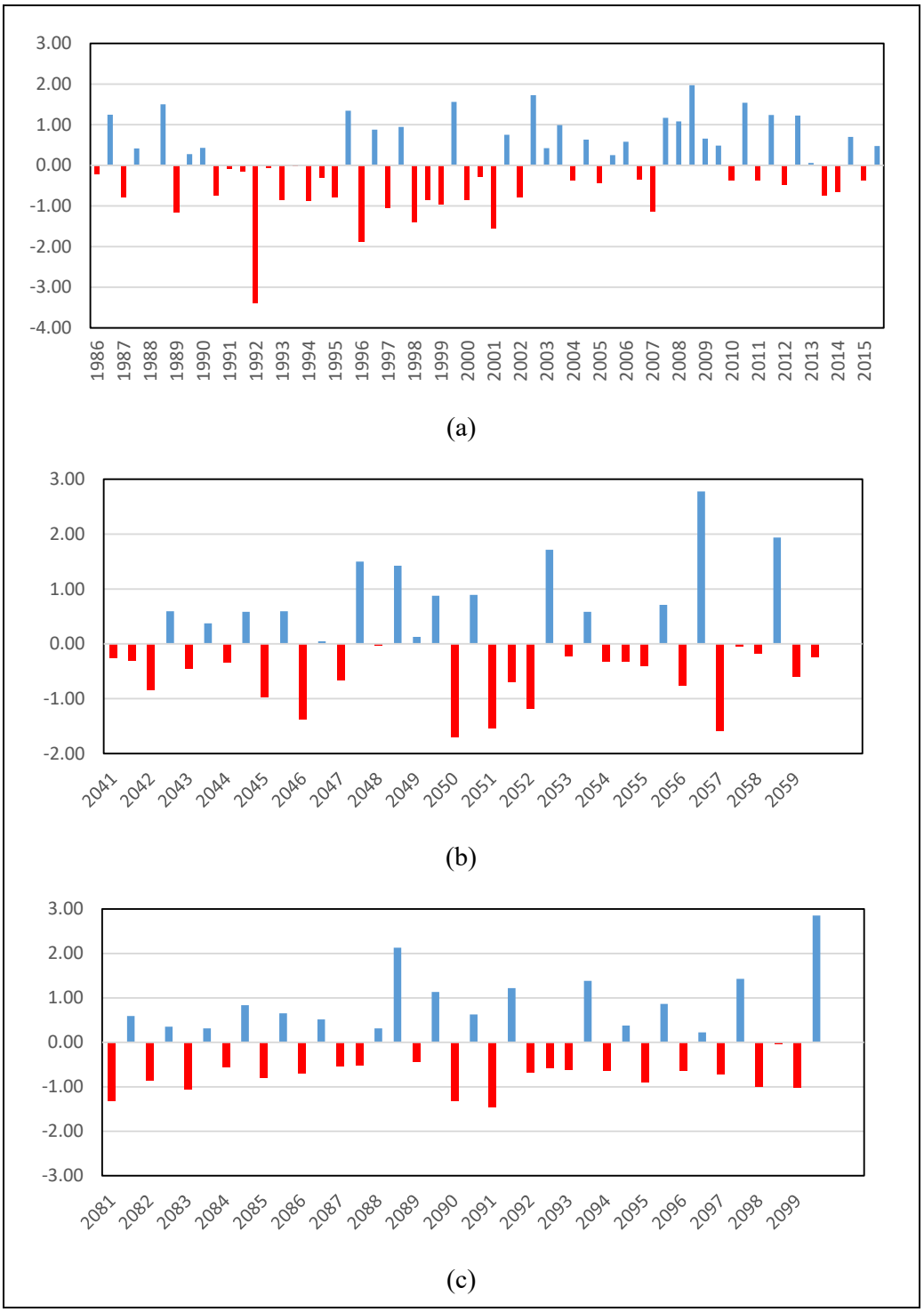

Figure 4-78 Standardized Precipitation Index in First Inter Monsoon for (a) observed period, (b) mid-century period, and (c) end-century period in Kelani River basin

Standardized Precipitation Index in First Inter Monsoon for the observed period, Mid-Century period, and End-Century period in Kelani River basin are shown in Figure 4-78. For the seasonal analysis, all those monthly SPI values are plotted as a graph. The First Inter Monsoon drought classification for different periods shows in Table 4-17. Compare the observed data all the drought types will reduce in the both mid and end-century.

Table 4-17 Event identification of SPI values in First Inter Monsoon and the percentage variation of the mid and end-century based on the observed period

Drought Type	Observed Period	Mid-Century	End-Century
Non-drought	28	15 (-46%)	17 (-39%)
Mild drought	25	18 (-28%)	15 (-40%)
Moderate drought	4	2 (-50%)	6 (50%)
Severe drought	2	3 (50%)	0 (-100%)
Extreme drought	1	0 (-100%)	0 (-100%)

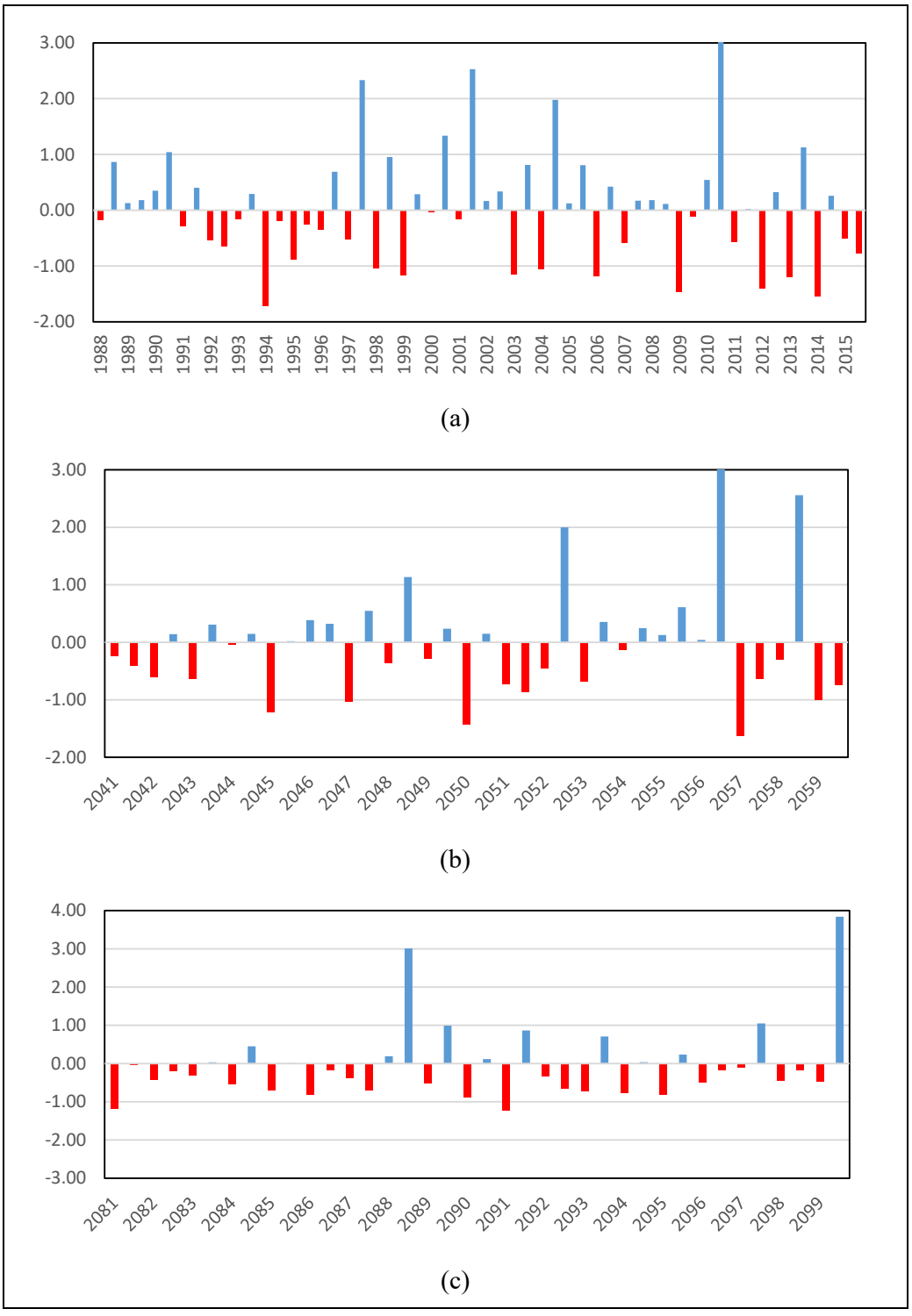

Figure 4-79 Streamflow Drought Index in First Inter Monsoon for (a) observed period, (b) mid-century period, and (c) end-century period in Kelani River basin

Streamflow Drought Index in First Inter Monsoon for the observed period, Mid-Century period, and End-Century period in Kelani River basin are shown in Figure 4-79. For the seasonal analysis, all those monthly SPI values are plotted as a graph. The First Inter Monsoon drought classification for different periods shows in Table 4-18. Compare the observed data all the drought types will reduce in the both mid and end-century.

Table 4-18 Event identification of SDI values in First Inter Monsoon and the percentage variation of the mid and end-century based on the observed period

Drought Type	Observed Period	Mid-Century	End-Century
Non-drought	30	18 (-40%)	13 (-57%)
Mild drought	19	15 (-21%)	23 (21%)
Moderate drought	8	4 (-50%)	2 (-75%)
Severe drought	3	1 (-67%)	0 (-100%)
Extreme drought	0	0 (0%)	0 (0%)

4.4.5.4 Southwest Monsoon Period

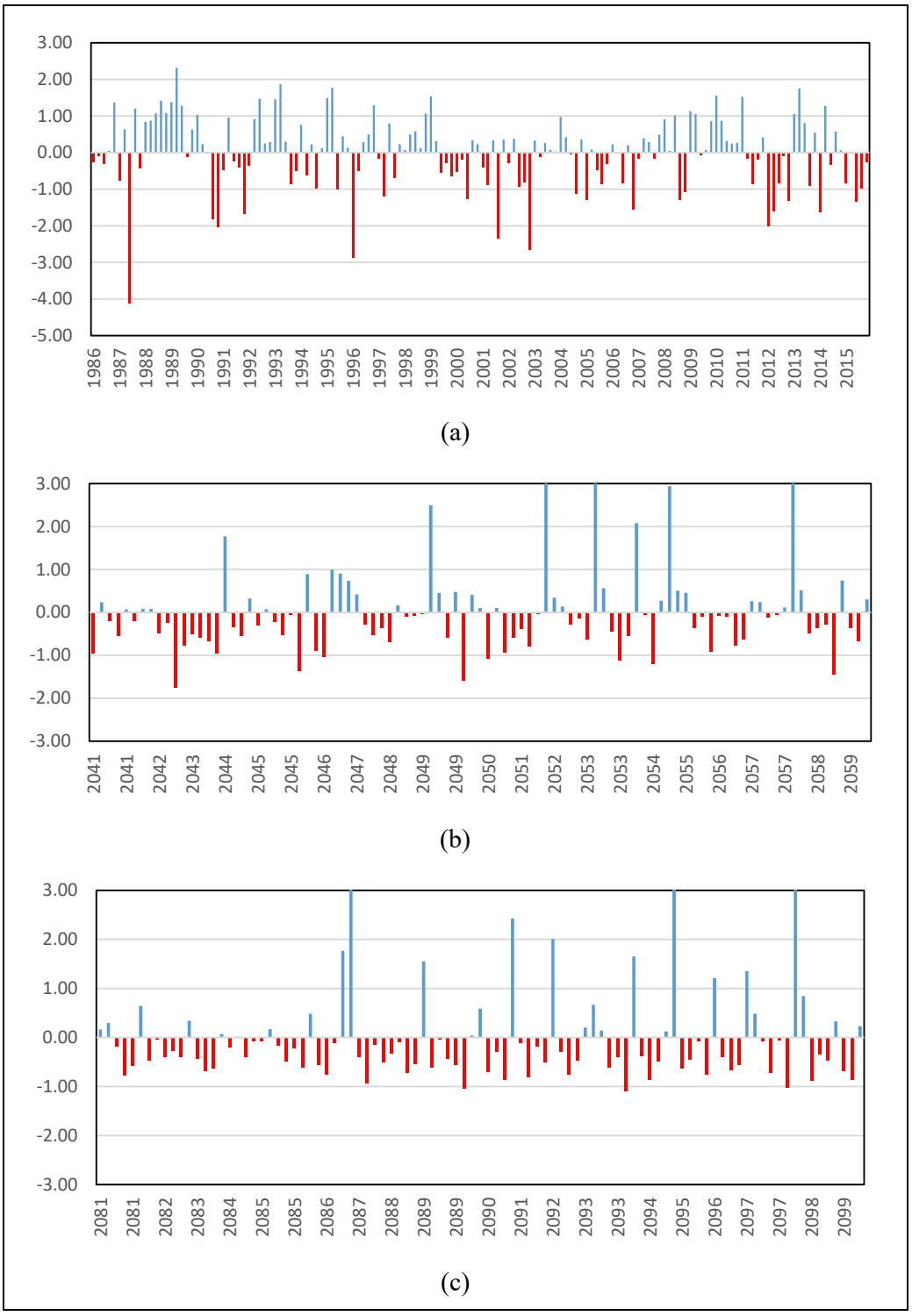

Figure 4-80 Standardized Precipitation Index in Southwest Monsoon for (a) observed period, (b) mid-century period, and (c) end-century period in Kelani River basin

Standardized Precipitation Index in Southwest Monsoon for the observed period, Mid-Century period, and End-Century period in Kelani River basin are shown in Figure 4-80. For the seasonal analysis, all those monthly SPI values are plotted as a graph. The Southwest Monsoon drought classification for different periods shows in Table 4-19. Compare the observed data all the drought types will reduce in the both mid and end-century.

Table 4-19 Event identification of SPI values in Southwest Monsoon and the percentage variation of the mid and end-century based on the observed period

Drought Type	Observed Period	Mid-Century	End-Century
Non-drought	81	36 (-56%)	28 (-65%)
Mild drought	50	51 (2%)	64 (28%)
Moderate drought	8	6 (-25%)	3 (-63%)
Severe drought	5	2 (-60%)	0 (-100%)
Extreme drought	6	0 (-100%)	0 (-100%)

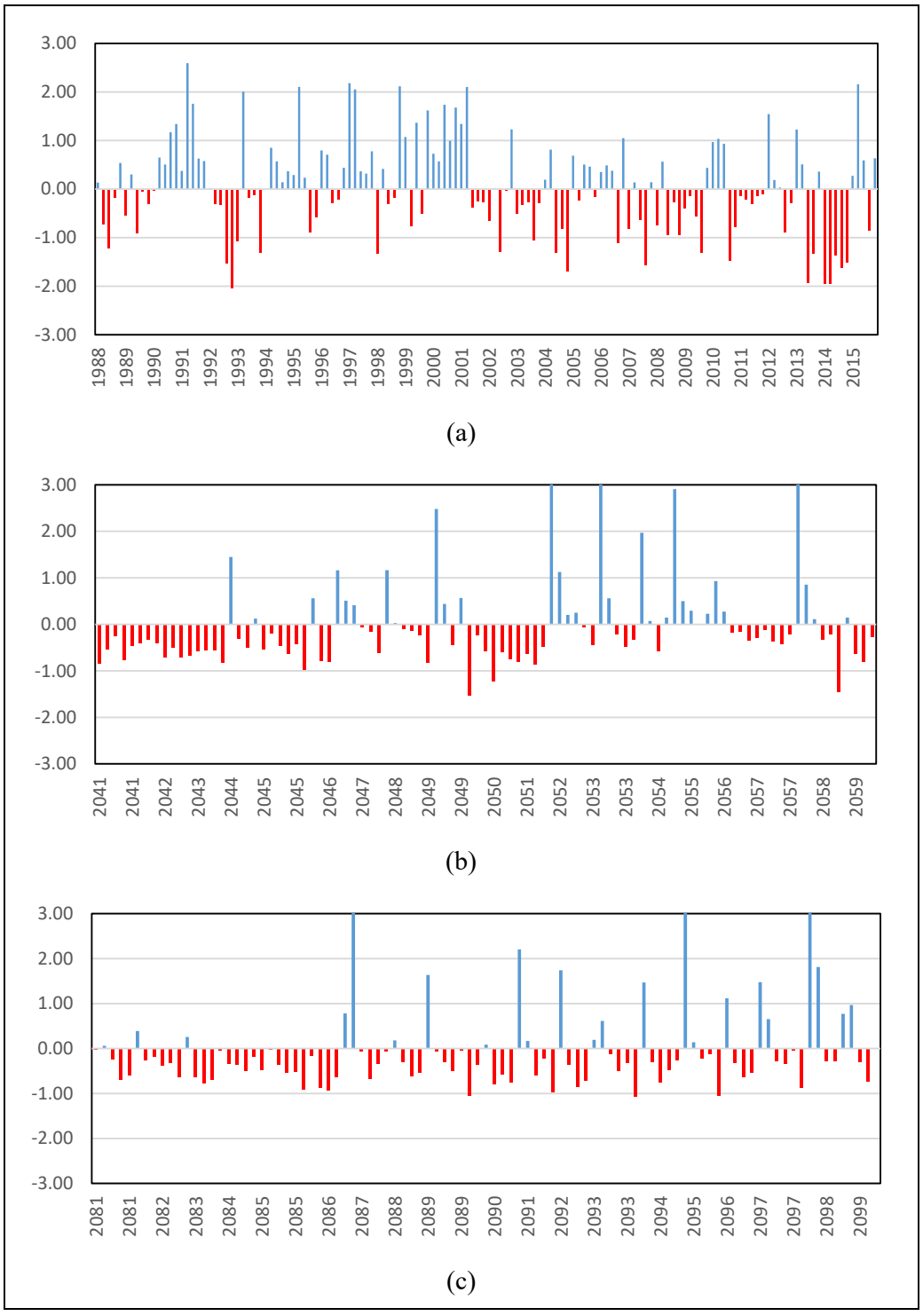

Figure 4-81 Streamflow Drought Index in Southwest Monsoon for (a) observed period, (b) mid-century period, and (c) end-century period in Kelani River basin

Streamflow Drought Index in Southwest Monsoon for the observed period, Mid-Century period, and End-Century period in Kelani River basin is shown in Figure 4-81. For the seasonal analysis, all those monthly SPI values are plotted as a graph. The Southwest Monsoon drought classification for different periods shows in Table 4-20. Compare the observed data all the drought types will reduce in the both mid and end-century.

Table 4-20 Event identification of SDI values in Southwest Monsoon and the percentage variation of the Mid and End-century based on the observed period

Drought Type	Observed Period	Mid-Century	End-Century
Non-drought	71	30 (-58%)	24 (-66%)
Mild drought	54	62 (15%)	68 (26%)
Moderate drought	13	2 (-85%)	3 (-77%)
Severe drought	11	1 (-91%)	0 (-100%)
Extreme drought	1	0 (-100%)	0 (-100%)

4.5 Discussion

Drought has a long-term effect, and its consequences are spread out across a broader geographical area than other natural disasters. Most policy reactions to drought tend to focus on meeting immediate demands to deliver more expensive solutions. Drought and flood-affected communities in Sri Lanka have been awarded billions of rupees for drought and disaster relief. Drought mitigation and preparedness, on the other hand, are inadequate, and drought and flooding are common in some parts of the country. According to the findings of this study, there may be distinct, tiny geographic locations that are more prone to drought and flooding. As a result, policymakers need to be able to identify places and intervals based on watersheds and river basins. It will be in lead to a more proactive method to risk management that stresses readiness, mitigation, forecast, and early indication. In this concern, the findings of this study will be beneficial to Sri Lankan representatives.

4.5.1 Bias Correction

The minimum 30 years period of precipitation data expected for bias correction according to the World Meteorological Organization (WMO). However, due to data scarcity, cost, and accuracy, 15 years of data (1985-2005) were employed as a baseline for bias correction (Sirisena et al., 2021).

4.5.2 Drought Condition

Agricultural, Metrological, and Hydrological drought have been calculated for the Kirindi Oya river basin. Agricultural drought indices NDVI calculated in GIS by using Landsat image on the other hand SPI and SDI have been calculated by using a respective formula which is mentioned in the 3.8 section. For the calculating of SPI and SDI have used three intervals three months, six months, and twelve months.

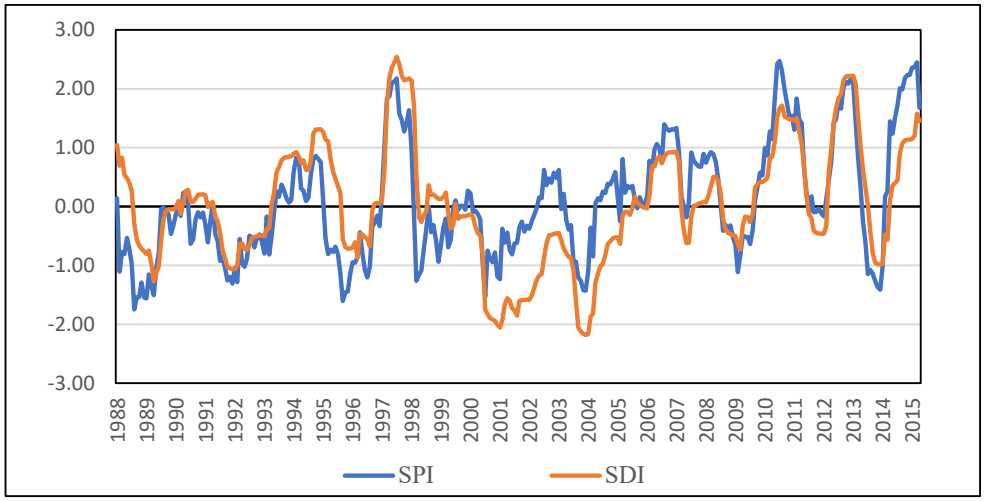

Figure 4-82 Variation of SPI and SDI in the 12-month interval of Kirindi Oya basin over the observed period

Table 4-21 Event identification of SPI values in 12 months period and the percentage variation of the mid and end-century based on the observed period in Kirindi Oya river basin

Drought Type	Observed Period	Mid-Century	End-Century
Non-drought	1009	699 (-31%)	661 (-34%)
Mild drought	840	584 (-30%)	630 (-25%)
Moderate drought	247	122 (-51%)	151 (-39%)
Severe drought	52	89 (71%)	42 (-19%)
Extreme drought	0	0 (0%)	10 (0%)

Table 4-22 Event identification of SDI values in 12 months period and the percentage variation of the mid and end-century based on the observed period in Kirindi Oya river basin

Drought Type	Observed Period	Mid-Century	End-Century
Non-drought	156	91 (-31%)	98 (-34%)
Mild drought	128	109 (-30%)	91 (-25%)
Moderate drought	16	29 (-51%)	40 (-39%)
Severe drought	21	0 (-100%)	0 (-100%)
Extreme drought	7	0 (-100%)	0 (-100%)

According to the SPI study, the Kirindi Oya river basin experienced droughts in the years 1989–1990, 1991–1992, 2000–2001, and 2013–2014, with 1991–1992 being a severe drought year (Abeysingha et al., 2020). Based on this project's finding has matched with the above-mentioned reference.

Agricultural, Metrological, and Hydrological drought have been calculated for the Kirindi Oya river basin. Agricultural drought indices NDVI calculated in GIS by using Landsat image on the other hand SPI and SDI have been calculated by using a respective formula which is mentioned in the 3.8 section. For the calculating of SPI and SDI have used three intervals three months, six months, and twelve months.

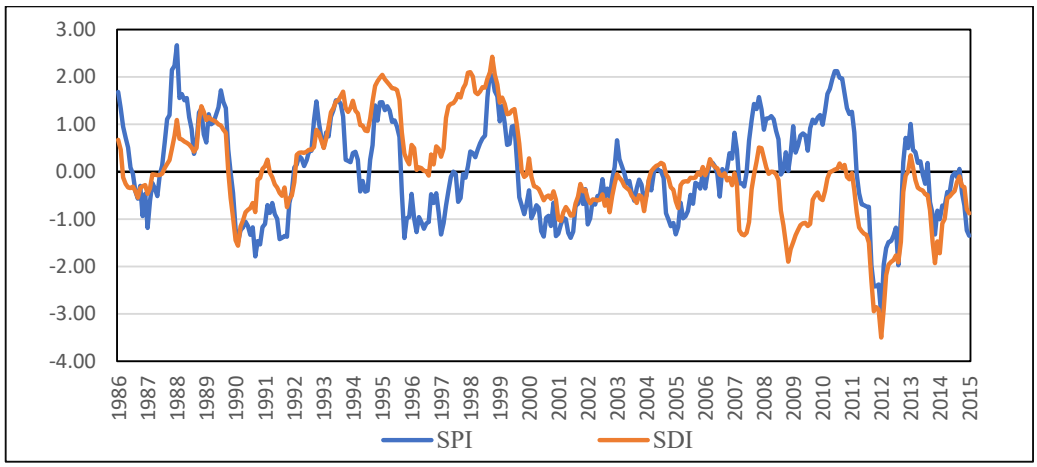

Figure 4-83 Variation of SPI and SDI in the 12-month interval of Kelani River basin over the observed period

Table 4-23 Event identification of SPI values in 12 months period and the percentage variation of the mid and end-century based on the observed period in the Kelani River basin

Drought Type	Observed Period	Mid-Century	End-Century
Non-drought	1094	637 (-42%)	496 (-55%)
Mild drought	801	516 (-36%)	833 (4%)
Moderate drought	304	158 (-48%)	84 (-72%)
Severe drought	42	102 (143%)	0 (-100%)
Extreme drought	30	0 (-100%)	0 (-100%)

Table 4-24 Event identification of SDI values in 12 months period and the percentage variation of the mid and end-century based on the observed period in the Kelani River basin

Drought Type	Observed Period	Mid-Century	End-Century
Non-drought	999	1413 (41%)	637 (-36%)
Mild drought	959	0 (-100%)	646 (-33%)
Moderate drought	188	0 (-100%)	121 (-36%)
Severe drought	69	0 (-100%)	9 (-87%)
Extreme drought	56	0 (-100%)	0 (-100%)

4.5.3 Model Calibration and Validation

Kirindi Oya River Basin

Daily time scale precipitation and observed river flow data were collected for the model process from 1985/86 to 2014/15 water years. The warmup period was taken from 1 October 2001 to 30 September 2002. When the warmup parameters are fixed then running the model for 5 years calibration (2002/03 to 2006/07) are considered for optimization. Four parameters (Recession Constant, Ratio to peak, Muskingum *K*, and Muskingum *X*) are optimized for calibrating the HEC-HMS model for the observed period and initial parameters and optimized parameters. Calibrated Objective function RMSE value is 0.60 which is performance level is good, NSE value is 0.59 which is a good category in performance level, and percent bias value is 7.63% which is very good in performance level.

Another 5 years (2010/11 to 2014/15) are used for validation and validated objectives functions are RMSE value is 0.70 which is performance level is satisfactory, NSE value is 0.505 which is a satisfactory category in performance level, and percent bias value is 3.22% which is very good in performance level. During this validity process, the model parameters which are determined from the calibration process were kept freeze. As military the calibrated model evaluation. After getting the fixed value of RMSE, NSE, and percent bias at a satisfactory level. After the model validates for the observed period, this model has been used for mid and end-century periods.

Kelani River Basin

Daily time scale precipitation and observed river flow data were collected for the model process from 1985/86 to 2014/15 water years. The warmup period was taken from 1 October 2001 to 30 September 1986. When the warmup parameters are fixed then run the model for 5 years calibration (1990/91 to 1994/95) are considered for optimization. Four parameters (Recession Constant, Ratio to peak, Muskingum *K*, and Muskingum *X*) are optimized for calibrating the HEC-HMS model for the observed period and initial parameters and optimized parameters. Calibrated Objective function RMSE value is 0.60 which is performance level is good, NSE value is 0.64 which is a satisfactory category in performance level, and percent bias value is 0.64% which is very good in performance level.

Another 5 years (2007/08 to 2011/12) are used for validation and validated objectives functions are RMSE value is 0.70 which is performance level is satisfactory, NSE value is 0.56 which is a satisfactory category in performance level, and percent bias value is -3.27% which is very good in performance level. During this validity process, the model parameters which are determined from the calibration process were kept freeze. As military the calibrated model evaluation. After getting the fixed value of RMSE, NSE, and percent bias at a satisfactory level. After the model validates for the observed period, this model has been used for mid and end-century periods.

4.5.4 Drought Assessment

Kirindi Oya River Basin

Seasonal analysis has been performed for the drought assessment. According to Sri Lankan, the hydrological water cycle is mentioned four-season. For the seasonal assessment, Figure 4-84 has been shown SPI and SDI variation together. SPI and SDI analyses, as well as their relationship, are valuable in monitoring drought and land use planning in the area. As per this graph, this study is a clear demonstration of SPI dynamics are matching with SDI dynamics in the observed period.

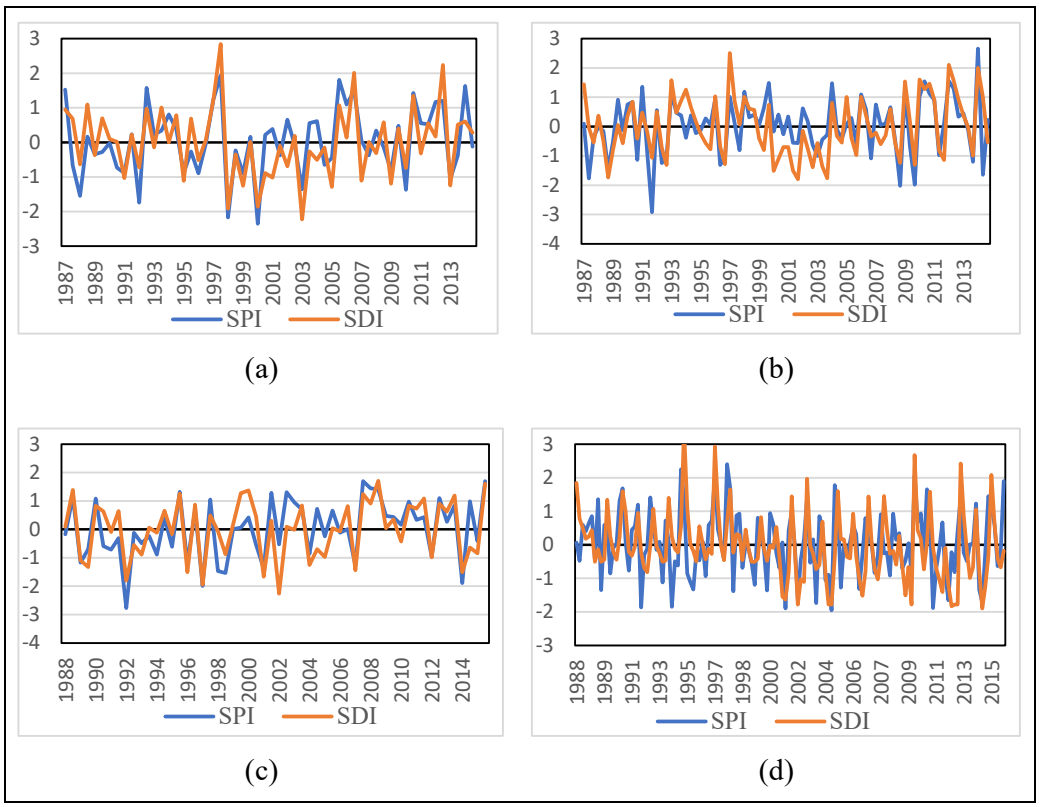

Figure 4-84 Variation of SPI and SDI in Kirindi Oya basin over the observed period where is (a) Second Inter Monsoon, (b) Northeast Monsoon, (c) First Inter Monsoon, and (d) Southwest Monsoon

Seasonal analysis has been performed for the drought assessment. According to Sri Lankan, the hydrological water cycle is mentioned four-season. For the seasonal assessment, Figure 4-85 has been shown SPI and SDI variation together. SPI and SDI analyses, as well as their relationship, are valuable in monitoring drought and land use planning in the area. As per this graph, this study is a clear demonstration of SPI dynamics are matching with SDI dynamics in the mid-century period of the 21st century.

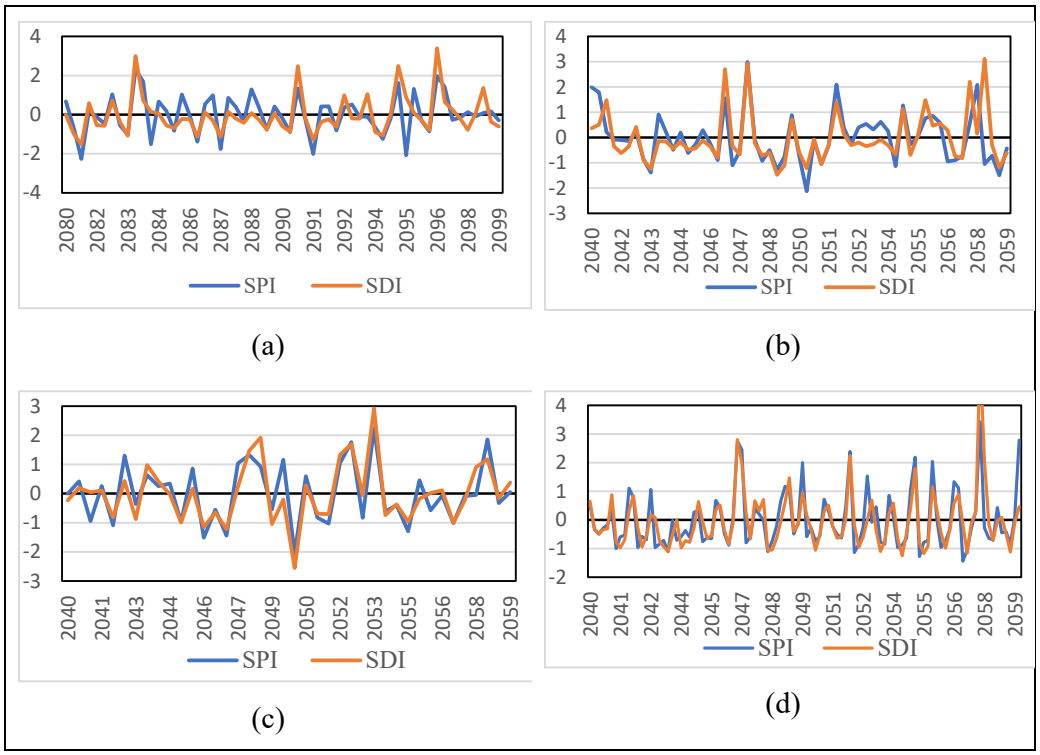

Figure 4-85 Variation of SPI and SDI in Kirindi Oya basin over the mid-century period where is (a) Second Inter Monsoon, (b) Northeast Monsoon, (c) First Inter Monsoon, and (d) Southwest Monsoon

Seasonal analysis has been performed for the drought assessment. According to Sri Lankan, the hydrological water cycle is mentioned four-season. For the seasonal assessment, with Figure 4-86 has been shown SPI and SDI variation together. SPI and SDI analyses, as well as their relationship, are valuable in monitoring drought and land use planning in the area. As per this graph, this study is a clear demonstration of SPI dynamics are matching with SDI dynamics in the end-century period of the 21st century.

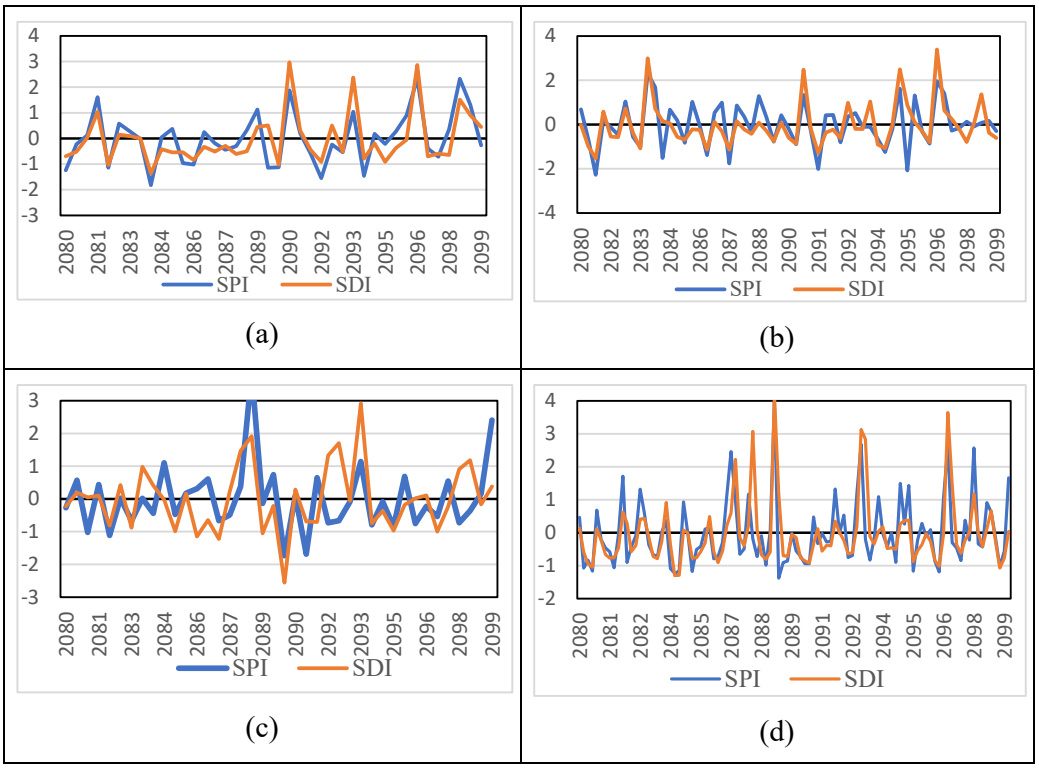

Figure 4-86 Variation of SPI and SDI in Kirindi Oya basin over the End-Century period where is (a) Second Inter Monsoon, (b) Northeast Monsoon, (c) First Inter Monsoon, and (d) Southwest Monsoon

Kelani River Basin

Seasonal analysis has been performed for the drought assessment. According to Sri Lankan, the hydrological water cycle is mentioned four-season. For the seasonal assessment, Figure 4-87 has been shown SPI and SDI variation together. SPI and SDI analyses, as well as their relationship, are valuable in monitoring drought and land use planning in the area. As per this graph, this study is a clear demonstration of SPI dynamics are matching with SDI dynamics in the observed period.

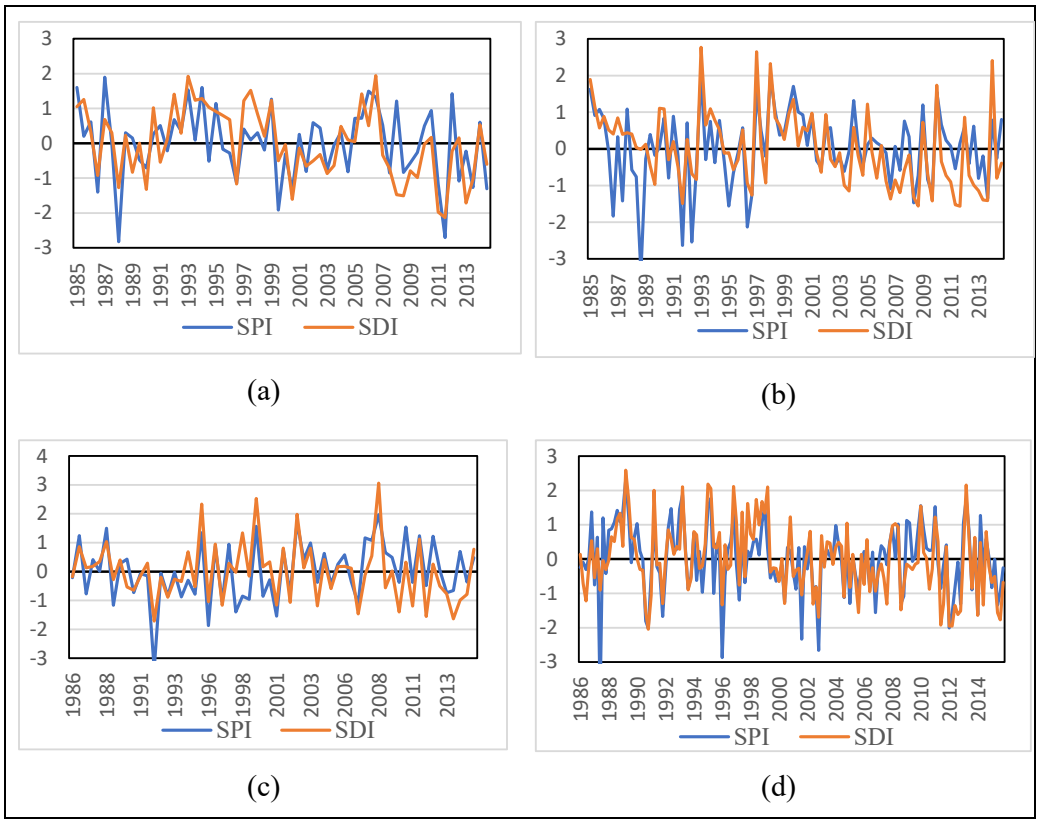

Figure 4-87 Variation of SPI and SDI in Kelani River basin over the observed period where is (a) Second Inter Monsoon, (b) Northeast Monsoon, (c) First Inter Monsoon, and (d) Southwest Monsoon

Seasonal analysis has been performed for the drought assessment. According to Sri Lankan, the hydrological water cycle is mentioned four-season. For the seasonal assessment, Figure 4-88 has been shown SPI and SDI variation together. SPI and SDI analyses, as well as their relationship, are valuable in monitoring drought and land use planning in the area. As per this graph, this study is a clear demonstration of SPI dynamics are matching with SDI dynamics in the mid-century period of the 21st century.

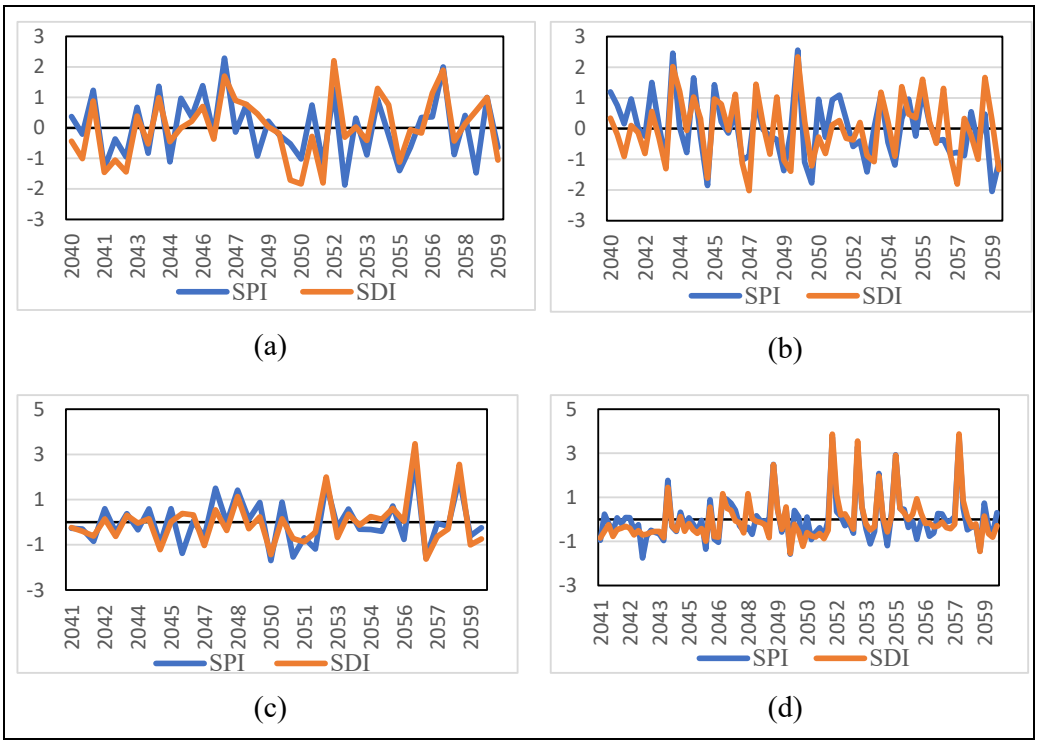

Figure 4-88 Variation of SPI and SDI in Kelani River basin over the mid-century period where is (a) Second Inter Monsoon, (b) Northeast Monsoon, (c) First Inter Monsoon and (d) Southwest Monsoon.

Seasonal analysis has been performed for the drought assessment. According to Sri Lankan, the hydrological water cycle is mentioned four-season. For the seasonal assessment, Figure 4-89 has been shown SPI and SDI variation together. SPI and SDI analyses, as well as their relationship, are valuable in monitoring drought and land use planning in the area. As per this graph, this study is a clear demonstration of SPI dynamics are matching with SDI dynamics in the end-century period of the 21st century.

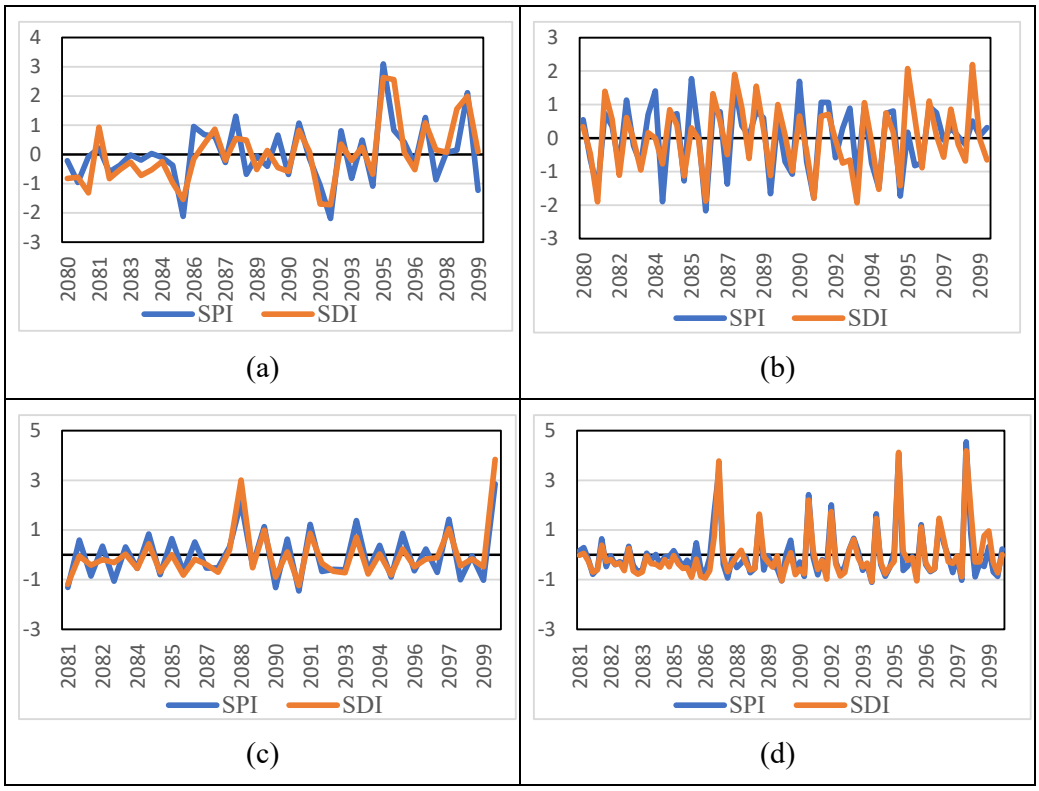

Figure 4-89 Variation of SPI and SDI in Kelani River basin over the end-century period where is (a) Second Inter Monsoon, (b) Northeast Monsoon, (c) First Inter Monsoon and (d) Southwest Monsoon.

According to seasonal analysis, each type of drought percentage variance of SPI in the mid-century in both Kirindi Oya and Kelani River basins are shown in Table 4-25. From this table, it has been clearly shown that in the SIM season moderate drought may increase double the number of events compared to the observed period and the extreme drought will not change in FIM and SWM. In the Kelani River basin, severe drought will no change in SIM and NEM and 50% will increase in FIM.

Table 4-25 Percentage variation in SPI according to seasonal analysis in both Kirindi Oya and Kelani River basin in mid-century Period

River Basin	Drought Type	SIM	NEM	FIM	SWM
Kirindi Oya	Non-drought	-25%	-47%	-40%	-49%
	Mild drought	-48%	0%	-12%	19%
	Moderate drought	100%	-13%	0%	-36%
	Severe drought	-50%	-100%	-67%	-100%
	Extreme drought	-50%	-50%	0%	0%
Kelani River	Non-drought	-41%	-44%	-46%	-56%
	Mild drought	-22%	-33%	-28%	2%
	Moderate drought	-14%	17%	-50%	-25%
	Severe drought	0%	0%	50%	-60%
	Extreme drought	-100%	-75%	-100%	-100%

According to seasonal analysis, each type of drought percentage variance of SPI in the end century is shown in Table 4-26. From this table, it has been clearly shown that extreme drought may increase 50% in NEM, and moderate drought may double the number compared to the observed period and the extreme drought will not change in SWM. In the Kelani River basin, extreme drought will no change in SIM and severe drought may increase 150% in NEM.

Table 4-26 Percentage variation in SPI according to seasonal analysis in both Kirindi Oya and Kelani River basin in end-century Period

River Basin	Drought Type	SIM	NEM	FIM	SWM
Kirindi Oya	Non-drought	-32%	-43%	-40%	-53%
	Mild drought	-38%	-8%	6%	17%
	Moderate drought	100%	-63%	-60%	0%
	Severe drought	0%	-33%	-33%	-100%
	Extreme drought	-100%	50%	-100%	0%
Kelani River	Non-drought	-47%	-29%	-39%	-65%
	Mild drought	0%	-60%	-40%	28%
	Moderate drought	-57%	-17%	50%	-63%
	Severe drought	-100%	150%	-100%	-100%
	Extreme drought	0%	-75%	-100%	-100%

Streamflow Drought Index

According to seasonal analysis, each type of drought percentage variance of SDI in the mid-century is shown in Table 4-27. From this table, it has been clearly shown that extreme drought may not change in FIM and SWM and moderate drought may not change in SIM and FIM compared to the observed period. In the Kelani River basin, extreme drought will no change in NEM and FIM and moderate drought may increase 20% in SIM.

Table 4-27 Percentage variation in SDI according to seasonal analysis in both Kirindi Oya and Kelani River basin in mid-century Period

River Basin	Drought Type	SIM	NEM	FIM	SWM
Kirindi Oya	Non-drought	-43%	0%	-39%	-29%
	Mild drought	0%	3%	7%	-21%
	Moderate drought	0%	-40%	0%	13%
	Severe drought	-100%	-100%	-100%	-100%
	Extreme drought	-100%	-100%	0%	0%
Kelani River	Non-drought	-41%	-31%	-40%	-58%
	Mild drought	-22%	-49%	-21%	15%
	Moderate drought	20%	-30%	-50%	-85%
	Severe drought	-75%	-33%	-67%	-91%
	Extreme drought	-100%	0%	0%	-100%

According to seasonal analysis, each type of drought percentage variance of SDI in the end century is shown in Table 4-28. From this table, it has been clearly shown that extreme drought may not change in SWM compared to the observed period. In the Kelani River basin, extreme drought will no change in NEM and FIM and severe drought may increase 67% in NEM.

Table 4-28 Percentage variation in SDI according to seasonal analysis in both Kirindi Oya and Kelani River basin in end-century Period

River Basin	Drought Type	SIM	NEM	FIM	SWM
Kirindi Oya	Non-drought	-50%	0%	-71%	-33%
	Mild drought	47%	-9%	107%	-12%
	Moderate drought	-63%	-50%	-100%	-38%
	Severe drought	-100%	-75%	-100%	-100%
	Extreme drought	-100%	-100%	-100%	0%
Kelani River	Non-drought	-41%	-33%	-57%	-66%
	Mild drought	-6%	-43%	21%	26%
	Moderate drought	-80%	-60%	-75%	-77%
	Severe drought	-25%	67%	-100%	-100%
	Extreme drought	-100%	0%	0%	-100%

- In the Second Inter Monsson, both river basins (Kirindi Oya and Kelani) percentage of drought variance are decreasing. For the extreme drought percentage of SPI values when Kirindi Oya 50% and Kelani double the number. Then it can be said that drought will reduce more in the Kelani River basin than Kirindi Oya river basin more than 50% in the mid-century. For the extreme drought percentage of SDI values when Kirindi Oya double the number and Kelani also double the number Then it can be said that drought will reduce equally in the Kelani River basin and Kirindi Oya both river basins in the mid-century.
- In the Northeast Monsson, both river basins (Kirindi Oya and Kelani) percentage of drought variance are decreasing. For the extreme drought percentage of SPI values when Kirindi Oya 50% and Kelani 75%. Then it can be said that drought

will reduce more in the Kelani River basin than Kirindi Oya river basin more than 25%. For the extreme drought percentage of SDI values when Kirindi Oya double the number and Kelani no change. Then it can be said that drought will reduce equally in the Kelani River basin and Kirindi Oya both river basins in the mid-century.

- In the First Inter Monsson, both river basins (Kirindi Oya and Kelani) percentage of drought variance are decreasing. For the extreme drought percentage of SPI values when Kirindi Oya no change and Kelani double the number. Then it can be said that drought will reduce more in the Kelani River basin than Kirindi Oya river basin more than double the number. For the extreme drought percentage of SDI values when Kirindi Oya no change and Kelani also no change. Then it can be said that drought will reduce equally in the Kelani River basin and Kirindi Oya both river basins in the mid-century.
- In the Southwest Monsson, both river basins (Kirindi Oya and Kelani) percentage of drought variance are decreasing. For the extreme drought percentage of SPI values when Kirindi Oya no change and Kelani double the number. Then it can be said that drought will reduce more in the Kelani River basin than Kirindi Oya river basin more than double the number. For the extreme drought percentage of SDI values when Kirindi Oya no change and Kelani double the number. Then it can be said that drought will reduce equally in the Kelani River basin and Kirindi Oya both river basins in the mid-century.
- In the Second Inter Monsson, both river basins (Kirindi Oya and Kelani) percentage of drought variance are decreasing. For the extreme drought percentage of SPI values when Kirindi Oya 50% and Kelani double the number. Then it can be said that drought will reduce more in the Kelani River basin than Kirindi Oya river basin more than 50% in the mid-century. For the extreme drought percentage of SDI values when Kirindi Oya double the number and Kelani also double the number. Then it can be said that drought will reduce equally in the Kelani River basin and Kirindi Oya both river basins in the end-century.
- In the Northeast Monsson, both river basins (Kirindi Oya and Kelani) percentage of drought variance are decreasing. For the extreme drought percentage of SPI

values when Kirindi Oya 50% and Kelani 75%. Then it can be said that drought will reduce more in the Kelani River basin than Kirindi Oya river basin more than 25%. For the extreme drought percentage of SDI values when Kirindi Oya double the number and Kelani no change. Then it can be said that drought will reduce equally in the Kelani River basin and Kirindi Oya both river basins in the mid-century.

- In the First Inter Monsson, both river basins (Kirindi Oya and Kelani) percentage of drought variance are decreasing. For the extreme drought percentage of SPI values when Kirindi Oya no change and Kelani double the number. Then it can be said that drought will reduce more in the Kelani River basin than Kirindi Oya river basin more than double the number. For the extreme drought percentage of SDI values when Kirindi Oya no change and Kelani also no change. Then it can be said that drought will reduce equally in the Kelani River basin and Kirindi Oya both river basins in the mid-century.
- In the Southwest Monsson, both river basins (Kirindi Oya and Kelani) percentage of drought variance are decreasing. For the extreme drought percentage of SPI values when Kirindi Oya no change and Kelani double the number. Then it can be said that drought will reduce more in the Kelani River basin than Kirindi Oya river basin more than double the number. For the extreme drought percentage of SDI values when Kirindi Oya no change and Kelani double the number. Then it can be said that drought will reduce equally in the Kelani River basin and Kirindi Oya both river basins in the mid-century.

CHAPTER 5

5 CONCLUSIONS AND RECOMMENDATIONS

5.1 Conclusions

- For attending the first objectives indices were calculated for both river basins. It has been shown in this research for the observed period Kirindi Oya basin observed 3- or 4-years drought affects frequently. on the other hand, the seasonal analysis showed different characteristics. For the second Inter monsoon in the observed 30 years severe drought identified only 4 different years but for Mid-century would occur for 6 different years but End-century only 3 years.
- According to the 2nd objective, the HEC-HMS model is developed for both river basins with respect to objective functions. For Kirindi Oya river basin calibrated value of RMSE is 0.6, NSE is 0.59, and the percent bias is 7.63% which is a good and satisfactory level. The validated value of RMSE is 0.7, NSE is 0.505, and the percent bias is 3.22% which is a good and satisfactory level.
- For the Kelani River basin, the calibrated value of RMSE is 0.6, NSE is 0.64, and the percent bias is 0.64% which is a good and satisfactory level. The validated value of RMSE is 0.7, NSE is 0.56, and the percent bias is -3.27% which is a good and satisfactory level.
- According to historical data, extreme drought may decrease by 50% in the mid-century period, and extreme drought may not occur that much in the end-of-century period. In the mid-century, severe droughts may decrease by 50%, and in the end-century, the same type of drought as observed may occur. In the case of mild drought, the probability of occurrence could be doubled as compared to the observed period. Mild drought is less harmful to the environment, however, in this study, the percentage variation of mild drought will decrease by 50% in the mid-century and by 30% at the end of the century. During the last non-drought

percentage variation may reduce by 25% in the mid-century and 30% in the end-century.

- As a result, gaining a better understanding of the drought situation in the Kirindi Oya basin will aid in fine-fine-tuning this irrigation project. The current study found that the Kirindi Oya river basin's drying propensity increases only from July to September (3 months).
- According to seasonal analysis, the probability of occurrence of extreme drought according to SPI values in Kirindi Oya basin is decreasing 25% for mid and 50% end-century, in the Kelani basin 90% for mid and 70% in end-century. According to SDI values in the Kirindi Oya basin is decreasing 25% for mid and 25% end-century, in the Kelani basin 95% for mid and 50% in end-century. First inter monsoon has been found more severe to drought for both SPI and SDI combination in Kirindi Oya river basin, the northeast monsoon period is the driest season for the Kelani River basin which is situated in wet zone in Sri Lanka.
- In the Kirindi Oya river basin, according to SPI calculation SIM moderate drought will increase 100% in mid-century but in the end-century extreme drought will increase 50% in NEM. On the other hand, according to SDI FIM and SWM may show the same drought event as the observed period in mid-century but in the end-century SWM only show the extreme drought as same as observed period.
- In the Kelani River basin, according to SPI calculation FIM, severe drought will increase 50% in mid-century but in the end-century severe drought will increase 150% in NEM and moderate will increase 50% in FIM. On the other hand, according to SDI moderate drought will increase 50% in SIM in mid-century and severe will increase 70% in NEM in the end of the century.

5.2 Recommendations

- SPI value is calculated along with four rainfall stations but there are so many rainfall stations are situated in the Kirindi Oya river basin. If possible, use all the rainfall stations it will show a more accurate result. Thus, it is recommended to use the maximum number of rainfall station data to identify meteorological droughts.

- In this research it has been used only three drought index Normalized Difference Vegetation (NDVI), Standardized Precipitation Index (SPI), and Streamflow Drought Index (SDI) but for the better result further it is recommended that use Palmer Drought Severity Index (PDSI), Vegetation Condition Index (VCI), Standardized Streamflow Index (SSI), and Temperature Condition Index (TCI).
- Drought has a long-term effect, and its consequences are spread out across a broader geographical area than other natural disasters. The majority of program reactions to drought tend to focus on meeting urgent demands to deliver frequently more expensive solutions. In Sri Lanka, billions of rupees are given for drought and flood relief in drought and flood-affected areas.
- For this research work, it has been assumed that the curve number is constant. But it has been recommended that future more accurate results land use may be considered.
- Drought modification and preparedness, on the other hand, are insufficient, and drought and flooding are common in several parts of the country. According to the findings of this study, there may be distinct tiny geographic locations that are more prone to drought and flooding.
- Therefore, policymakers need to be able to identify places and seasons depending on watershed and river basin. It will result in a more proactive risk management strategy that stresses readiness, mitigation, forecast, and early warning. This research provides helpful data for Sri Lankan representatives in this regard.

BIBLIOGRAPHY

References

Aadhar, S., & Mishra, V. (2017). Data Descriptor: High-resolution near real-time drought monitoring in South Asia. *Scientific Data*, *4*, 1–14. https://doi.org/10.1038/sdata.2017.145

Abeysingha, N. S., Wickramasuriya, M. G., & Meegastenna, T. J. (2020). *Assessment of meteorological and hydrological drought ; a case study in Kirindi Oya river basin in Sri Lanka*. *10*(5), 429–447.

Agrawal, A. (2005). *A data model with pre-and-post processor for HEC-HMS*. *August*, 321–325.

Ahbari, A., Stour, L., Agoumi, A., & Serhir, N. (2018). Estimation of initial values of the HMS model parameters: Application to the basin of Bin El Ouidane (Azilal, Morocco). *Journal of Materials and Environmental Science*, *9*(1), 305–317. https://doi.org/10.26872/jmes.2018.9.1.34

Al-Qinna, M. I., Hammouri, N. A., Obeidat, M. M., & Ahmad, F. Y. (2011). Drought analysis in Jordan under current and future climates. *Climatic Change*, *106*(3), 421–440. https://doi.org/10.1007/s10584-010-9954-y

Amarsaikhan, D., Battsengel, V., Nergui, B., Ganzorig, M., & Bolor, G. (2014). A Study on Air Pollution in Ulaanbaatar City, Mongolia. *Journal of Geoscience and Environment Protection*, *02*(02), 123–128. https://doi.org/10.4236/gep.2014.22017

Belal, A. A., El-Ramady, H. R., Mohamed, E. S., & Saleh, A. M. (2014). Drought risk assessment using remote sensing and GIS techniques. *Arabian Journal of Geosciences*, *7*(1), 35–53. https://doi.org/10.1007/s12517-012-0707-2

Bravar, L., & Kavvas, M. L. (1991). On the physics of droughts. II. Analysis and simulation of the interaction of atmospheric and hydrologic processes during

droughts. *Journal of Hydrology*, *129*(1–4), 299–330. https://doi.org/10.1016/0022-1694(91)90056-N

Brown, J. F., Reed, B. C., Falls, S., Hayes, M. J., Wilhite, D. A., Hall, L. W. C., Hubbard, K., & Hall, L. W. C. (2002). *A PROTOTYPE DROUGHT MONITORING SYSTEM INTEGRATING CLIMATE AND SATELLITE DATA*.

Chandimala, J., & Zubair, L. (2007). Predictability of stream flow and rainfall based on ENSO for water resources management in Sri Lanka. *Journal of Hydrology*, *335*(3–4), 303–312. https://doi.org/10.1016/j.jhydrol.2006.11.024

De Châtel, F. (2014). The Role of Drought and Climate Change in the Syrian Uprising: Untangling the Triggers of the Revolution. *Middle Eastern Studies*, *50*(4), 521–535. https://doi.org/10.1080/00263206.2013.850076

De Silva, C. S., Weatherhead, E. K., Knox, J. W., & Rodriguez-Diaz, J. A. (2007). Predicting the impacts of climate change-A case study of paddy irrigation water requirements in Sri Lanka. *Agricultural Water Management*, *93*(1–2), 19–29. https://doi.org/10.1016/j.agwat.2007.06.003

De Silva, M. M. G. T., Weerakoon, S. B., & Herath, S. (2014). Modeling of Event and Continuous Flow Hydrographs with HEC–HMS: Case Study in the Kelani River Basin, Sri Lanka. *Journal of Hydrologic Engineering*, *19*(4), 800–806. https://doi.org/10.1061/(asce)he.1943-5584.0000846

Dessai, S., & Sims, C. (2010). Public perception of drought and climate change in southeast england. *Environmental Hazards*, *9*(4), 340–357. https://doi.org/10.3763/ehaz.2010.0037

Filho, W. L. (2015). Handbook of Climate Change Adaptation. In *Handbook of Climate Change Adaptation* (Issue January). https://doi.org/10.1007/978-3-642-38670-1

Gunathilake, G. R. M. B., Panditharathne, P., Gunathilake, A. S., & Warakagoda, N. D. (2019). Application of HEC-HMS Model on Event-Based Simulations in the Seethawaka. *Scholar Journal of Applied Sciences and Research*, *2*(9), 32–40.

Hamedi, A., & Fuentes, H. R. (2015). Comparative effectiveness and reliability of

NEXRAD data to predict outlet hydrographs using the GSSHA and HEC-HMS hydrologic models. *World Environmental and Water Resources Congress 2015: Floods, Droughts, and Ecosystems - Proceedings of the 2015 World Environmental and Water Resources Congress*, *September 2005*, 1444–1453. https://doi.org/10.1061/9780784479162.142

Hasan, M. M., & Croke, B. F. W. (2013). Filling gaps in daily rainfall data: A statistical approach. *Proceedings - 20th International Congress on Modelling and Simulation, MODSIM 2013*, *December*, 380–386. https://doi.org/10.36334/modsim.2013.a9.hasan

Himanshu, S. K., Singh, G., & Kharola, N. (2015). Monitoring of drought using satellite data. *International Research Journal of Earth Sciences*, *3*(1), 66–72.

Ismail, wan, & Ibrahim, W. (2017). Estimation of rainfall and stream flow missing data for Terengganu, Malaysia by using interpolation technique methods. *Malaysian Journal of Fundamental and Applied Sciences*, *13*(3), 213–217. https://doi.org/10.11113/mjfas.v13n3.578

Jayakrishnan, R., Srinivasan, R., Santhi, C., & Arnold, J. G. (2005). Advances in the application of the SWAT model for water resources management. *Hydrological Processes*, *19*(3), 749–762. https://doi.org/10.1002/hyp.5624

Kashani, M. H., & Dinpashoh, Y. (2012). Evaluation of efficiency of different estimation methods for missing climatological data. *Stochastic Environmental Research and Risk Assessment*, *26*(1), 59–71. https://doi.org/10.1007/s00477-011-0536-y

Kottawa-Arachchi, J. D., & Wijeratne, M. A. (2017). Climate change impacts on biodiversity and ecosystems in sri lanka: A review. *Nature Conservation Research*, *2*(3), 2–22. https://doi.org/10.24189/ncr.2017.042

Liu, L., Hong, Y., Bednarczyk, C. N., Yong, B., Shafer, M. A., Riley, R., & Hocker, J. E. (2012). Hydro-Climatological Drought Analyses and Projections Using Meteorological and Hydrological Drought Indices: A Case Study in Blue River Basin, Oklahoma. *Water Resources Management*, *26*(10), 2761–2779. https://doi.org/10.1007/s11269-012-0044-y

Lyon, B., Zubair, L., Ralapanawe, V., & Yahiya, Z. (2009). Finescale evaluation of drought in a tropical setting: Case study in Sri Lanka. *Journal of Applied Meteorology and Climatology*, *48*(1), 77–88. https://doi.org/10.1175/2008JAMC1767.1

Malpass, A., Shaw, A., Sharp, D., Walter, F., Feder, G., Ridd, M., & Kessler, D. (2009). "Medication career" or "Moral career"? The two sides of managing antidepressants: A meta-ethnography of patients' experience of antidepressants. *Social Science and Medicine*, *68*(1), 154–168. https://doi.org/10.1016/j.socscimed.2008.09.068

Marj, A. F., & Meijerink, A. M. J. (n.d.). *International Journal of Remote Agricultural drought forecasting using satellite images , climate indices and artificial neural network*. *December 2014*, 37–41. https://doi.org/10.1080/01431161.2011.575896

Mckee, T. B., Doesken, N. J., & Kleist, J. (1993). *The relationship of drought frequency and duration to time scales*. *January*, 17–22.

Mishra, A. K., & Singh, V. P. (2010). A review of drought concepts. *Journal of Hydrology*, *391*(1–2), 202–216. https://doi.org/10.1016/j.jhydrol.2010.07.012

Murad, H., & Islam, A. K. M. S. (2011). Drought Assessment Using Remote Sensing and Gis in North-West Region of Bangladesh. *3rd International Conference on Water and Flood Management*, 861–877.

Refsgaard, J. C., Storm, B., & Refsgaard, A. (1995). Validation and applicability of distributed hydrological models. *IAHS-AISH Publication*, *231*, 387–397.

Sepulcre-Canto, G., Horion, S., Singleton, A., Carrao, H., & Vogt, J. (2012). Development of a Combined Drought Indicator to detect agricultural drought in Europe. *Natural Hazards and Earth System Science*, *12*(11), 3519–3531. https://doi.org/10.5194/nhess-12-3519-2012

Sirisena, T. A. J. G., Maskey, S., Bamunawala, J., Coppola, E., & Ranasinghe, R. (2021). Projected streamflow and sediment supply under changing climate to the coast of the kalu river basin in tropical sri lanka over the 21st century. *Water*

(Switzerland), *13*(21). https://doi.org/10.3390/w13213031

Subramanya, K. (2013). *Engineering Hydrology By K Subramanya*.

Tabari, H., Nikbakht, J., & Hosseinzadeh Talaee, P. (2013). Hydrological Drought Assessment in Northwestern Iran Based on Streamflow Drought Index (SDI). *Water Resources Management*, *27*(1), 137–151. https://doi.org/10.1007/s11269-012-0173-3

Taufik, A., Syed Ahmad, S. S., & Azmi, E. F. (2019). Classification of landsat 8 satellite data using unsupervised methods. *Lecture Notes in Networks and Systems*, *67*(January), 275–284. https://doi.org/10.1007/978-981-13-6031-2_46

Tucker, C. J., & Choudhury, B. J. (1987). Satellite remote sensing of drought conditions. *Remote Sensing of Environment*, *23*(2), 243–251. https://doi.org/10.1016/0034-4257(87)90040-X

Tucker, C. J., Pinzon, J. E., Brown, M. E., Slayback, D. A., Pak, E. W., Mahoney, R., Vermote, E. F., & El Saleous, N. (2005). An extended AVHRR 8-km NDVI dataset compatible with MODIS and SPOT vegetation NDVI data. *International Journal of Remote Sensing*, *26*(20), 4485–4498. https://doi.org/10.1080/01431160500168686

US Army Corps of Engineers. (2018). Hydrologic Modeling System HEC-HMS, Hydrologic Modeling System HEC-HMS, User's Manual. Version 4.3. Hydrologic Engineering Centre. *Hydrologic Engineering Centre*, (Version 4.3), 640.

USDA-NRCS. (2010). *National Engineering Handbook Chapter 15, Time of Concentration*. 1–15.

Wang, G. (2005). *Agricultural drought in a future climate : results from 15 global climate models participating in the IPCC 4th assessment*. 739–753. https://doi.org/10.1007/s00382-005-0057-9

Wijesekera, N. T. S., & Perera, L. R. H. (2012). Key Issues of Data and Data Checking for Hydrological Analyses - Case Study of Rainfall Data in the Attanagalu Oya Basin of Sri Lanka. *Engineer: Journal of the Institution of Engineers, Sri Lanka*,

45(2), 1. https://doi.org/10.4038/engineer.v45i2.6936

Wilhite, D. A. (2021). Drought As a Natural Hazard. *Droughts*, 33–33. https://doi.org/10.4324/9781315830896-24

Wipulanusat, W., Nakrod, S., & Prabnarong, P. (2009). Multi-hazard Risk Assessment Using GIS and RS Applications : A Case Study of Pak Phanang Basin. *Walailak Journal of Science and Technology*, *6*(1), 109–125. https://doi.org/10.2004/wjst.v6i1.76

Wu, H., Hayes, M. J., Weiss, A., & Hu, Q. (2001). An evolution of the standardized precipitation index, the China-Z index and the statistical Z-score. *International Journal of Climatology*, *21*(6), 745–758. https://doi.org/10.1002/joc.658

Wu, Z., Lin, Q., Lu, G., He, H., & Qu, J. J. (2015). Analysis of hydrological drought frequency for the Xijiang River Basin in South China using observed streamflow data. *Natural Hazards*, *77*(3), 1655–1677. https://doi.org/10.1007/s11069-015-1668-z

Xing, Z., Ma, M., Su, Z., Lv, J., Yi, P., & Song, W. (2020). A review of the adaptability of hydrological models for drought forecasting. *Proceedings of the International Association of Hydrological Sciences*, *383*, 261–266. https://doi.org/10.5194/piahs-383-261-2020

Zubair, L., Ralapanawe, V., Yahiya, Z., Perera, R., Tennakoon, U., Chandimala, J., Razick, S., & Lyon, B. (2005). *Fine Scale Natural Hazard Risk and Vulnerability Identification Informed by Climate in Sri Lanka, Project Report*. 20. http://iri.columbia.edu/publications/id=985

Zubair, Lareef, Rao, S. A., & Yamagata, T. (2003). Modulation of Sri Lankan Maha rainfall by the Indian Ocean Dipole. *Geophysical Research Letters*, *30*(2), 2–5. https://doi.org/10.1029/2002GL015639

ANNEXURE 1

SEASONAL ANALYSIS OF KIRINDI OYA

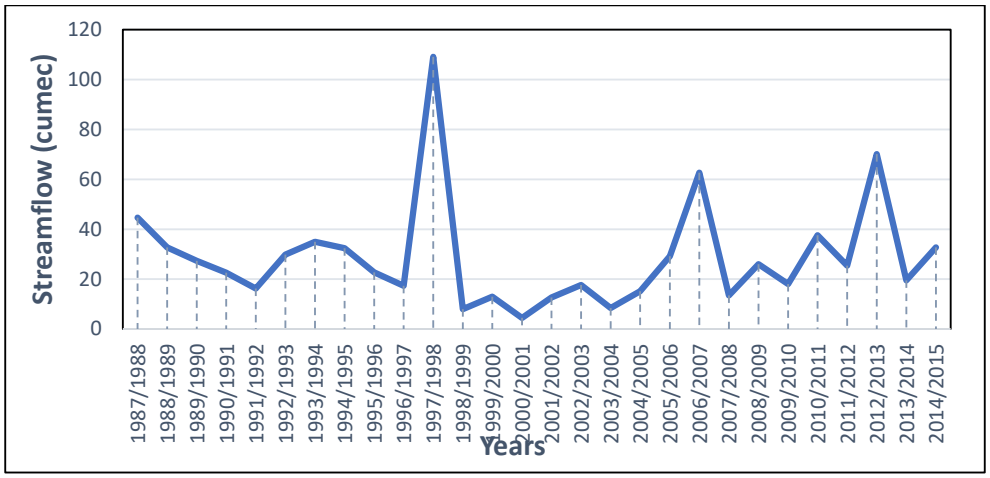

Figure A1- 1 Streamflow Seasonal Variation of Thanamalwila Streamflow gauging stations Second Inter monsoon seasons in Sri Lanka

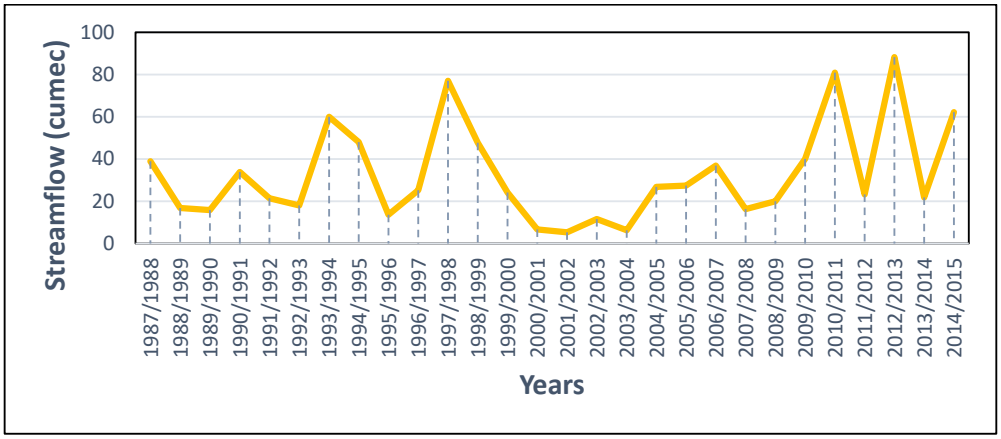

Figure A1- 2 Streamflow Seasonal Variation of Thanamalwila Streamflow gauging stations Northeast monsoon seasons in Sri Lanka

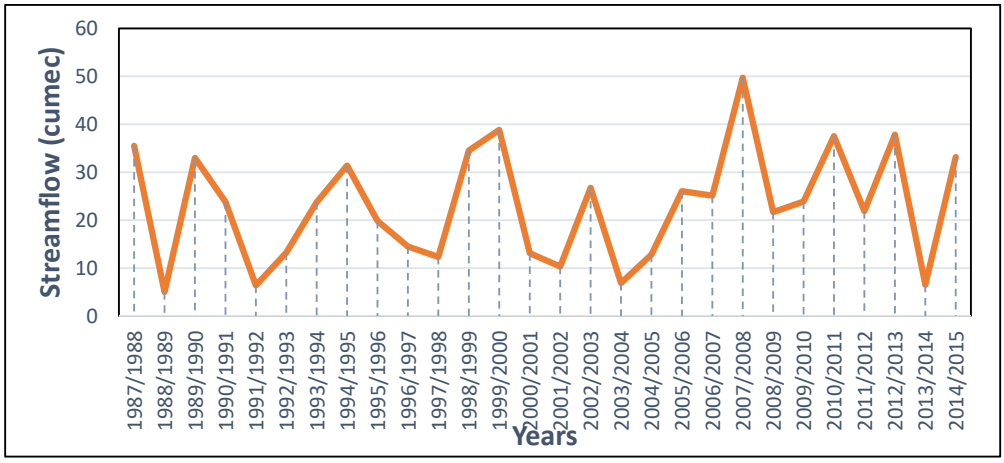

Figure A1- 3 Streamflow Seasonal Variation of Thanamalwila Streamflow gauging stations First Inter monsoon seasons in Sri Lanka

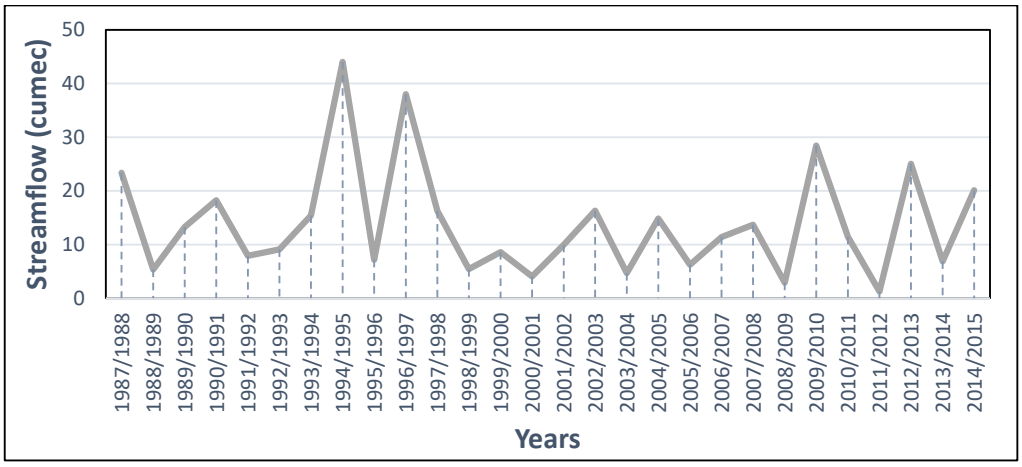

Figure A1- 4 Streamflow Seasonal Variation of Thanamalwila Streamflow gauging stations Southwest monsoon seasons in Sri Lanka

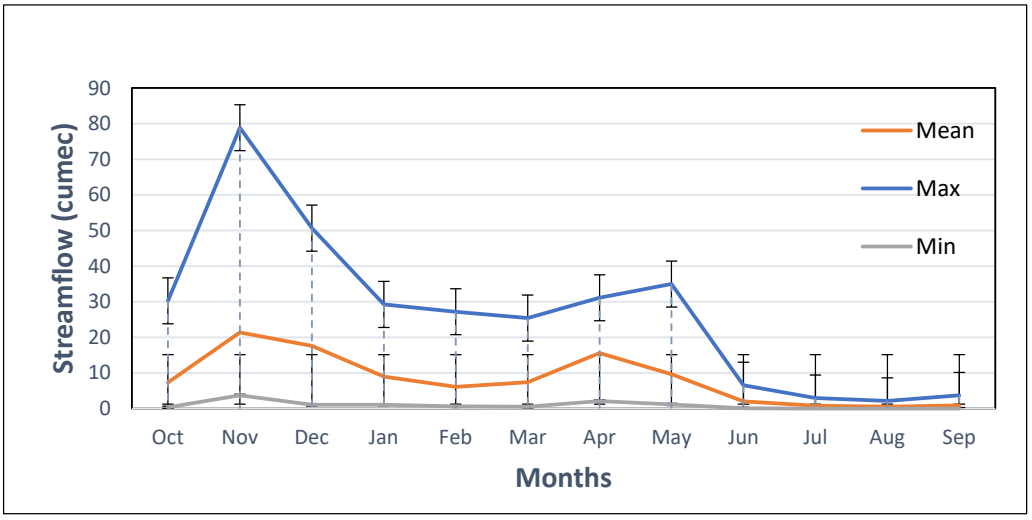

Figure A1- 5 Monthly Mean, Maximum and Minimum of Streamflow in Thanamalwila gauging station in Kirindi Oya river basin

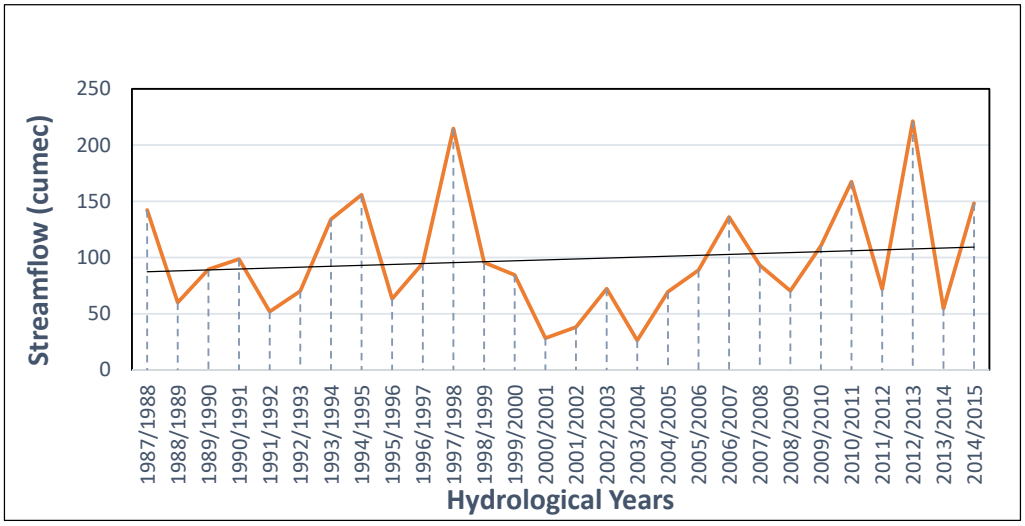

Figure A1- 6 Yearly total of Thanamalwila Streamflow Gauging Station in Kirindi Oya River Basin

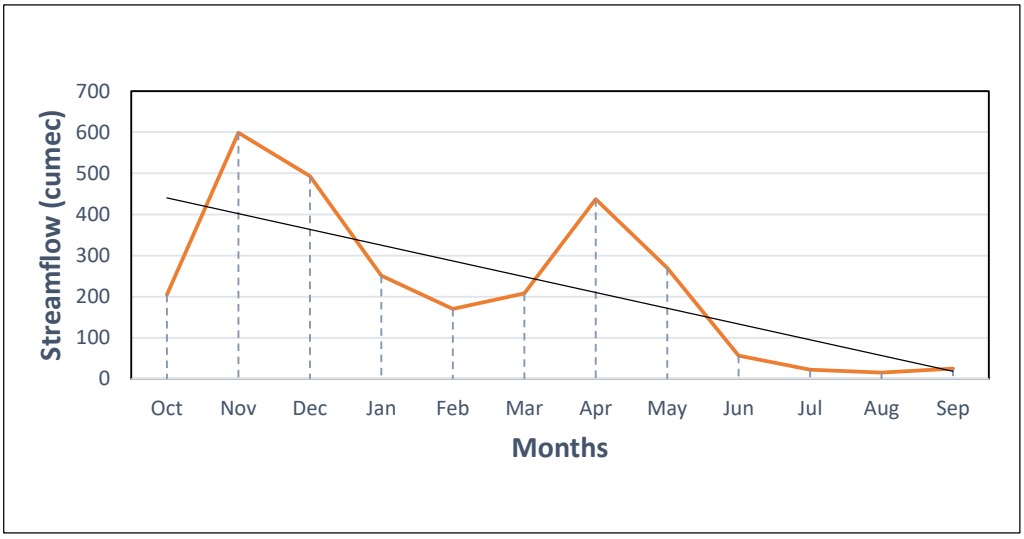

Figure A1- 7 Monthly total of Tanamalwila Streamflow Gauging Station in Kirindi Oya River Basin

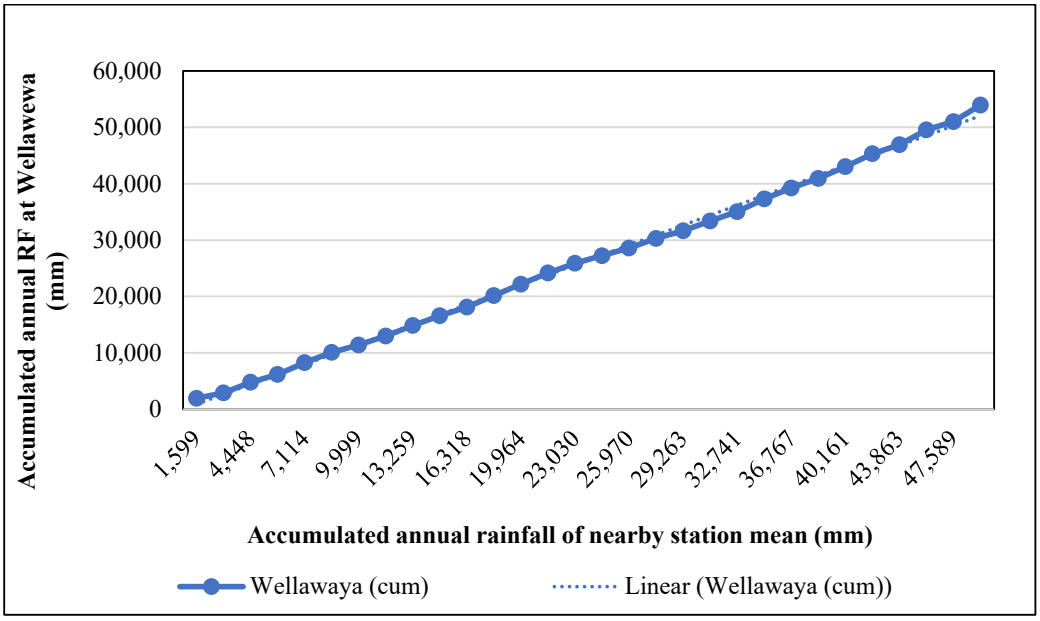

Figure A1- 8 Double Mass Curve of Wellawaya rainfall station in the Kirindi Oya River Basin

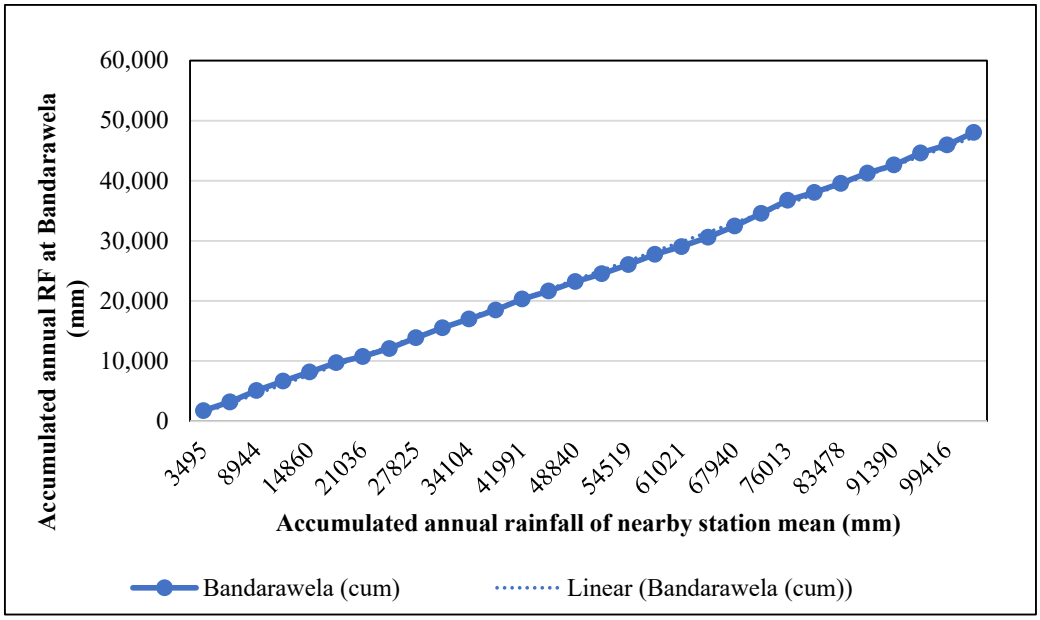

Figure A1- 9 Double Mass Curve of Bandarawela rainfall station in the Kirindi Oya River Basin

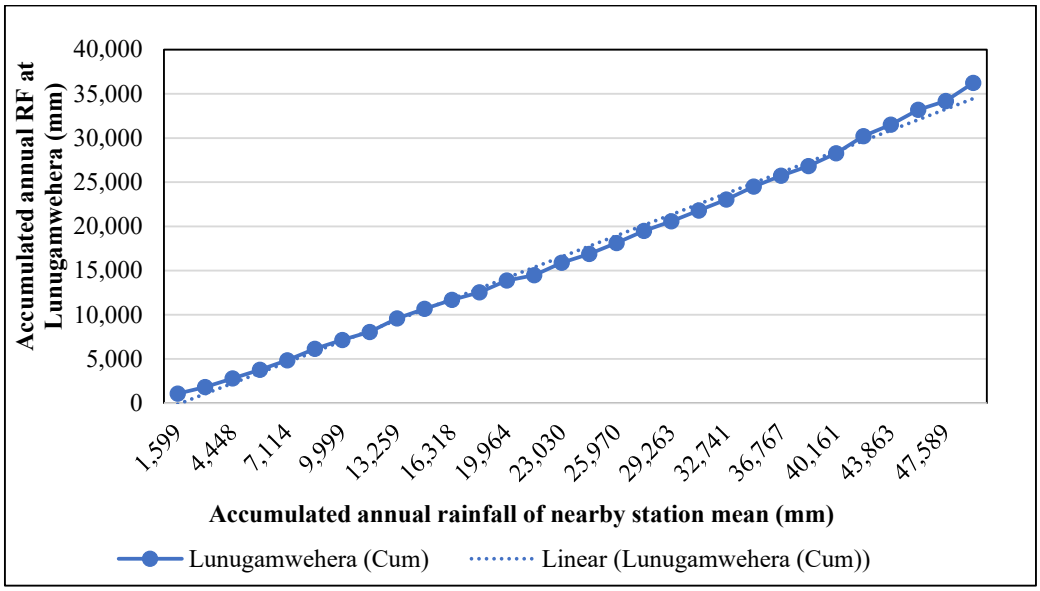

Figure A1- 10 Double Mass Curve of Lunugamwehera rainfall station in the Kirindi Oya River Basin

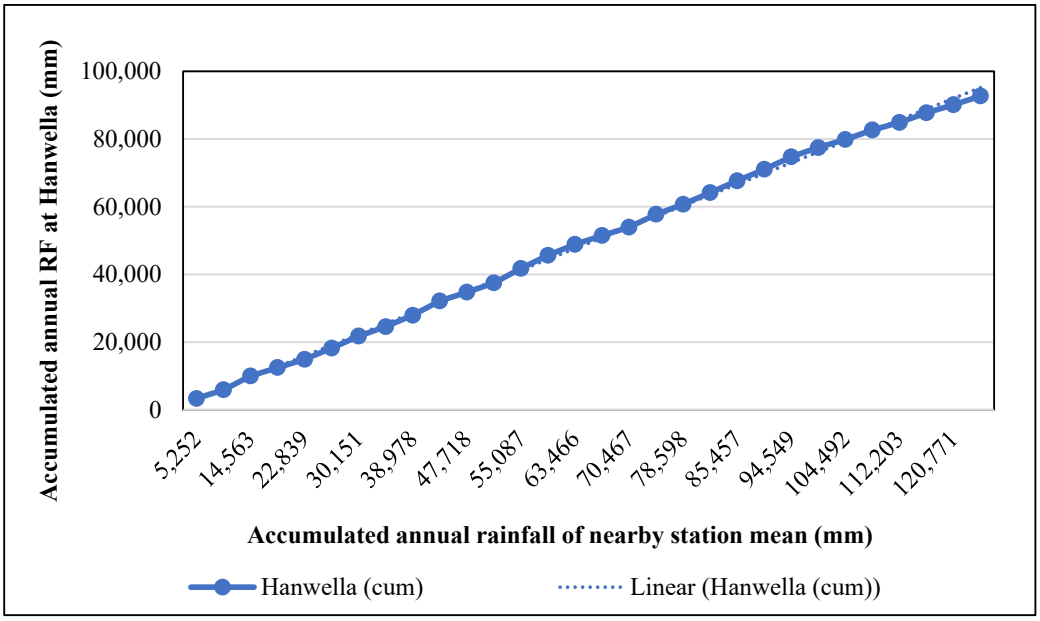

Figure A1- 11 Double Mass Curve of Hanwella rainfall station in the Kelani River Basin

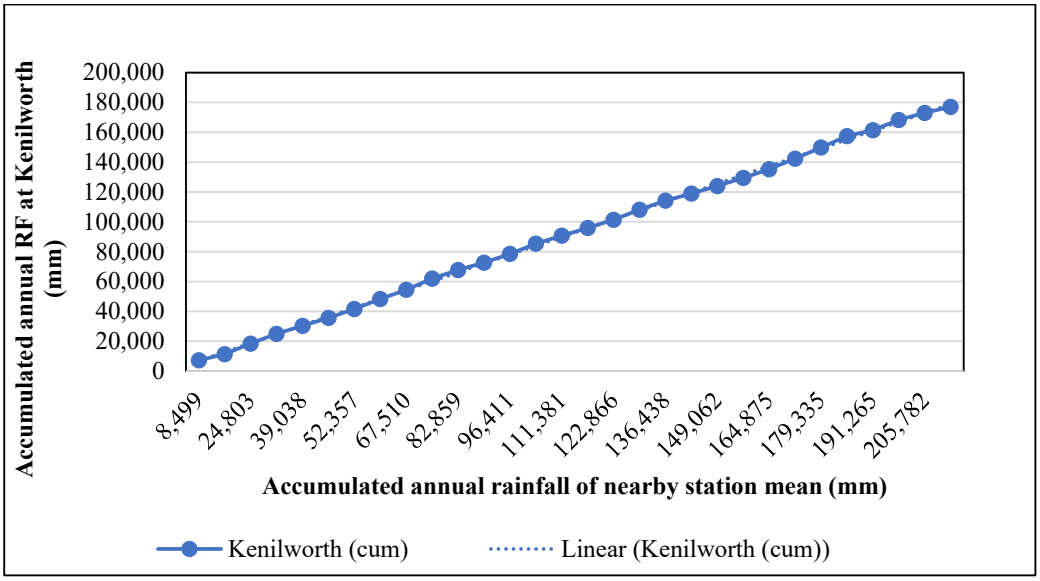

Figure A1- 12 Double Mass Curve of Kenilworth rainfall station in the Kelani River Basin

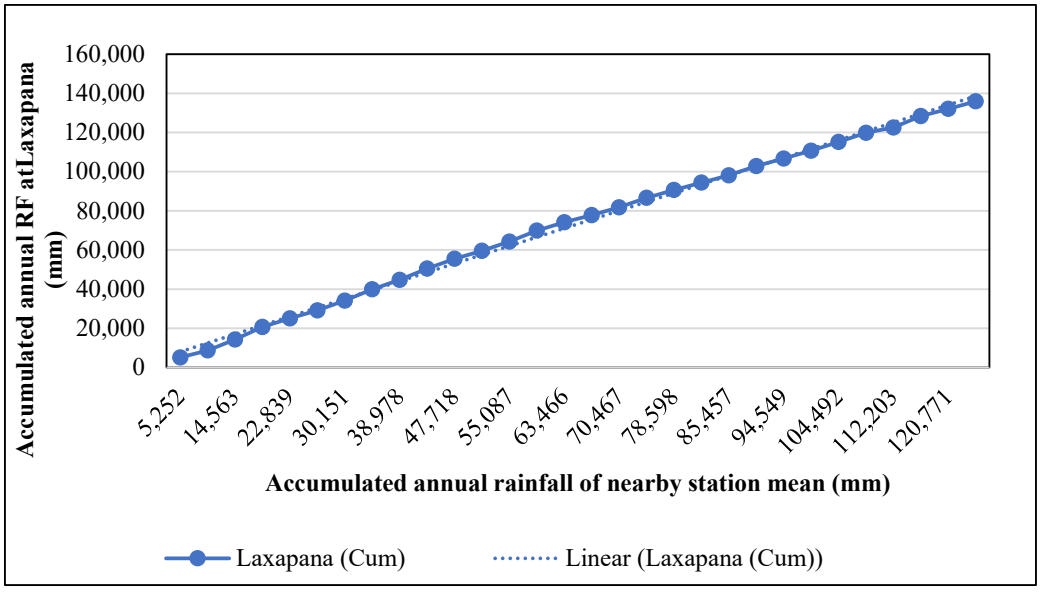

Figure A1- 13 Double Mass Curve of Laxapana rainfall station in the Kelani River Basin

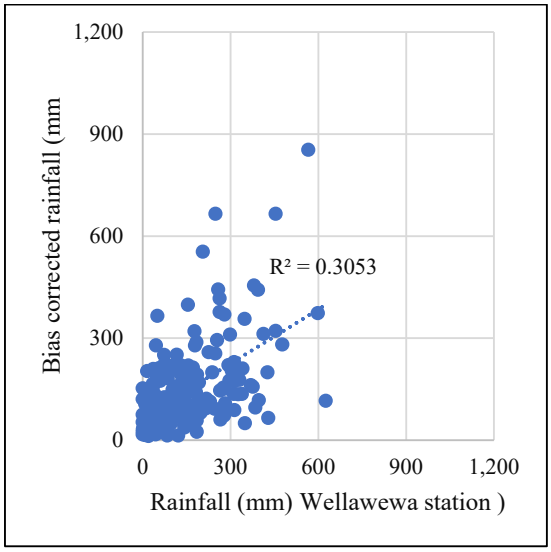

Figure A1- 14 Bias corrected rainfall (mm) for WAS_22_MIROC-MIROC5

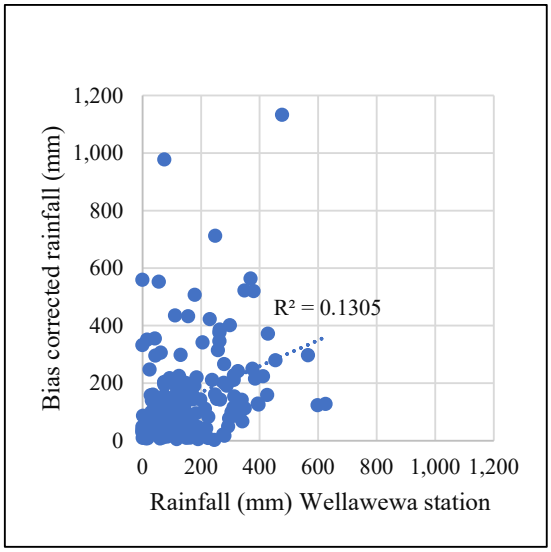

Figure A1- 15 Bias corrected rainfall (mm) for WAS_44i MPI-M-MPI-ESM-LR

The findings, interpretations and conclusions expressed in this thesis/dissertation are entirely based on the results of the individual research study and should not be attributed in any manner to or do neither necessarily reflect the views of UNESCO Madanjeet Singh Centre for South Asia Water Management (UMCSAWM), nor of the individual members of the MSc panel, nor of their respective organizations.